INTERIM RESULTS ON THE CORROSION BEHAVIOR OF ENGINEERING ALLOYS IN OZONATED ARTIFICIAL SEAWATER

W.E. Wyllie II, B.E. Brown and D.J. Duquette
Rensselaer Polytechnic Institute
Troy, NY 12180

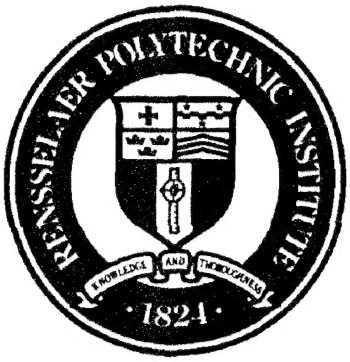

MARCH 1996

Report No. 2 to the Office of Naval Research
Contract No. N00014-94-1-0093

Unclassified

SECURITY CLASSIFICATION OF THIS PAGE

REPORT DOCUMENTATION PAGE

1a. REPORT SECURITY CLASSIFICATION: Unrestricted	1b. RESTRICTIVE MARKINGS: None
2a. SECURITY CLASSIFICATION AUTHORITY	3. DISTRIBUTION/AVAILABILITY OF REPORT: Unrestricted
2b. DECLASSIFICATION/DOWNGRADING SCHEDULE	
4. PERFORMING ORGANIZATION REPORT NUMBER(S): 2	5. MONITORING ORGANIZATION REPORT NUMBER(S)
6a. NAME OF PERFORMING ORGANIZATION: Rensselaer Polytechnic Institute; 6b. OFFICE SYMBOL (If applicable)	7a. NAME OF MONITORING ORGANIZATION
6c. ADDRESS (City, State and ZIP Code): Materials Science and Engineering Dept. Troy, NY 12180-3590	7b. ADDRESS (City, State and ZIP Code)
8a. NAME OF FUNDING/SPONSORING ORGANIZATION: Office of Naval Research; 8b. OFFICE SYMBOL (If applicable): Code 1131M	9. PROCUREMENT INSTRUMENT IDENTIFICATION NUMBER
8c. ADDRESS (City, State and ZIP Code): 800 N. Quincy Street Arlington, VA 22217-5000	10. SOURCE OF FUNDING NOS. — PROGRAM ELEMENT NO.; PROJECT NO.: N00014-94-10093; TASK NO.; WORK UNIT NO.

11. TITLE (Include Security Classification): Interim Results on the Corrosion Behavior of Engineering Alloys In Ozonated Artificial Seawater

12. PERSONAL AUTHOR(S): W. E. Wyllie II, B. E. Brown and D. J. Duquette

13a. TYPE OF REPORT	13b. TIME COVERED	14. DATE OF REPORT (Yr., Mo., Day)	15. PAGE COUNT
Technical	FROM 10/94 TO 3/96	March 1996	

16. SUPPLEMENTARY NOTATION: None

17. COSATI CODES		
FIELD	GROUP	SUB. GR.

18. SUBJECT TERMS (Continue on reverse if necessary and identify by block number): ozone, bromate, bromide, bromine, hypobromous acid, chlorine, corrosion control, biofouling control, oxidizing biocide, (continued on reverse side)

19. ABSTRACT (Continue on reverse if necessary and identify by block number)

Initial testing of metal alloys in ozonated vs. aerated artificial seawater has been completed for exposure times of up to 16 weeks. Five alloy groups were tested: nickel-based, stainless steel-based, titanium-based, aluminum-based, and copper-based. Three types of samples were used to evaluate corrosion behavior: weight loss, creviced and wire (electrochemical). Of the five alloy groups, titanium was the most resistant, showing little difference in the corrosion behavior between aerated and ozonated solutions. Although evidence of crevice corrosion was found on titanium crevice samples in ozonated solutions, data indicate that this is due to the breakdown of the Teflon washers used to create the crevice. Solutions containing alloys with nickel precipitated a black corrosion product which contains hydrated nickel chlorate. However, the percentage of weight lost by these nickel-containing alloys did not indicate a significant weight change. Nickel alloys behaved in a transpassive manner when exposed to ozonated solution. Nickel alloys and highly alloyed stainless steels were resistant to classical crevice corrosion (continued on reverse)

20. DISTRIBUTION/AVAILABILITY OF ABSTRACT	21. ABSTRACT SECURITY CLASSIFICATION
UNCLASSIFIED/UNLIMITED ☒ SAME AS RPT. ☐ DTIC USERS ☐	Unrestricted

22a. NAME OF RESPONSIBLE INDIVIDUAL	22b. TELEPHONE NUMBER (Include Area Code)	22c. OFFICE SYMBOL
D. J. Duquette	(518) 276-6448	

DD FORM 1473, 83 APR — EDITION OF 1 JAN 73 IS OBSOLETE.

SECURITY CLASSIFICATION OF THIS PAGE

18. Continued
seawater, corrosion, nickel, stainless steel, copper, aluminum, titanium.

19. Continued
in ozonated solution, however differential oxidation cell corrosion was noted between free surfaces (high ozone concentration) and slots between multiple crevice washer plateaus (low ozone concentration). Ozonation appeared to be beneficial to the corrosion of aluminum alloys, decreasing corrosion rates and the amount of crevice corrosion compared to aerated seawater. The general corrosion resistance of copper was higher in ozonated vs. aerated solutions, however, the crevice corrosion behavior was adversely affected. Although nickel is beneficial to the corrosion resistance of copper-nickel alloys in aerated seawater, alloys with higher nickel concentrations were adversely affected both in terms of both general and crevice corrosion. The only ozonated samples which experienced significant crevice corrosion relative to their aerated counterparts were 304 stainless steel, 316 stainless steel, and Inconel 690; all have low molybdenum concentrations. Overall, the general corrosion of all of the alloys exposed to ozonated solutions did not appear to be very significant, although in the case of low molybdenum-containing stainless steels and nickel alloys, tight crevices should be avoided.

TABLE OF CONTENTS

LIST OF TABLES

LIST OF FIGURES

ACKNOWLEDGMENT

The authors wish to acknowledge the financial support of the Office of Naval Research under contract N00014-94-1-0093.

The authors also wish to acknowledge the donation of materials by the following companies:

Allegheny Ludlum
Rolled Alloys
Haynes International
Langley Alloys
RMI Titanium

We would also like to thank those who aided us in our background research regarding the chemical reactions in ozonated seawater:

Gordon Grguric, Richard Stockton College, Pomona, NJ
Chris Costen, EPCOT: The Living Seas, Orlando, FL
David LaBonne and Andy Aiken, National Aquarium in Baltimore, Baltimore, MD
Kitty Brown, U.C. Davis Marine Lab, Bodega Bay, CA

We would also like to thank all of the undergraduates who helped with this project.

ABSTRACT

Initial testing of metal alloys in ozonated *vs.* aerated artificial seawater has been completed for exposure times of up to 16 weeks. Five alloy groups were tested: nickel-based, stainless steel-based, titanium-based, aluminum-based, and copper-based. Three types of samples were used to evaluate corrosion behavior: weight loss, creviced and wire (electrochemical). Of the five alloy groups, titanium was the most resistant, showing little difference in the corrosion behavior between aerated and ozonated solutions. Although evidence of crevice corrosion was found on titanium crevice samples in ozonated solutions, data indicate that this is due to the breakdown of the Teflon washers used to create the crevice. Solutions containing alloys with nickel precipitated a black corrosion product which contains hydrated nickel chlorate. However, the percentage of weight lost by these nickel-containing alloys did not indicate a significant weight change. Nickel alloys behaved in a transpassive manner when exposed to ozonated solution. Nickel alloys and highly alloyed stainless steels were resistant to classical crevice corrosion in ozonated solution, however differential oxidation cell corrosion was noted between free surfaces (high ozone concentration) and slots between multiple crevice washer plateaus (low ozone concentration). Ozonation appeared to be beneficial to the corrosion of aluminum alloys, decreasing corrosion rates and the amount of crevice corrosion compared to aerated seawater. The general corrosion resistance of copper was higher in ozonated *vs.* aerated solutions, however, the crevice corrosion behavior was adversely affected. Although nickel is beneficial to the corrosion resistance of copper-nickel alloys in aerated seawater, alloys with higher nickel concentrations were adversely affected both in terms of both general and crevice corrosion. The only ozonated samples which experienced significant crevice corrosion relative to their aerated counterparts were 304 stainless steel, 316 stainless steel, and Inconel 690; all have low molybdenum concentrations. Overall, the general corrosion of all of the alloys exposed to ozonated solutions did not appear to be very significant, although in the cases of low molybdenum-containing stainless steels and nickel alloys, tight crevices should be avoided.

Keywords: ozone, bromate, bromide, bromine, hypobromous acid, chlorine, corrosion control, biofouling control, oxidizing biocide, seawater, nickel, stainless steel, copper, aluminum, titanium.

INTRODUCTION

In the early 1900s, ozone was first used for the disinfection of municipal drinking water in Nice, France.[1] Since then, water treatment by ozonation has been favored over chlorination in Europe because of improved taste, odor control and disinfection. Today, due to the environmental hazards of chlorination byproducts, ozone is currently being used in many fresh water treatment applications in the United States, where only chlorine has been used in the past. These applications include the sterilization of drinking water, treatment of sewage and waste water, algae control in swimming pools, and biofouling control in cooling tower waters.

Although most applications of ozone are in fresh waters, there is a growing number of applications for the use of ozone in seawater. Ozone has already been used successfully in several large aquaria for the treatment of biotoxins in recirculating seawater systems.[2] It is also being investigated for use in preventing biofouling in the process of desalination, as well as in heat exchangers which use marine waters for cooling.[3]

Research on ozonated seawater is only about 20 years old, with the majority of the work having been performed in the field of marine biology. This paper summarizes the reactions that occur between ozone and the constituents of seawater and presents the results of corrosion testing of nickel, stainless steel, titanium, aluminum and copper alloys in ozonated artificial seawater.

The Chemistry of Ozone in Seawater

Ozone is one of the strongest oxidizers used in water treatment. Table I compares the reduction potentials in the standard state and at nominal conditions of seawater with the oxidant present.[4]

Table I. Reduction potentials of oxidants present in ozonated seawater.

Redox Couple	e^o (V_{SHE})	Nominal conditions in artificial seawater, pH 8.2	e (V_{SHE}) at nominal conditions
O_3/O_2	2.08	Ozonated, $p(O_3)$ = 0.024 atm	1.55
$HOCl/Cl^-$	1.48	Chlorinated, [HOCl] = 25 mg/l	1.15
$HOBr/Br^-$	1.33	Brominated, [HOBr] = 25 mg/l	1.08
O_2/OH^-	1.23	Oxygenated, $p(O_2)$ = 0.95 atm	0.75
O_2/OH^-	1.23	Aerated, $p(O_2)$ = 0.2 atm	0.73

Ozone can be produced directly from molecular oxygen, either through ultraviolet radiation or from corona discharge. The solubility of ozone in water, as with other gases, depends on the temperature of the water and the presence of species in the water which are readily oxidized by the ozone (ozone demand). Ozone has a theoretical solubility 10 times that of oxygen in pure water, but in solutions other than pure water, it has been reported to be more on the order of 1 to 1.5 times that of oxygen.[5,6] This discrepancy between theory and practice is due to ozone-depleting impurities in real solutions, which are not accounted for in theory, as well as to the low partial pressure of ozone in the feed gas.[5,6]

Ozone Reactions in Sea Water

Reactions involving ozone become much more complicated in seawater, because of the large number of dissolved species, shown in Table II. Readily oxidizable species, particularly halides, create an ozone demand. In addition, the presence of organics, amines, or impurities such as sulfides, iron(II), or manganese(II) ions further increase the variation in ozone demand during water treatment. The ozone demand must be met before ozone is available for biological control.

Table II. The ionic composition of seawater(1)

Ion	mg/L or ppm
Chloride, Cl^-	19000
Sulfate, SO_4^{2-}	2700
Bicarbonate, HCO_3^-	140
Bromide, Br^-	65
Fluoride, F^-	1
Boric acid, H_3BO_3	26
Sodium, Na^+	10550
Magnesium, Mg^{2+}	1300
Calcium, Ca^{2+}	400
Potassium, K^+	380
Strontium, Sr^{2+}	13

(1) From "Characteristics of Seawater," A.C. Redfield, in The Corrosion Handbook, H.H. Uhlig, ed., J. Wiley & Sons: New York (1948) p. 1111 (Original references: H.U. Sverdrup, M.W. Johnson, and R.H. Fleming, The Oceans, Prentice-Hall, Inc. (1942); J. Lyman and R.H. Fleming, *J. Marine Research,* **3**, (1940) pp. 134-146)

Bromide, Hypobromite, and Bromate The bromide reaction with ozone is very important in seawater. Research on ozonated seawater chemistry has shown that bromide is oxidized by ozone to hypobromite, in a manner similar to the oxidation of bromide by hypochlorite to hypobromite in chlorinated waters.[7-10]

$$O_3 + Br^- \longrightarrow O_2 + BrO^- \qquad k_1 = 160\ M^{-1}s^{-1} \qquad (1)^{11}$$

Once formed by ozonation, the BrO^- can react again with ozone along a path that returns to Br^-,

$$O_3 + BrO^- \longrightarrow 2O_2 + Br^- \qquad k_2 = 330\ M^{-1}s^{-1} \qquad (2)^{11}$$

effectively creating a catalytic decomposition loop for molecular ozone (Figure 1).[12] The hypobromite ion also associates with H^+ ion and forms hypobromous acid (HOBr), which is a very effective disinfectant.[13-15]

Ozone oxidizes BrO^- to form bromate (BrO_3^-):[10,11,16]

$$2O_3 + BrO^- \longrightarrow 2O_2 + BrO_3^- \qquad k_3 = 100\ M^{-1}s^{-1} \qquad (3)^{11}$$

Once bromate forms it does not react further with ozone and terminates the ozone-bromide reaction loop (Figure 1). The bromate ion is not particularly useful as a disinfectant and its toxicity to animal life is a concern.[10,17]

Ozone can also oxidize the chloride ion to hypochlorite, followed by a similar reaction scheme for hypochlorite as exists as for hypobromite:

$$O_3 + Cl^- \longrightarrow O_2 + ClO^- \qquad k_4 = 0.003\ M^{-1}s^{-1} \qquad (4)^{18}$$

$$O_3 + ClO^- \longrightarrow 2O_2 + Cl^- \qquad k_5 = 110\ M^{-1}s^{-1} \qquad (5)^{19}$$

$$2O_3 + ClO^- \longrightarrow 2O_2 + ClO_3^- \qquad k_6 = 30\ M^{-1}s^{-1} \qquad (6)^{18}$$

Because of the much higher rate constant for the oxidation of bromide (1) compared to that for chloride ion (4), the bromide oxidation by ozone occurs more rapidly. The small fraction of hypochlorite that does form via reaction (4) reacts quickly to oxidize Br^- to BrO^-:

$$ClO^- + Br^- \rightarrow Cl^- + BrO^- \qquad k_7 = 6.7\text{x}10^3\ M^{-1}s^{-1} \qquad (7)^{20}$$

BrO^- will react to form bromate by reaction (3), explaining higher bromate levels in

solutions with both Br^- and Cl^- present rather than Br^- alone.[21] Accordingly, free hypochlorite levels are expected to be low in ozonated seawater.

Complete conversion of Br^- to BrO^-/HOBr by ozone results in a theoretical maximum concentration of 78 mg/L HOBr. However, the typical concentrations of HOBr observed lie between 25 - 50 mg/L at a pH of 8 - 8.3 based on a series of 150 hour ozonation tests in 1 liter artificial seawater cells (0.16 wt.% ozone in air @ 0.03 m^3/hr [1 SCFH]).[22] The maximum level of HOBr is not reached because of the competing reaction of ozone with BrO^- to form the bromate ion.

As the pH increases or as bromide concentration decreases in ozonated solutions, it has been shown that the oxidation of BrO^- to BrO_3^- is predominant.[17,23] Research has shown that all Br^- in seawater is effectively converted to BrO_3^- through exhaustive ozonation (ozonation beyond the level necessary to react with the initial Br^- + other oxidizable species). The theoretical maximum concentration of 104 mg/L BrO_3^- was achieved by Crecelius[10] using a high ozone dose (5 wt.% ozone in oxygen @ 0.012 m^3/hr [0.43 SCFH]) in 200 mL artificial seawater.

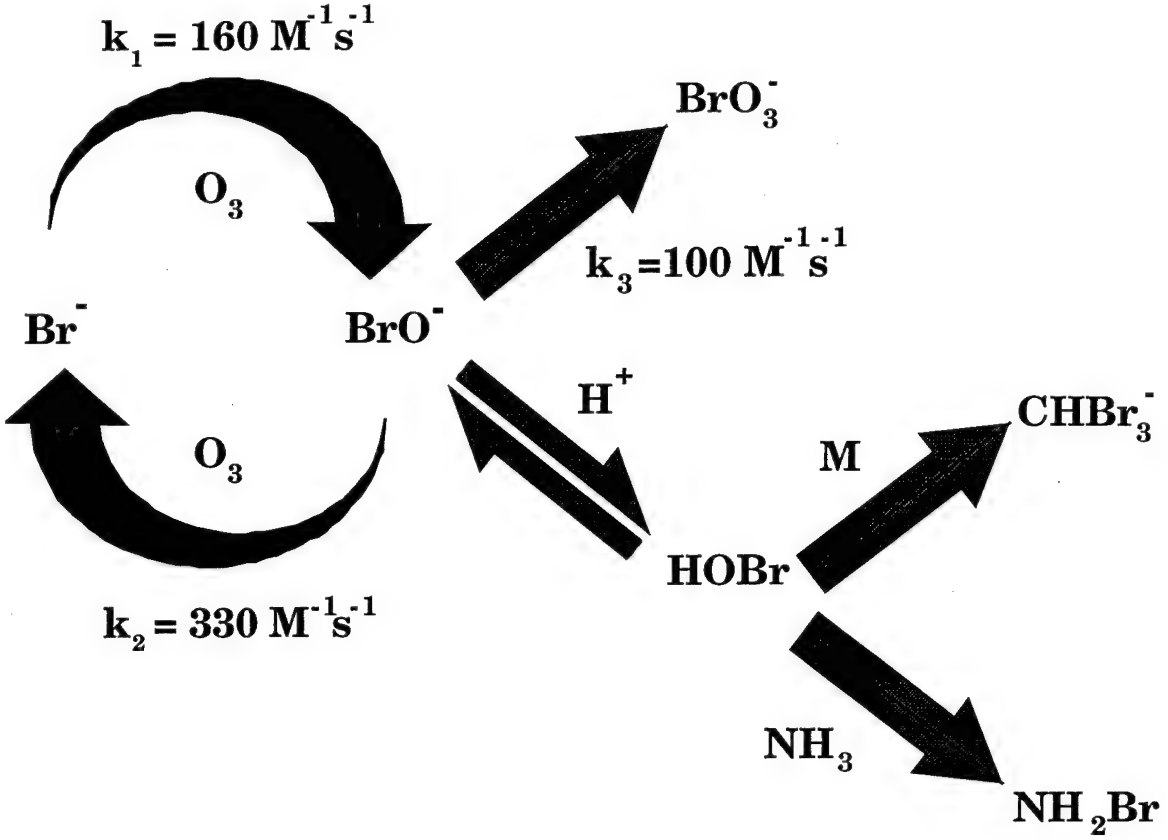

Figure 1. Reaction cycle caused by the ozonation of bromide in seawater.[11]

Corrosion of Alloys in Seawater

Nickel Alloys

Nickel is resistant to general corrosion in seawater, with corrosion rates typically less than 25 μm/y (1 mpy) .[24] However, its passive film is not resistant to pitting breakdown due to the presence of chloride ions. The addition of copper decreases the severity (depth/width ratio) of pitting somewhat, but pitting susceptibility persists up to 69 weight percent (wt.%) of copper. Chromium imparts resistance to oxidizing environments, and increases the resistance to tarnishing and pitting, but Ni-Cr alloys are still susceptible to localized corrosion. The crevice corrosion resistance is greatly enhanced by molybdenum additions, by increasing the resistance to breakdown in the reducing environment created within crevices.[25] Tungsten has a similar effect on increasing the resistance to reducing acid environments, however molybdenum is more effective on a weight percent of alloyed element basis.[26] Hastelloy C, a Ni-Cr-Mo-W alloy, is considered immune to general and localized corrosion in seawater.[24] Corrosion of IN625, a Ni-Cr-Mo-Ta alloy, was reported to have a corrosion rate of 0.4 μm/y in seawater with no pitting or crevice attack.[27] In the analysis by Streicher,[28] nickel base alloys C276 and IN625 were considered immune to crevice corrosion in filtered seawater.

Related literature has reported that the crevice corrosion rate of IN625 in low level chlorinated artificial seawater (1 mg/L HOCl, deaerated) is expected to be lower than in aerated artificial seawater[29] based on a lower cathodic currents measured during cathodic polarization in chlorinated versus aerated seawater. In the case of ozonated seawater, ozone, HOBr and oxygen (feed gas) reduction together should result in a greater cathodic current than for aerated conditions. As a result, any crevices that initiate on IN625 and any other Ni-Cr-Mo alloys may grow faster with ozonation.

Stainless Steel Alloys

The general corrosion susceptibility of austenitic stainless steels in seawater is considered to be negligible, owing to the protective passive film. Rather, pitting and crevice corrosion are the most deleterious forms of attack to these alloys in seawater, resulting in deep penetration of 304 and 316 stainless steels.[24] Alloying to increase the localized corrosion resistance of stainless steels typically involves increased chromium and molybdenum, which raise the critical pitting potential (Ep). Molybdenum provides the greatest increase in resistance to crevice corrosion, on a wt.% alloyed element basis, possibly by increasing the resistance to passive film breakdown in reducing crevice environments, or by forming a protective molybdenum

salt film.[30]

Streicher's analysis[28] of multiple crevice assembly data in filtered seawater resulted in the ranking of stainless steels based on resistance to crevice corrosion. Crevice corrosion resistance was observed to be based on some general alloy composition trends: alloys with high chromium contents (≥ 25 wt.% Cr), low nickel content, and at least 3.5 wt.% molybdenum were virtually immune. Factors that increased the crevice corrosion susceptibility were low chromium (≤ 20 wt.% Cr), substantial nickel (≥ 20 wt.% Ni) and copper.

Corrosion data for stainless steels in ozonated seawater is more scarce than for non-ozonated seawater. Electrochemical testing of 304L stainless steel in ozonated 0.5 N NaCl[31] and 304 stainless steel in ozonated artificial seawater[32] indicated enhanced passive films but increased susceptibility to crevice corrosion compared to non-ozonated conditions.

Titanium Alloys

Titanium is inert in most oxidizing environments over a wide range of pH values, due to the highly stable passive film. In seawater, titanium is considered inert with respect to general corrosion, with rates of less than 2.5 μm/y (0.1 mpy) for Grade-2 (commercial purity) and Grade-5 (Ti-6Al-4V). After 3 years exposure to ambient seawater, pitting and crevice corrosion are nonexistent.[26] Based on research in the titanium industry,[33] crevice corrosion will not occur on titanium alloys in seawater, regardless of pH, below a temperature range of 75-80°C. To increase the crevice corrosion resistance at higher temperatures, palladium (Grade-7) or molybdenum+nickel (Grade-12) are added to titanium.[26] These alloying additions increase the stability of the passive film in the reducing acidic environment which forms within a crevice. Although resistant to chloride ion, titanium is more susceptible to passivity breakdown in other acid halide solutions such as HBr and HF.[26]

Titanium Grade-2 has been used successfully in seawater-cooled power plant and ship condensers.[34,35] Because titanium is not as inherently biofouling-resistant as the 90Cu-10Ni alloy that was originally used in this application,[35] treatment with a biocide such as chlorine or ozone is necessary.

In ozonated artificial seawater at room temperature, titanium Grade-2 showed a few small pits under a PTFE crenelated washer.[32] No pitting was observed under aerated conditions. It has been proposed that the fluoride ion, produced from degradation of the PTFE washer in the crevice of the ozonated sample, formed HF and was responsible for the breakdown of the passive film.[36]

Aluminum Alloys

Aluminum readily forms a protective film in the presence of oxygen or oxidizing environments, such as ozone. Although general corrosion resistance is excellent, the main form of corrosion in seawater is pitting, observed at crevices and surface deposits.[37] This is due to the breakdown of the protective oxide in the presence of chloride ion, at potentials noble to the pitting potential.[25] Copper, present in heat treatable, high strength 2xxx and 7xxx alloys, accelerates the pitting attack. Initiation is easier due to the influence of copper, shifting the corrosion potential noble to the pitting potential, and pit growth is accelerated by galvanic action between cathodic copper sites and anodic aluminum pits.[25]

Lightweight, high strength aluminum alloys have been used extensively for structures in marine applications. The 1xxx series (pure Al) and 5xxx series (Al-Mg-Mn, Al-Mg-Cr, Al-Mg-Mn-Cr) show good corrosion resistance in seawater service. The magnesium present in solid solution and as Al_6Mg_5 in the 5xxx series provides better performance than the 1xxx alloys. Uniform corrosion rates for 5xxx alloys are about 5 μm/y (0.20 mpy) maximum;[26] 7 μm/y (0.28 mpy) for 1100 and 6061.[27] Pitting penetration rates decrease with time. Maximum pit depths after 1 year of exposure were 75-125 μm (3-5 mils) for 1100-H14 and 5052-H3, and 275-500 μm (11-20 mils) for 6061-T6 and 7075-T6. The 6xxx alloys shows greater general corrosion resistance but greater susceptibility to deep pitting, and the Cu-bearing 2xxx and 7xxx alloys are even more susceptible to deep pitting in seawater.[26]

Copper Alloys

The copper-based alloys (Copper, 90Cu-10Ni, 70Cu-30Ni) are considered to have adequate corrosion resistance in seawater due to the formation of a protective scale. Nickel, as well as iron (0.5 - 1.5 wt.%) increases the corrosion resistance of copper alloys to impingement attack.[25] Typical general corrosion rates for seawater are about 13-75 μm/y (0.52-3.0 mpy) for copper, 3-40 μm/y (0.12-1.6 mpy) for 90Cu-10Ni, and 3-70 μm/y (0.12-2.8 mpy) for 70Cu-30Ni.[24,37]

Copper-nickel alloys with 10-30 wt.% nickel do not exhibit active-passive behavior, and are generally not susceptible to pitting in seawater.[24,25] These alloys resist general corrosion in fast-flowing seawater as well. Generally, increasing the nickel content of the Cu-Ni alloys decreases the pitting resistance in stagnant seawater; beyond 30% Ni, flowing conditions must exist to avoid serious pitting damage.[25,27] Results of a 3-month exposure test in flowing seawater on creviced copper alloys[38] ranked the localized corrosion resistance as follows: pure copper > 70Cu-30Ni > 35Cu-65Ni. Preferential attack was outside the plateaus of a multiple

crevice, rather than under the crevice, as is seen in passive stainless alloys in the same test. This result was attributed to metal ion concentration cell corrosion. The authors noted that the cathode-to-anode area ratio had no significant effect on the copper alloys, indicating that the localized corrosion was limited by the anodic dissolution kinetics.[38]

A recent review of the literature[32], showed that the corrosion behavior of copper and its alloys was not affected by the presence of ozone in fresh cooling waters. Literature regarding copper base alloys in ozonated saline solutions is limited. Electrochemical testing on 70Cu-30Ni in ozonated 0.5 N NaCl[31] resulted in an increase in E_{corr} and an apparent enhancement in the protective film over the deaerated condition based on a potentiostatic current *vs.* time experiment. Naval brass did not show a significant effect of ozonation compared to aeration of seawater after a 30 day creviced sample immersion test.[32] However, the color of the corrosion product was gold with ozonation *vs.* greenish white with aeration, indicating that the ozone reduction had an effect on the character of the protective film which formed.

EXPERIMENTAL

Solutions

Ten, 60-liter tanks of artificial seawater were prepared by adding 1946 g of Forty Fathoms Bio-Crystals™ Marinemix to 56L of distilled water in each tank. Marinemix is a brand of artificial seawater that contains all of the components of natural seawater, in accordance with ASTM D 1141-90[39].

The initial bromine concentration of each tank was tested using a titration procedure (Appendix I) and adjusted by the addition of Marinemix or distilled water, until the bromide concentration was in the range of 800-860 mM/L (63-69 mg/L).

Five tanks were ozonated at a rate of 0.03 m^3/hr (1 SCFH [standard cubic feet per hour]) using fritted glass bubblers; five tanks, used as controls, were aerated at a rate of 0.03 m^3/hr (1 SCFH).

Ozonated tanks were measured for changes in pH as well as concentrations of apparent residual ozone, bromide, hypohalite, and bromate, after 1 day and 1 week of ozonation before samples were immersed. After sample immersion, these values were measured at the same intervals as which samples were removed for testing. The residual ozone was measured using the Indigo Trisulfonate Method.[40,41] Bromide, hypohalite, and bromate concentrations were measured using the titrations described in Appendix I. Aerated control tanks were aerated for 4 days before immersion of samples; free bromide concentration and pH of these solutions were tested prior to sample immersion.

In order to compensate for evaporation and prevent adverse build-up of byproducts, 6L of artificial seawater, in both the aerated and ozonated tanks, was changed out weekly and replaced with fresh solution.

Ozone Generation and Delivery

Ozone was generated using a combination of an AirSep® AS-12 oxygen generator and American Ozone™ GS2-14 ozone generator. The Airsep unit was set to operate at a pressure of 69 kPa (10 psi) and 55% of maximum output, delivering 90-95% oxygen (nitrogen balance) to the ozone generator at a flow rate of 0.28 m^3/hr (10 SCFH). With the ozone generator operating at a pressure of 21 kPa (3 psi) and at 85% power setting, this produced an ozone output of approximately 47 g O_3/m^3 (3.35 wt.% O_3 in 90-95% O_2).

The ozone was supplied to a set of 6 valved, glass-lined, stainless steel ball flow meters (0-2 SCFH range). The flow of ozone to each tank was controlled by an individual flow meter set to 0.03 m^3/hr (1 SCFH), giving a rate of ozone input into

each tank of 1.3 g O_3/hr with an oxygen input rate of 39 g O_2/hr. From the flow meters, ozone was delivered to each tank via Teflon™ and norprene® tubing. Only Teflon tubing was used inside the tanks.

Unbleached polyvinyl chloride (PVC) sheets were used as lids to cover both aerated and ozonated tanks. Holes were placed in the sheets for incoming air/ozone Teflon tubes. In the case of ozonated tanks, a section of flexible vinyl tubing was placed in a hole in the center of the lid, and sealed with silicone sealant, to duct away off-gassing ozone. Two external fans helped to pull and direct the excess ozone from the tanks, as well as the outflow valve, to a nearby fume hood where it was further diluted to the hood system (Figure 2). The ozonated tank lids were completely sealed to the tanks with duct tape. A corner opening was cut in the ozonated tank lids to facilitate measurement of tank pH, ozone concentration, and to perform periodical water change outs, without the removal of the entire tank lid.

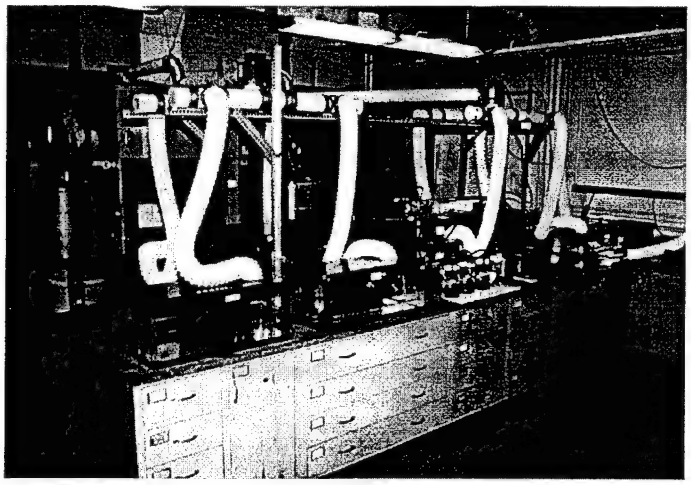

Figure 2. Exhaust system for ozonated seawater tanks.

Samples

The materials in these experiments include metals and alloys which are generally considered to be "active" or "passive" in aerated chloride containing environments. These include iron-based (stainless steels), nickel-based, aluminum-based and copper-based alloys, as well as a limited number of titanium alloys.

Four basic types of samples were used in these experiments:

1.) Weight Loss
2.) Crevice
3.) Large Cathode Crevice
4.) Wire

Table III below shows the different alloys used in the test program. The weight loss and crevice samples were 2.5x5.1 cm (1.0x2.0 in) coupons cut from plate, in which a 0.95 cm (0.38 in) hole had been drilled. Three samples were used as weight loss samples, and the rest were used as crevice samples. Large cathode area crevice samples, measuring 3.8x7.6 cm (1.5x3.0 in), were cut from sheet or plate stock, with a 0.95 cm (0.38 in) hole drilled in the center. Wire samples were typically alloys that could be obtained as weld wire, and varied in diameter. Eight samples of each of the wire alloys were prepared for testing. All samples were ground through 600 grit abrasive, rinsed with distilled water, ultrasonically cleaned in distilled water, and then rinsed again with distilled water.

Table III: Alloys used for weight loss and crevice samples.

Iron-Based[1]	Nickel-Based[1]	Copper-Based	Aluminum-Based	Titanium-Based
304 SS[2]	IN625[2]	ETP Copper	1100[2]	Grade-2[2]
316SS[2]	C276[2]	90Cu-10Ni	5052	Grade-5[2]
AL6XN[2]	C22[2]	Hiduron	6061	Grade-7
654SMO	VDM Alloy 59	Marinel	7075	Grade-12
Remanit 4565S	IN690	70Cu-30Ni[2]	5356[3]	ß21S
				ßC

[1] Included large cathode area crevice samples.
[2] Wire samples were included for additional electrochemical testing.
[3] Included as wire sample only, to represent 5xxx series aluminum alloys.

Table IV. Chemical composition (wt.%) based on mill analyses of stainless steel plate samples used for seawater immersion tests.

	C	Cr	Fe	Mn	Mo	Ni	P	S	Si	Other
304 SS	0.06	18.1	bal.	1.83	-	8.03	0.034	0.004	0.46	
316 SS	0.057	16.56	bal.	1.67	2.44	11.84	0.033	0.015	0.66	
AL6XN	0.02	20.30	bal.	0.52	6.25	23.93	0.026	0.000	0.39	0.27 Cu, 0.24 N
654SMO	0.015	24.60	bal.		7.3	21.9				0.40 Cu, 0.487 N
Remanit 4565S	0.022	23.57	bal.	5.57	4.2	17.65	0.018	<0.003	0.19	0.48 N, 0.04 Nb

Table V. Chemical composition (wt.%) based on mill analyses of nickel-base alloy plate samples used for seawater immersion tests.

	C	Cr	Fe	Mn	Mo	Ni	P	S	Si	Other
IN625	0.02	21.71	3.97	0.08	8.82	bal.	0.007	0.001	0.09	0.27 Ti, 3.41 (Ta+Nb)
C276	0.003	16.02	6.27	0.45	15.89	bal.	0.011	<0.002	0.04	1.83 Co, 0.16 V, 3.51 W
C22	0.004	20.65	2.61	0.21	14.08	bal.	0.004	<0.001	0.03	0.06 Cu, 0.11 Co, 0.02 V, 3.29 W
VDM 59	0.005	22.65	0.29	0.15	15.6	bal.	0.002	0.002	0.03	0.03 Co, 0.14 V, 0.08 W
IN690	0.01	29.10	10.26	0.42	-	bal.	-	0.003	0.30	0.29 Ti, 0.22 Al

Table VI. Chemical composition (wt.%) based on mill analyses of titanium alloy plate samples used for seawater immersion tests.

	Al	C	Fe	Mo	N	O	Ti	V	Other
Ti Grade-2	-	0.020	0.10	-	0.012	0.12	bal.	-	0.001 H
Ti Grade-5	6.30	0.030	0.18	-	0.012	0.012	bal.	4	38 ppm H
Ti Grade-7	-	0.010	0.04	-	0.008	0.13	bal.	-	0.13 Pd
Ti Grade-12	-	0.020	0.03	0.40	0.01	0.13	bal.	-	0.72 Ni
Beta C Ti	3.00	0.010	0.06	3.90	0.018	0.09	bal.	8	3.8 Zr, 6.00 Cr
Beta 21S	3.20	0.012	0.32	14.45	0.016	0.14	bal.	-	2.56 Nb, 0.19 Si

Table VII. Chemical composition (wt.%) based on mill analyses of copper-base alloy plate samples used for seawater immersion tests.

	Al	C	Cr	Cu	Fe	Mn	Ni	P	S	Zn	Other
ETP Copper	-	-	-	99.9	-	-	-	-	-		
90Cu-10Ni	-	0.006	-	bal.	1.10	0.36	9.4	0.0	0.006	0.17	0.04 Pb
Hiduron 191	1.38	0.01	0.01	bal.	0.91	4.36	14.00	0.005	0.005	0.02	0.005 Pb, 0.005 Sn, 0.05 Si
Marinel	1.83	0.01	0.44	bal.	1.13	4.30	17.80	0.011	0.011	0.01	0.007 Pb, 0.78 Nb, 0.009 Sn, 0.05 Si
70Cu-30Ni	-	0.008	-	bal.	0.56	0.39	29.52	0.01	0.010	0.22	0.01 Pb

Table VIII. Nominal composition (wt.%) of aluminum alloy samples used for seawater immersion tests.

	Al	Cr	Cu	Fe	Mg	Mn	Si	Ti	Zn
1100-H14	99.00	-	0.05-0.2	0.95	-	0.05	0.95	-	-
5052-H3	bal.	0.15-0.35	0.10	0.40	2.2-2.8	0.10	0.25	-	0.1
5356 (wire only)	bal.	0.05-0.20	0.10	0.40	4.5-5.5	0.05-0.20	0.25	0.06-0.20	0.10
6061-T6	bal.	0.04-0.35	0.15-0.4	0.70	0.8-1.2	0.15	0.4-0.8	0.15	0.25
7075-T6	bal.	0.18-0.28	1.2-2.0	0.50	2.1-2.9	0.30	0.40	0.20	5.1-6.1

Sample Fixturing

Each of the alloy groups was placed in its own tank, for both the aerated and ozonated conditions. All samples were either threaded directly, or suspended using Teflon thread and O-rings, on removable 0.63 cm (0.25 in) glass rods which were fixtured on a glass rack (Figure 3). Creviced samples were placed on the lower portion of the rack, while weight loss samples and wires were placed on the upper portion.

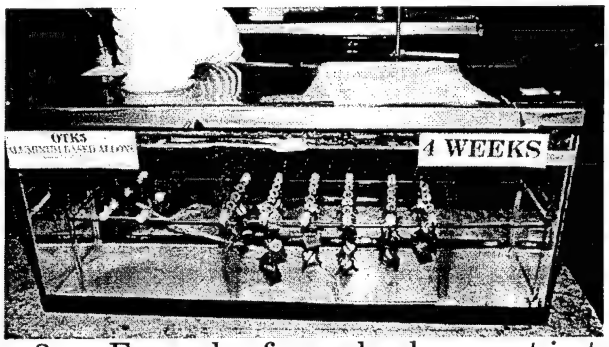

Figure 3. Example of sample placement in tanks.

Three weight loss samples of each alloy were threaded through their holes onto a glass rod, using Teflon tubing as spacers between the samples. Crevice samples were assembled between two Teflon crenelated washers, surrounding the hole. The sample and Teflon washers were clamped between Grade-2 titanium washers and secured with a Grade-2 titanium bolt and nut (Fig. 4). For purposes of discussion, the portion of the crenelated Teflon washer which is in contact with the surface of the sample to form the crevice will be called the "plateau", while the region separating the plateaus will be referred to as the "slot". A Teflon thread was tied to one of the Teflon washers used for each sample; the other end of the thread was tied to a Teflon O-ring

for later fixturing. In order to prevent any contact between the sample and the bolt, the bolt was first wrapped with Teflon tape to insulate it. The crevice samples were assembled while submerged in aerated artificial seawater, in order to minimize air pockets and to initiate wetting in the Teflon crenelated washers. After crevice samples were tightened up with one and a quarter turns from finger tight, the resistance was checked between the sample and the bolt with a voltmeter. Each sample was re-checked after final removal from the tanks to be sure that there was no contact between the sample and fixture.

A metal to metal crevice was also created, but only with Grade-2 titanium. Two Grade-2 titanium washers were ground to 600 grit abrasive, ultrasonically cleaned in distilled water, and rinsed again before being placed on either side of a Grade-2 titanium crevice sample to create the metal to metal crevice.

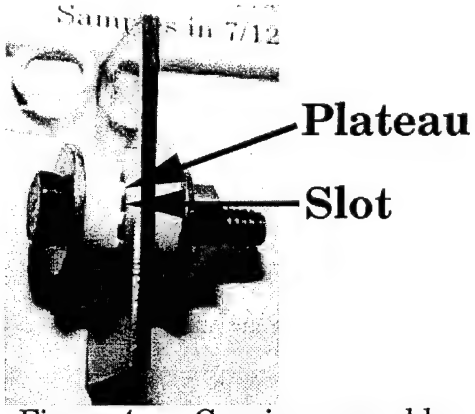

Figure 4. Crevice assembly.

Wire samples were bent such that one end rose significantly out of the solution, while being supported by the glass rod, to allow corrosion potential data to be collected directly in the tank without disturbing the wire (Figure 5). An effort was made to prevent the other end of the wire from being submerged as well in order to avoid preferential corrosion on the transverse wire sections.

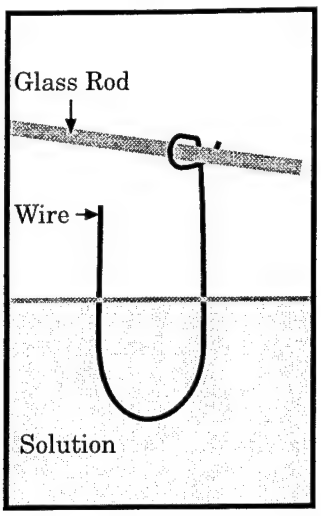

Figure 5. Wire schematic.

Testing

Tests were performed at the intervals listed in Table IX. Before any samples were removed or tested in the tanks, the water chemistry was checked (see "solutions" in this section).

Table IX. Time intervals that samples were tested after immersion.

1 WEEK
2 WEEKS
4 WEEKS
8 WEEKS
16 WEEKS
24 WEEKS
48 WEEKS

At each time interval, weight loss samples were removed, rinsed in distilled water and allowed to air dry before weighing. After weighing, the samples were photographed, replaced on the glass rod(s) and returned to the tank.

One crevice sample and one large cathode area crevice sample of each alloy was removed at each time interval and rinsed in distilled water. The resistance between the sample and the titanium bolt fixturing was then checked to determine if contact existed between them. The assembly was then carefully taken apart, and the crenelated washer and fixture saved, if corrosion product was present. The samples were then rinsed in distilled water again and allowed to air dry. The samples were then weighed, photographed, and stored in a dessicator.

At each interval, one wire of each alloy was carefully removed from the tank for testing in a one-liter cell. Care was taken to keep the wire submerged while removing both the wire and tank solution in the one liter cell. A bubbler was placed in the cell, bubbling either air or ozone at a rate of approximately 0.003 m^3/h (0.1 SCFH). Electrochemical measurements of steady state corrosion potential, linear polarization resistance and cyclic polarization were then performed on the wire. Afterwards, the wire was removed from the cell and the submerged length of the wire recorded in order to determine the area to be used for corrosion rate calculations.

A single wire of each alloy remained in the tank over the course of the entire experiment. At each interval, the steady state corrosion potential and linear polarization resistance of these wires were measured while they remained in the tank.

Linear polarization resistance (LPR) measurements were collected at a scan rate of 0.6 V/hr for all wire samples. Corrosion rates for all alloys were then calculated from the LPR data based on $\beta_a=\beta_c=0.12$. Cyclic potentiodynamic polarization scans of all wires were performed at a rate of 10 V/hr, with the exception of the stainless steel alloys which were scanned at 1V/hr.

RESULTS

Solution Chemistry

Figures 6-15 show the typical change in pH, residual ozone, free bromide, hypohalites, and bromate for each ozonated tank with time. Values for brominated species are given as percentages of total bromide, which is in the range of 820-880 μM (65-70 mg/L) for all tanks.

Tanks were ozonated for a week before samples were immersed. After a week of ozonation, the solution chemistry of the artificial seawater in the tanks showed relatively stable values with only slight variations between tanks. The pH decreased slightly in most of the tanks to a value between 8.1-8.2. The residual ozone concentration stabilized to between 0.3-0.4 mg/L, with 82-89% of the total bromide in solution oxidized to bromate. The amount of free Br^- was between 10-15% of the total bromide in solution, while HOBr and OBr^- were from 0-5%.

After samples were immersed, a reduction in the amount of residual ozone was observed in all of the tanks, occurring over a period of 4 to 8 weeks. This decrease is believed to be due to an increase in ozone demand created by metallic corrosion of the samples, as well as subsequent oxidation of metal ions by ozone. After the initial decrease, the residual ozone concentration in the tanks recovered to higher values. The ozonated tanks containing nickel-base, stainless steels, and copper-base alloys recovered to ozone concentrations of 0.33, 0.26, and 0.2 mg/L, respectively, by 16 weeks of sample exposure. These values were lower than the initial concentration prior to sample immersion, reflecting the ozone demand associated with ongoing metallic corrosion. In contrast, the tanks containing titanium and aluminum alloys showed recovery to steady values of 0.52 and 0.39 mg/L ozone, respectively, which were higher than the initial values. This would indicate that the ozone demand due to metallic corrosion was lower than in the tanks containing nickel base, stainless steel, and copper alloys. It is important to note that, in the absence of metal corrosion, ozone concentration would be expected to rise above initial values, due to decreased chemical demand associated with decreasing concentration of unreacted Br^- ion.

After 4 weeks exposure to ozone, the concentration of bromide and its byproducts stabilized in all of the tanks. In general, the stable values for each tank were similar to one another, within 93-95 % as BrO_3^-, 3-5 % as free Br^- and 1-3 % as HOBr (% of total Br) The pH stabilized to approximately 8.2 in ozonated tanks for the duration of the experiment, once samples were immersed.

The total bromide concentration of each aerated tank was measured initially and adjusted to be within 820-880 μM (65-70 mg/L); at sampling intervals, only the

pH of the aerated tanks was recorded. Little change was seen in the pH of the aerated tanks over time after samples were immersed; all tanks were stable within the 8.2 - 8.3 pH range.

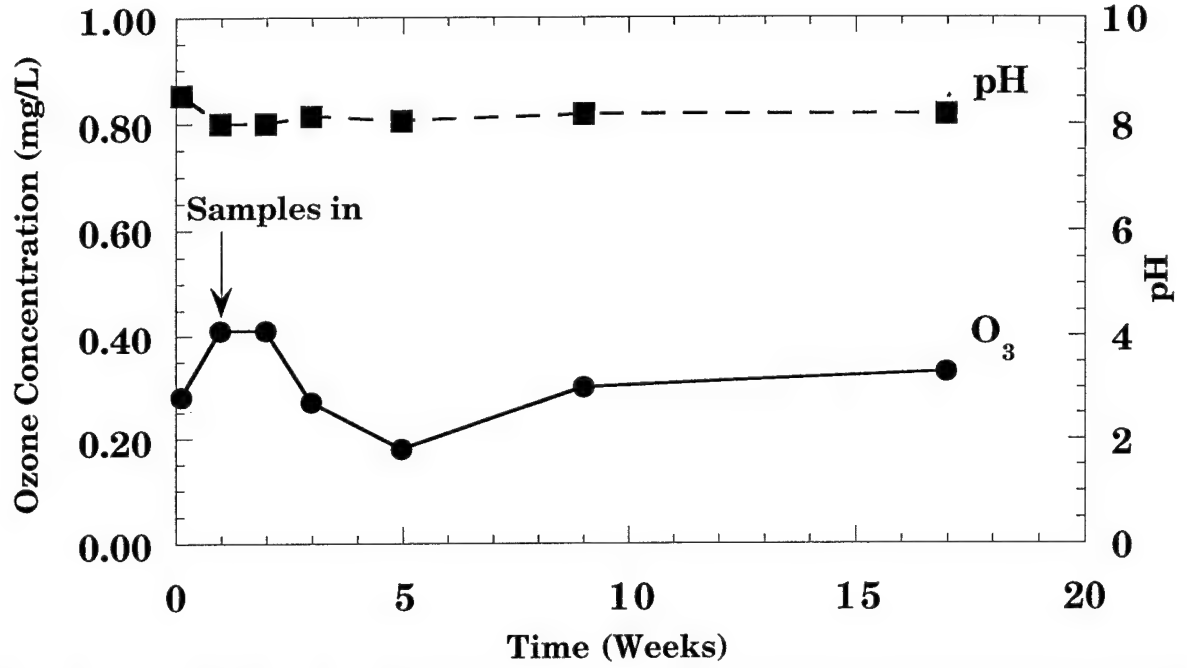

Figure 6. Change in pH and measured residual ozone concentration with time, forsolutions containing nickel alloys.

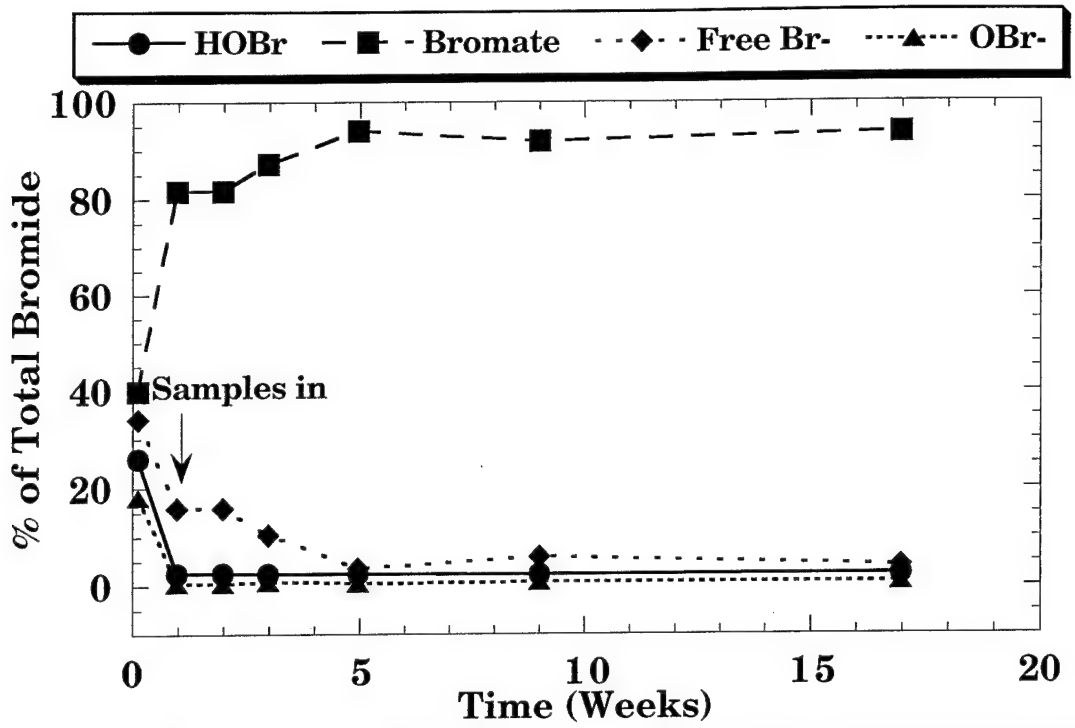

Figure 7. Change in concentration of bromide, hypohalites, and bromate with time, forsolutions containing nickel alloys.

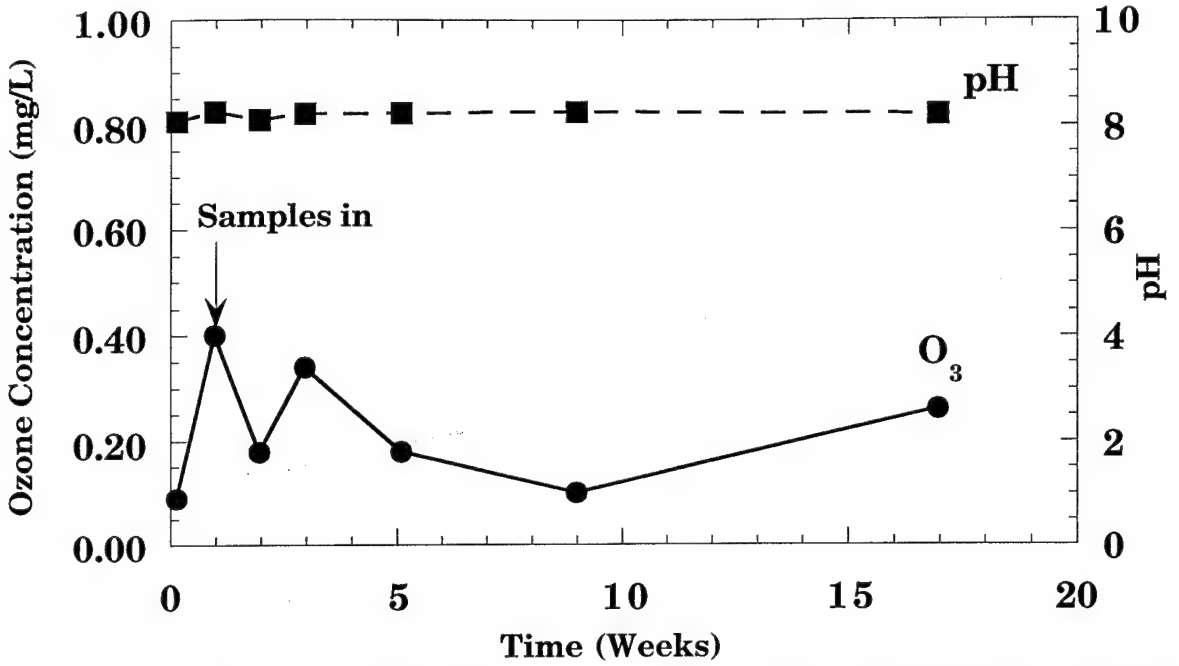

Figure 8. Change in pH and measured residual ozone concentration with time, forsolutions containing stainless steel alloys.

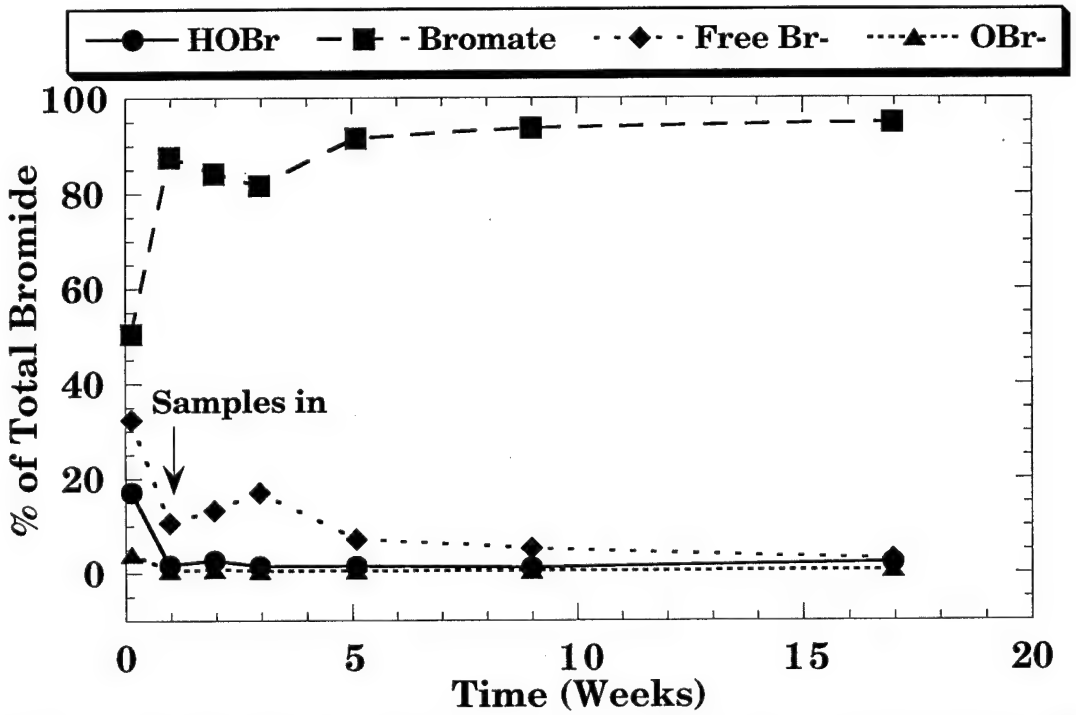

Figure 9. Change in concentration of bromide, hypohalites, and bromate with time, forsolutions containing stainless steel alloys.

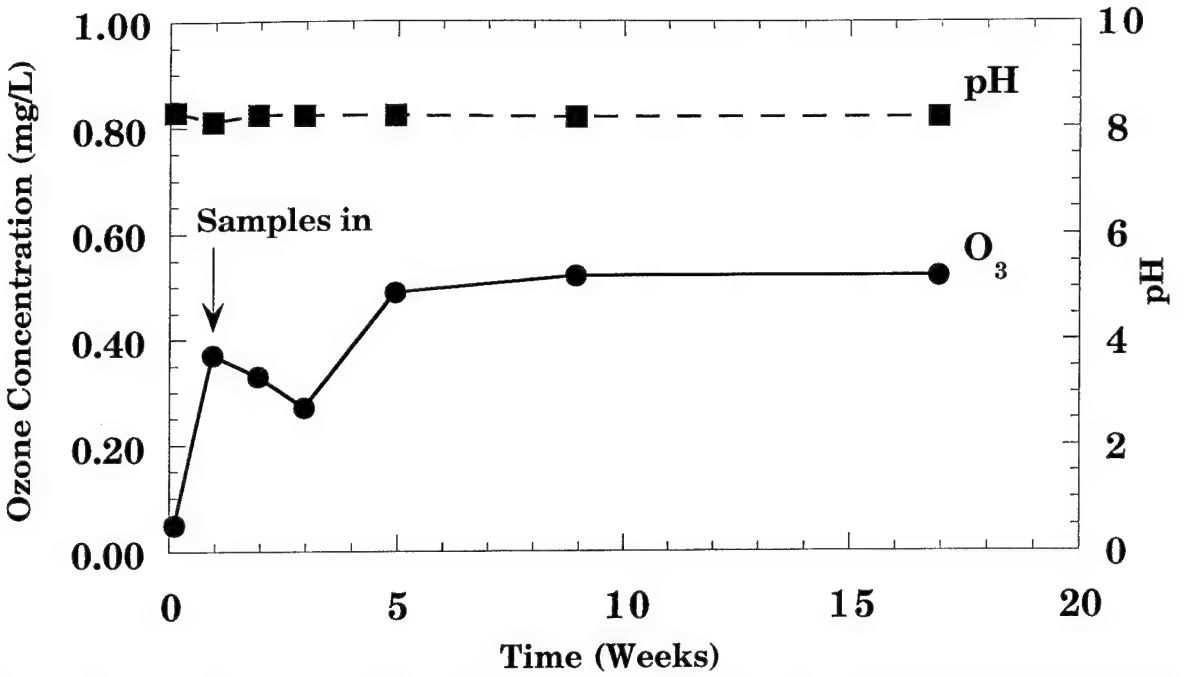

Figure 10. Change in pH and measured residual ozone concentration with time, forsolutions containing titanium alloys.

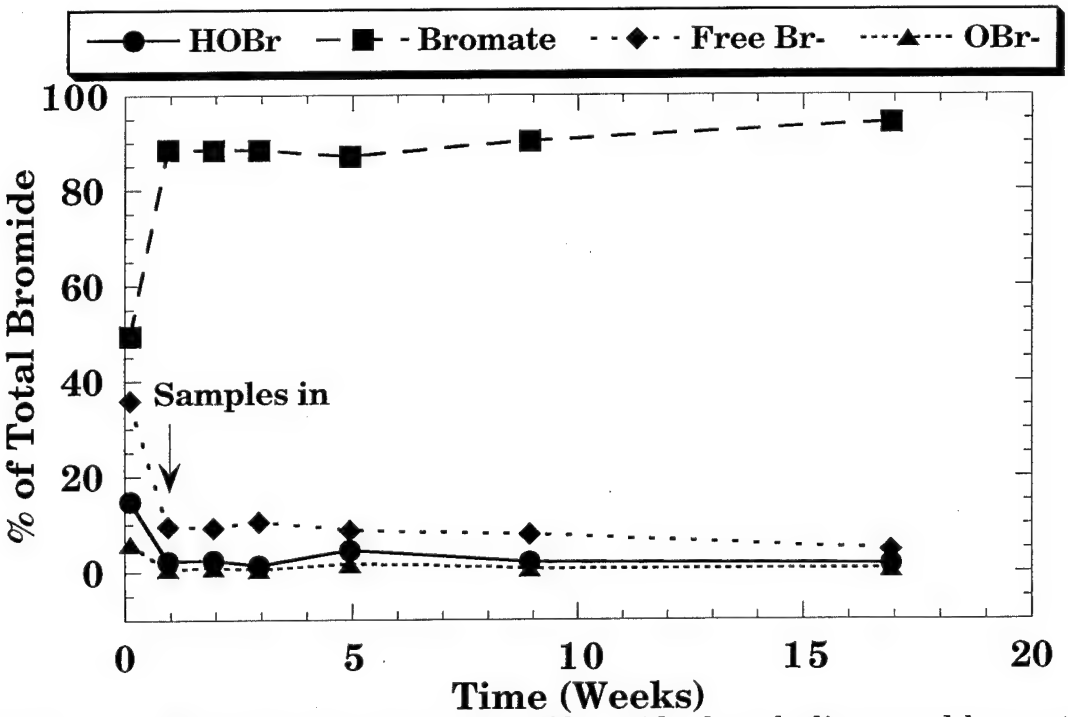

Figure 11. Change in concentration of bromide, hypohalites, and bromate with time, forsolutions containing titanium alloys.

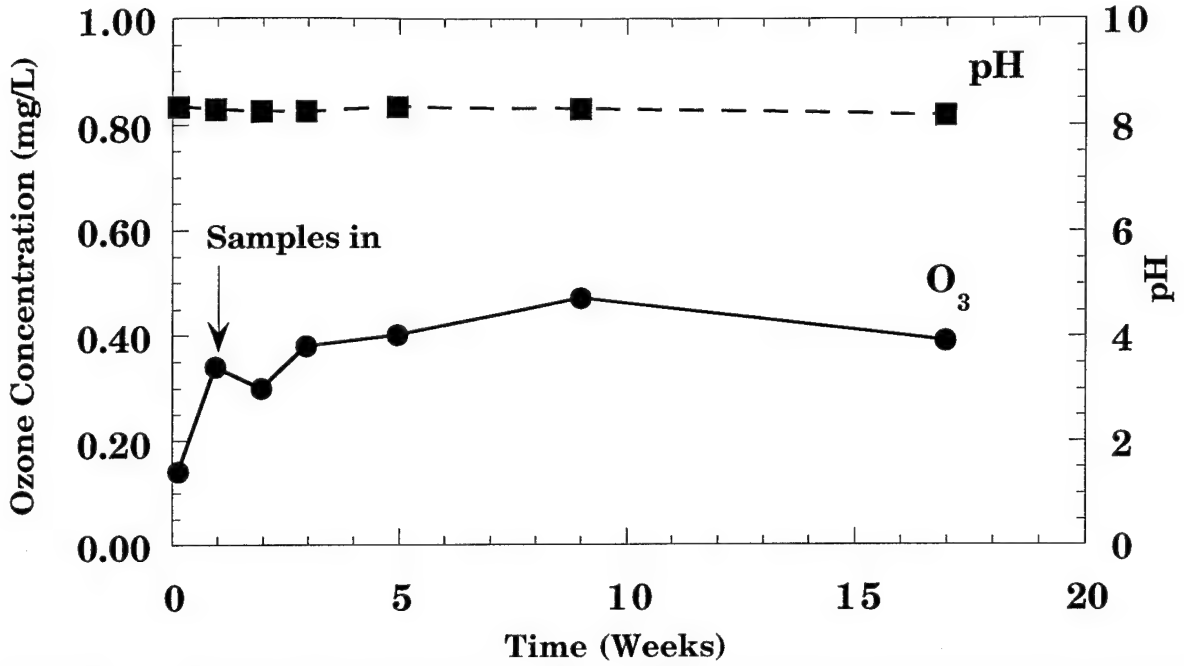

Figure 12. Change in pH and measured residual ozone concentration with time, forsolutions containing aluminum alloys.

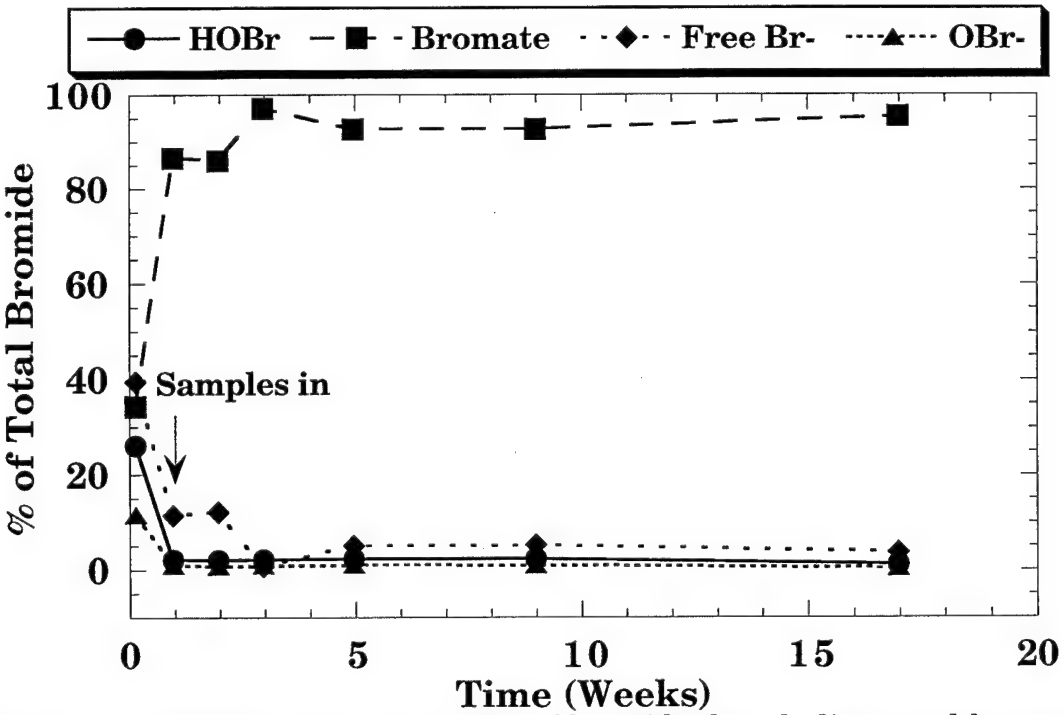

Figure 13. Change in concentration of bromide, hypohalites, and bromate with time, forsolutions containing aluminum alloys.

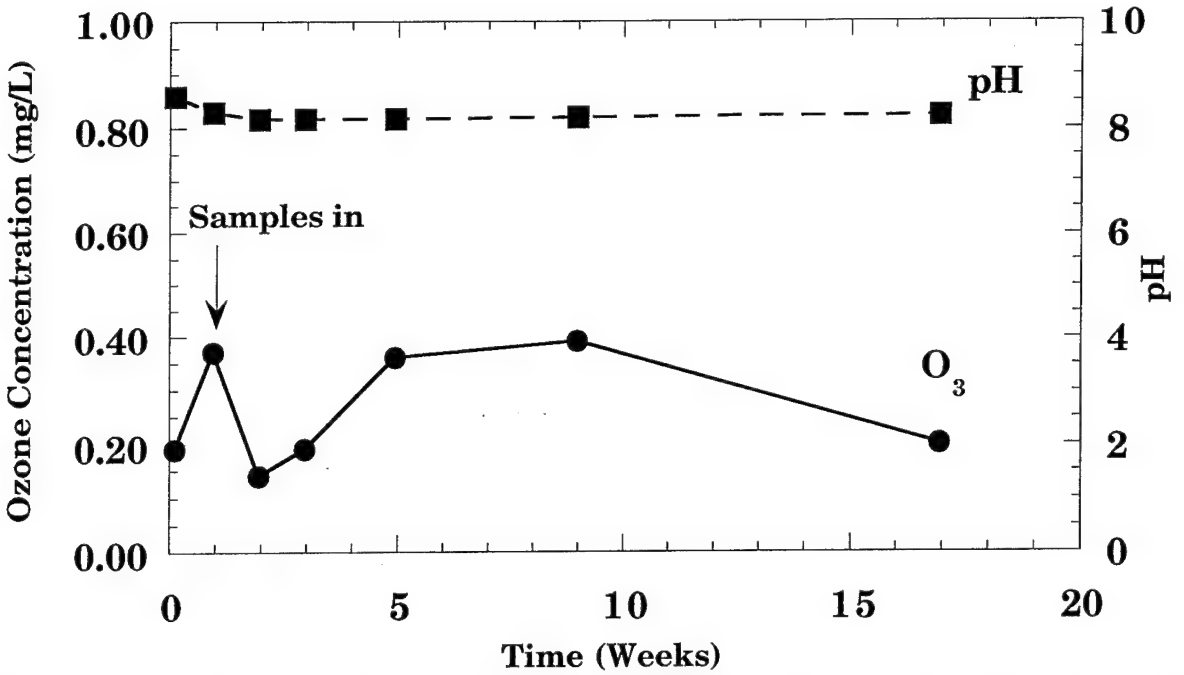

Figure 14. Change in pH and measured residual ozone concentration with time, forsolutions containing copper alloys.

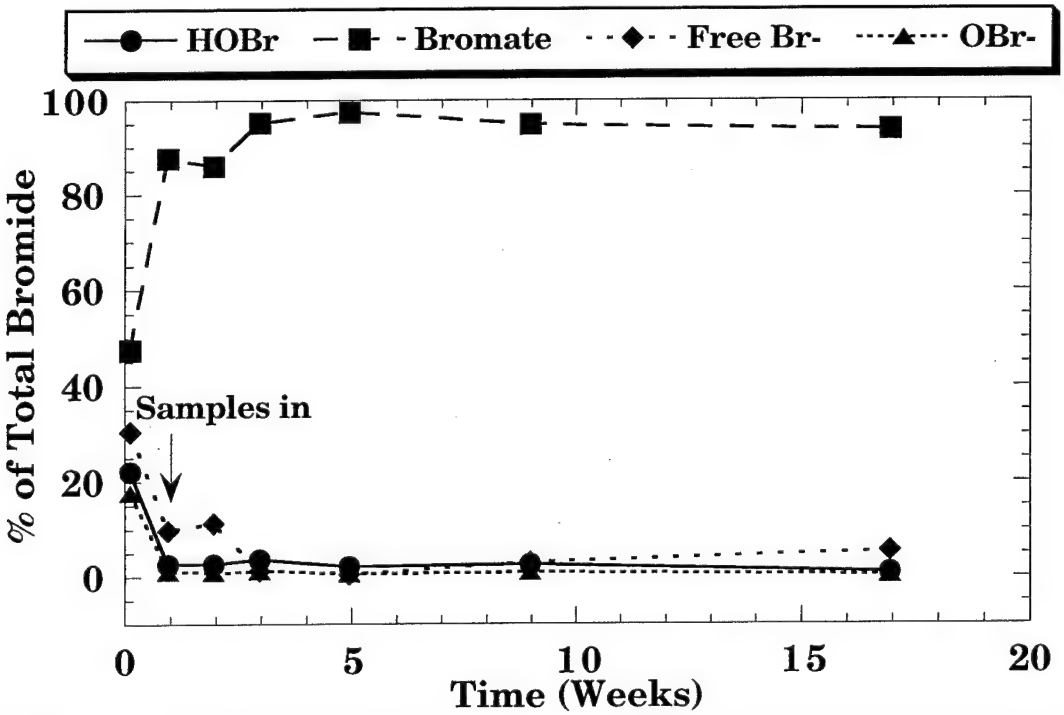

Figure 15. Change in concentration of bromide, hypohalites, and bromate with time, forsolutions containing copper alloys.

Nickel Alloys

In ozonated seawater, voluminous amounts of black flocculent corrosion product precipitated in the tanks containing nickel based alloys, and alloys with significant amounts of nickel (e.g., AL6XN and 70Cu-30Ni). For the tank containing the nickel alloys, this precipitation occurred within 24 hours of the immersion of the samples. For copper-nickel and stainless steel samples, the black corrosion product did not begin to precipitate for several days. This precipitation resulted in the plating of the black corrosion product onto the glass sides of the tanks, however, the submerged samples remained free of black corrosion product. Partially submerged wire samples were covered with the black corrosion product, but only above the waterline, possibly due to condensation and evaporation of water on the surface in combination with exposure to gaseous ozone as it exited the tank.

Black corrosion product was collected from the ozonated tank containing the nickel alloys, filtered and dried. Examination using energy dispersive spectroscopy (EDS) in the scanning electron microscope (SEM) revealed primarily calcium, oxygen, chloride, and nickel. Further analysis by x-ray diffraction indicated the presence of calcium oxide, sodium chloride, and a hydrated nickel chlorate.

C276

Weight Loss Samples Figure 16 shows the percent weight loss (%WTL) in C276 samples after exposure to either aerated or ozonated artificial seawater. The error bars shown in the figure are a combination of the standard deviation from taking an average of the weight change of three samples, as well as the maximum uncertainty associated with the balanced used (± 0.001 g). The samples exposed to ozonated seawater showed a steady increase in the percent of weight lost over time, while aerated samples showed a slight initial weight gain which became constant with time. Corrosion of the weight loss samples was enhanced in ozonated solutions where the samples were in contact with the glass rod and Teflon spacers, indicating that the slight crevice set up by these conditions was enough to produce crevice corrosion.

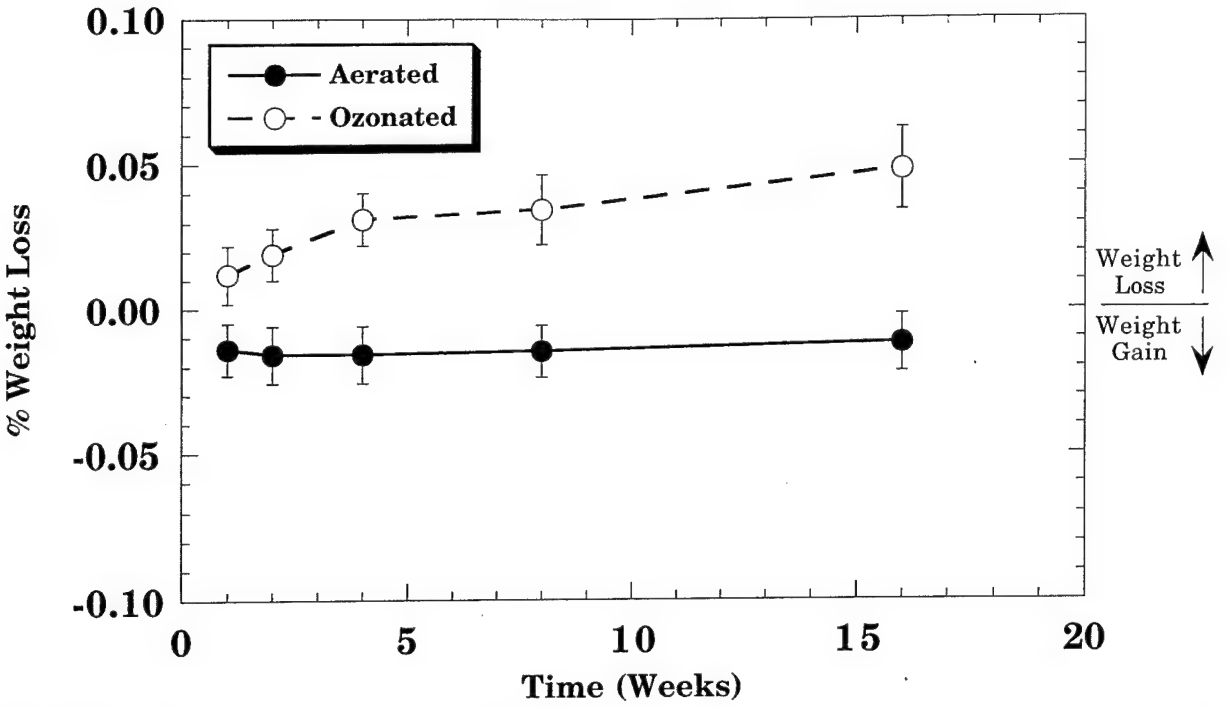

Figure 16. Percent weight loss of C276 in aerated and ozonated artificial seawater. Note that the corrosion product was not removed because the samples were re-immersed at each time period.

Crevice Samples Figures 17-18 show the change in aerated and ozonated small C276 crevice samples, 2.5x5.1 cm (1.0x2.0 in), at 4 weeks and 16 weeks. At 4 weeks (Fig. 17), there are a few small pits evident in the creviced region of the aerated sample, but the surface of the sample is otherwise similar in appearance to when the sample was initially immersed. The ozonated sample, on the other hand, is significantly different. The bulk surface is covered by what appears to be a thin oxide which refracts a yellow/orange coloration. The oxide is thin as indicated by the original polishing scratches that can be seen on the discolored surface. Surrounding the creviced region is a dark brown ring which appears to extend only a few millimeters under and beyond the creviced region. A bright metal region is apparent in the top half of Figure 17b between the ring of brown coloration and the crevice. These metallic appearing regions are areas where corrosion has occurred, leaving the base metal exposed. The slot regions vary from a rainbow effect of oxidized corrosion product to a light brown corrosion product. The plateaus, which were in contact with the crenelated washer to form crevices, are uncorroded with no real change in coloration or evidence of pitting. Original polishing scratches can still be seen on the surface of the plateaus. After 16 weeks (Fig. 18), there is little change in the aerated sample, however, the ozonated sample shows a much larger ring of dark brown

corrosion product, which appears to "drain" out of the crevice region. The bright metal regions, where relatively significant corrosion has occurred, are much larger, extending down into the slot regions, as well as further outside the crevice.

Figures 19-21 show the change in the large cathode area crevice samples, 3.8x7.6 cm (1.5x3.0 in), from 2 weeks to 16 weeks. At 2 weeks of exposure (Fig. 19), the aerated sample is similar to the small aerated crevice sample, with only a few small pits in the creviced region. The ozonated sample is covered with a light yellow oxide which turns to a light blue color around the creviced region. A light brown corrosion product forms a border between the bulk metal and the creviced region at the top of the creviced region pictured. The slots vary from light brown with dots of darker corrosion product to a light oxide coloration, while the plateaus of the crevice appear to be clean, uncorroded metal. At 4 weeks (Fig. 20), the only difference from the smaller C276 crevice samples of an equivalent time period is that for the ozonated sample there appears to be a buildup of dark brown corrosion product in 3 of the slots located at the top of the crevice pictured, with a brown "drain" stain. At 16 weeks (Fig. 21) there is little change in the aerated sample, while the ozonated sample resembles the small cathodic area crevice sample of the same time period. Areas of corrosion which have exposed the base metal extend from the slot regions into the brown stained regions, as well as to a spot completely outside the crevice area (lower right corner in Fig. 21b).

Using SEM and EDS, the dark brown stained regions (Fig. 22) were found to be semi-adherent solid corrosion product films showing high iron, oxygen, and silicon concentrations. The origin of this phenomenon is not understood at this time. In contrast to the solid corrosion product, original polishing scratches can be seen on the discolored surface of the bulk region.

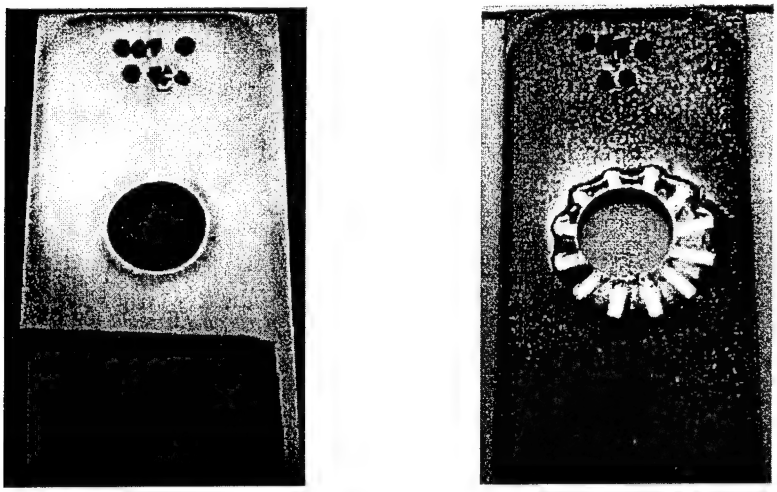

(a) (b)

Figure 17. Small C276 crevice samples, 2.5x5.1 cm (1.0x2.0 in), exposed for 4 weeks: (a) aerated artificial seawater (b) ozonated artificial seawater.

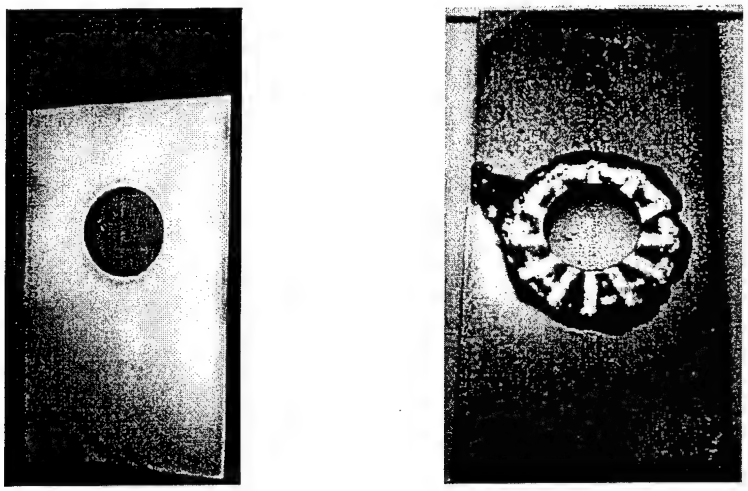

(a) (b)

Figure 18. Small C276 crevice samples, 2.5x5.1 cm (1.0x2.0 in), exposed for 16 weeks: (a) aerated artificial seawater (b) ozonated artificial seawater.

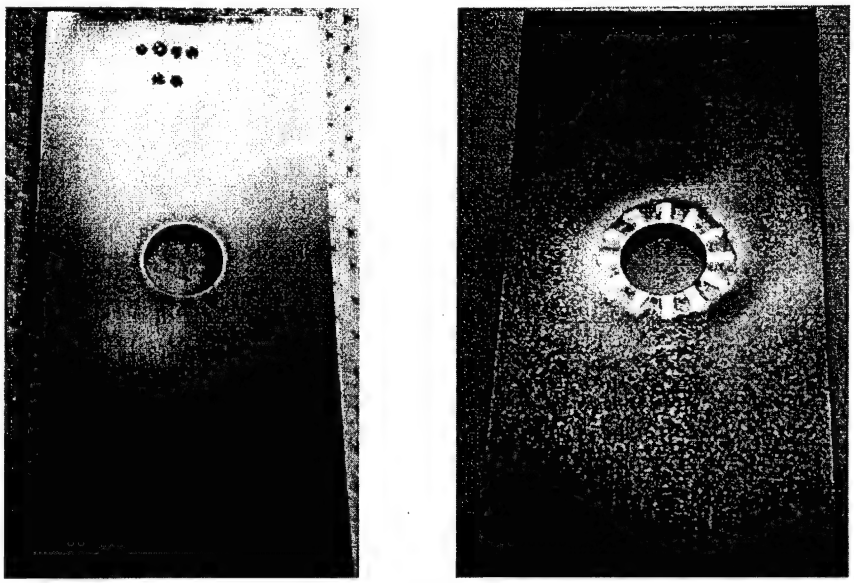

(a) (b)

Figure 19. Large C276 crevice samples, 3.8x7.6 cm (1.5x3.0 in), exposed for 2 weeks: (a) aerated artificial seawater (b) ozonated artificial seawater.

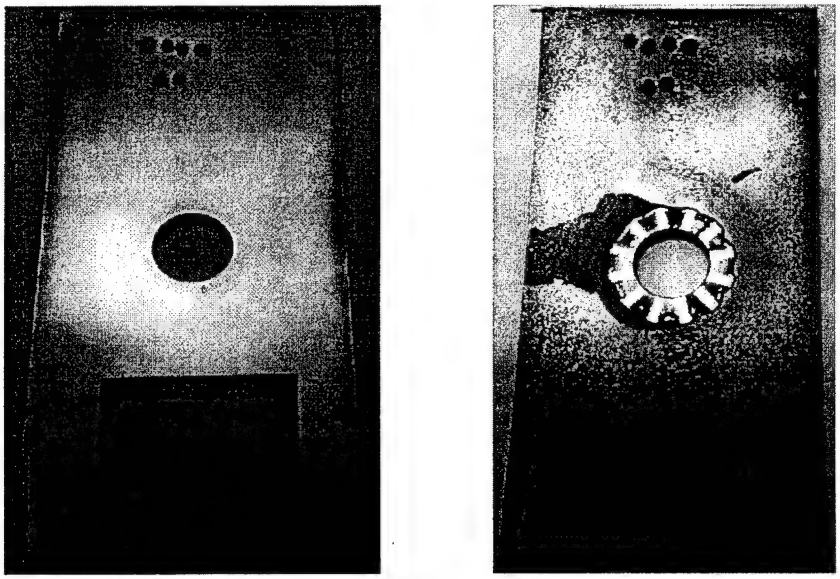

(a) (b)

Figure 20. Large C276 crevice samples, 3.8x7.6 cm (1.5x3.0 in), exposed for 4 weeks: (a) aerated artificial seawater (b) ozonated artificial seawater.

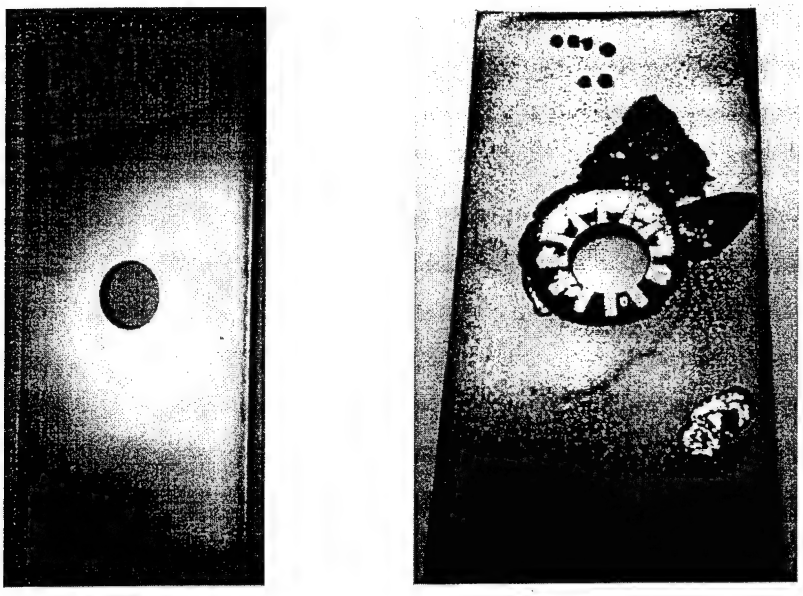

(a) (b)

Figure 21. Large C276 crevice samples, 3.8x7.6 cm (1.5x3.0 in), exposed for 16 weeks: (a) aerated artificial seawater (b) ozonated artificial seawater.

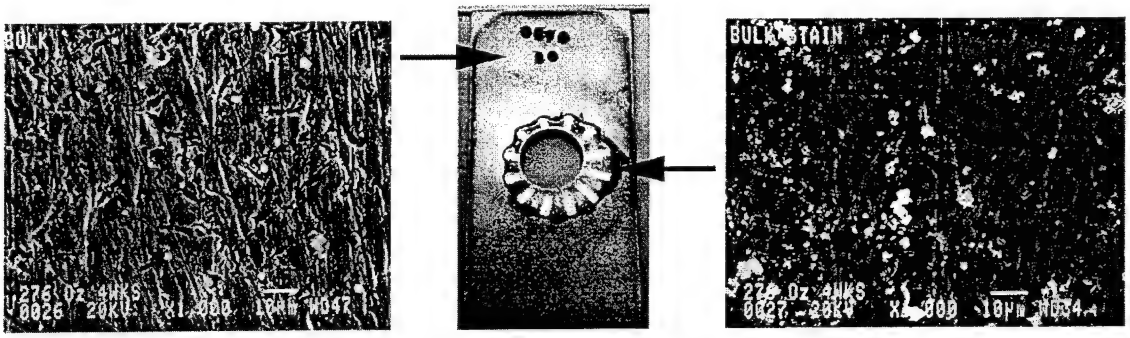

Figure 22. Small C276 crevice sample, 2.54x5.1 cm (1.0x2.0 in), after 4 weeks of exposure to ozonated artificial seawater. SEM photograph on the left depicts the bulk, uncreviced surface of the sample at 1000x, while SEM photo on the right shows the cracked surface of the corrosion product outside of the crevice washer at 1000x.

Wire Samples Electrochemical testing of C276 wires in the tanks showed that the corrosion potential of wires exposed to ozonated artificial seawater is shifted from 0.4 to 0.8 V noble to the corrosion potential of C276 wires in aerated seawater (Figure 23).

Figure 24 shows that the corrosion rates calculated from LPR measurements on C276 wires are higher in ozonated *vs.* aerated seawater. The corrosion rate of C276 in ozonated solutions decreased from an initial value of 7μm/y to 1.5 μm/y (0.28 to 0.06 mpy) after 16 weeks of exposure. Corrosion rates in aerated solutions are

negligible (<0.5 μm/y [0.02 mpy]) over the entire time period.

Figures 25 and 26 show the polarization curves of C276 wires in aerated and ozonated seawater at 4 and 8 week time intervals. The zero current potential of the aerated C276 wire shifts from -0.35 to -0.30 V_{SCE} as time is increased from 4 weeks to 8 weeks. At both time periods, the aerated wires exhibited primary and secondary passivity. The potential at which the aerated curve shifts to transpassive behavior is 0.28 V_{SCE} at 4 weeks and 0.25 V_{SCE} at 8 weeks. Very little hysteresis was observed in the aerated wire curves of either time period.

At 4 weeks, the zero current potential of the ozonated C276 wire sample is $0.28V_{SCE}$, 0.6V noble to the aerated sample zero current potential. This potential correlates to the transition observed in aerated solutions, indicating the ozonated wires are in the transpassive region under steady state corrosion conditions. At 4 weeks, the ozonated curve exhibits a slight region of secondary passivity, with hysteresis occurring upon reversal of the potential. Examination of the wires after polarization showed that significant amounts of pitting had occurred on the polarized portions of both wires below the waterline. This is of interest since no hysteresis was seen in the aerated polarization curve.

At 8 weeks, the zero current potential of the ozonated C276 wire remains 0.6V noble to the zero current potential of the aerated wire, and is slightly noble to the aerated breakdown potential for primary passivity. The 8 week ozonated wire polarization curve shows a distinct region of secondary passivity, which was not as evident at 4 weeks. The passive current density in this region is approximately $5x10^{-5}$ A/cm^2, more than an order of magnitude lower than the secondary passive current density for the 8 week aerated wire. The 8 week ozonated curve also shows a very distinct hysteresis loop upon reversal, indicating an increase in pitting and crevice corrosion compared to exposure at 4 weeks. Examination of the wires showed, once again, significant pitting had occurred for both cases below the waterline. However, corrosion was enhanced at the polarization waterline in the case of the ozonated sample. The appearance of this waterline corrosion was similar to the crevice corrosion seen on ozonated C276 crevice samples, with the formation of a dark brown corrosion product which spalled away to reveal shiny metallic base metal.

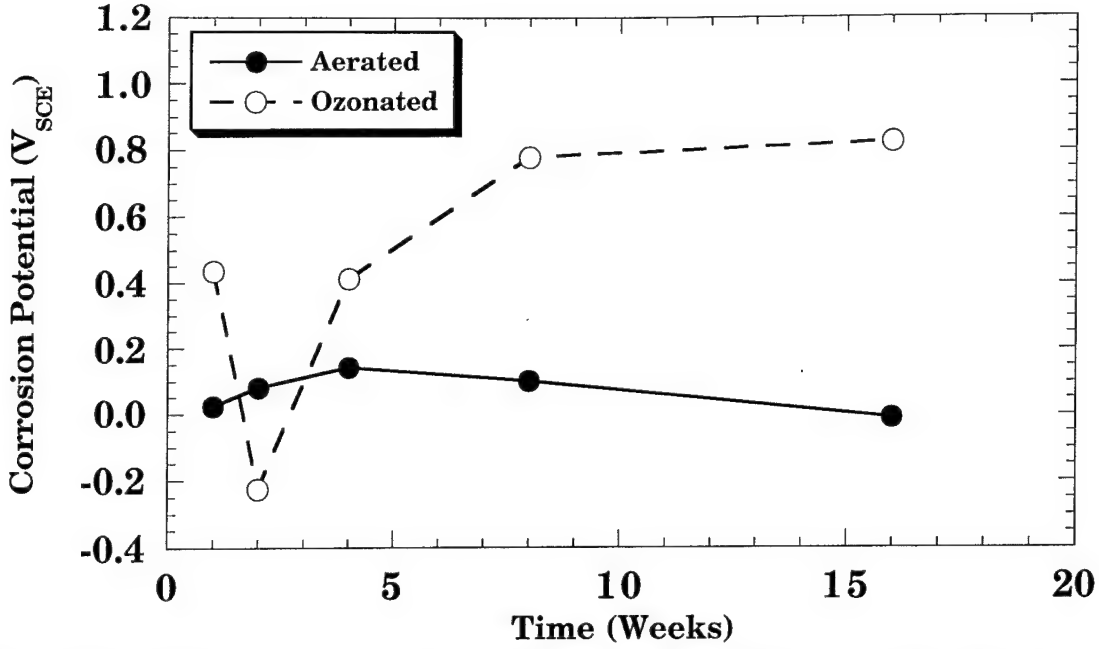

Figure 23. The steady state corrosion potential of C276 wire exposed to aerated or ozonated artificial seawater.

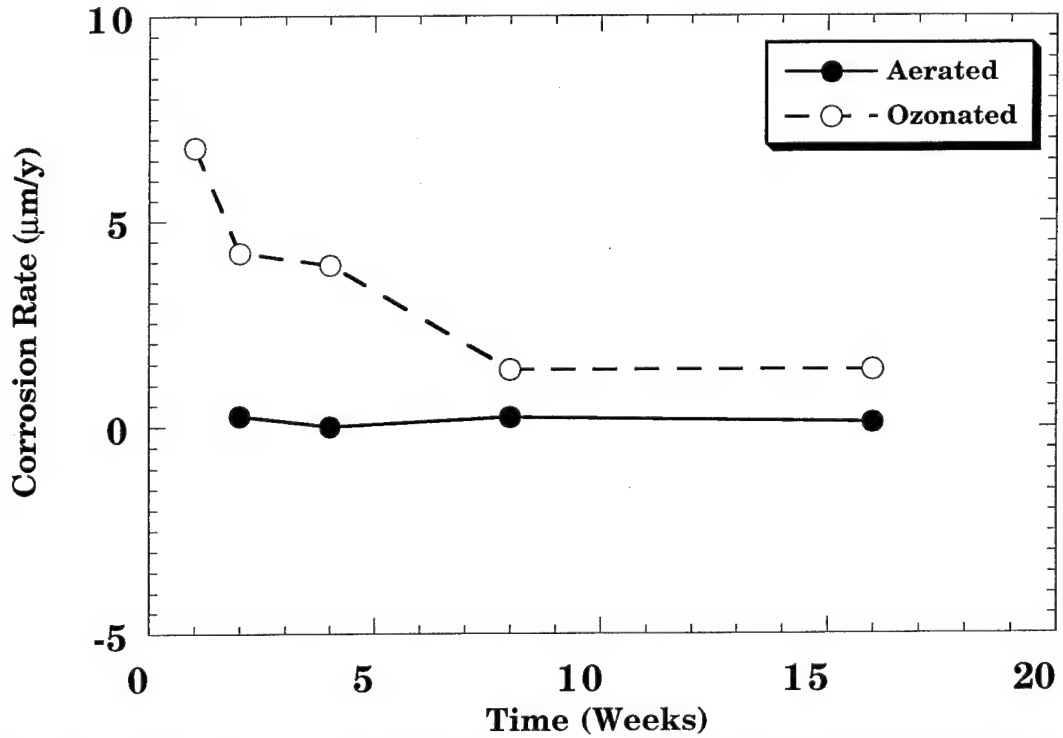

Figure 24. A comparison of the corrosion rates of C276 calculated from LPR measurements in aerated and ozonated artificial seawater.

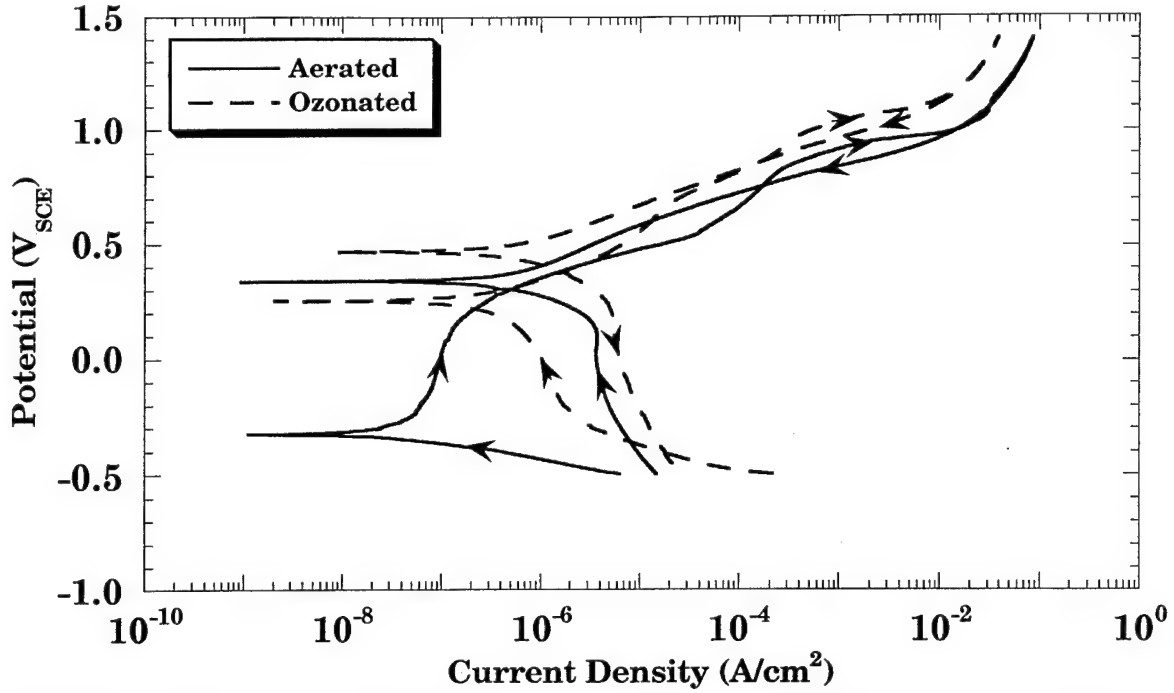

Figure 25. A comparison of the polarization curves of C276 wires exposed to aerated or ozonated artificial seawater for 4 weeks.

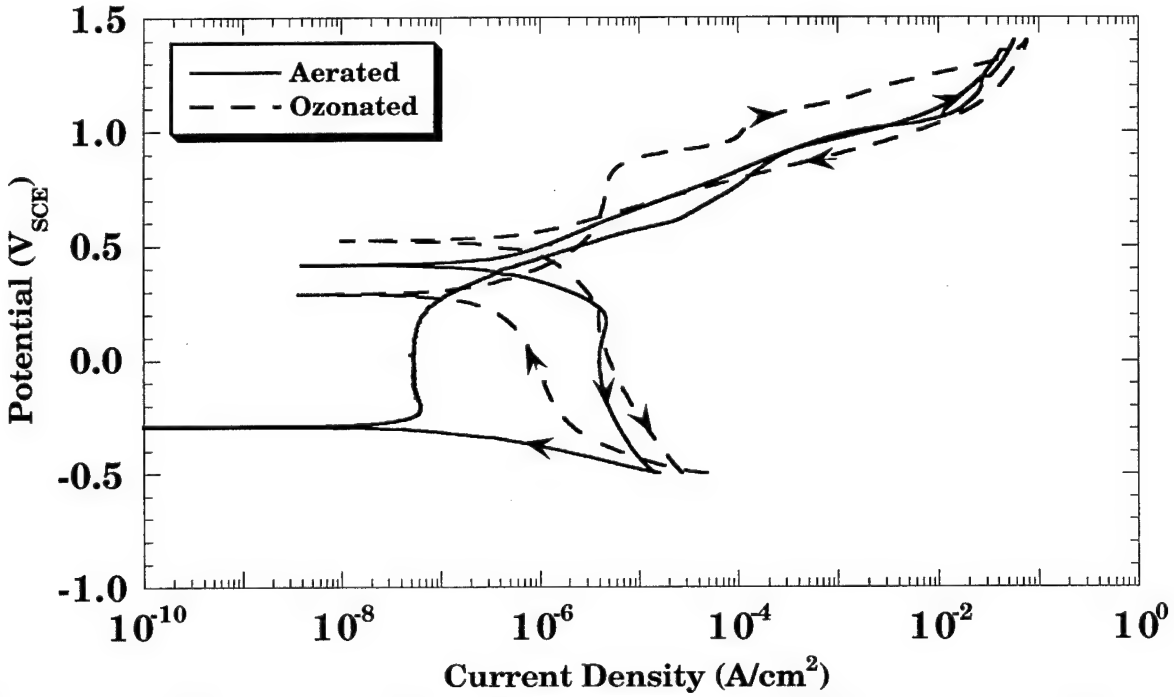

Figure 26. A comparison of the polarization curves of C276 wires exposed to aerated or ozonated artificial seawater for 8 weeks.

C22

Weight Loss Samples Figure 27 shows the percent weight loss (%WTL) in C22 samples after exposure to either aerated or ozonated artificial seawater. The samples exposed to ozonated seawater showed a steady increase in the percent of weight lost over time, while aerated samples showed no change in weight until 16 weeks, where a slight weight loss was measured. Corrosion on the weight loss samples in ozonated solutions was enhanced where the samples were in contact with the glass rod and Teflon spacers, indicating that the slight crevice set up by these conditions was enough to produce crevice corrosion.

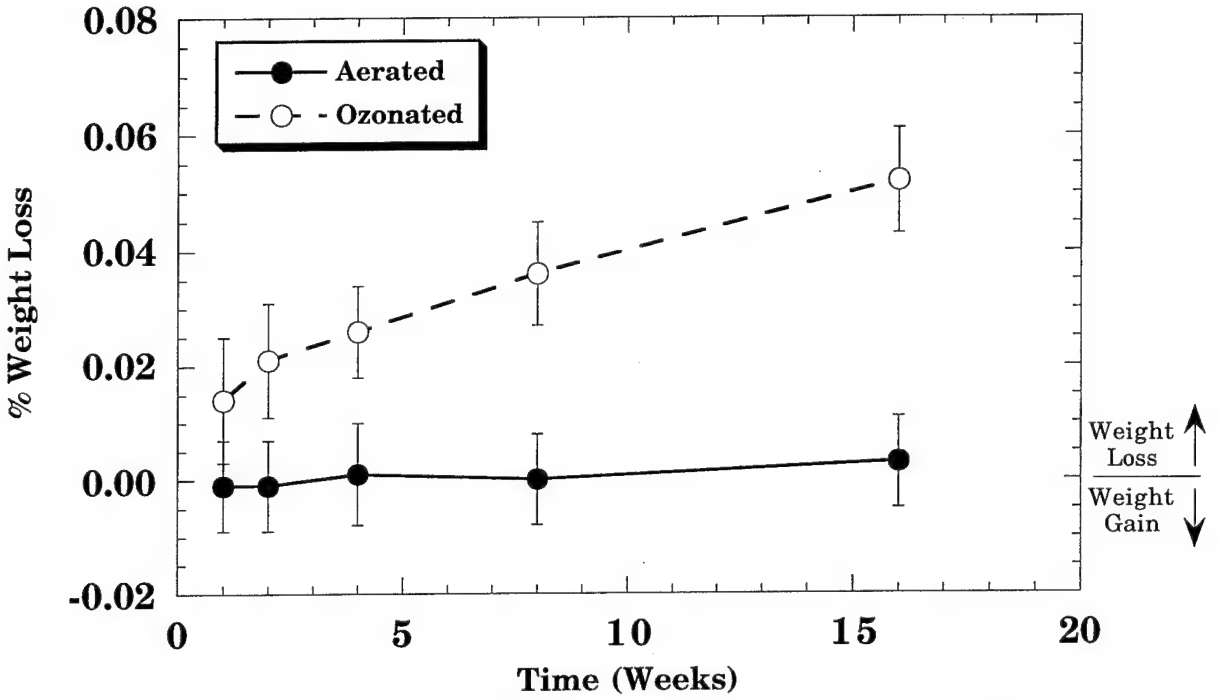

Figure 27. Percent weight loss of C22 in aerated and ozonated artificial seawater. Note that the corrosion product was not removed because the samples were re-immersed at each time period.

Crevice Samples Figure 28 shows the difference in damage between small aerated and ozonated crevice samples, 2.5x5.1 cm (1.0x2.0 in), at 4 weeks. A few very small pits are scattered under the crevice region of the aerated sample, barely visible by eye, but the surface is otherwise unattacked. The bulk surface of the ozonated sample is covered by a thin oxide which refracts a blue/green coloration (Fig. 28b). Surrounding the crevice region is a different color oxide of yellow/orange coloration. The slot regions vary from a light blue to brown coloration, with 2 slots filled with dark brown corrosion product. The plateaus, which were in contact with

the crenelated washer to form tight crevices, are uncorroded with no change in coloration or evidence of pitting.

Figures 29-30 show that there is little change in the large cathode area, 3.8x7.6 cm (1.5x3.0 in), crevice samples from 2 weeks to 4 weeks. The only real difference is the change in coloration of the bulk oxide. At 2 weeks the coloration is a dark maroon, with a dark blue swirl around the crevice region, while at 4 weeks the bulk coloration is a gold/brown, with a blue/brown swirl around the crevice region. The slots on both of the samples show the formation of dark brown corrosion product in the form of spots edging the uncorroded plateau regions.

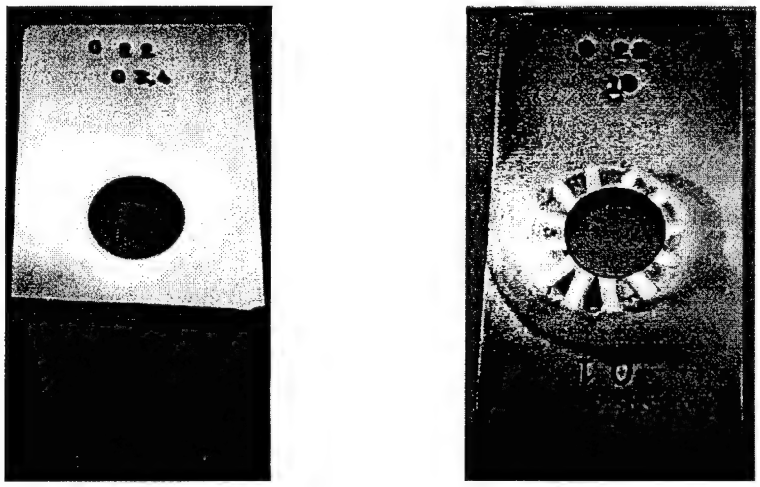

(a) (b)

Figure 28. Small C22 crevice samples, 2.5x5.1 cm (1.0x2.0 in), exposed for 4 weeks: (a) aerated artificial seawater (b) ozonated artificial seawater.

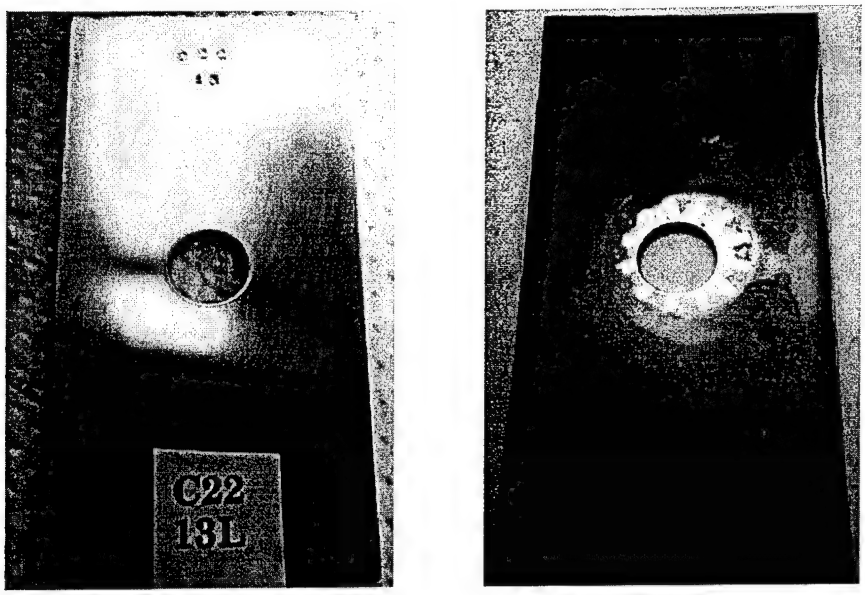

(a) (b)

Figure 29. Large C22 crevice samples, 3.8x7.6 cm (1.5x3.0 in), exposed for 2 weeks: (a) aerated artificial seawater (b) ozonated artificial seawater.

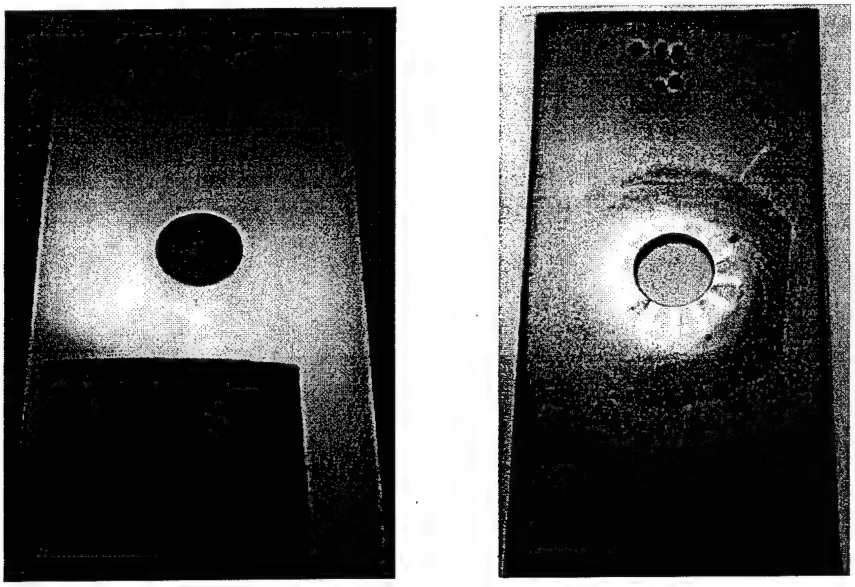

(a) (b)

Figure 30. Large C22 crevice samples, 3.8x7.6 cm (1.5x3.0 in), exposed for 4 weeks: (a) aerated artificial seawater (b) ozonated artificial seawater.

Wire Samples Electrochemical testing of C22 wires in the tanks showed that the corrosion potential of the nickel alloys exposed to ozonated artificial seawater is shifted from 0.4 to 0.8 V noble to the corrosion potential of aerated seawater, depending on the time of exposure (Fig. 31).

Corrosion rates calculated from LPR measurements on C22 wires are shown

in Figure 32. Rates were found to be higher in ozonated *vs.* aerated seawater. Wires exposed to ozone exhibit a peak corrosion rate of 6.5 μm/y (0.26 mpy) after 4 weeks of exposure, which dropped with continued exposure time to a value of 2.0 μm/y (0.08 mpy) after 16 weeks. Corrosion rates of C22 samples in aerated solutions are shown to be negligible (<0.5 μm/y [0.02 mpy]) over the entire time period.

Figure 33 shows the polarization curves of C22 wires in aerated and ozonated seawater after 4 weeks of exposure. The aerated wire exhibited both primary and secondary passivity, with the primary breakdown occurring at a potential of 0.29 V_{SCE}. The zero current potential of the ozonated sample is 0.40 V_{SCE}, 0.75 V noble to the aerated sample zero current potential. This potential is also noble to the transition observed in aerated solutions, indicating that the ozonated wires are in the transpassive region under steady state conditions. The polarization curve of the ozonated wire sample also exhibits a hysteresis loop upon reversal, which is not observed for the aerated case. The passive current density (measured 0.3 V noble to the zero current potential) of the aerated sample was found to be almost 100 times less than the ozonated sample. After polarization, neither of the wires showed evidence of pitting below the waterline. However, the ozonated wire did show evidence of corrosion similar to that seen on the crevice samples and wires of C276. Regions of the C22 ozonated wire were discolored more darkly than other regions. Within these regions of discoloration were bright metallic areas in which the oxide had spalled off to expose the base metal beneath.

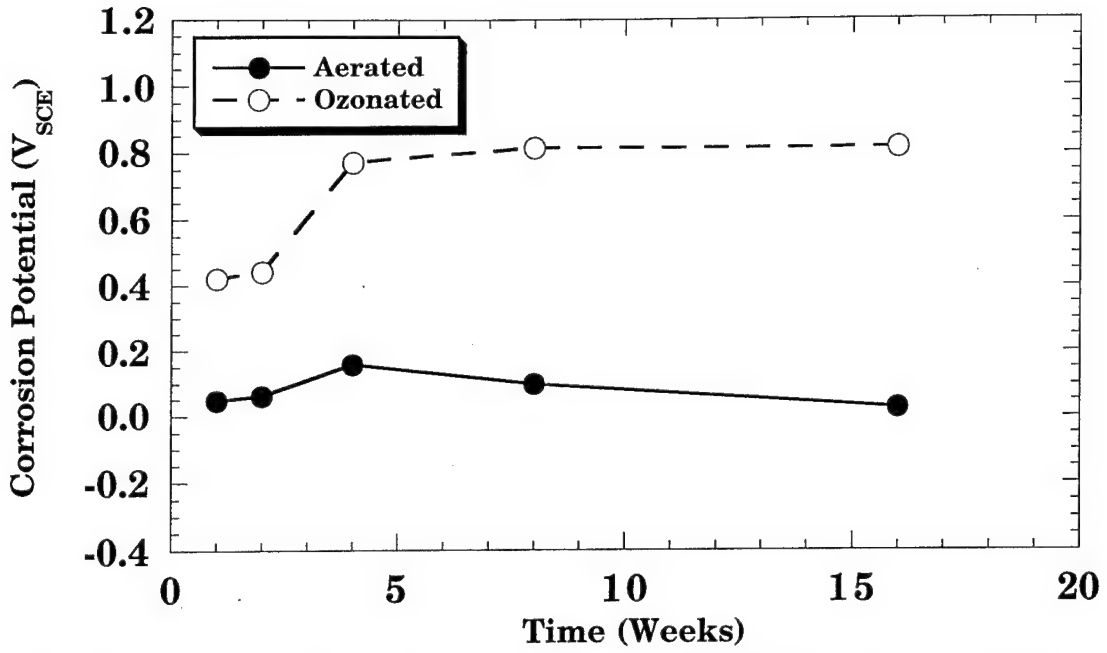

Figure 31. The steady state corrosion potential of C22 wire exposed to aerated or ozonated artificial seawater.

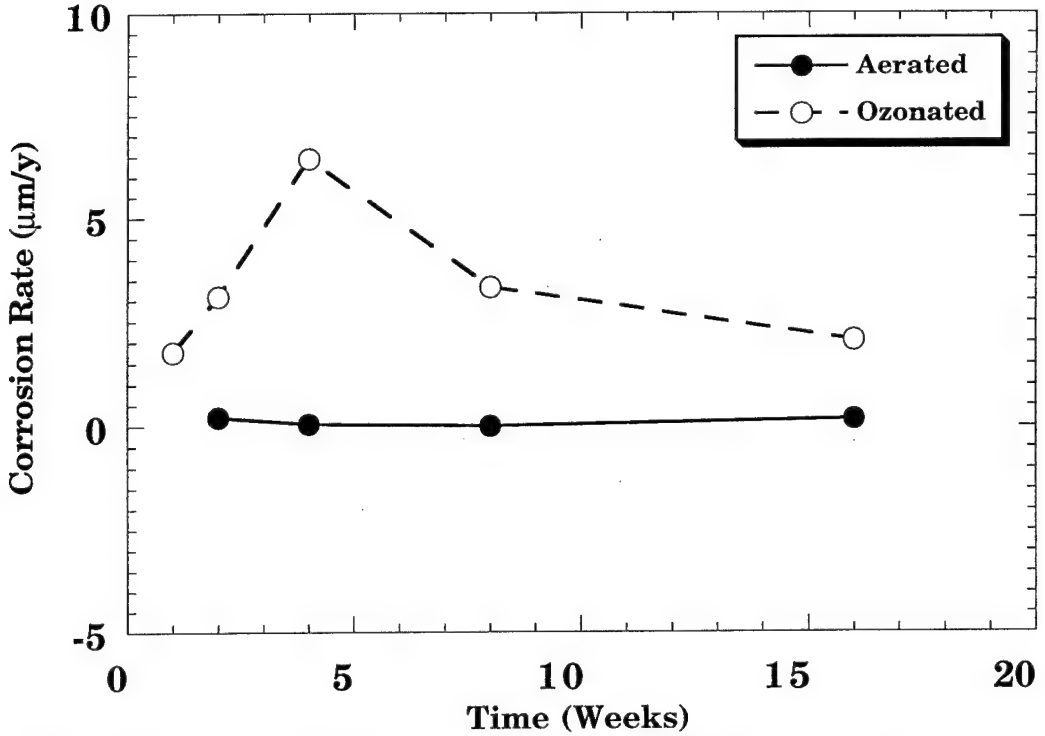

Figure 32. A comparison of the corrosion rates of C22 wire samples calculated from LPR measurements in aerated and ozonated artificial seawater.

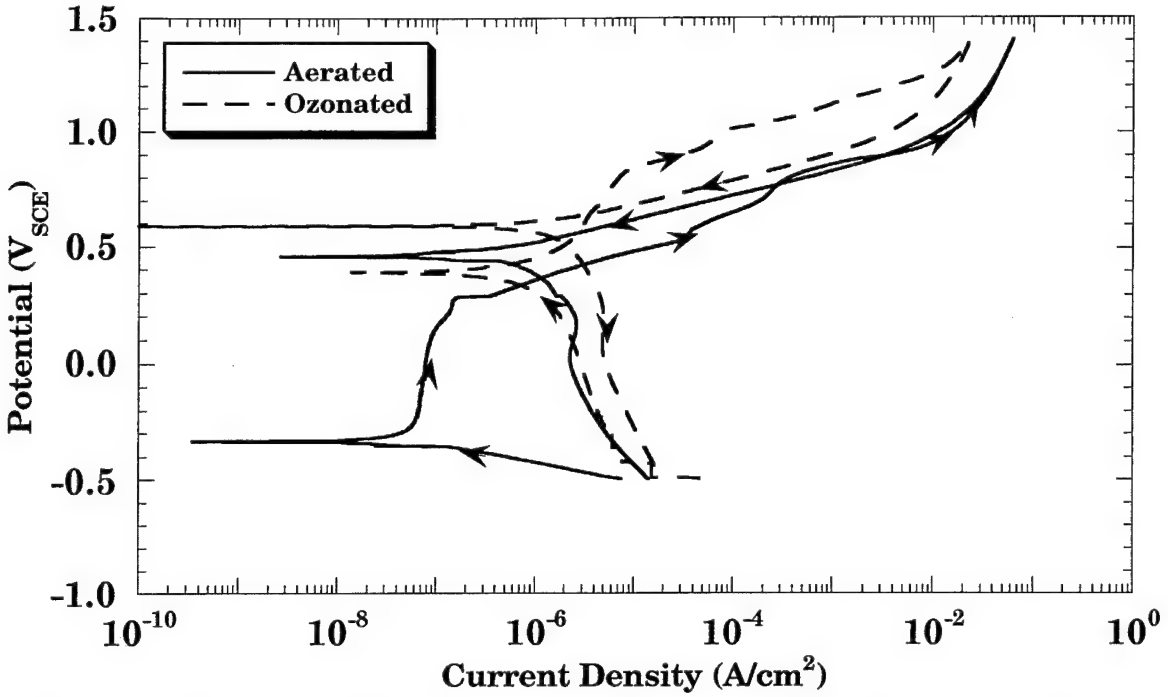

Figure 33. A comparison of the polarization curves of C22 wires exposed the aerated or ozonated artificial seawater for 4 weeks.

IN625

Weight Loss Samples Figure 34 shows the percent weight loss (%WTL) in IN625 samples after exposure to either aerated or ozonated artificial seawater. The samples exposed to ozonated seawater showed a steady rate of increase in the percent of weight lost over time up to 4 weeks of exposure, and then a slightly slower rate of increasing weight loss from 4 to 16 weeks. Aerated samples showed a weight gain which was constant with time. Corrosion on the weight loss samples in ozonated solutions was enhanced where the samples were in contact with the glass rod and Teflon spacers, indicating that the slight crevice set up by these conditions was enough to produce crevice corrosion.

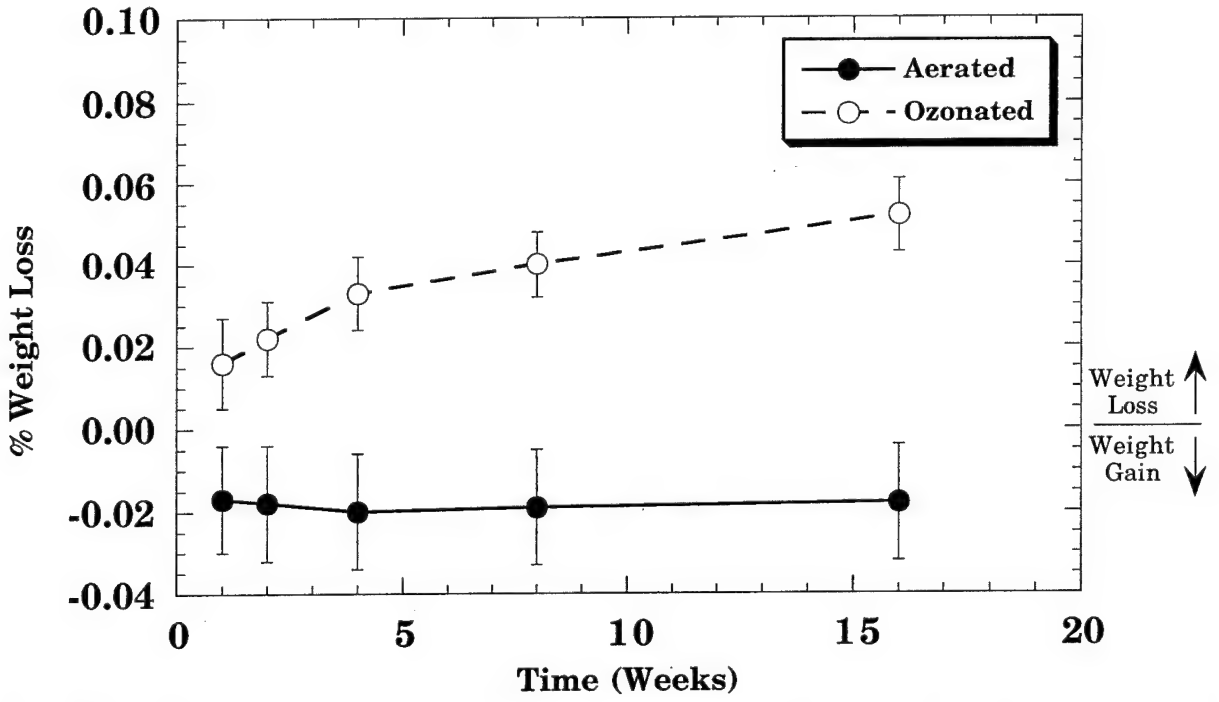

Figure 34. Percent weight loss of IN625 in aerated and ozonated artificial seawater. Note that the corrosion product was not removed because the samples were re-immersed at each time period.

Crevice Samples Figure 35-36 shows the difference in damage between small aerated and ozonated crevice samples, 2.5x5.1 cm (1.0x2.0 in), at 4 and 8 weeks. Under the crevice region of the aerated samples for both time periods there are only a few very small scattered pits, with the surface otherwise unattacked. The bulk surface of the 4 week ozonated sample is covered by a thin oxide which refracts a yellow/orange coloration (Fig. 35b). The slot regions vary from a light blue to brown in coloration. The plateaus, which were in contact with the crenelated washer to form

tight crevices, are uncorroded with no change in coloration or pitting evident, although there does appear to be slight "seepage" of corrosion product at the plateau edges. At 8 weeks, the bulk region of the ozonated sample is a dark maroon, with almost a rainbow appearance in some areas (Fig. 36b). Several of the slots on the 8 week sample also contain dark brown corrosion product. The plateaus of the 8 week ozonated samples are similarly uncorroded as with the 4 week ozonated sample.

Figures 37-38 show the change in the large cathode area, 3.8x7.6 cm (1.5x3.0 in), crevice samples at 2 weeks and 4 weeks. The only real difference is the change in coloration of the bulk and slot regions. At 2 weeks the coloration is blue, with a brown swirl around the crevice region, while at 4 weeks the bulk coloration is a gold/brown, with a reddish brown swirl around the crevice region. The slots on both of the samples show the formation of dark brown corrosion product in the form of spots edging the uncorroded plateau regions.

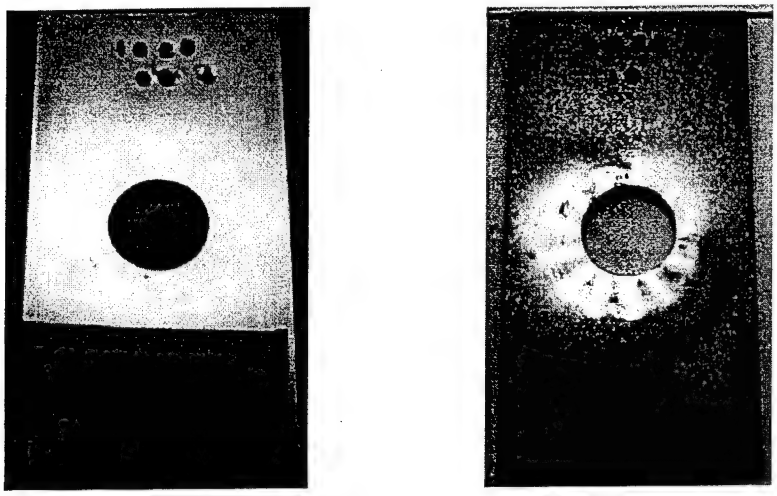

(a) (b)

Figure 35. Small IN625 crevice samples, 2.5x5.1 cm (1.0x2.0 in), exposed for 4 weeks: (a) aerated artificial seawater (b) ozonated artificial seawater.

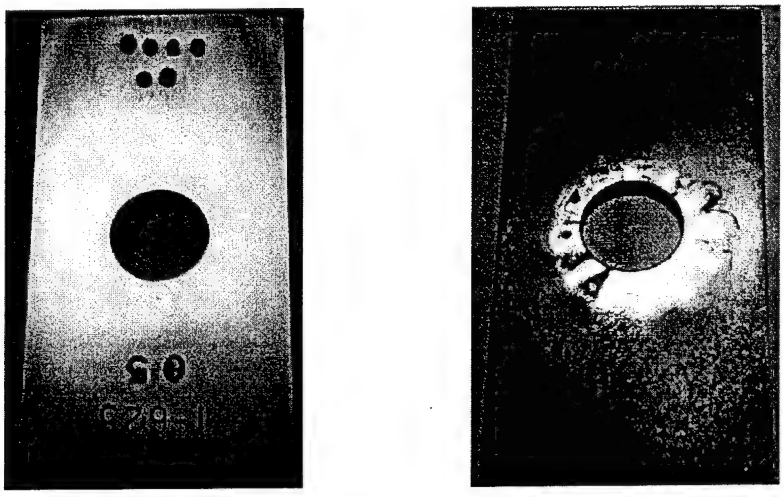

(a) (b)

Figure 36. Small IN625 crevice samples, 2.5x5.1 cm (1.0x2.0 in), exposed for 8 weeks: (a) aerated artificial seawater (b) ozonated artificial seawater.

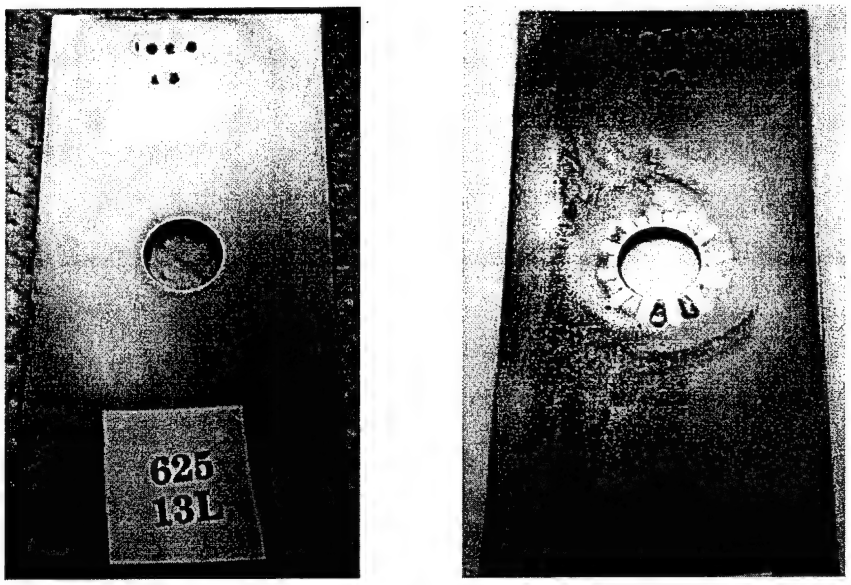

(a) (b)

Figure 37. Large IN625 crevice samples, 3.8x7.6 cm (1.5x3.0 in), exposed for 2 weeks: (a) aerated artificial seawater (b) ozonated artificial seawater.

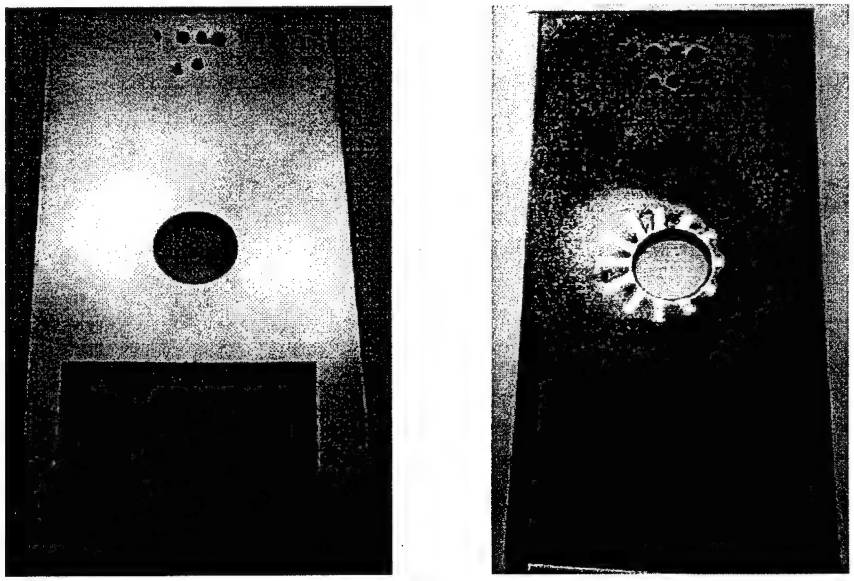

(a) (b)

Figure 38. Large IN625 crevice samples, 3.8x7.6 cm (1.5x3.0 in), exposed for 4 weeks: (a) aerated artificial seawater (b) ozonated artificial seawater.

Wire Samples Electrochemical testing of IN625 wires in the tanks showed that the corrosion potential of the nickel alloys exposed to ozonated artificial seawater is shifted from 0.2 to 0.4 V noble to the corrosion potential of aerated seawater, depending on the time of exposure (Figure 39).

Corrosion rates calculated from LPR measurements on IN625 wires are

shown in Figure 40. Corrosion rates were found to be higher in ozonated *vs.* aerated seawater. Wires exposed to ozone had a high initial corrosion rate of 34 μm/y (1.4 mpy) after one week of exposure, dropping thereafter to a constant value of 10 μm/y (0.4 mpy). Corrosion rates of IN625 wires in aerated solutions showed an initial rate of 3 μm/y (0.1 mpy), which dropped to less than 0.5 μm/y (0.02 mpy) after a week of immersion.

Polarization curves of IN625 wires show little difference between aeration and ozonation (Figure 41). In marked contrast to the noble shifts in potential of the other nickel curves, the ozonated zero current potential of IN625 wire is 0.2 V active to the aerate counterpart. Unlike the two other nickel alloy wires, there is also no evidence of a hysteresis loop. Examination of the wires after polarization confirmed that there was no evidence of pitting corrosion, or the type corrosion observed on the C276 or C22 wires.

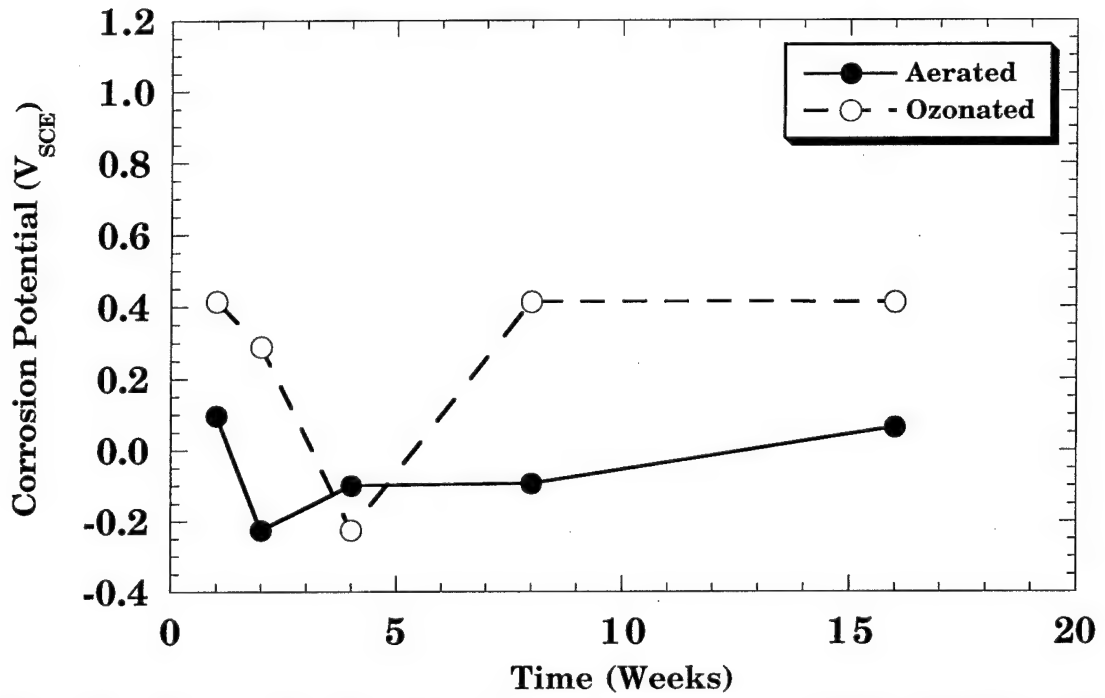

Figure 39. The steady state corrosion potential of IN625 wire exposed to aerated or ozonated artificial seawater.

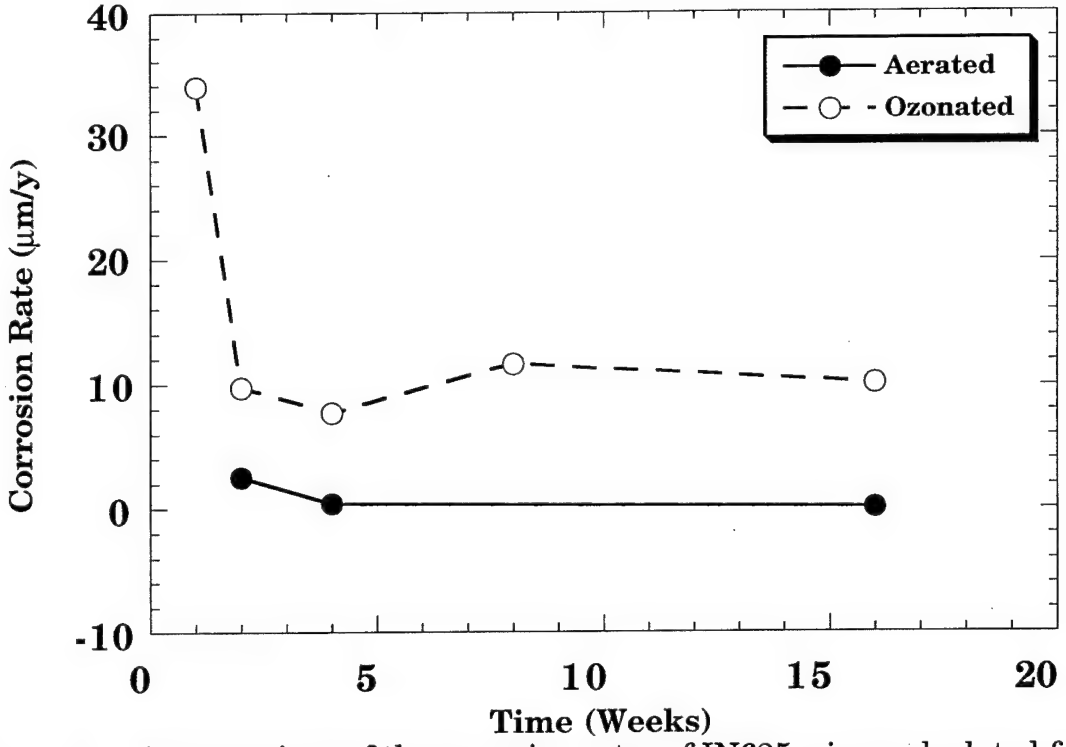

Figure 40. A comparison of the corrosion rates of IN625 wires calculated from LPR measurements in aerated and ozonated artificial seawater.

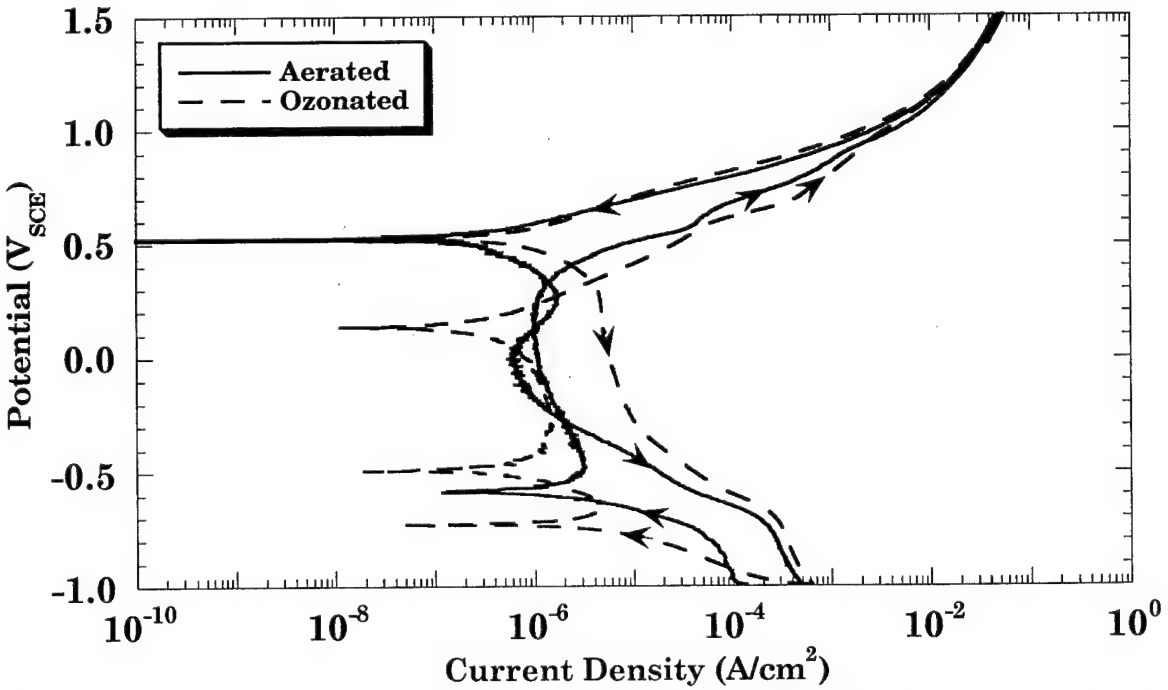

Figure 41. A comparison of the polarization curves of IN625 wires exposed to aerated or ozonated artificial seawater for 4 weeks.

VDM59

Weight Loss Samples Figure 42 shows the percent weight loss (%WTL) of VDM59 samples after exposure to either aerated or ozonated artificial seawater. The samples exposed to ozonated seawater showed a slight steady rate of increase in the percent of weight lost over time up to 4 weeks of exposure, and then a higher rate of weight change from 4 to 16 weeks. Aerated samples showed no real change in weight over time. Corrosion on the weight loss samples in ozonated solutions was enhanced where the samples were in contact with the glass rod and Teflon spacers, indicating that the slight crevice set up by these conditions was enough to produce crevice corrosion.

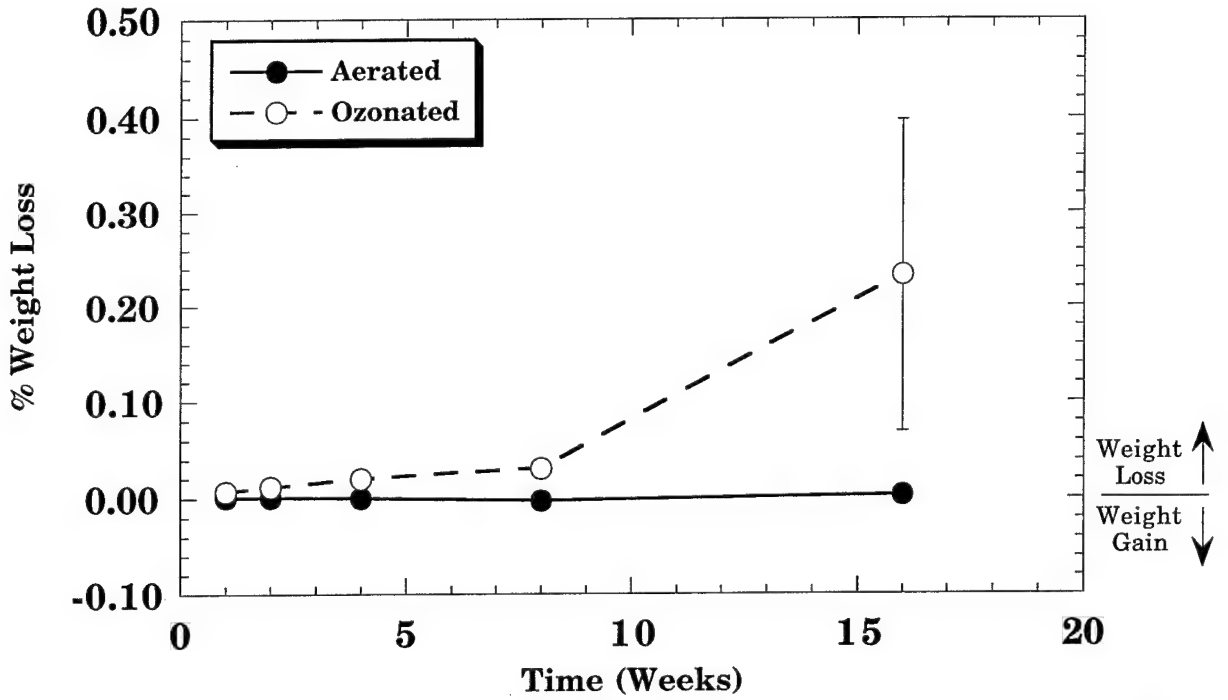

Figure 42. Percent weight loss of VDM59 in aerated and ozonated artificial seawater. Note that the corrosion product was not removed because the samples were re-immersed at each time period.

Crevice Samples Figure 43 shows the difference in damage between small aerated and ozonated samples, 2.5x5.1 cm (1.0x2.0 in), after 4 weeks of exposure. A few very small pits are scattered under the crevice region of the aerated sample, barely visible to the naked eye, but the surface is otherwise unattacked. The bulk surface of the ozonated sample is covered by a thin oxide which refracts a bronze coloration (Fig. 43b). Surrounding the creviced region is a swirl of blue/brown colored oxide. The slot regions vary from light blue to brown colorations, with many of the

slots containing small amounts of dark brown corrosion product which outlines the crevice plateaus. The plateaus, which were in direct contact with the crenelated washer to form tight crevices, are uncorroded, with no change in coloration or pitting evident.

Figures 44-46 show the change in the large cathode area, 3.8x7.6 cm (1.5x3.0 in), crevice samples at 2, 4, and 8 weeks. At both 2 and 4 weeks the bulk region of the ozonated samples have a light brown coloration, with the slots having a light brown to blue coloration. At 8 weeks there is a dramatic change in coloration in both the bulk and slot regions of the ozonated sample. The bulk region of the 8 week ozonated sample is dark blue, with a light brown swirl surrounding the crevice region, while the slot regions are either gold in color or dark brown with corrosion product. The plateau regions of 2, 4, and 8 week samples all appear to be uncorroded.

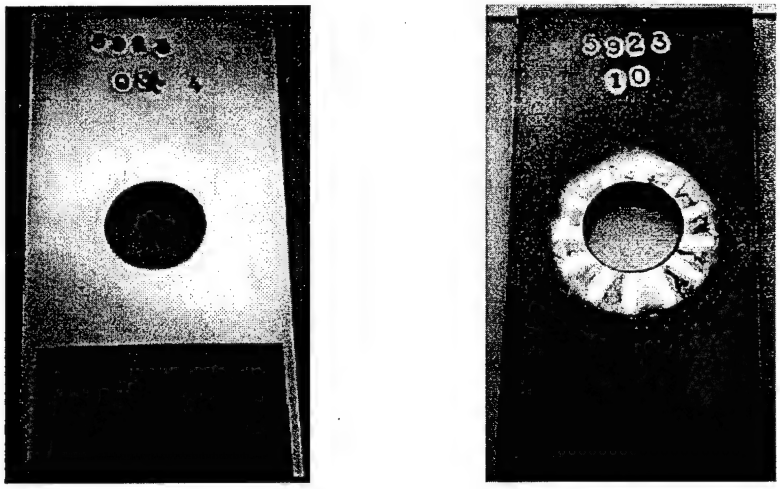

(a) (b)

Figure 43. Small VDM59 crevice samples, 2.5x5.1 cm (1.0x2.0 in), exposed for 4 weeks: (a) aerated artificial seawater (b) ozonated artificial seawater.

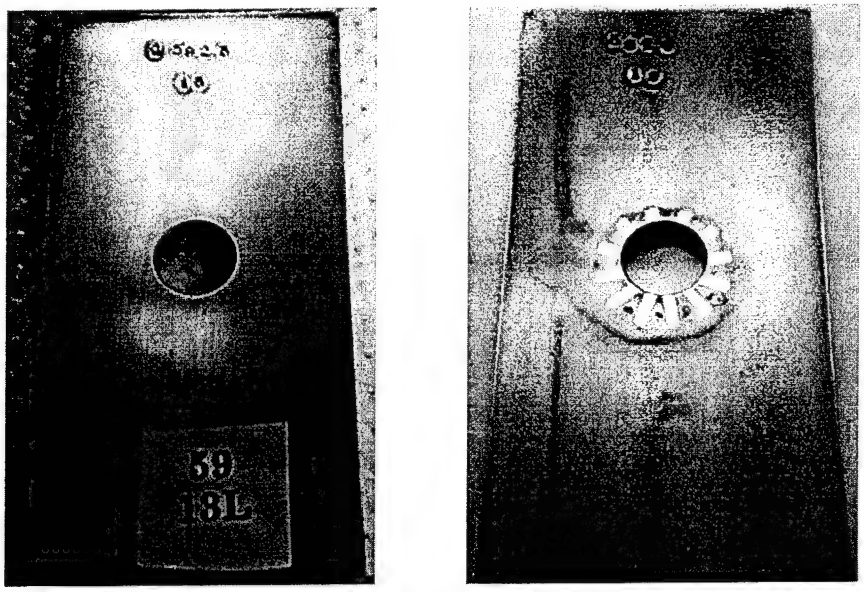

(a) (b)

Figure 44. Large VDM59 crevice samples, 3.8x7.6 cm (1.5x3.0 in), exposed for 2 weeks: (a) aerated artificial seawater (b) ozonated artificial seawater.

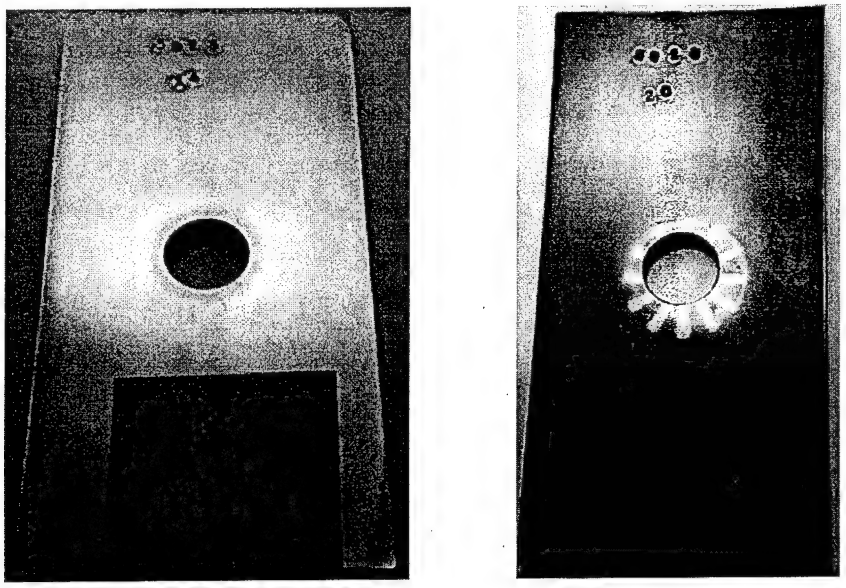

(a) (b)

Figure 45. Large VDM59 crevice samples, 3.8x7.6 cm (1.5x3.0 in), exposed for 4 weeks: (a) aerated artificial seawater (b) ozonated artificial seawater.

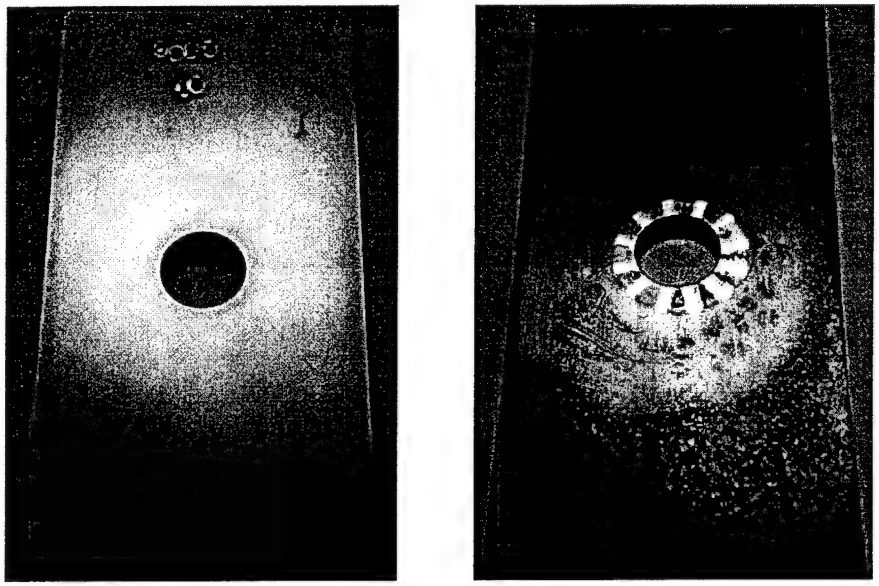

(a) (b)

Figure 46. Large VDM59 crevice samples, 3.8x7.6 cm (1.5x3.0 in), exposed for 8 weeks: (a) aerated artificial seawater (b) ozonated artificial seawater.

IN690

Weight Loss Samples Figure 47 shows the percent weight loss (%WTL) of IN690 samples after exposure to either aerated or ozonated artificial seawater. The samples exposed to ozonated seawater showed a steady rate of increase in the percent of weight lost over time up to 4 weeks of exposure, and then a slightly lower rate of weight change from 4 to 16 weeks. Aerated samples showed no real change in weight over time. Corrosion on the weight loss samples in ozonated solutions was enhanced where the samples were in contact with the glass rod and Teflon spacers, indicating that the slight crevice set up by these conditions was enough to produce crevice corrosion.

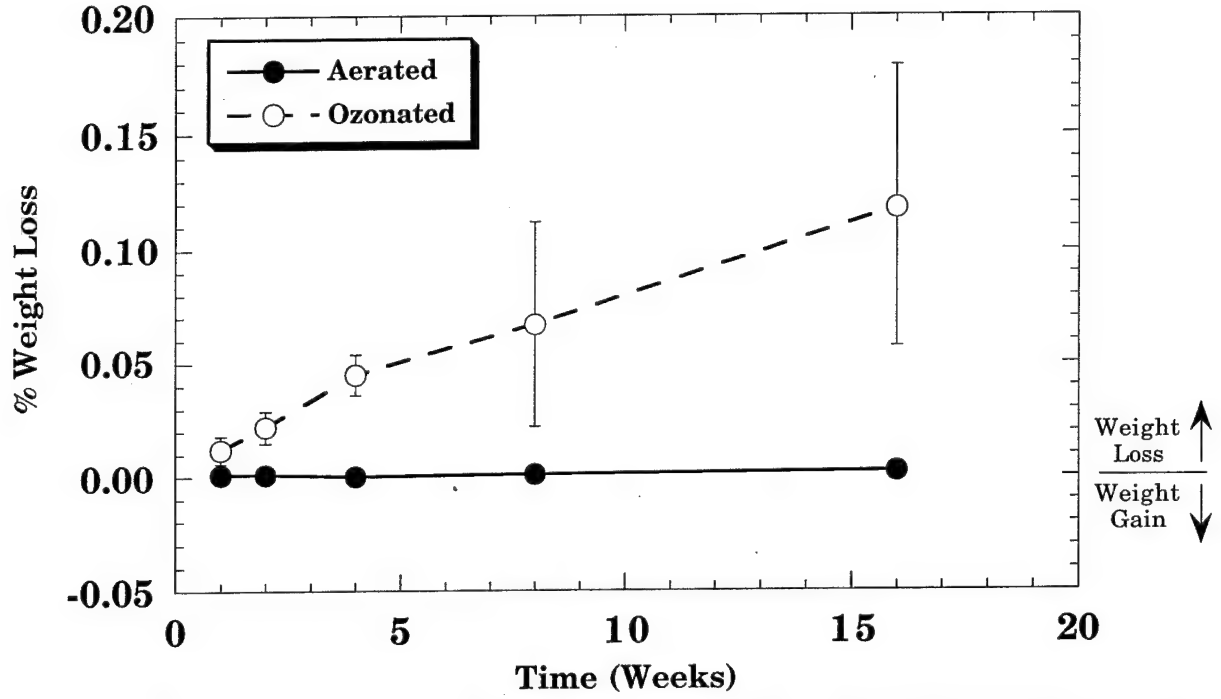

Figure 47. Percent weight loss of IN690 in aerated and ozonated artificial seawater. Note that the corrosion product was not removed because the samples were re-immersed at each time period.

Crevice Samples Figures 48 shows the difference in damage between small aerated and ozonated crevice samples, 2.5x5.1 cm (1.0x2.0 in), after 4 weeks of exposure. A few small pits are scattered under the crevice region of the aerated sample, barely visible to the naked eye, but the surface is otherwise unattacked. The ozonated sample, on the other hand, has several plateaus at which crevice corrosion has resulted in deep gouging pits. Other plateaus on the ozonated sample are not as greatly affected; showing only the initiation of a deep pit at the interface of the

plateau with the slot region. The bulk region of IN690 in ozone is unaffected, with only a slight discoloration around the crevice region. This is in contrast to the other nickel alloys which had all shown coloration due to an oxide on the surface. The slot regions of the ozone sample have an oxide that is light blue in color with brown corrosion product dispersed throughout.

Figures 49-50 show the change in the large cathode area, 3.8x7.6 cm (1.5x3.0 in), crevice samples at 2 weeks and 4 weeks. As with the small ozonated crevice sample, exposed for 4 weeks, these samples suffer from extremely severe crevice corrosion in random plateaus. At this time, there is no real correlation to the number of massively attacked plateau sites on an ozonated sample and exposure time for either the small or large crevice samples.

Using SEM and EDS, the brown corrosion product in the slot region of the 4 week ozonated small, 2.5x5.1 cm (1.0x2.0 in), crevice sample (Fig. 51) was found to be a semi-adherent film showing high iron and oxygen concentrations, possibly iron oxide. Probing into one of the massive pits on an actively corroding plateau (Fig. 52), showed pure titanium crystallites, high titanium, chrome and silicon concentrations, as well as a decreased amount of iron. Trace amounts of niobium were also found to be present, possibly as an "impurity" from the titanium which appeared to be dissolved in the crevice and redeposited.

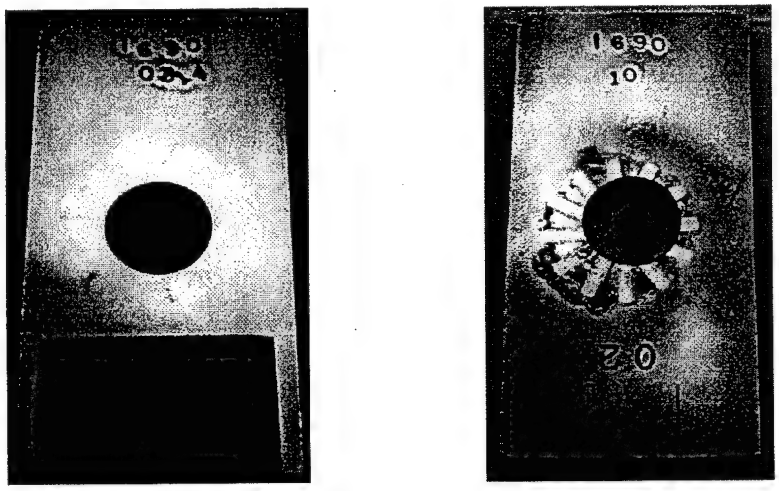

(a) (b)

Figure 48. Small IN690 crevice samples, 2.5x5.1 cm (1.0x2.0 in), exposed for 4 weeks: (a) aerated artificial seawater (b) ozonated artificial seawater.

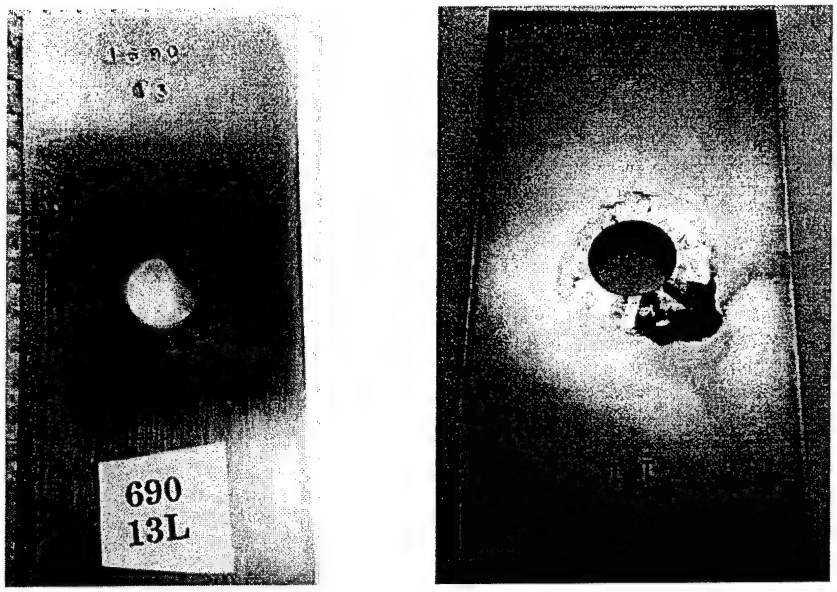

(a) (b)

Figure 49. Large IN690 crevice samples, 3.8x7.6 cm (1.5x3.0 in), exposed for 2 weeks: (a) aerated artificial seawater (b) ozonated artificial seawater.

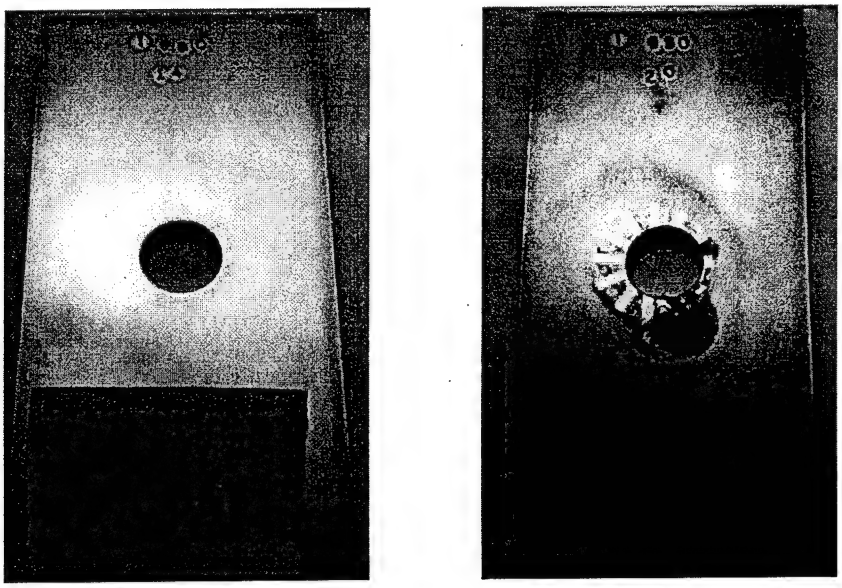

(a) (b)

Figure 50. Large IN690 crevice samples, 3.8x7.6 cm (1.5x3.0 in), exposed for 4 weeks: (a) aerated artificial seawater (b) ozonated artificial seawater.

Figure 51. Small IN690 crevice sample, 2.5x5.1 cm (1.0x2.0 in), after 4 weeks of exposure to ozonated artificial seawater. SEM photograph on the right depicts the semi-adherent brown corrosion product in the slot regions, which was found to have high concentrations of iron and oxygen.

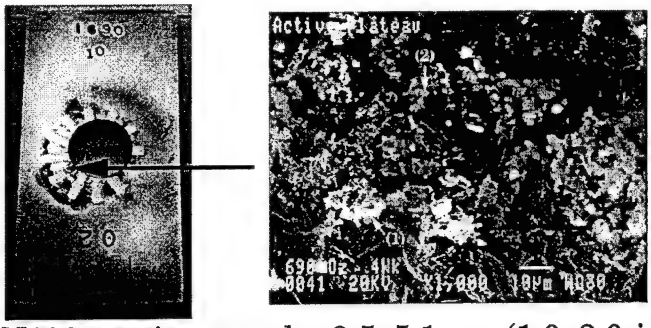

Figure 52. Small IN690 crevice sample, 2.5x5.1 cm (1.0x2.0 in), after 4 weeks of exposure to ozonated artificial seawater. SEM photograph on the right depicts an active pit on a plateau. EDS spot analysis of area (1) showed a pure titanium crystallite, while area (2) showed high amounts of titanium, chrome, silicon, and a trace of niobium.

Stainless Steel Alloys

304 Stainless Steel

Weight Loss Samples Figure 53 shows the percent weight loss (%WTL) of 304 stainless steel samples exposed to aerated and ozonated artificial seawater, as a function of time of exposure. Note that there is a significant increase in metal loss of 304 stainless steel samples in ozonated *vs.* aerated artificial seawater. No pitting was visible on the free surfaces in either aerated or ozonated seawater. Most of the corrosion of the ozonated samples occurred at the point where the samples were in contact with the glass support rod and Teflon spacers. This observation was based on the large volume of red corrosion product seen in this area. No such corrosion product was observed on the aerated weight loss samples. This indicates that crevice corrosion occurs readily in ozonated seawater, even at a slight contact crevice.

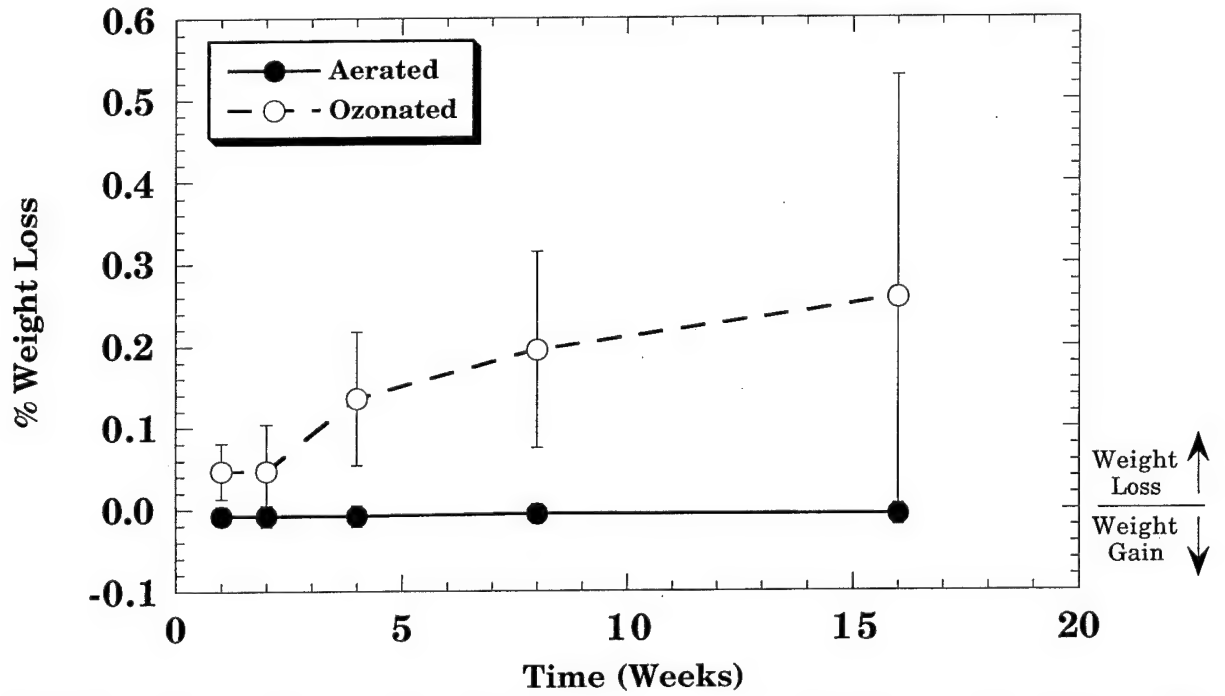

Figure 53. Percent weight loss of 304 stainless steel in aerated and ozonated artificial seawater. Note that the corrosion product was not removed because samples were re-immersed after each time period.

Crevice Samples Figures 54-55 show the severe crevice attack that occurred on 304 stainless steel samples exposed to aerated *versus* ozonated seawater. The small 2.5x5.1 cm (1.0x2.0 in) aerated samples exhibited no attack at crevice plateaus, and only one large cathode area, 3.8x7.6 cm (1.5x3.0 in), sample showed

attack at one crevice site at 4 weeks (Fig. 57a). In contrast, the small ozonated samples exhibited deep penetration under at least one plateau by 4 weeks and under 5 plateaus by 16 weeks. Large volumes of red corrosion product were associated with the crevice corrosion in ozonated seawater. In general, the number of sites attacked and the severity of attack increased as the duration of exposure to ozonated seawater increased. Large uncreviced (cathode) area samples exposed to ozonated seawater showed deep penetration under one plateau as early as 2 weeks (Fig. 56a); at 4 weeks there are 3 sites of attack at different plateaus. The effect of the larger cathode area results in earlier initiation in ozonated seawater compared to the smaller area samples, but at 4 weeks and later, the degree of crevice attack is generally independent of the cathode area.

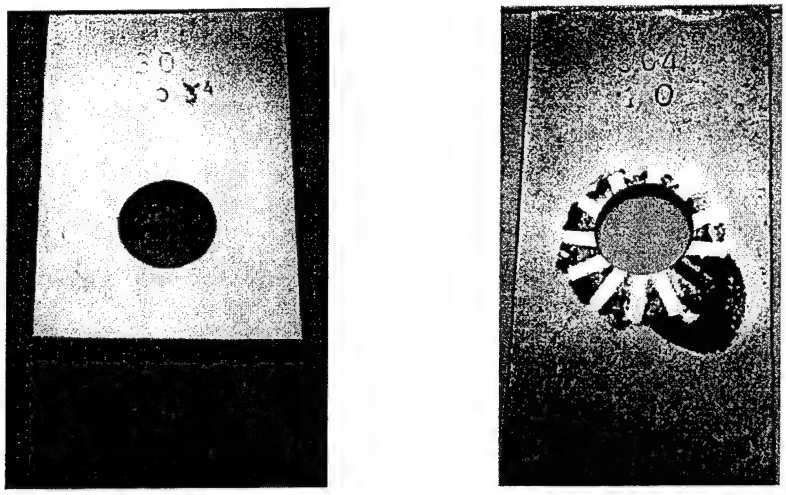

(a) (b)

Figure 54. Small 304 stainless steel samples, 2.5x5.1 cm (1.0x2.0 in) exposed for 4 weeks: (a) aerated artificial seawater, (b) ozonated artificial seawater.

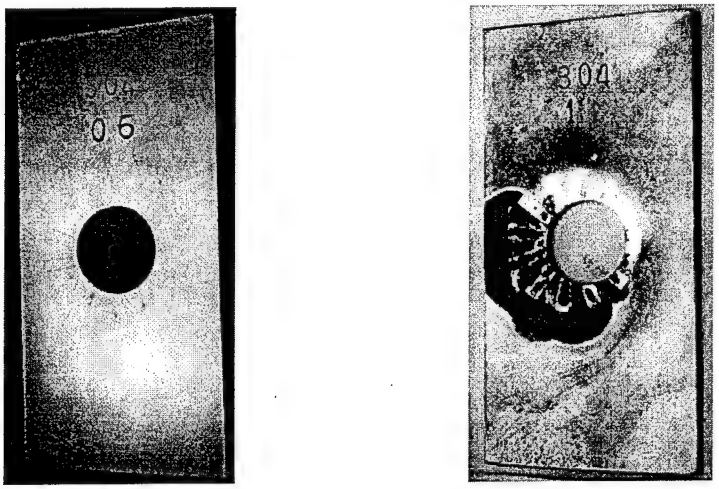

(a) (b)

Figure 55. Small 304 stainless steel samples, 2.5x5.1 cm (1.0x2.0 in) exposed for 16 weeks: (a) aerated artificial seawater, (b) ozonated artificial seawater.

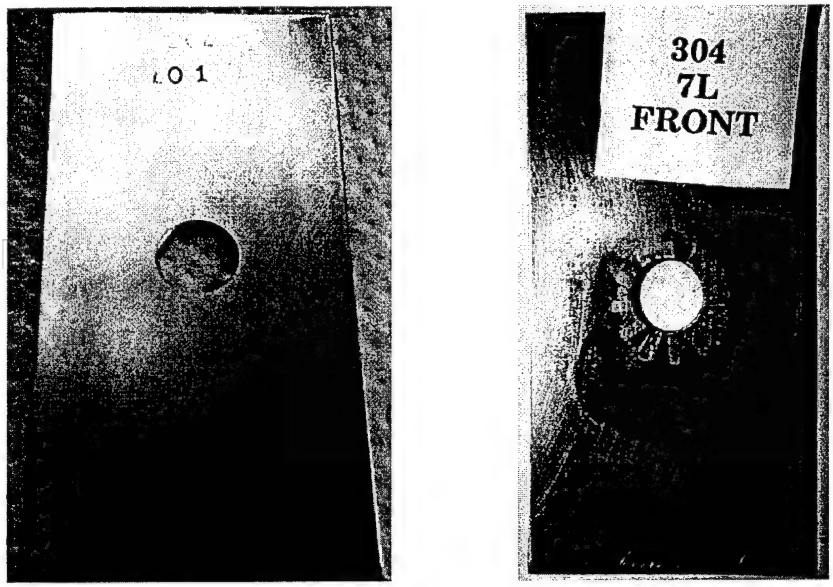

(a) (b)

Figure 56. Large 304 stainless steel samples, 3.8x7.6 cm (1.5x3.0 in), exposed for 2 weeks: (a) aerated artificial seawater, (b) ozonated artificial seawater.

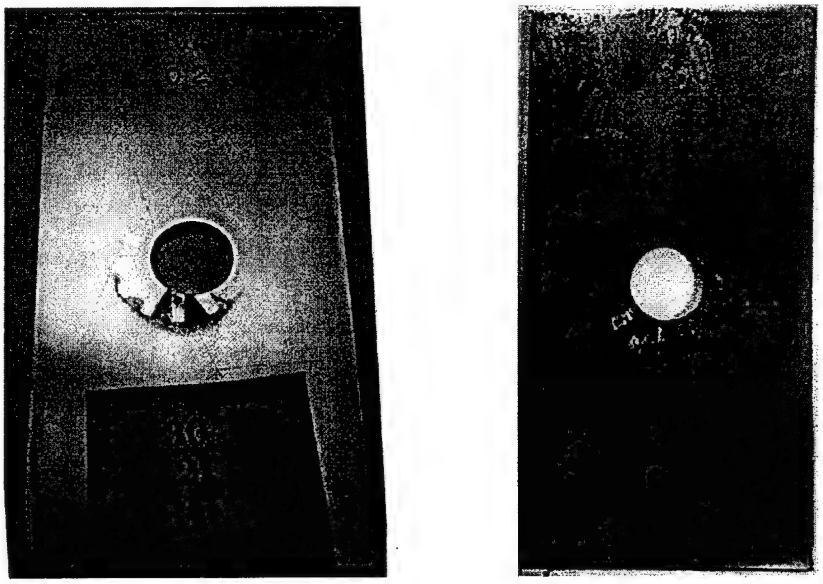

(a) (b)

Figure 57. Large 304 stainless steel samples, 3.8x7.6 cm (1.5x3.0 in), exposed for 4 weeks: (a) aerated artificial seawater, (b) ozonated artificial seawater.

Wire Samples Electrochemical testing of stainless steel wires in the tanks showed that the corrosion potential of 304 stainless steel exposed to ozonated artificial seawater was shifted in the noble direction with respect to the aerated corrosion potential. By 4 weeks exposure, the ozonated corrosion potential was 0.8 to 0.9 V higher than the aerated corrosion potential. Beyond 4 weeks, a steady

corrosion potential of approximately 0.82 V_{SCE} was reached in ozonated seawater, while the aerated potential decreased from 0.0 to -0.2 V_{SCE} by 16 weeks (Fig. 58).

Figure 59 shows corrosion rates calculated from LPR measurements on wire samples which were exposed to the aerated or ozonated seawater. The aerated condition shows consistent corrosion rates near zero. The ozonated case shows a sharp increase in corrosion rate to 22 μm/y (0.9 mpy) at 2 weeks, followed by a decrease to less than 5 μm/y (0.2 mpy). The aerated and ozonated corrosion rates are equal and zero at 16 weeks.

Cyclic potentiodynamic polarization (CPP) experiments were performed on 304 stainless steel wire samples at each test interval. The CPP test was conducted in one-liter test volumes, as described in the experimental section. Results for the 4 and 8 week test interval are shown in Figures 60 and 61. The aerated seawater CPP for both time intervals shows a large hysteresis loop, with a breakdown potential (E_b) and a repassivation potential (E_{rp}) of approximately 0.4 and 0.0 V_{SCE}, respectively. The repassivation potential is slightly active to the zero-current potential, indicating slight susceptibility to crevice corrosion. The crevice data support this, with only one sample (4 weeks, large) of the 1, 2, 4, 8, or 16 week samples showing crevice attack at plateaus. The noise in the passive region of the 8 week data (Figure 61) is attributed to transient pit nucleation and annihilation. Based on visual examination at 16x, aerated CPP scans caused large, subsurface, cavernous pits to develop on the wire surfaces. The large hysteresis area and degree of pitting from CPP testing was typical for aerated conditions at 1, 2 and 16 weeks, as well. The areas of the wire not subjected to the CPP, but exposed to the aerated open circuit potential conditions in the tank (due to a shallower depth of submersion in the one-liter cell compared to the tank), were not pitted. This observation indicates that polarization of the wires noble to the pitting potential initiated stable pits, but pitting does not occur at open circuit corrosion potential conditions active to the pitting potential.

The CPP results for 304 stainless steel exposed to ozonated artificial seawater at 1 and 2 weeks resulted in large hysteresis areas and large subsurface, undercutting pits, similar to the aerated counterparts. By 4 weeks exposure, the effects of the stronger oxidant were apparent, as seen by the 0.4 V noble shift in zero-current potential. Comparing 4 week ozonated *versus* aerated seawater CPP results, a slope change is seen at approximately 0.84 V_{SCE} with ozonation. This is believed to be the intersection of the anodic polarization curve with the oxygen evolution line. However, a large hysteresis loop is evident, with the E_{rp} active to the zero current potential by greater than 0.1 V. Visual observation at 16x revealed very deep,

narrow pits at and below the waterline from CPP testing. This damage required a more active repassivation potential to arrest the pit growth. Analysis of the open circuit potentials (E_{corr}) *versus* the repassivation potential data support the greater susceptibility to crevice corrosion in ozonated seawater, as seen on the crevice samples in Figures 54-57. The E_{corr} value of ozonation from Figure 58, 0.82 V_{SCE}, is more noble to E_{rp} by a greater difference (0.82 - 0.35 = +0.47 V) compared to the aerated counterpart (0.01 - 0.00 = +0.01 V). The greater potential difference corresponds to the larger driving force between the base metal (cathode) during ozonation and the potential within the deep pit/crevice (anode), leading to greater crevice penetration.

At 8 weeks, the aerated cyclic polarization has not changed significantly, but the polarization curve for 304 stainless steel in ozonated seawater is much different, seen in Figure 61. In the ozonated case, the zero current potential is positioned near the intersection with the oxygen evolution line. A small secondary passive range is recorded from 1.00- 1.04 V_{SCE}. There is no hysteresis in the ozonated CPP at 8 weeks, with the forward and reverse curves tracking the same path. Visual observation at 16x showed small, hemispherical pits that developed during the 8 weeks exposure at open circuit conditions, however these pits did not grow during the CPP test, and no new pitting was observed. It appears that the ozonated 304 stainless steel wire surface is acting as a reversible gas electrode during the CPP. This behavior has been noted at 16 weeks as well. However, large hemispherical pits were observed at the original waterline in the ozonated tank seawater, under corrosion product that had accumulated. These data suggest that, for actively exposed surfaces, ozone stabilizes the passive film against pit initiation. However, for creviced alloys, the increased driving force of ozone versus that of oxygen results in enhanced crevice corrosion.

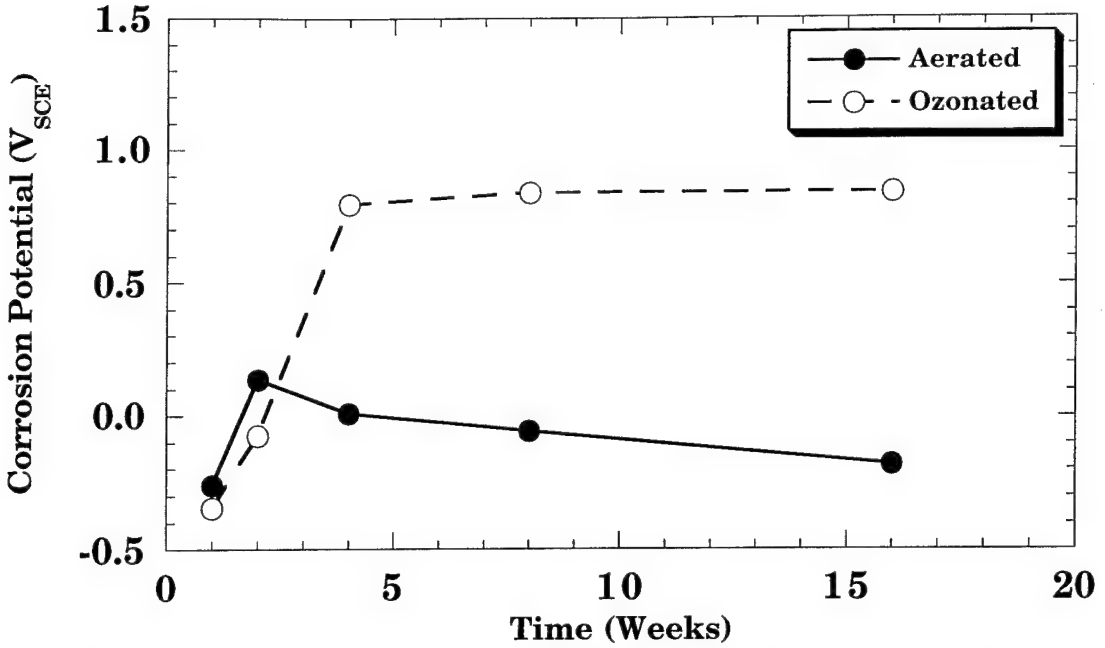

Figure 58. The steady state corrosion potential of 304 stainless steel wire exposed to aerated or ozonated artificial seawater.

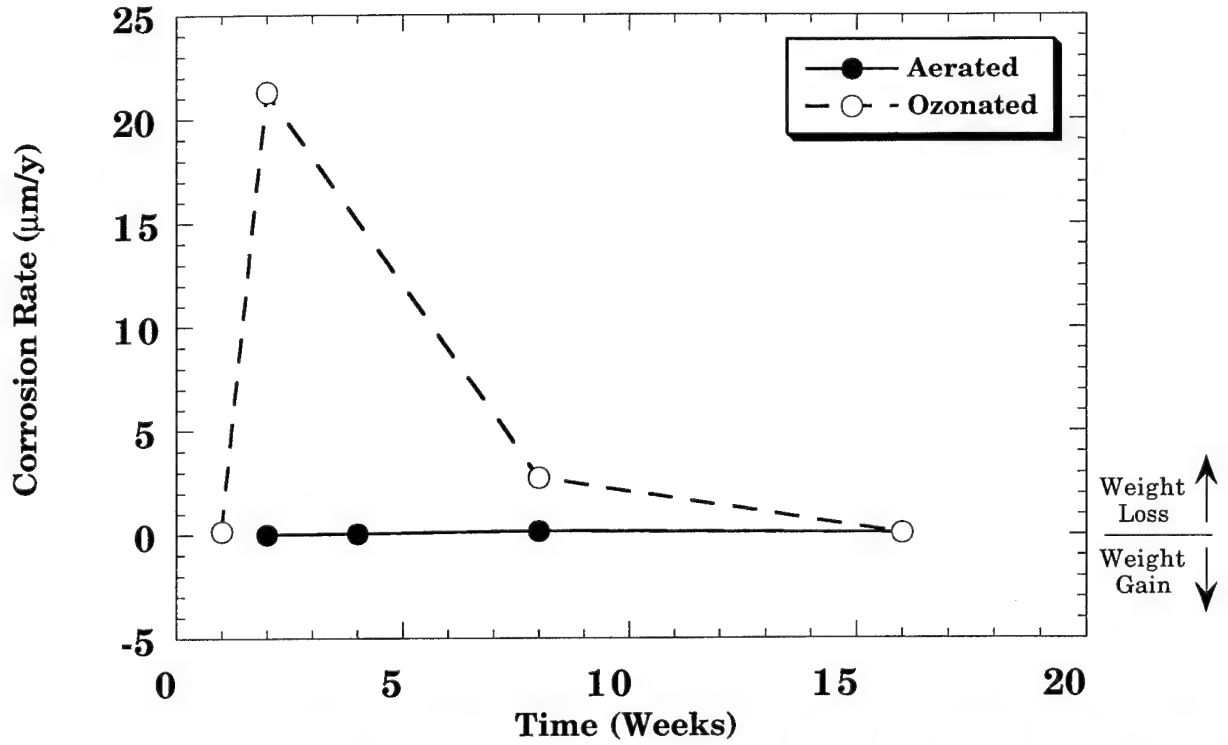

Figure 59. A comparison of corrosion rates calculated from LPR measurements for 304 stainless steel in aerated and ozonated artificial seawater.

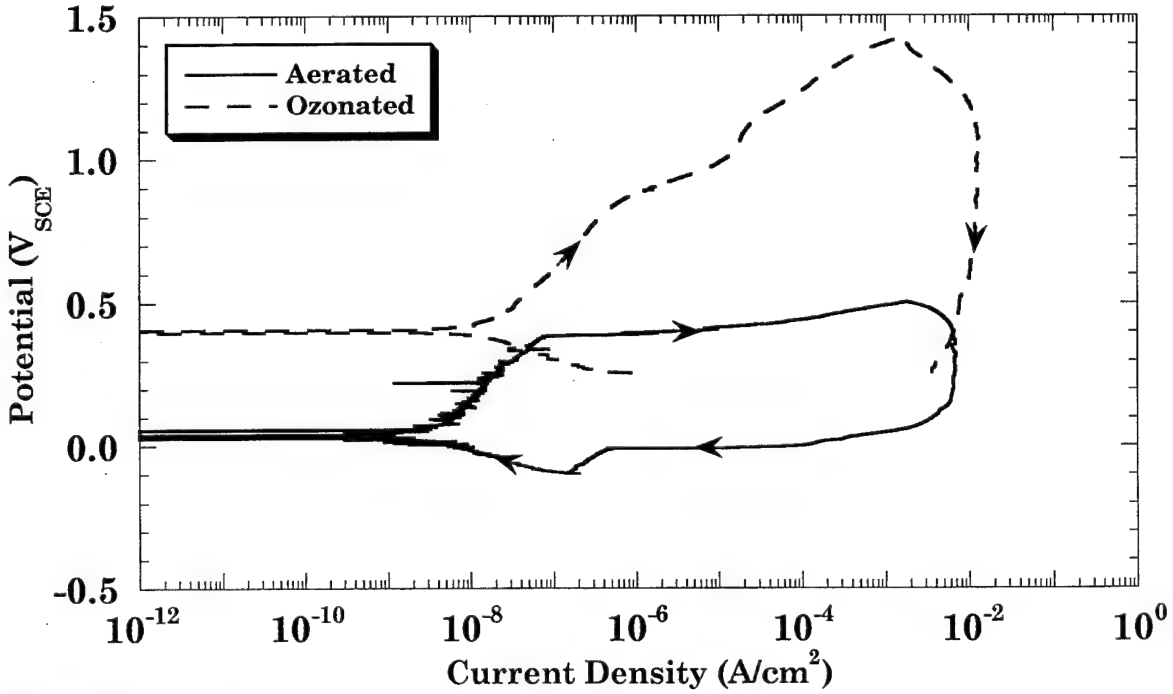

Figure 60. A comparison of polarization curves of 304 stainless steel wires exposed to aerated or ozonated artificial seawater for 4 weeks.

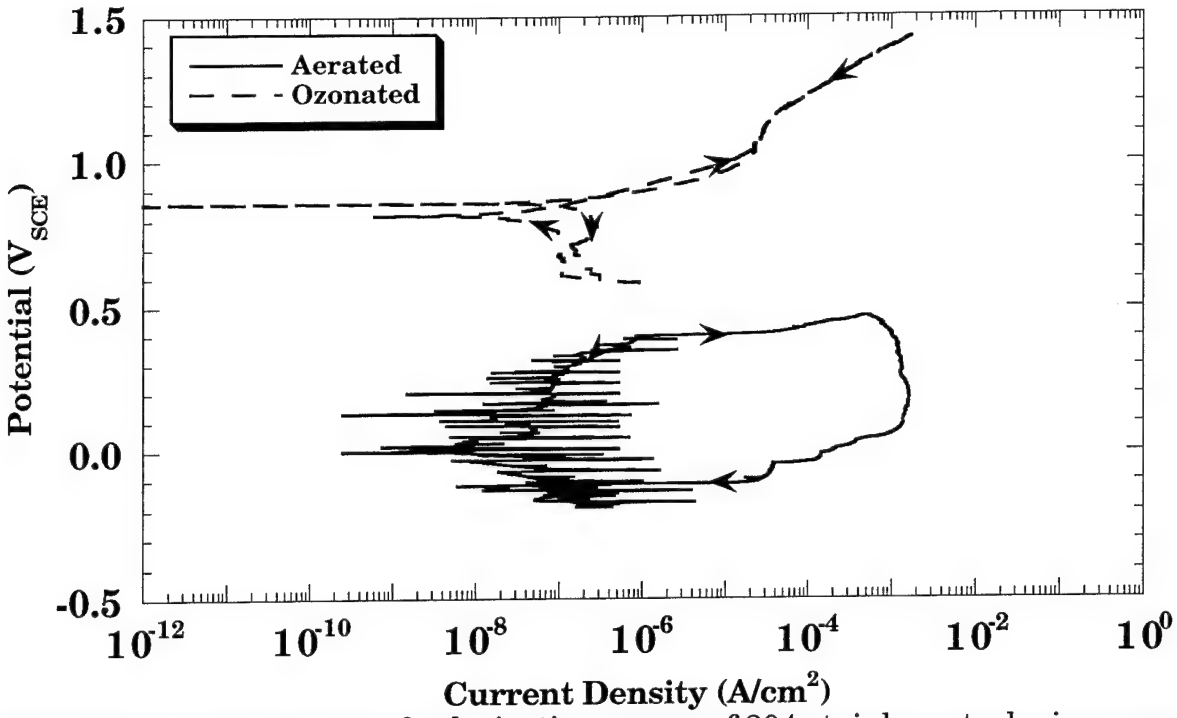

Figure 61. A comparison of polarization curves of 304 stainless steel wires exposed to aerated or ozonated artificial seawater for 8 weeks.

316 Stainless Steel

Weight Loss Samples The percent weight loss (%WTL) of 316 stainless steel samples exposed to aerated and ozonated artificial seawater are shown in Figure 62, as a function of time of exposure. Note the significant increase in metal loss of 316 stainless steel samples in ozonated *vs.* aerated artificial seawater. The corrosion behavior in ozonated *vs.* aerated seawater is similar to that for 304 stainless steel; large volumes of red corrosion product had accumulated at the slight contact crevice formed between the glass support rod, Teflon spacers, and the sample. No pitting was visible on the free surfaces in either aerated or ozonated seawater. No corrosion product was observed on the aerated weight loss samples.

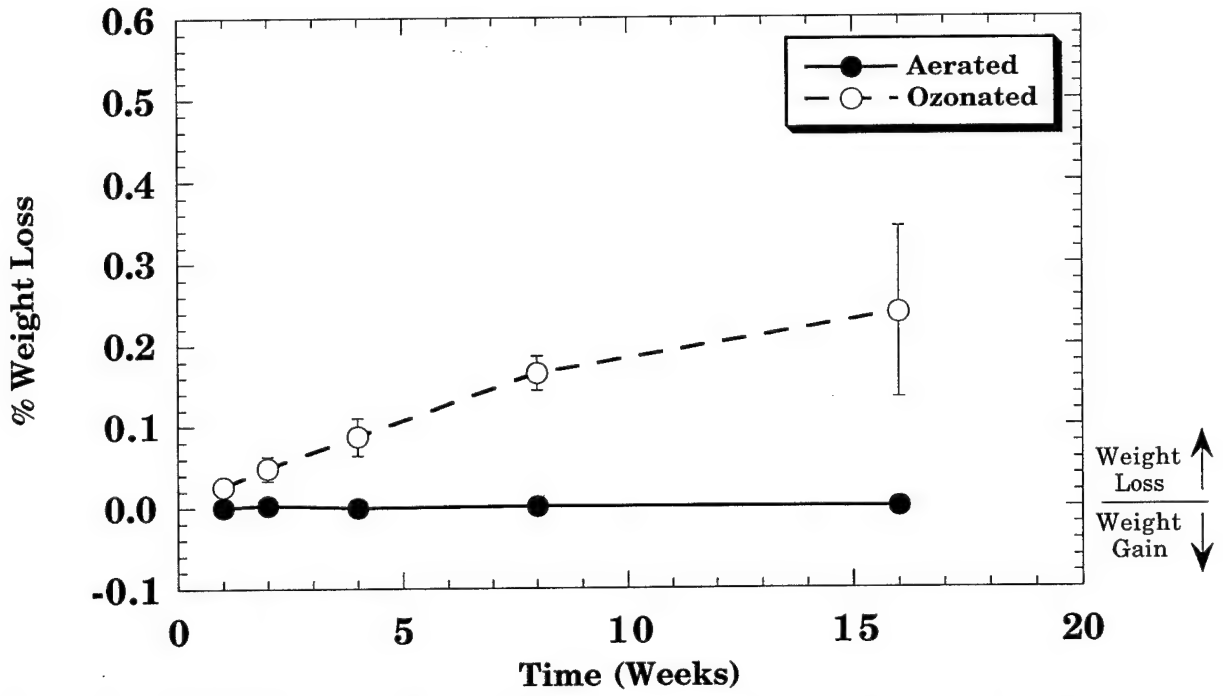

Figure 62. Percent weight loss of 316 stainless steel in aerated and ozonated artificial seawater. Note that the corrosion product was not removed because samples were re-immersed after each time period.

Crevice Samples The general appearance of the small, 2.5x5.1 cm (1.0x2.0 in), crevice samples of 316 stainless steel is presented in Figures 63 and 64 from 4 and 8 weeks exposure data, respectively, for aerated *versus* ozonated seawater. Exposure to aerated seawater resulted in one crevice plateau being attacked at 4 weeks, shown in Figure 63(a), however the 8 week sample did not show similar attack. Note the severe crevice attack that occurred on 316 stainless steel samples exposed to ozonated seawater. Two crevice plateaus were attacked by 4 weeks, and

6 plateaus at 8 weeks. Large volumes of red corrosion product was associated with the crevice corrosion in ozonated seawater. As with 304 stainless steel, the number of sites attacked and the severity of attack generally increased as the duration of exposure to ozonated seawater increased. Large uncreviced (cathode) area samples in ozonated seawater also showed the same behavior, starting as early as 2 weeks, while the aerated samples did not show attack at the plateaus (Fig. 65-66). The larger cathode area has the same effect for 316 as for 304 stainless steel; earlier crevice corrosion initiation in ozonated seawater was comparable to the smaller area samples, but beyond 4 weeks, the degree of crevice attack is generally independent of the cathode area.

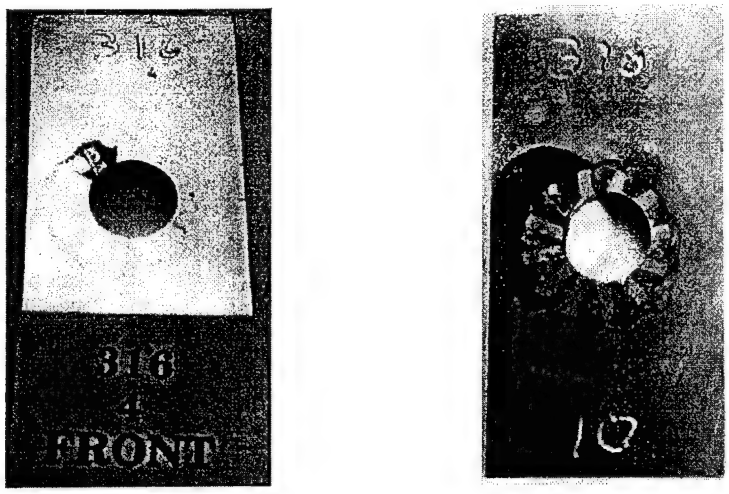

(a) (b)

Figure 63. Small stainless steel samples, 2.5x5.1 cm (1.0x2.0 in) exposed for 4 weeks: (a) aerated artificial seawater, (b) ozonated artificial seawater.

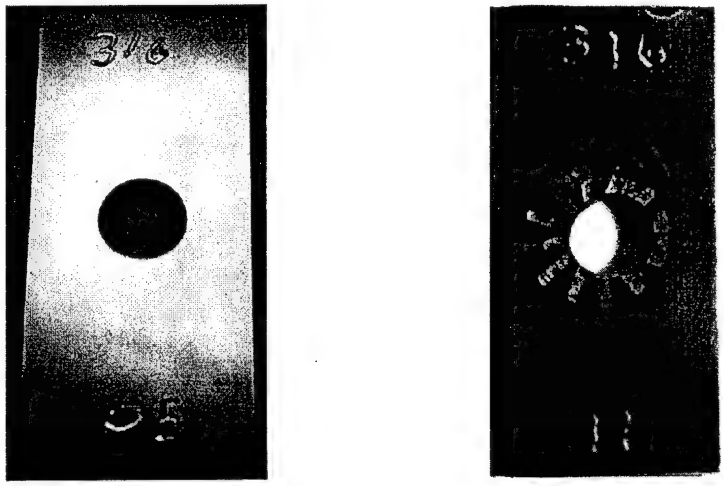

(a) (b)

Figure 64. Small 316 stainless steel samples, 2.5x5.1 cm (1.0x2.0 in), exposed for 8 weeks: (a) aerated artificial seawater, (b) ozonated artificial seawater.

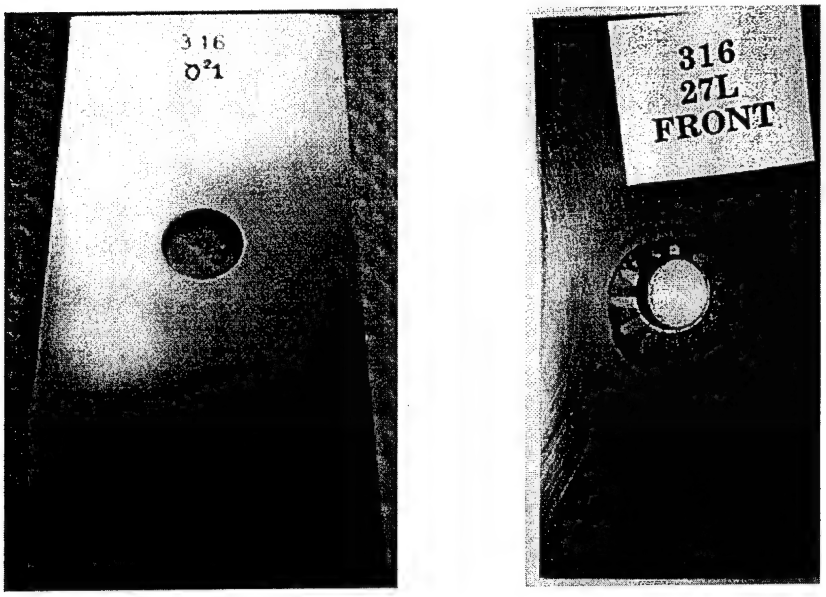

(a) (b)

Figure 65. Large 316 stainless steel samples, 3.8x7.6 cm (1.5x3.0 in), exposed for 2 weeks: (a) aerated artificial seawater, (b) ozonated artificial seawater.

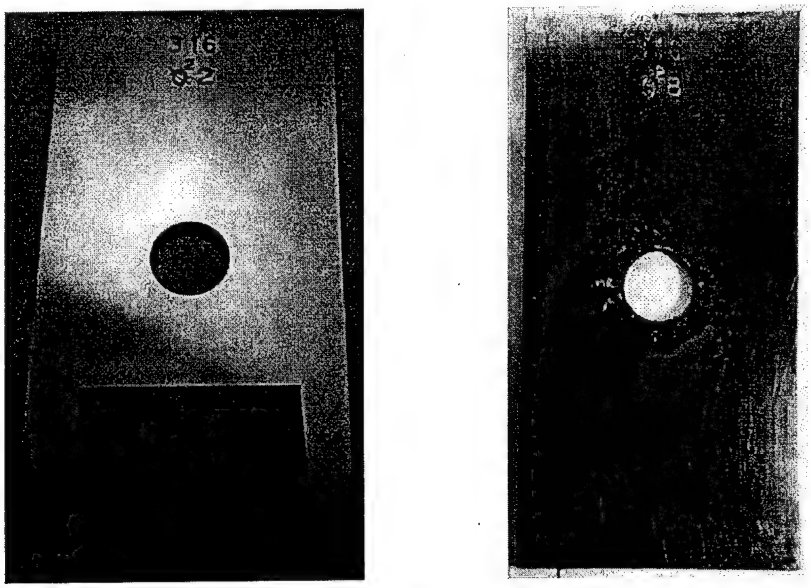

(a) (b)

Figure 66. Large 316 stainless steel samples, 3.8x7.6 cm (1.5x3.0 in), exposed for 4 weeks: (a) aerated artificial seawater, (b) ozonated artificial seawater.

Wire Samples Electrochemical testing of stainless steel wires in the tanks showed that the open circuit corrosion potential of 316 stainless steel exposed to ozonated artificial seawater was shifted in the noble direction by +0.8 to +0.9 V compared to the aerated corrosion potential. The ozonated corrosion potential reached a steady value of approximately 0.81 V_{SCE} by 4 weeks exposure, where the aerated potential varied only slightly from a stable value of 0.1 V_{SCE} (Fig. 67).

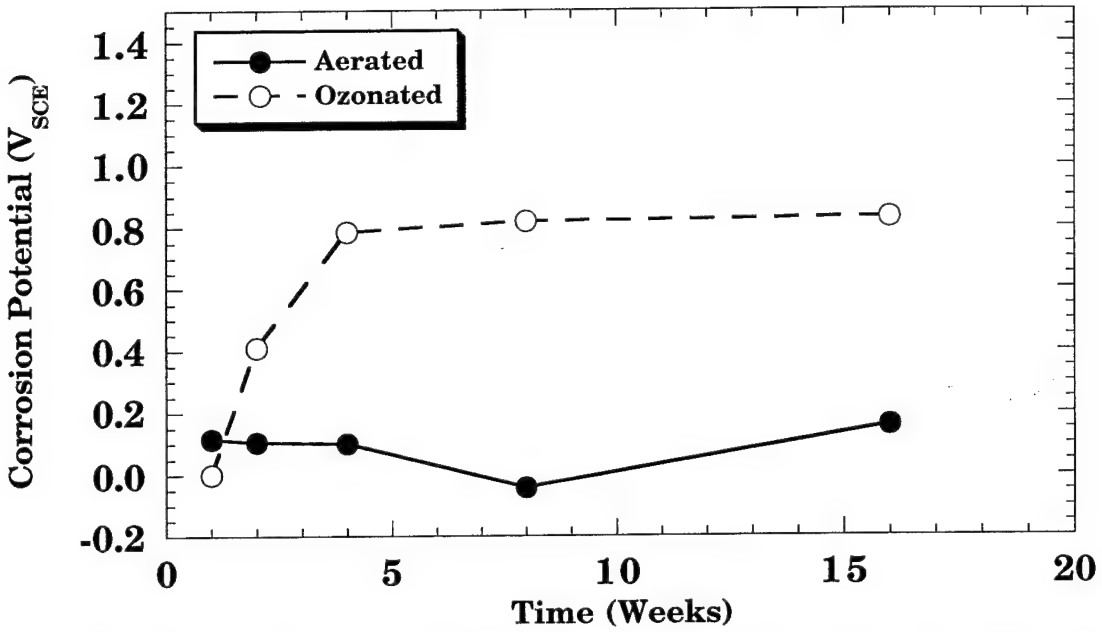

Figure 67. The steady state corrosion potential of 316 stainless steel wire exposed to aerated or ozonated artificial seawater.

Figure 68 shows corrosion rates calculated from LPR measurements on wire samples which were exposed to the aerated or ozonated seawater. With the exception of the first point at 1 week, the aerated condition shows consistent corrosion rates near zero. From 4 to 16 weeks, the corrosion rate increases somewhat, but does not exceed 1 μm/y (0.04 mpy).

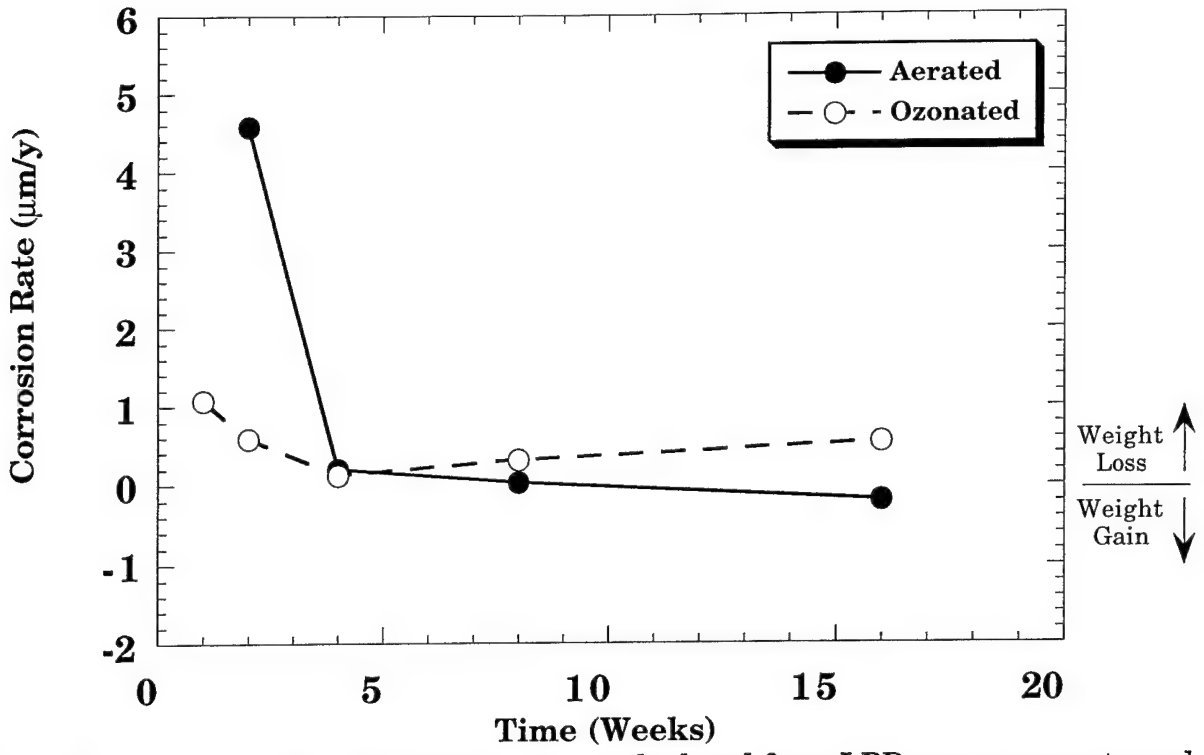

Figure 68. A comparison of corrosion rates calculated from LPR measurements and weight loss measurements for 316 stainless steel in aerated and ozonated artificial seawater.

The results of cyclic potentiodynamic polarization (CPP) tests on 316 stainless steel are shown in Figure 69, after 8 weeks exposure to aerated and ozonated seawater. The wire sample tested in aerated seawater shows a primary passive region, a transpassive range at 0.5 to 0.7 V_{SCE}, and secondary passivity from 0.7 to 0.9 V_{SCE}. Breakdown occurs after reversal of the scan, with partial repassivation "steps" in the curve before reaching the final repassivation potential at 0.3 V_{SCE}. Visual examination revealed that the breakdown occurred at large, hemispherical pits at the waterline of the CPP test. The area of the sample not subject to the CPP test, but exposed to the open circuit conditions in the aerated seawater tank (due to the depth of wire submersion being less in the one-liter cell than in the tank), was not pitted.

In contrast to the behavior of the aerated CPP test, the sample tested after 8 weeks in ozonated seawater did not show breakdown at the waterline or anywhere on the submerged surface. The CPP curve shown in Figure 69 tracks from a zero-current potential in the secondary passive range of the aerated test, shows no hysteresis, and follows reversible gas electrode behavior similar to 304 stainless steel

at 8 weeks (Figure 61). This behavior has been observed after 1, 2, 16, and 26 weeks in ozonated seawater as well. However, small hemispherical pits were observed at the original waterline from 8 weeks exposure, where green/black scale was attached. The preliminary conclusion is that the exposure to ozone for extended time periods enhances the passive film on completely submerged surfaces, but at a crevice formed by corrosion product, ozonation results in crevice corrosion.

The CPP waterline pitting in aerated seawater was also observed at 2 and 16 weeks, but it was not seen at 4 weeks, 26 weeks, or during any preliminary CPP tests in aerated seawater. The sporadic nature of the breakdown and pitting on 316 stainless steel shows that the alloy is "borderline" to localized corrosion in aerated seawater; it is more resistant than 304 stainless steel, which was shown to pit severely during every aerated CPP test, but 316 stainless steel is not immune.

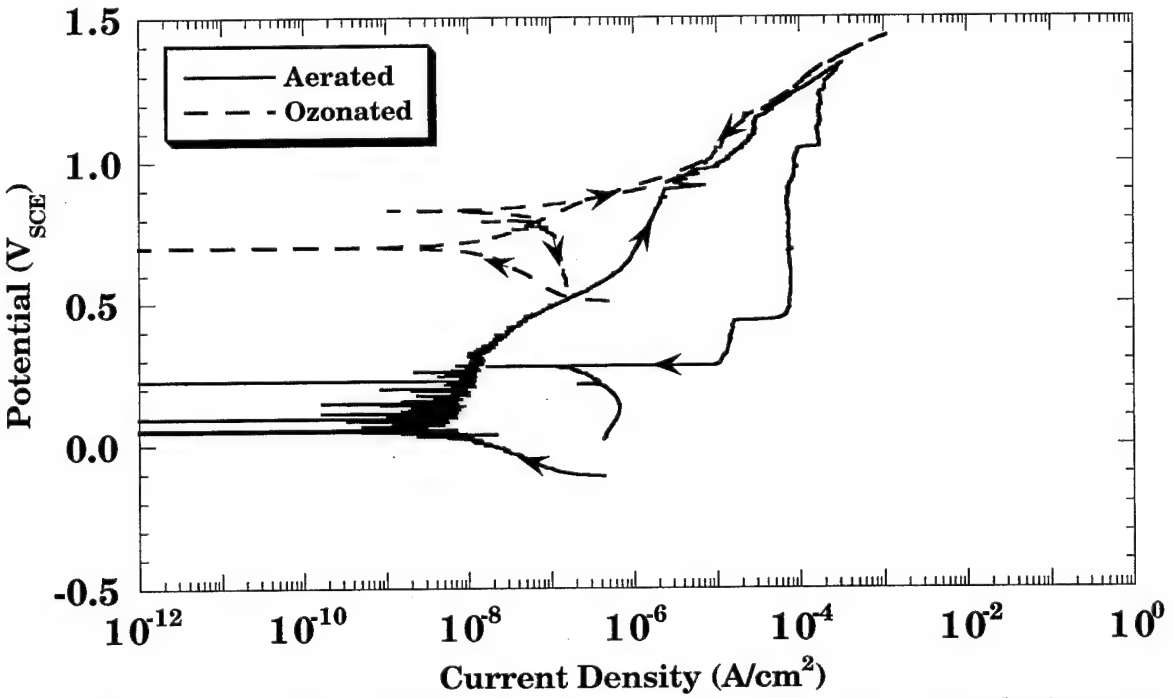

Figure 69. A comparison of polarization curves of 316 stainless steel wires exposed to aerated or ozonated artificial seawater for 8 weeks.

AL6XN Stainless Steel

Weight Loss Samples Figure 70 shows the percent weight loss (%WTL) of AL6XN stainless steel samples exposed to aerated and ozonated artificial seawater, as a function of time of exposure. The curves show that there was no significant weight change in either aerated or ozonated artificial seawater. The results for AL6XN in ozonated seawater are in marked contrast with the %WTL results for 304 and 316 stainless steel, where significant corrosion was observed at the metal/glass rod/Teflon spacer interface. For AL6XN stainless steel, no corrosion product was observed at this interface.

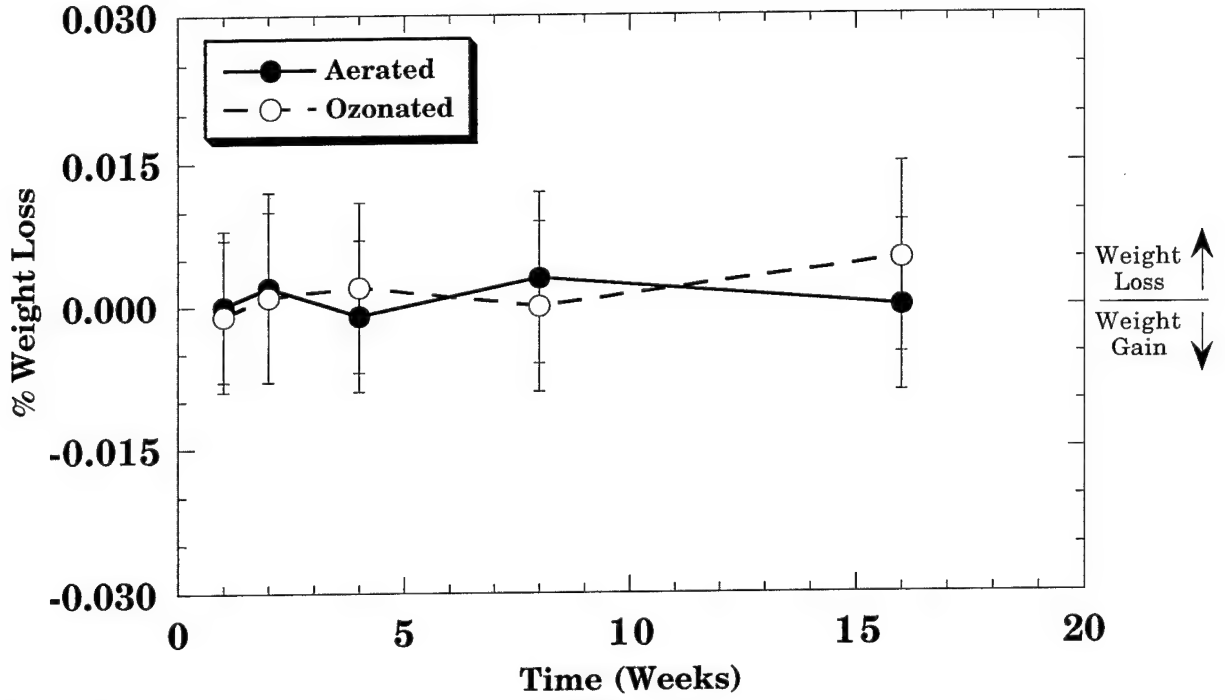

Figure 70. Percent weight loss of AL6XN stainless steel in aerated and ozonated artificial seawater. Note that the corrosion product was not removed because samples were re-immersed at each time period.

Crevice Samples Figures 71-72 show the corrosion around the crevice areas that occurred on AL6XN stainless steel samples exposed to aerated and ozonated seawater, after 4 and 16 weeks exposure. Discoloration from oxide build up is visible in the slot regions between crevice plateaus on the ozonated samples; the aerated samples show virtually no effect of the crevice. Large cathodic area crevice samples also showed the same behavior, seen in Figures 73-74. Black corrosion product was seen at the mouth of slot, along the outer perimeter of the crevice washer. The black corrosion product is similar to the voluminous precipitates found in the ozonated tanks containing nickel base alloys, stainless steels, and copper-nickel alloys. Based

on visual observation at 16x of the large 16 week ozonated sample, the crevice plateaus were relatively unaffected, appearing dark grey or slightly yellow in color. At the boundary between the edge of the Teflon plateau and the slot, the surface is yellow/green in color. When moving away from the plateau edge into the center of the slot, the oxide layer in the slot regions becomes thicker, more cracked, and the color of the oxide changes from yellow/green -> orange -> red/brown. Comparing the general appearance of slots at 2, 4, 8, and 16 weeks, increasing exposure time generally results in thickening and cracking of the oxide, with a greater area fraction of dark oxide present in a given slot.

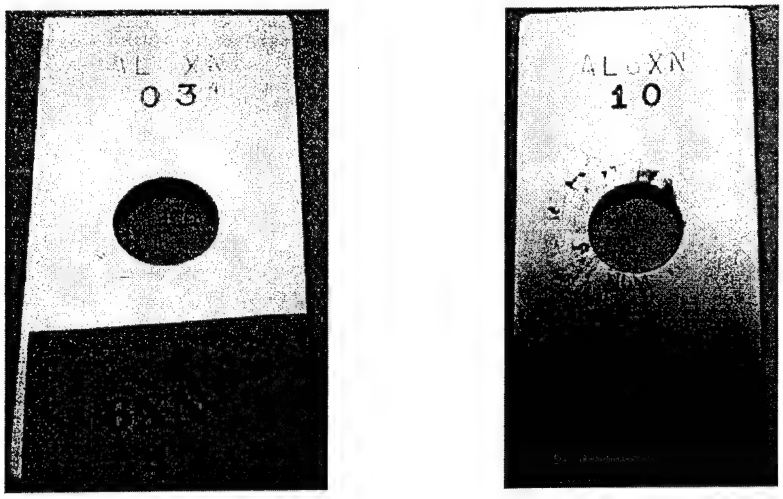

(a) (b)

Figure 71. Small AL6XN stainless steel samples, 2.5x5.1 cm (1.0x2.0 in), exposed for 4 weeks: (a) aerated artificial seawater, (b) ozonated artificial seawater.

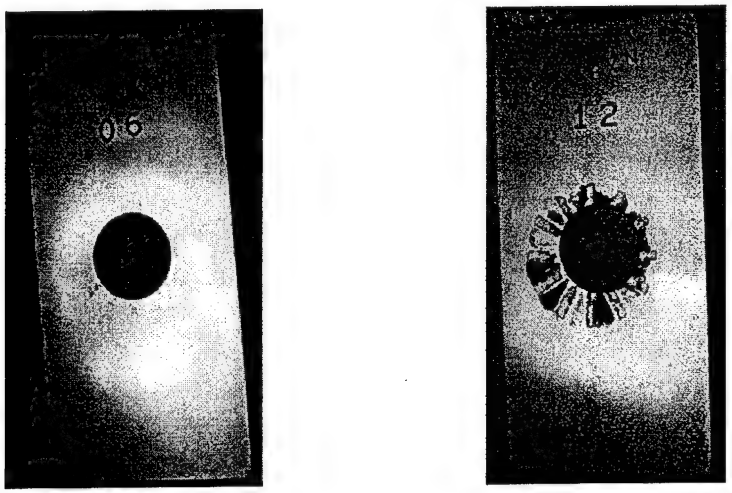

(a) (b)

Figure 72. Small AL6XN stainless steel samples, 2.5x5.1 cm (1.0x2.0 in), exposed for 16 weeks: (a) aerated artificial seawater, (b) ozonated artificial seawater.

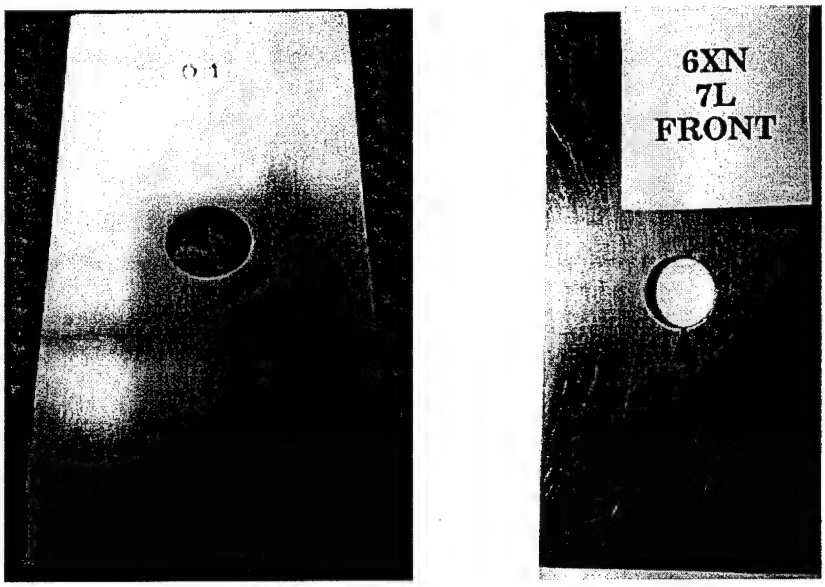

(a) (b)

Figure 73. Large AL6XN stainless steel samples, 3.8x7.6 cm (1.5x3.0 in), exposed for 2 weeks: (a) aerated artificial seawater, (b) ozonated artificial seawater.

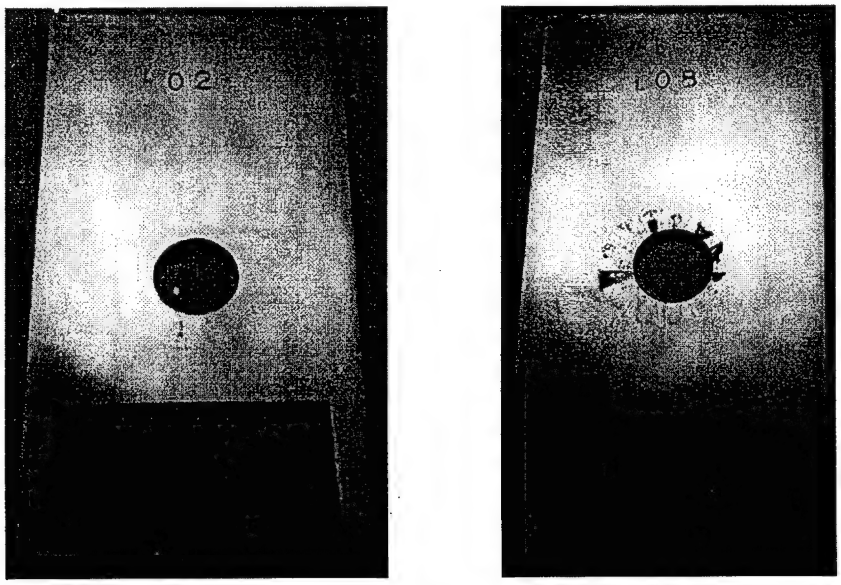

(a) (b)

Figure 74. Large AL6XN stainless steel samples, 3.8x7.6 cm (1.5x3.0 in), exposed for 4 weeks: (a) aerated artificial seawater, (b) ozonated artificial seawater.

Wire Samples Figure 75 presents the corrosion potential of AL6XN stainless steel as a function of exposure time in aerated and ozonated artificial seawater. After 2 weeks of exposure in ozonated seawater, the corrosion potential is shifted by 1.0 V noble to the aerated corrosion potential. The ozonated corrosion potential reached a steady state value of 0.8 V_{SCE} after 8 weeks exposure.

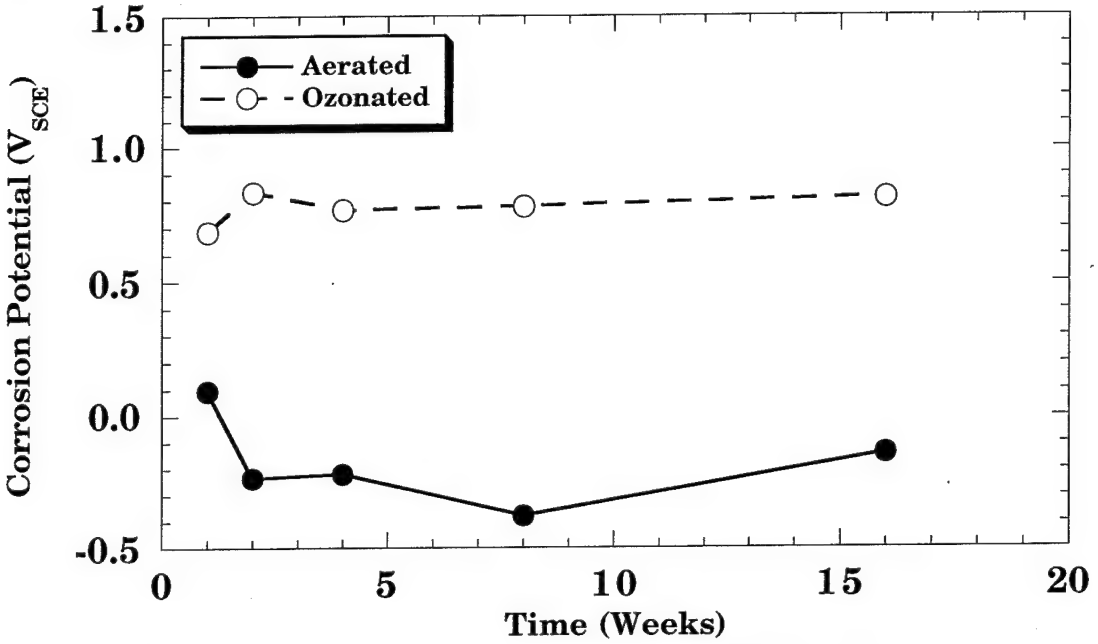

Figure 75. The steady state corrosion potential of AL6XN stainless steel wire samples, exposed to aerated or ozonated artificial seawater.

Figure 76 shows a comparison of corrosion rates calculated from LPR measurements for AL6XN stainless steel, in aerated and ozonated seawater. The aerated condition shows essentially a corrosion rate of zero at all test intervals. The corrosion rate in ozonated seawater shows a maximum of approximately 4 μm/y (0.16 mpy) at two weeks. After 2 weeks, the corrosion rate decreases with time to a value ≤ 1 μm/y (0.04 mpy) after 16 weeks of exposure.

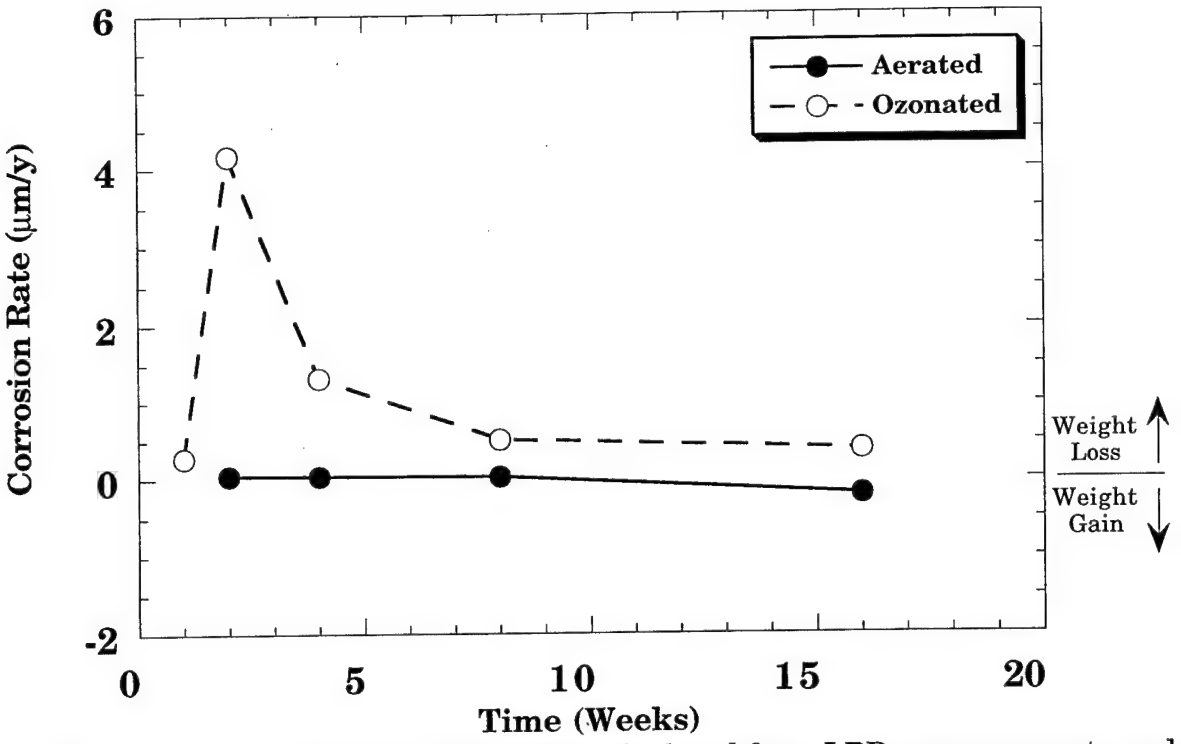

Figure 76. A comparison of corrosion rates calculated from LPR measurements and weight loss measurements for AL6XN stainless steel in aerated and ozonated artificial seawater.

Cyclic potentiodynamic polarization (CPP) experiments performed on AL6XN exposed for the test periods show distinct differences between aerated and ozonated seawater. After 4 and 8 weeks exposure, the CPP curves in aerated seawater are essentially the same. As seen in Figures 77-78, the curves contain a primary passive range, a transpassive range (0.35 - 0.6 V_{SCE}), a secondary passive range (0.6 -0.9 V_{SCE}), and slight hysteresis evident at 1.1 V_{SCE}. The reverse curve follows the oxygen evolution curve back to a final zero-current potential at 0.7 V_{SCE}, in the secondary passive range. The lack of significant hysteresis and the position of the breakdown and repassivation potentials indicates resistance to localized corrosion. Visual observation of the aerated CPP sample revealed no pitting on the free surfaces or at the waterline, consistent with the observations of the CPP curve.

After 4 weeks of ozonation, the zero-current potential is shifted to 0.8 V_{SCE}, which is within the secondary passive range as defined on the aerated CPP curve. The forward scan intersects a narrow passive range, followed by breakdown at 1.12 V_{SCE}. However, a hysteresis loop develops upon reversal of the scan. The 8 week cyclic polarization data (Figure 78) shows similar behavior, however the repassivation potential has shifted active to about 0.85 V_{SCE} and subsequently the

hysteresis is greater. Visual examination of both 4 and 8 week CPP samples for ozonated seawater revealed small, hemispherical pits on free surfaces. No pitting was noted on the surfaces of the sample exposed to the open circuit conditions in the ozonated seawater tank. Creviced immersion samples do not show signs of classical crevice corrosion from exposure to ozonated seawater. The pitting seen in the CPP test in not believed to be indicative of pitting or crevice susceptibility in the open circuit condition, but rather local secondary transpassive dissolution during CPP testing, enhanced by ozone.

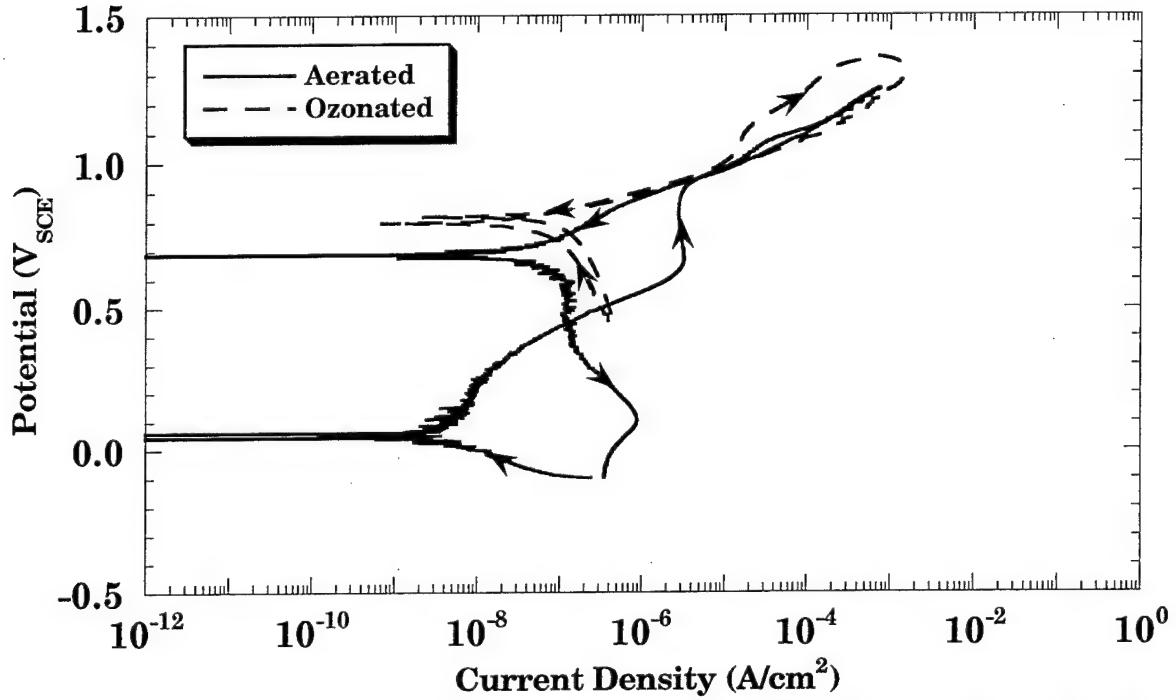

Figure 77. A comparison of polarization curves of AL6XN Stainless Steel wires exposed to aerated or ozonated artificial seawater for 4 weeks.

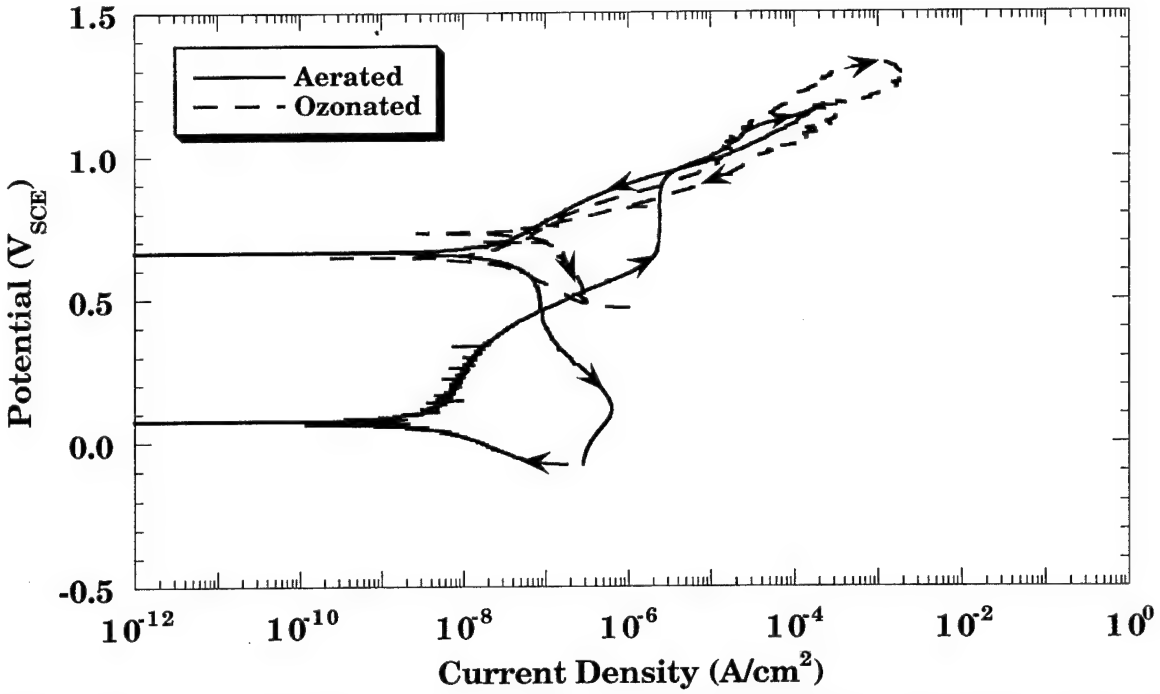

Figure 78. A comparison of polarization curves of AL6XN Stainless Steel wires exposed to aerated or ozonated artificial seawater for 8 weeks.

654SMO Stainless Steel

Weight Loss Samples The percent weight loss values of 654SMO stainless steel in aerated and ozonated artificial seawater are shown in Figure 79, as a function of time of exposure. The data indicate that there was no significant weight loss in either aerated or ozonated artificial seawater.

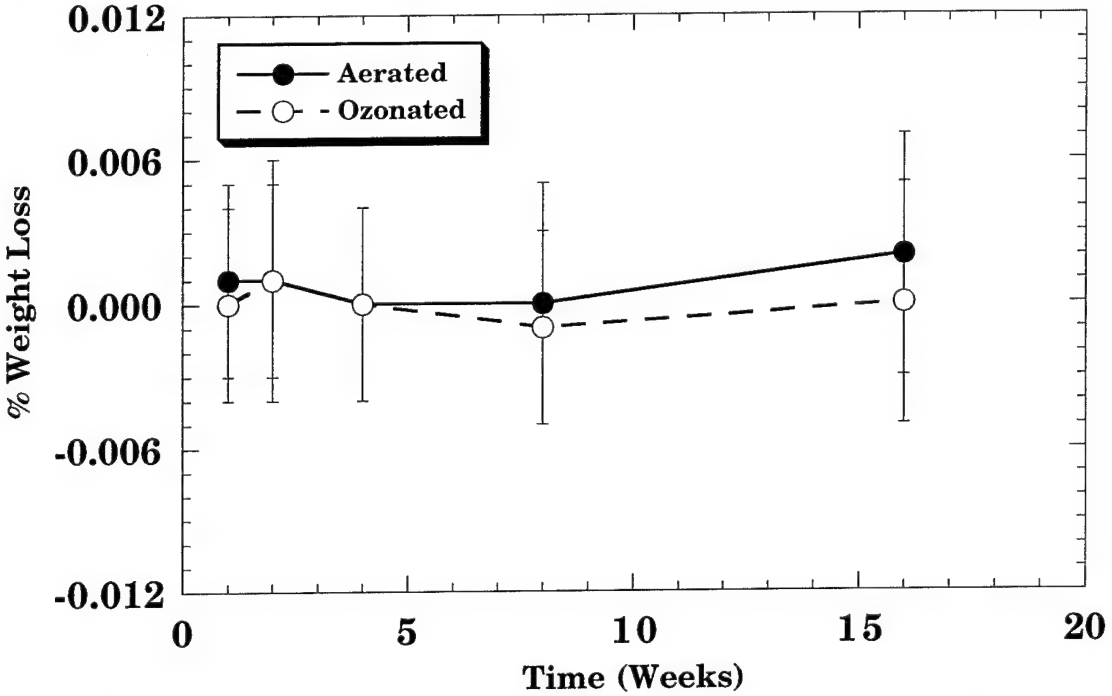

Figure 79. Percent weight loss of 654SMO stainless steel in aerated and ozonated artificial seawater. Note that the corrosion product was not removed because samples were re-immersed after each time period.

Crevice Samples The appearance of corrosion around the crevice areas that occurred on 654SMO stainless steel samples is shown in Figure 80, after 4 weeks of exposure to aerated and ozonated seawater. The appearance of 654SMO samples exposed ozonated and aerated seawater is similar to that of AL6XN stainless steel. Oxide discoloration is visible in the slot regions between crevice plateaus on the ozonated samples; black corrosion product was seen at the mouths of slot regions. The aerated samples show virtually no effect of the crevice. Large cathodic area crevice samples also showed the same behavior, as seen in Figures 81-82. Visual observation at 16x of the ozonated samples revealed the same color pattern as seen on AL6XN samples, with the exception that a blue/violet colored oxide was also present in the center of the slot region after 16 weeks exposure. As is the case with AL6XN stainless steel, increasing exposure time generally results in thickening and cracking of the oxide, with a greater area fraction of dark colored oxide present on

average in the slots.

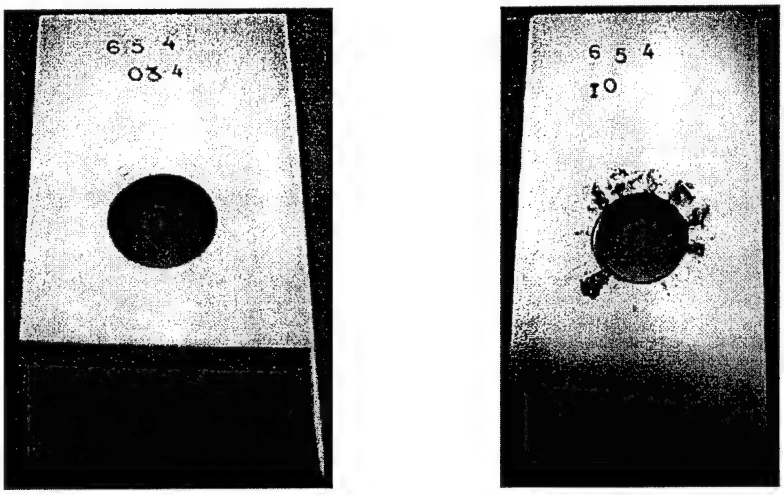

(a) (b)

Figure 80. Small 654SMO stainless steel samples, 2.5x5.1 cm (1.0x2.0 in), exposed for 4 weeks: (a) aerated artificial seawater, (b) ozonated artificial seawater.

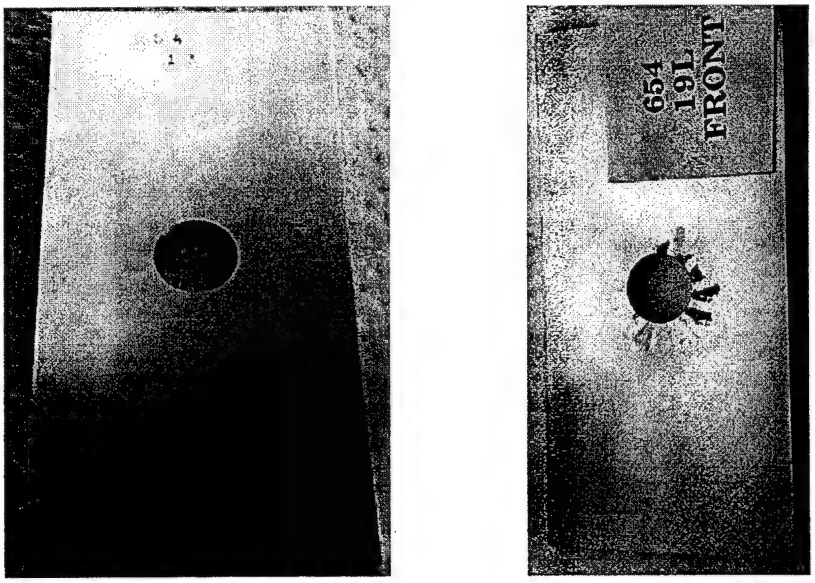

(a) (b)

Figure 81. Large 654SMO stainless steel samples, 3.8x7.6 cm (1.5x3.0 in), exposed for 2 weeks: (a) aerated artificial seawater, (b) ozonated artificial seawater.

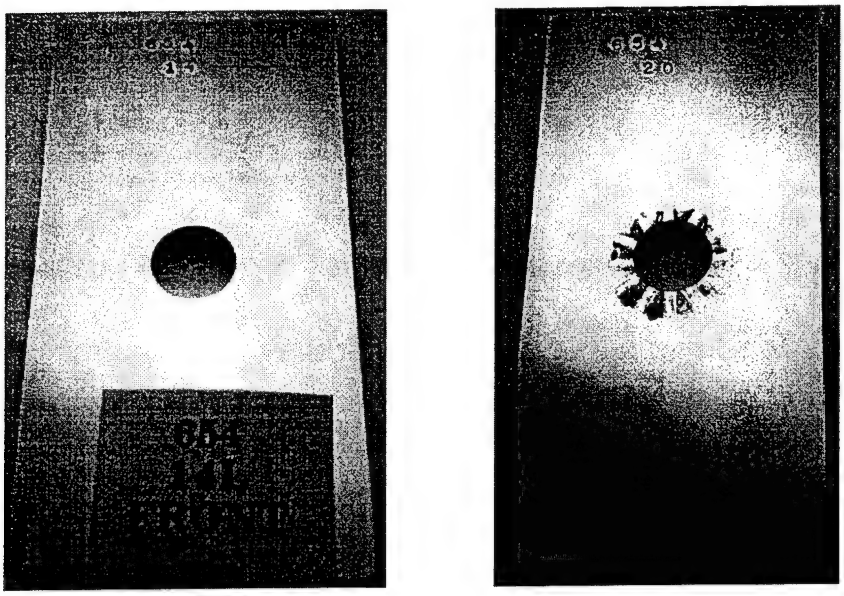

(a) (b)

Figure 82. Large 654SMO stainless steel samples, 3.8x7.6 cm (1.5x3.0 in), exposed for 4 weeks: (a) aerated artificial seawater, (b) ozonated artificial seawater.

Remanit 4565S Stainless Steel

Weight Loss Samples Figure 83 presents the percent weight loss of 4565S stainless steel as a function of exposure time, after exposure to aerated and ozonated artificial seawater. As observed with AL6XN and 654SMO stainless steels, there was no significant weight change in either aerated or ozonated artificial seawater.

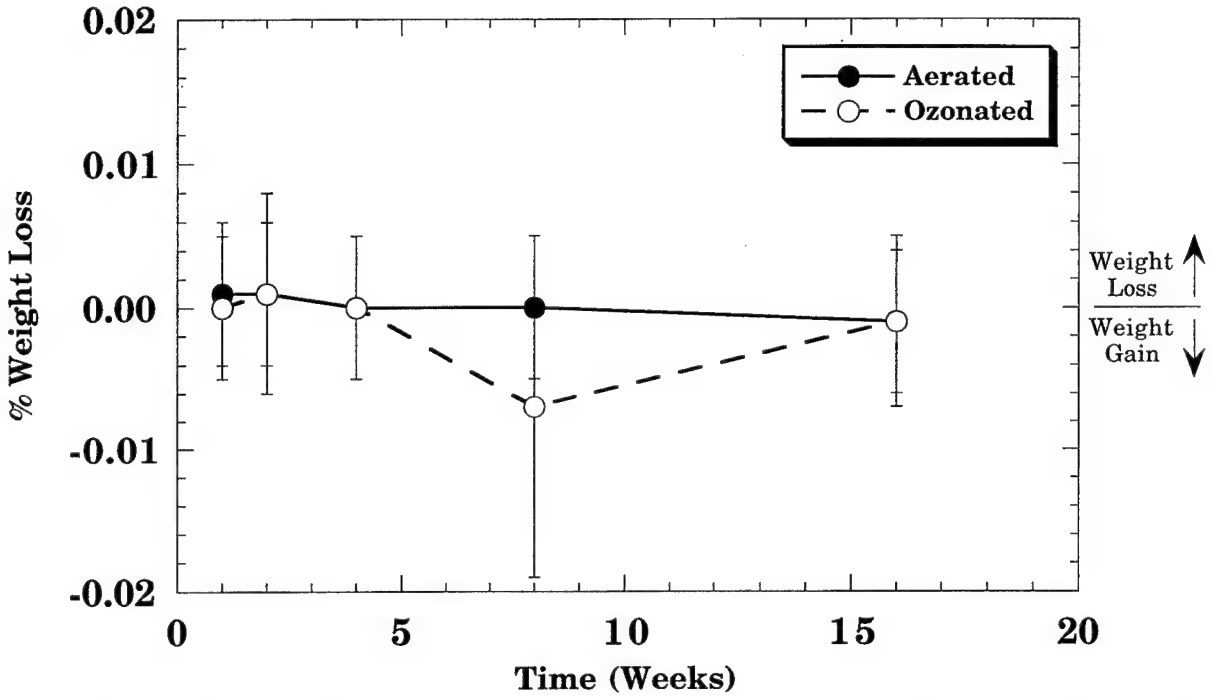

Figure 83. Percent weight loss of Remanit 4565S stainless steel in aerated and ozonated artificial seawater. Note that the corrosion product was not removed because samples were re-immersed at each time period.

Crevice Samples Figure 84 shows the corrosion around the crevice areas that occurred on Remanit 4565S stainless steel samples exposed to aerated and ozonated seawater, after 4 weeks exposure. The appearance is similar to that seen on 654SMO stainless steel. Oxide discoloration is visible in the slot regions between crevice plateaus on the ozonated samples; the aerated samples show virtually no effect of the crevice. Large cathodic area crevice samples also showed the same behavior, as early as 2 weeks, seen in Figures 85-86. Black corrosion product was seen at the mouth of slot, along the outer perimeter of the crevice washer. The color pattern of the plateau and slot surfaces in similar to the appearance of those areas on 654SMO stainless steel. As seen with 654SMO and AL6XN stainless steels, increasing exposure time generally results in thickening and cracking of the oxide, with a greater area fraction of dark oxide present on average in the slots.

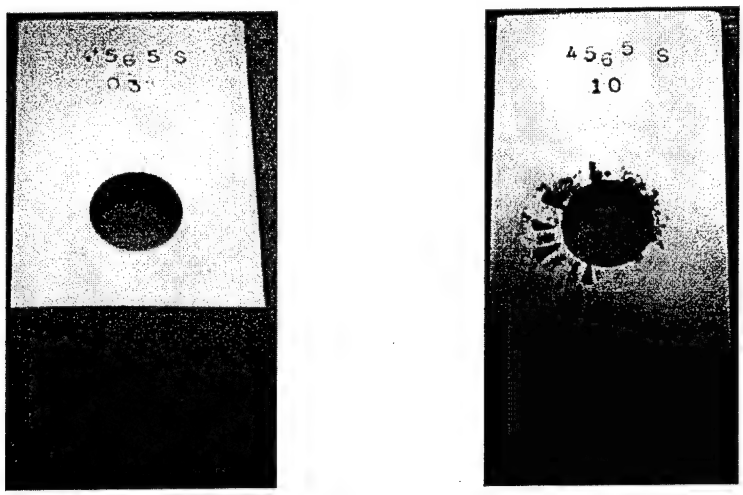

(a) (b)

Figure 84. Small Remanit 4565S stainless steel samples, 2.5x5.1 cm (1.0x2.0 in), exposed for 4 weeks: (a) aerated artificial seawater, (b) ozonated artificial seawater.

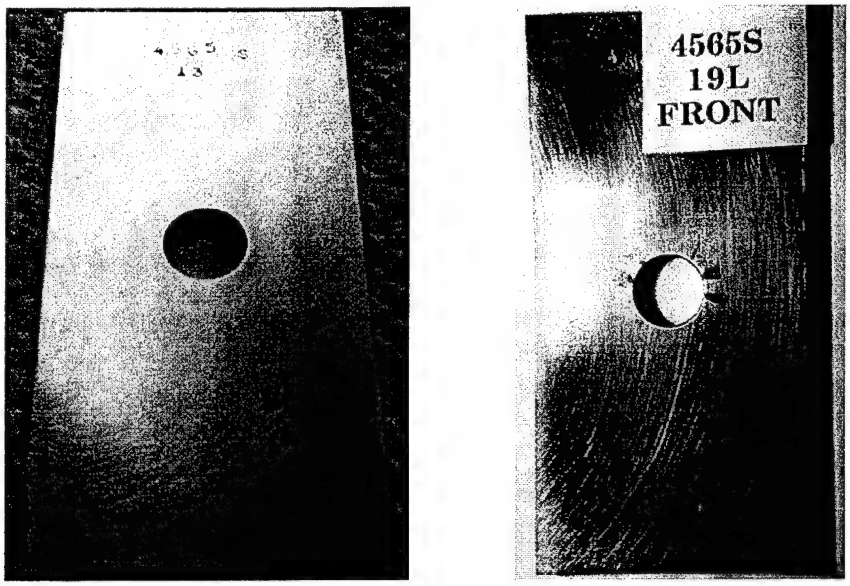

(a) (b)

Figure 85. Large Remanit 4565S stainless steel samples, 3.8x7.6 cm (1.5x3.0 in), exposed for 2 weeks: (a) aerated artificial seawater, (b) ozonated artificial seawater.

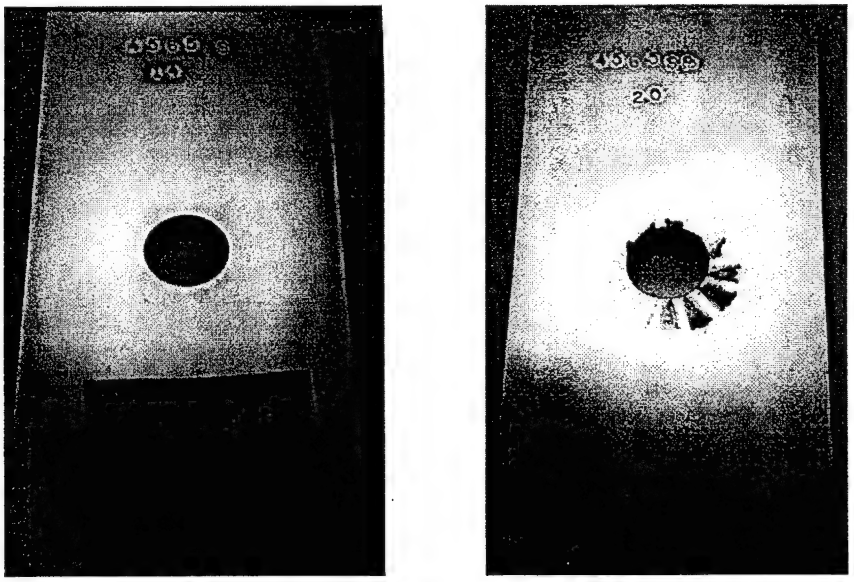

(a) (b)

Figure 86. Large Remanit 4565S stainless steel samples, 3.8x7.6 cm (1.5x3.0 in), exposed for 4 weeks: (a) aerated artificial seawater, (b) ozonated artificial seawater.

Titanium Alloys

Titanium Grade-2

Weight Loss Samples Figure 87 shows the percent weight loss (%WTL) of titanium Grade-2 samples after exposure to either aerated or ozonated seawater. No significant weight change occurred in either condition.

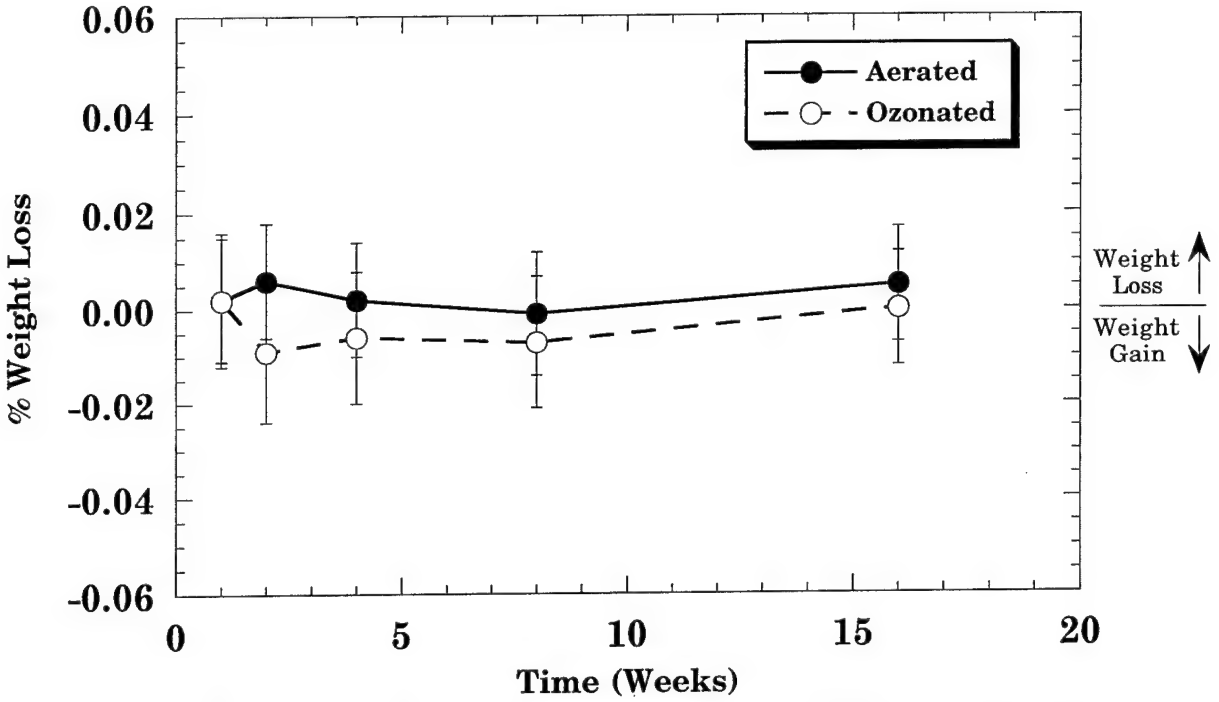

Figure 87. Percent weight loss of titanium Grade-2 in aerated and ozonated artificial seawater. Note that the corrosion product was not removed because samples were re-immersed at each time period.

Crevice Samples Small titanium Grade-2 crevice samples, 2.5x5.1 cm (1.0x2.0 in), exposed for 4 weeks showed enhanced pitting under crevices created with Teflon crenelated washers when solutions were ozonated (Fig. 88), and no evidence of crevice corrosion in solutions that were aerated.

Analyses of the corrosion products of small titanium Grade-2 Teflon creviced samples exposed to the ozonated solutions for 4 weeks indicate that a measurable amount of fluorine is contained within the corrosion product. No similar corrosion product was observed for metal-to-metal crevices, or for crevices in aerated solutions. Thus it can be concluded that ozone enhanced the degradation of the Teflon washers used to create the crevices, and could be responsible for enhanced crevice corrosion. This observation is of particular interest since discussions with the manufacturer of

the Teflon indicated that Teflon is considered to be inert to ozone. In view of the fact that engineering alloys can be expected to be in contact with a number of polymeric gasketing materials, many of which are based on chlorinated hydrocarbons, the observation of degradation of a relatively inert material such as Teflon is of considerable interest.

A brown ring, found by EDS to contain iron based corrosion products, was formed at the mouth of the crevice of the metal to metal crevice samples in both aerated and ozonated seawater (Fig. 89). The sample exposed to ozone appeared to have a darker and more substantial ring, indicating that ozone enhanced the dissolution of the small amount of iron alloyed with the titanium Grade-2 (0.3 wt.%). This preferential corrosion appears to be confined to the surface layers of the titanium (Fig. 90) and does not result in the pitting morphology often associated with crevice corrosion.

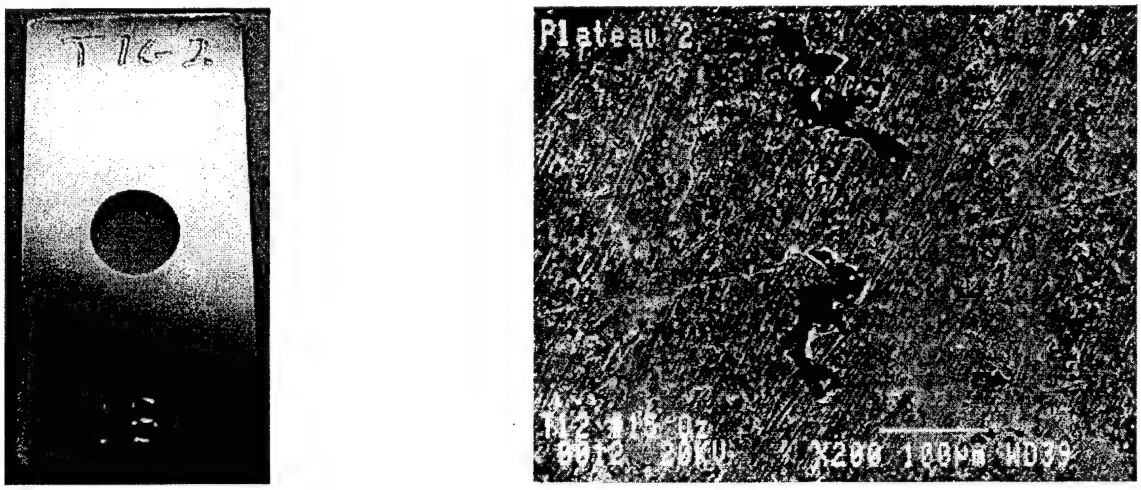

(a) (b)

Figure 88. Small Titanium Grade-2 crevice sample, 2.5x5.1 cm (1.0x2.0 in), ozonated for 4 weeks. (a) Very little damage evident macroscopically, although damage (b) becomes apparent under the SEM at 200x.

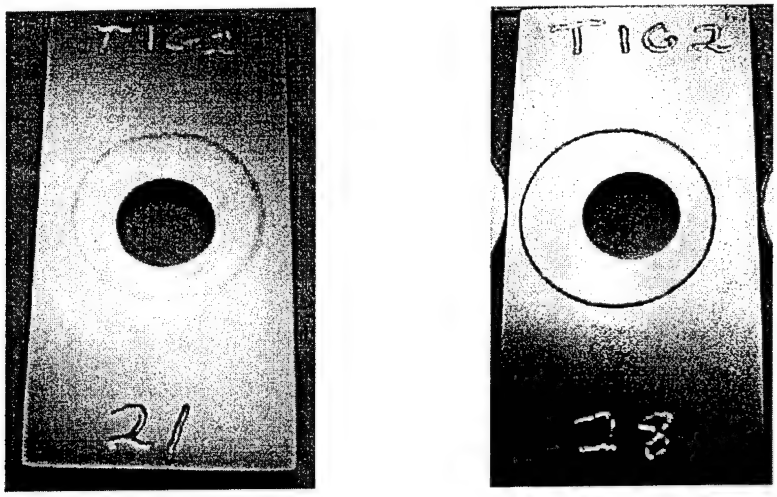

(a) (b)

Figure 89. Small Titanium Grade-2 crevice samples, 2.5x5.1 cm (1.0x2.0 in), with a metal-metal crevice exposed for 4 weeks: (a) aerated artificial seawater (b) ozonated artificial seawater. Note the brown iron corrosion product ring which formed at the interface between the sample and the metal washer.

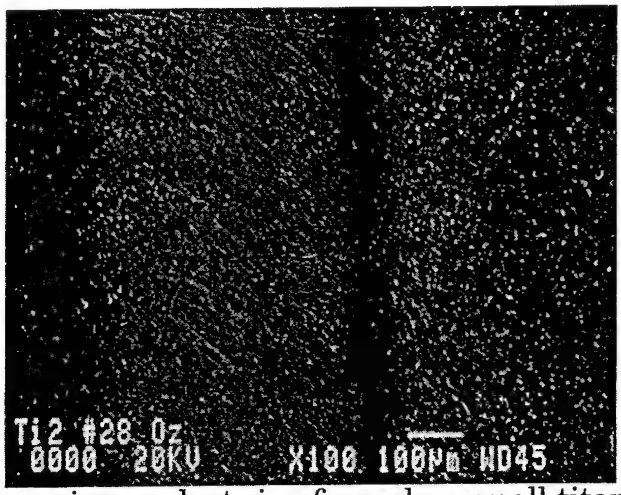

Figure 90. Iron corrosion product ring formed on small titanium Grade-2 crevice sample with a metal-metal crevice exposed for 4 weeks in ozonated artificial seawater.

Wire Samples Electrochemical testing of titanium Grade-2 wires in the tanks showed that the corrosion potential of wires in ozonated artificial seawater is shifted 0.6 to 0.8 V noble to the corrosion potential of aerated seawater, depending on the time of exposure (Fig. 91).

Corrosion rate values calculated from LPR measurements on titanium Grade 2 wires are shown in Figure 92. Rates in both aerated and ozonated seawater were less than 0.5 μm/y (0.02 mpy) at 4 weeks of exposure. The corrosion rate of ozonated wires increased to 1 μm/y (0.04 mpy) at 8 weeks, then decreased to less than 0.5 μm/y (0.02 mpy). Aerated samples showed the opposite trend at 8 and 16 week exposure times.

Polarization curves of titanium Grade-2 show a noble shift in the zero current potential, as well as a decrease in current density, in ozonated compared to aerated artificial seawater (Fig. 93).

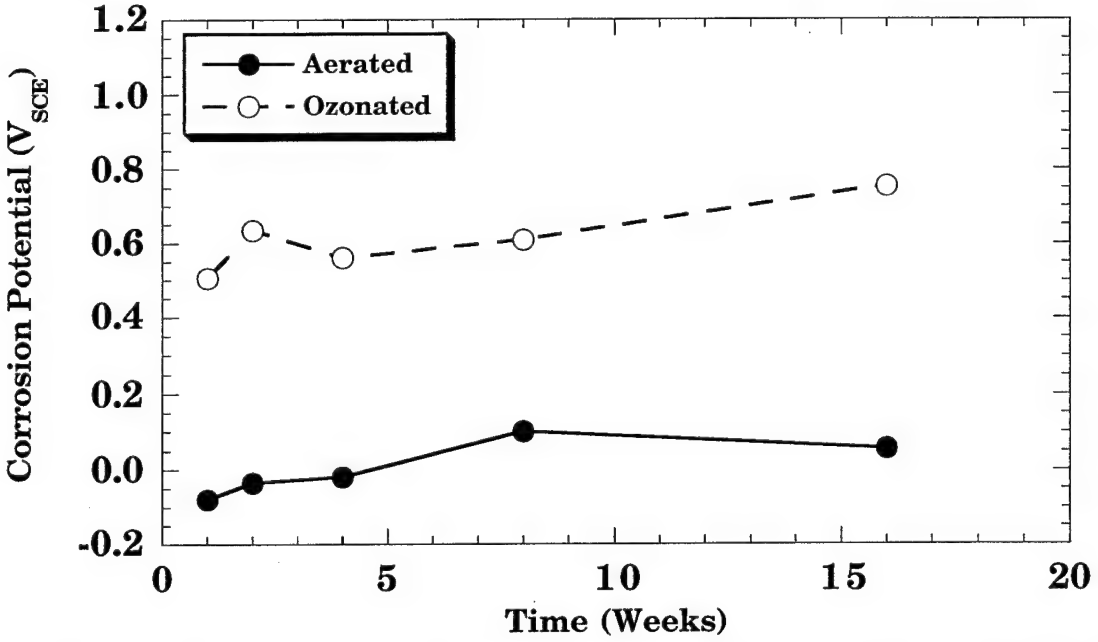

Figure 91. The steady state corrosion potential of titanium Grade-2 wire exposed to aerated or ozonated artificial seawater.

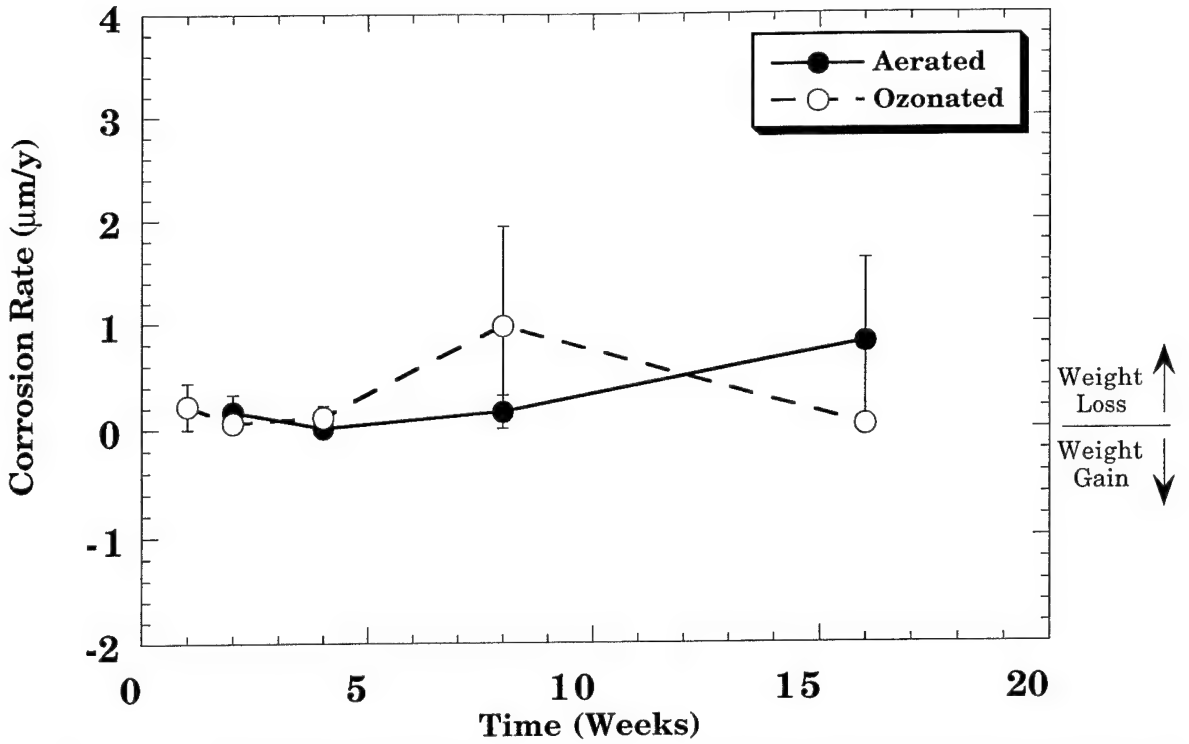

Figure 92. A comparison of the corrosion rates of titanium Grade-2 wire samples calculated from LPR measurements in aerated and ozonated seawater.

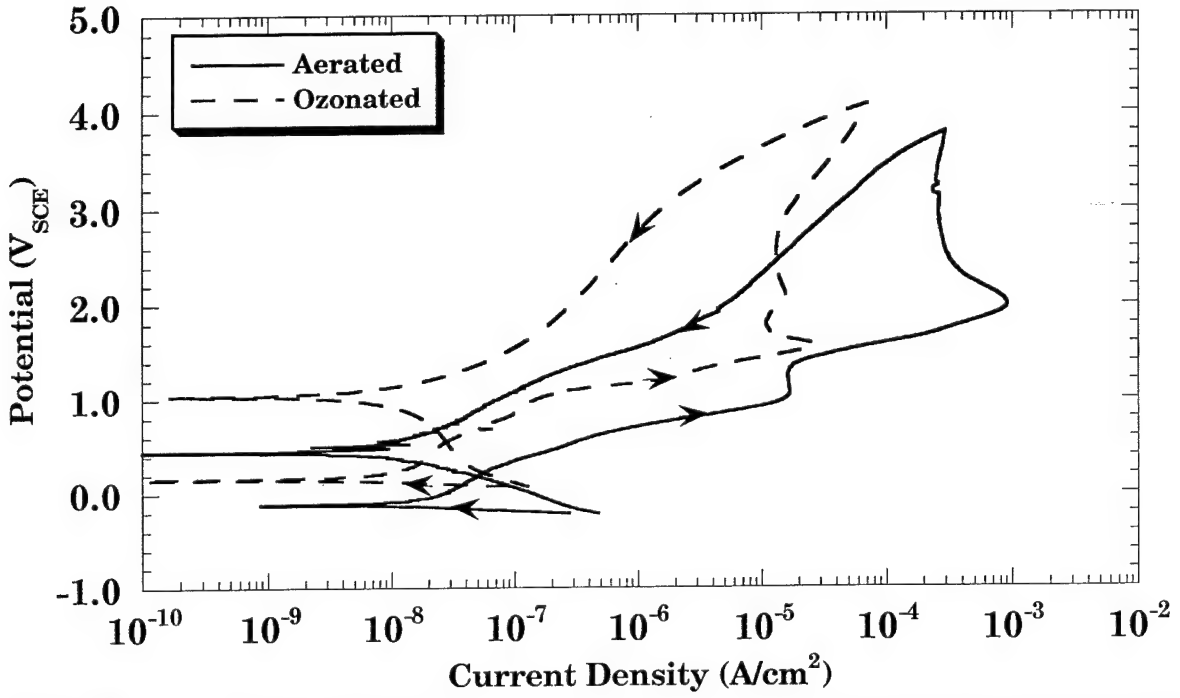

Figure 93. A comparison of the polarization curves of titanium Grade-2 wires exposed to aerated or ozonated artificial seawater for 4 weeks.

Titanium Grade-5

Weight Loss Samples As seen for titanium Grade-2, the %WTL on the titanium Grade-5 samples was very small, as shown in Figure 94.

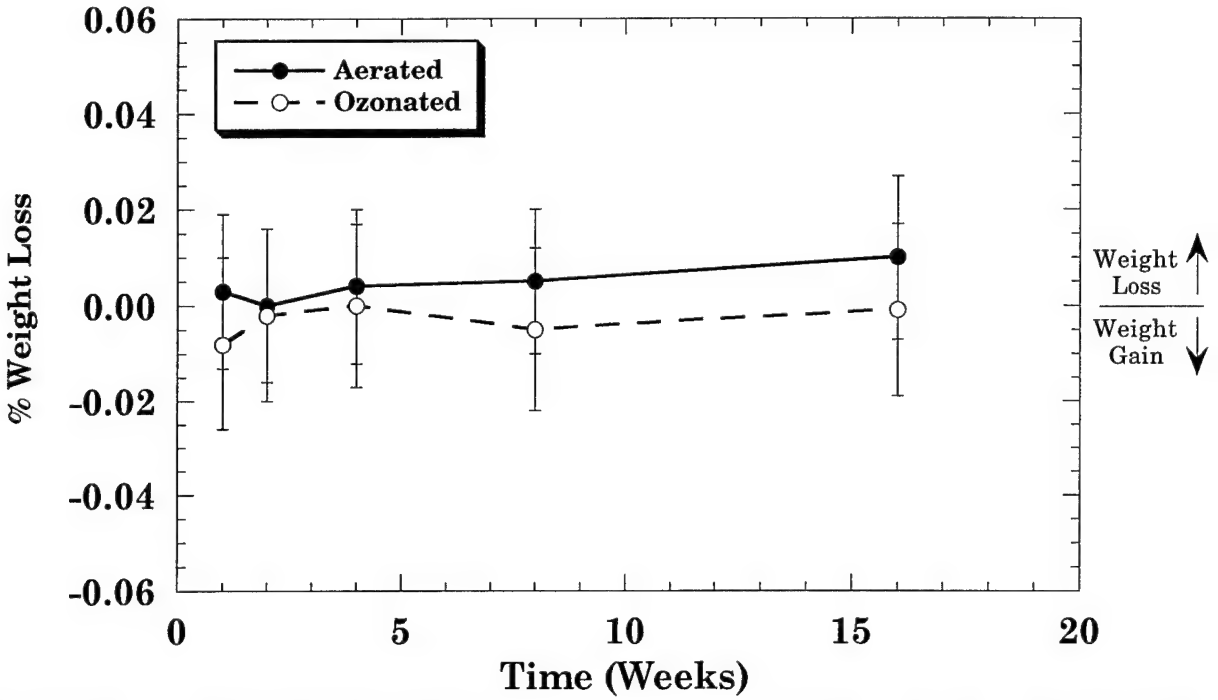

Figure 94. Percent weight loss of titanium Grade-5 in aerated and ozonated artificial seawater. Note that the corrosion product was not removed because samples were re-immersed at each time period.

Crevice Samples Titanium Grade-5 alloys showed enhanced pitting under crevices created with Teflon crenelated washers when exposed for more than 4 weeks in ozonated seawater (Fig. 95-96). No evidence of crevice corrosion was found on samples exposed to aerated solutions. This enhanced crevice corrosion may be due to the breakdown of the Teflon crenelated washer in ozonated solutions.

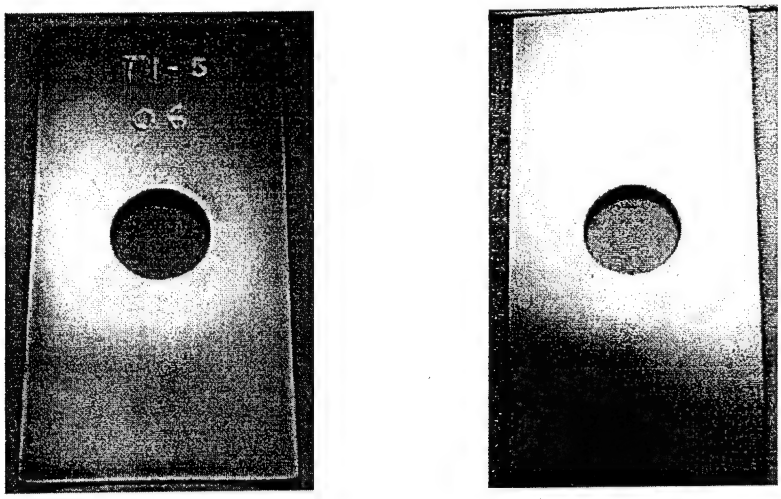

(a) (b)

Figure 95. Small titanium Grade-5 crevice samples, 2.5x5.1 cm (1.0x2.0 in), exposed for 4 weeks: (a) aerated artificial seawater (b) ozonated artificial seawater.

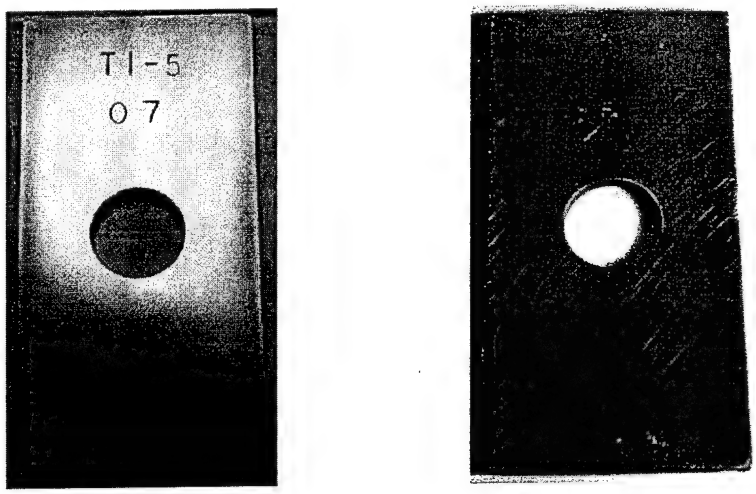

(a) (b)

Figure 96. Small titanium Grade-5 crevice samples, 2.5x5.1 cm (1.0x2.0 in), exposed for 8 weeks: (a) aerated artificial seawater (b) ozonated artificial seawater.

Wire Samples Electrochemical testing of titanium Grade-5 wires in the tanks showed that the corrosion potential of wires in ozonated artificial seawater is shifted 0.6 to 0.8 V noble to the corrosion potential of aerated seawater, to a steady state value in the range of 0.75 - 0.85 V_{SCE} (Fig. 97).

Corrosion rate values calculated from LPR measurements are very low, consistent with the low %WTL seen in Figure 94. The aerated seawater results show increasing corrosion rates with time, while the corrosion rate in ozonated seawater

stays relatively constant (Fig. 98).

Cyclic polarization curves of titanium Grade-5 show a noble shift in the zero current potential, as well as a decrease in current density, in ozonated compared to aerated artificial seawater (Fig. 99).

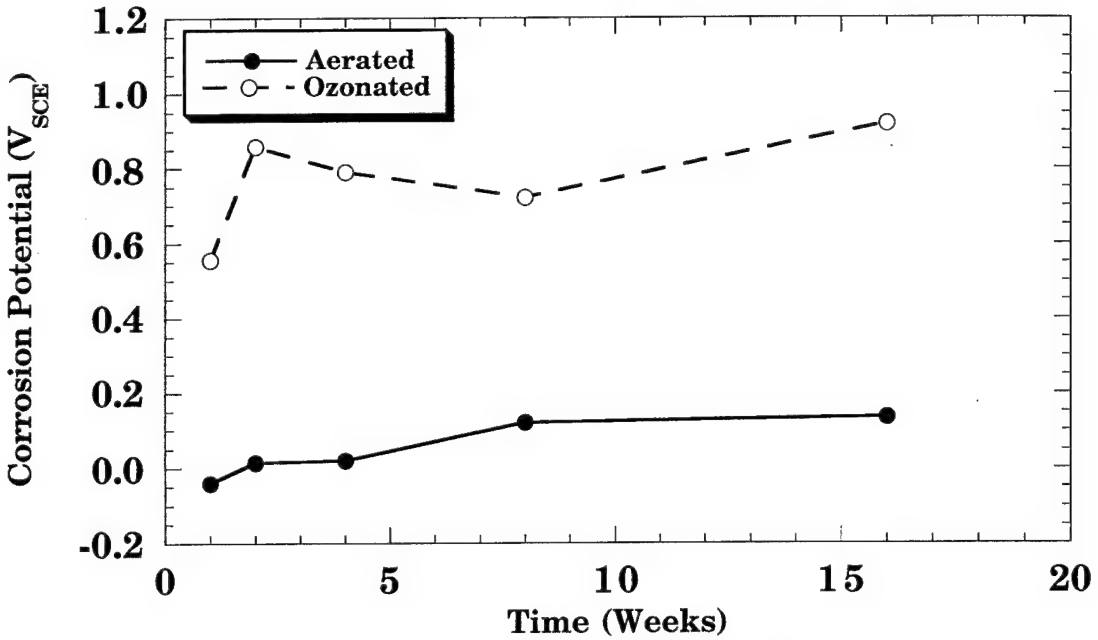

Figure 97. The steady state corrosion potential of titanium Grade-5 wire exposed to aerated or ozonated artificial seawater.

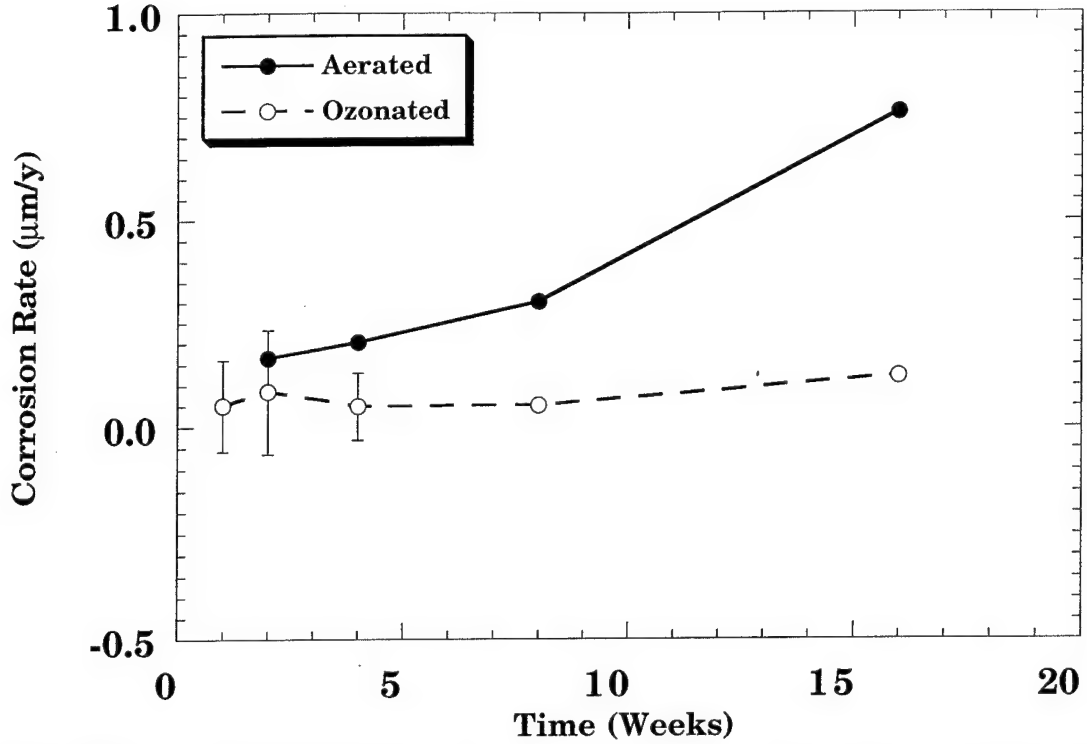

Figure 98. A comparison of the corrosion rates calculated from LPR measurements for titanium Grade-5 in aerated and ozonated seawater.

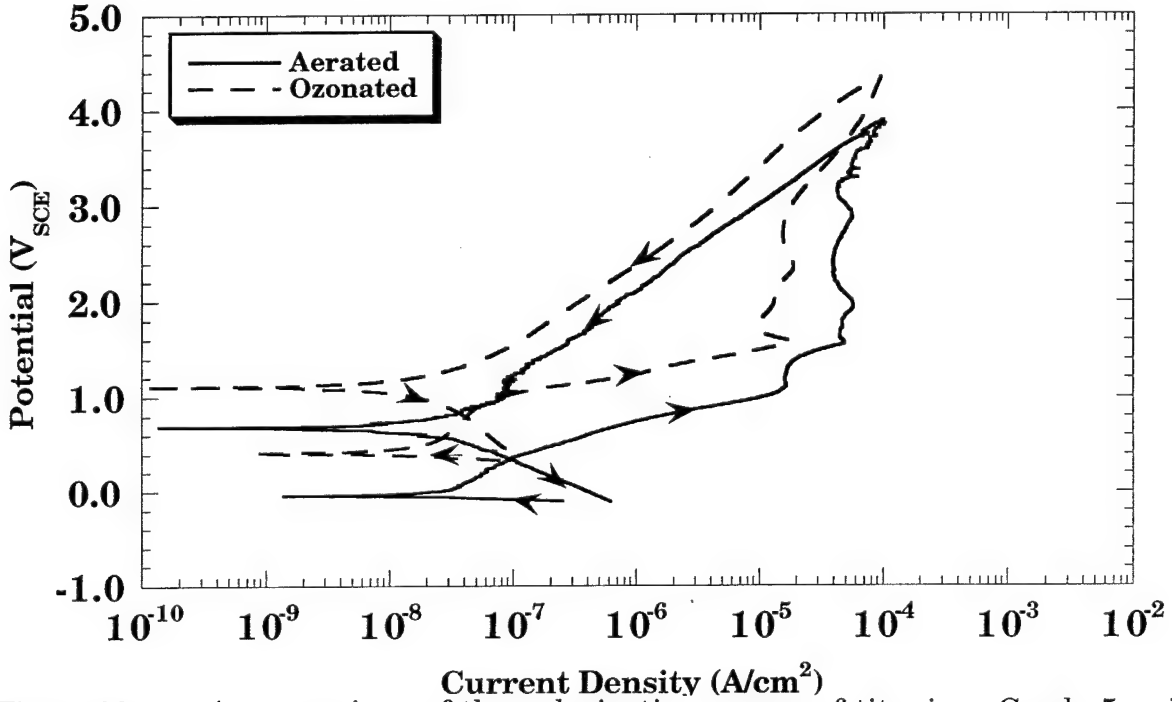

Figure 99. A comparison of the polarization curves of titanium Grade-5 wires exposed to aerated or ozonated artificial seawater for 4 weeks.

Titanium Grade-7

Weight Loss Samples The percent weight loss (%WTL) for titanium Grade-7 exposed to aerated and ozonated seawater is shown in Fig. 100. The results show very little weight loss in either case.

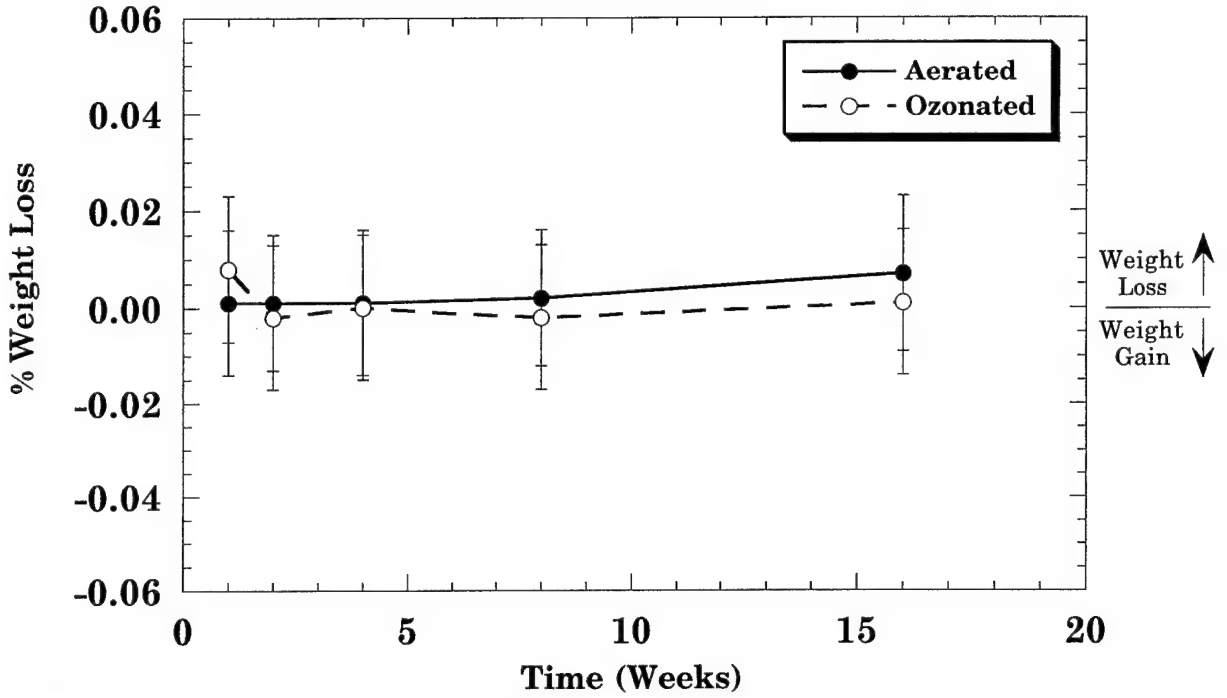

Figure 100. Percent weight loss for titanium Grade-7 in aerated and ozonated artificial seawater. Note that the corrosion product was not removed because samples were re-immersed at each time period.

Crevice Samples Titanium Grade-7 alloys showed enhanced pitting under crevices created with Teflon crenelated washers when solutions were ozonated for more than 4 weeks (Fig. 101-102), and no evidence of crevice corrosion in solutions that were aerated. This enhanced crevice corrosion could be due to the breakdown of the Teflon crenelated washer in ozonated solutions.

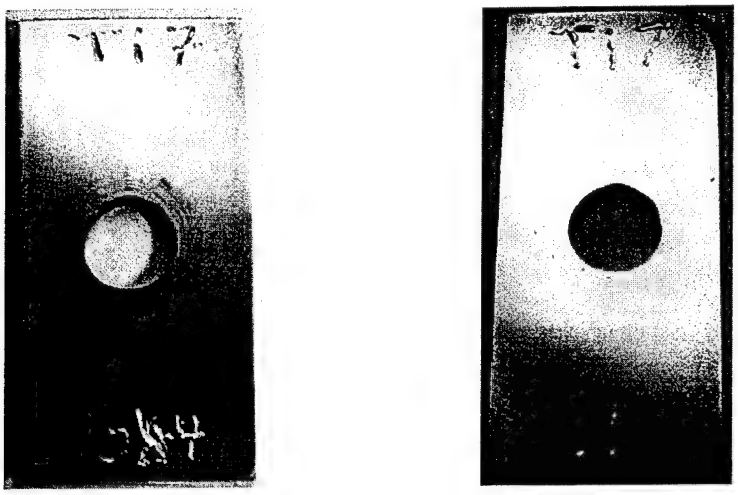

(a) (b)

Figure 101. Small Titanium Grade-7 crevice sample, 2.5x5.1 cm (1.0x2.0 in), exposed for 4 weeks: (a) aerated artificial seawater (b) ozonated artificial seawater.

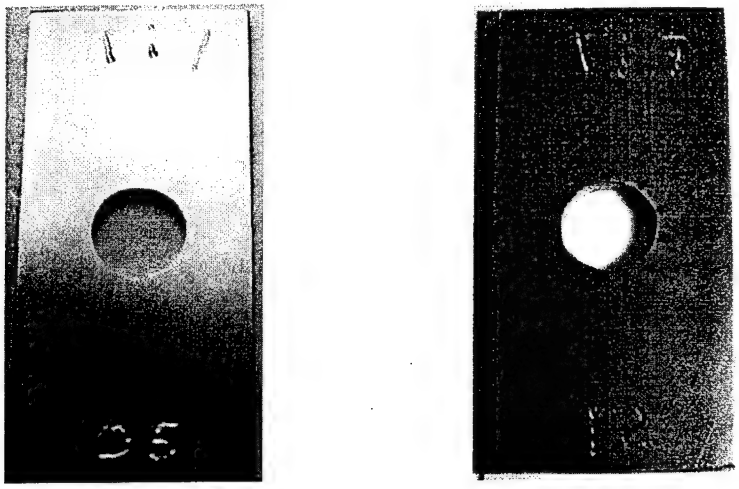

(a) (b)

Figure 102. Small Titanium Grade-7 crevice sample, 2.5x5.1 cm (1.0x2.0 in), exposed for 4 weeks: (a) aerated artificial seawater (b) ozonated artificial seawater.

Titanium Grade-12

Weight Loss Samples Consistent with other titanium grades, the %WTL on the titanium Grade-12 samples was very small in aerated and ozonated seawater, as shown in Figure 103.

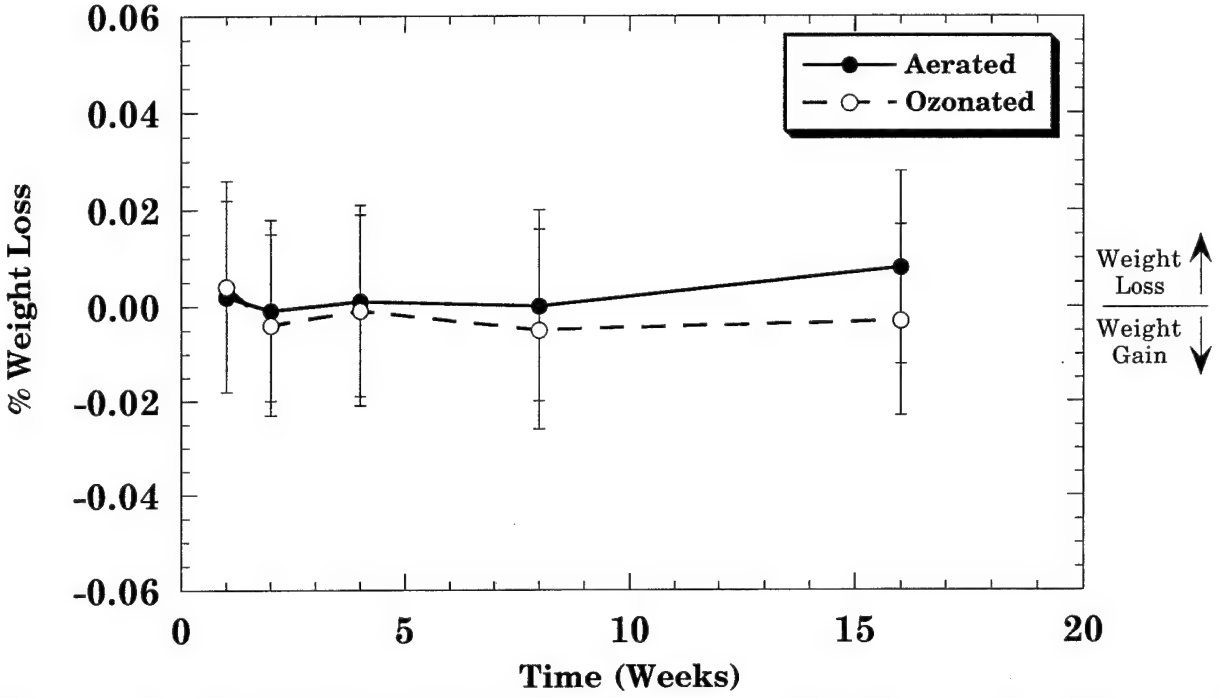

Figure 103. Percent weight loss of titanium Grade-12 in aerated and ozonated artificial seawater. Note that the corrosion product was not removed because samples were re-immersed at each time period.

Crevice Samples Titanium Grade-12 alloys showed enhanced pitting under crevices created with Teflon crenelated washers when solutions were ozonated, but no significant difference was seen until 16 weeks (Fig. 104-105), and no evidence of crevice corrosion in solutions that were aerated. This enhanced crevice corrosion may be due to the breakdown of the Teflon crenelated washer in ozonated solutions.

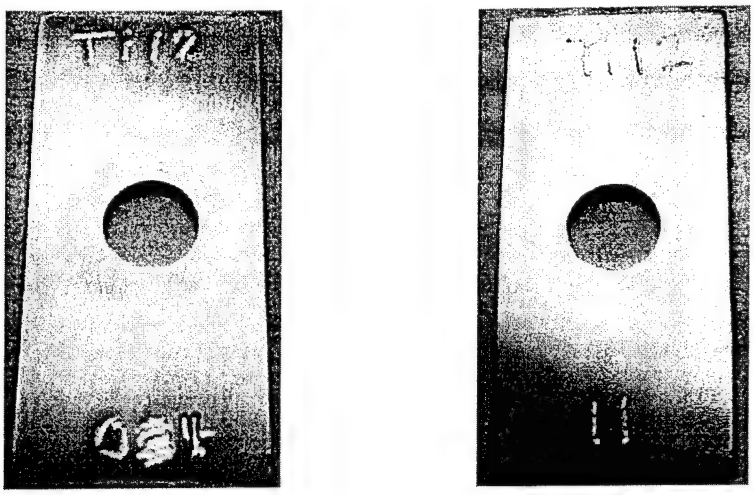

(a) (b)

Figure 104. Small Titanium Grade-12 crevice samples, 2.5x5.1 cm (1.0x2.0 in), exposed for 4 weeks: (a) aerated artificial seawater (b) ozonated artificial seawater.

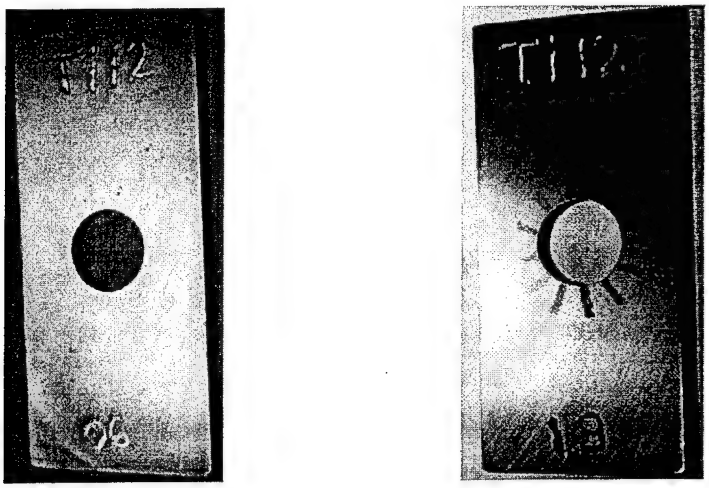

(a) (b)

Figure 105. Small Titanium Grade-12 crevice samples, 2.5x5.1 cm (1.0x2.0 in), exposed for 16 weeks: (a) aerated artificial seawater (b) ozonated artificial seawater.

β-C Titanium

Weight Loss Samples The %WTL the β-C titanium samples was very small for both aerated and ozonated seawater, as shown in Figure 106.

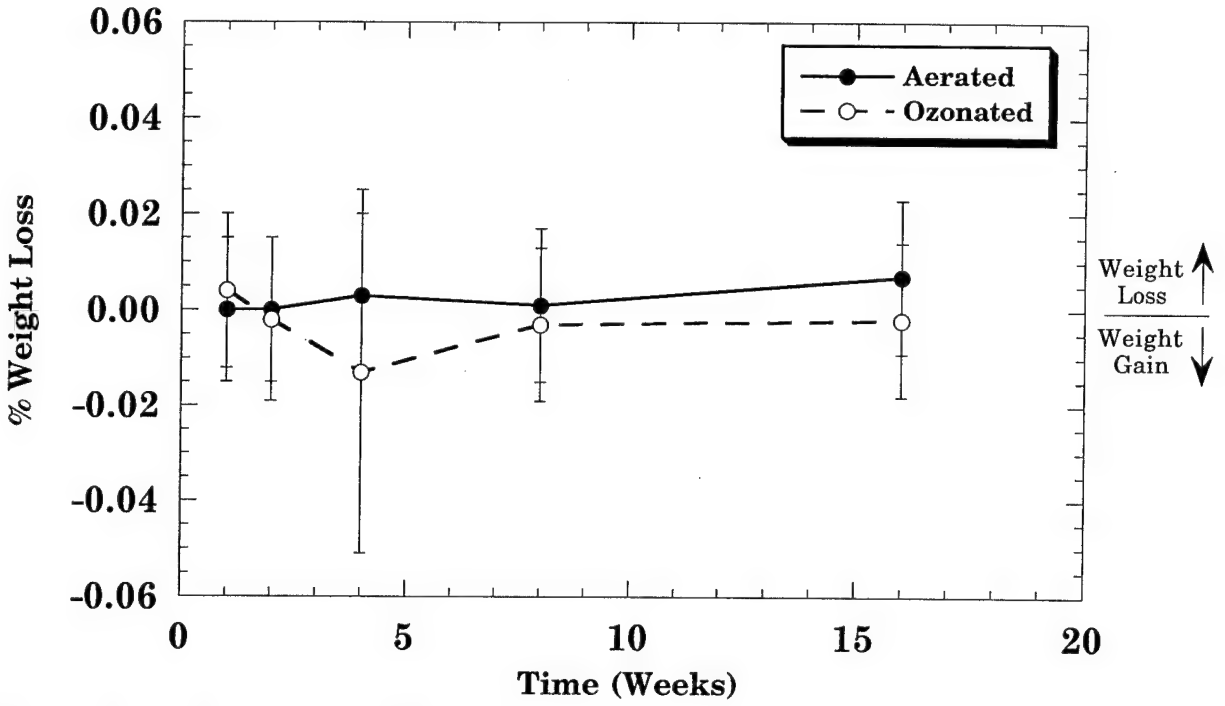

Figure 106. Percent weight loss of β-C titanium in aerated and ozonated artificial seawater. Note that the corrosion product was not removed because samples were re-immersed at each time period.

Crevice Samples Titanium β-C alloys showed enhanced pitting under crevices created with Teflon crenelated washers when solutions were ozonated, with the largest difference in behavior occurring between 4 and 8 weeks (Fig. 107-108). No real evidence of crevice corrosion was observed in solutions that were aerated. This enhanced crevice corrosion may be due to the breakdown of the Teflon crenelated washer in ozonated solutions.

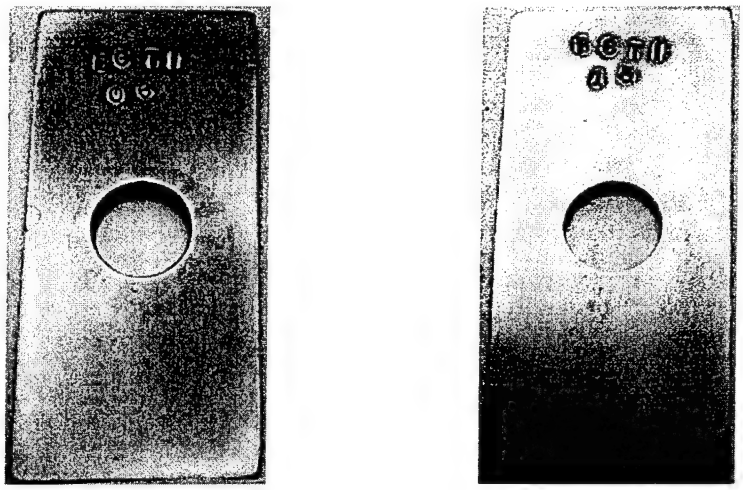

(a) (b)

Figure 107. Small β-C titanium crevice samples, 2.5x5.1 cm (1.0x2.0 in), exposed for 4 weeks: (a) aerated artificial seawater (b) ozonated artificial seawater.

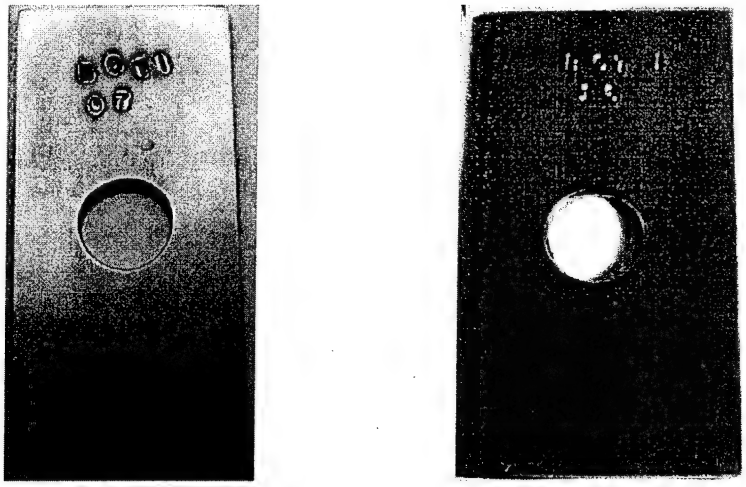

(a) (b)

Figure 108. Small β-C titanium crevice samples, 2.5x5.1 cm (1.0x2.0 in), exposed for 8 weeks: (a) aerated artificial seawater (b) ozonated artificial seawater.

β-21S Titanium

Weight Loss Samples Consistent with other titanium alloys, the %WTL is very low in both aerated and ozonated seawater, as shown in Figure 109.

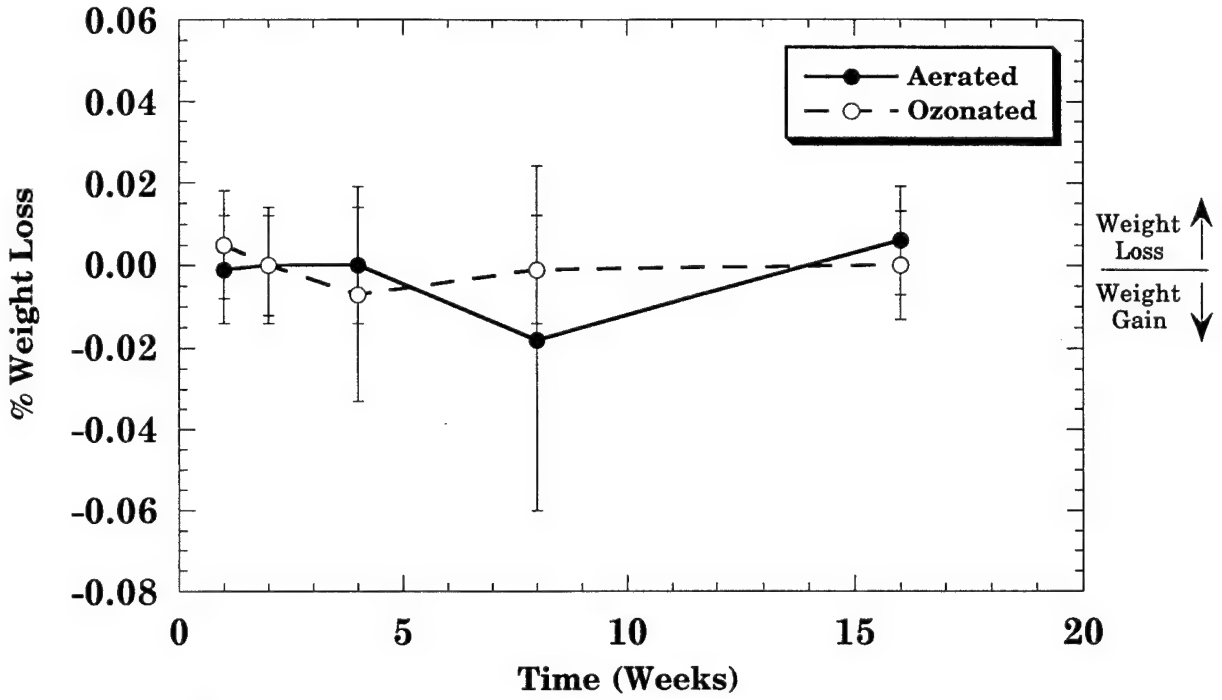

Figure 109. Percent weight loss of β-21S titanium in aerated and ozonated artificial seawater. Note that the corrosion product was not removed because samples were re-immersed at each time period.

Crevice Samples Titanium β-21S alloys showed enhanced pitting under crevices created with Teflon crenelated washers when solutions were ozonated, with the largest difference in behavior occurring between 4 and 8 weeks (Fig. 110-111). No real evidence of crevice corrosion was observed in solutions that were aerated. This enhanced crevice corrosion may be due to the breakdown of the Teflon crenelated washer in ozonated solutions.

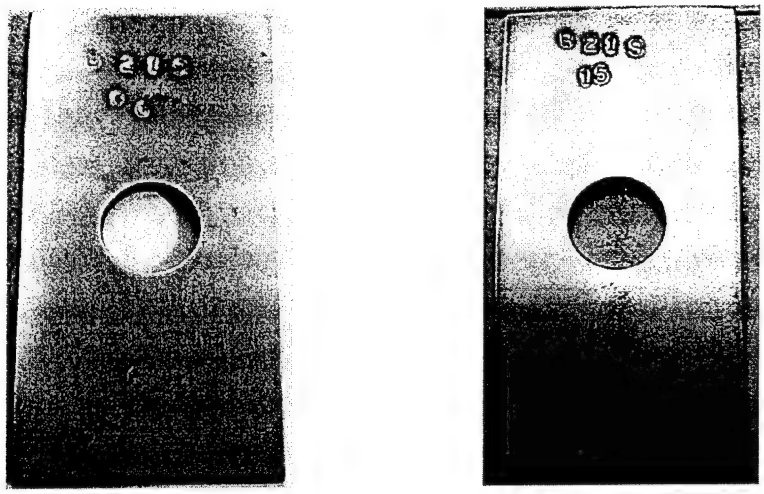

(a) (b)

Figure 110. Small β-21S titanium crevice samples, 2.5x5.1 cm (1.0x2.0 in.), exposed for 4 weeks: (a) aerated artificial seawater (b) ozonated artificial seawater.

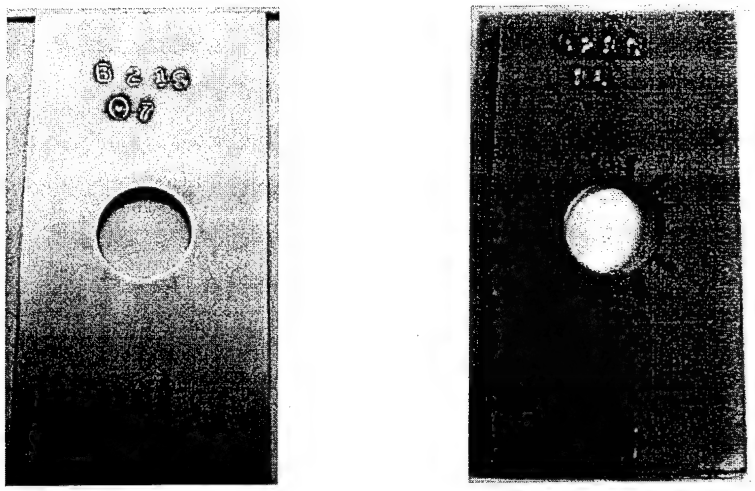

(a) (b)

Figure 111. Small β-21S titanium crevice samples, 2.5x5.1 cm (1.0x2.0 in.), exposed for 8 weeks: (a) aerated artificial seawater (b) ozonated artificial seawater.

Aluminum Alloys

As in the case for the nickel alloys, the general appearance of the surfaces of the aluminum alloys are visibly different when samples exposed to ozonated *vs.* aerated solutions are compared (Fig. 112). Aluminum alloys, virtually independent of alloy content, exhibit a light gray surface discoloration with extensive pitting and the production of large amounts of white corrosion product (hydrated aluminum oxides), when exposed to aerated seawater. Aluminum alloys exposed to ozonated solutions, on the other hand, exhibit a dark slate color (almost black), very adherent general corrosion product. These samples show considerably less pitting and much less of the white corrosion product than samples exposed for equivalent periods of time in aerated seawater.

AL1100

Weight Loss Samples Aluminum alloys, whether creviced or uncreviced, appear to show reduced corrosion in ozonated *vs.* aerated seawater solutions. The exact corrosion rates are difficult to ascertain at this time since no corrosion product has been removed. Figure 112 shows the percent weight loss (%WTL) of AL1100 in aerated *vs.* ozonated seawater. The %WTL for the aerated samples is negative, reflecting the weight gained by the precipitation of white corrosion product on the samples.

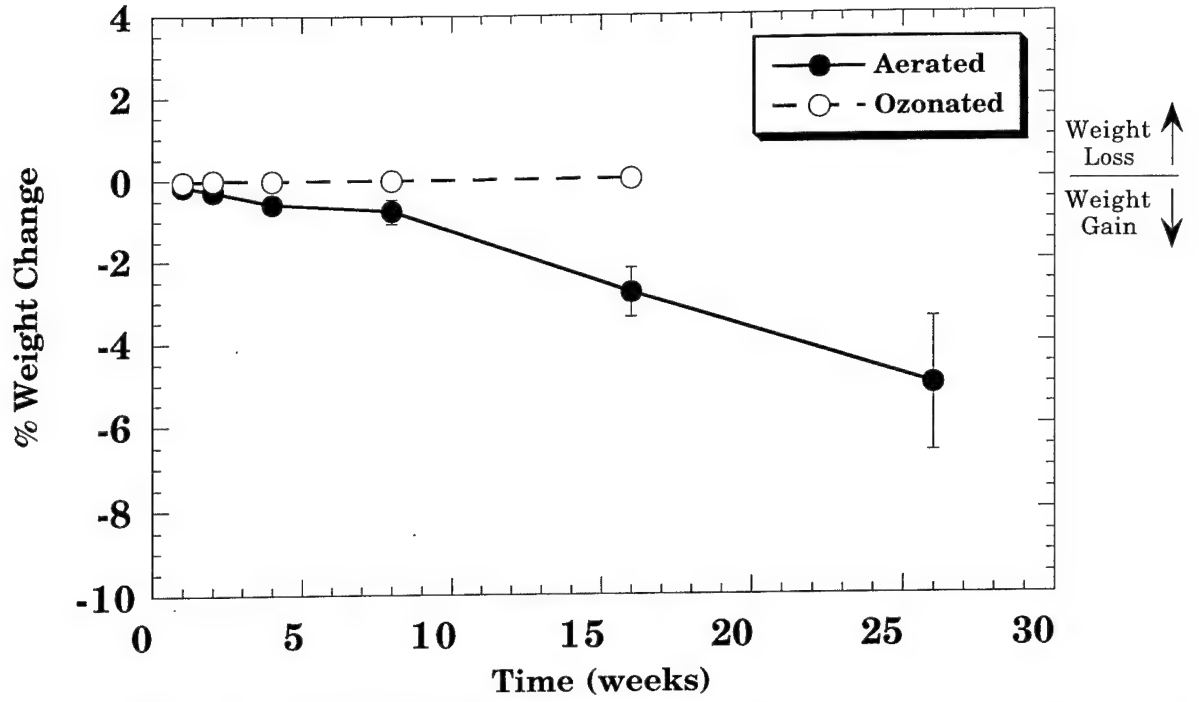

Figure 112. Percent weight of AL1100 in aerated and ozonated artificial seawater calculated from weight loss measurements. Note that the corrosion product was not removed because samples were re-immersed at each time period.

Crevice Samples For creviced aluminum alloys, the area at the mouth of the creviced slots is virtually devoid of corrosion products in ozonated solutions, while the same areas in aerated solutions show extensive production of voluminous corrosion product.

Figure 113 shows the difference between aerated and ozonated samples of AL1100 after 4 weeks of exposure. The aerated sample (Fig. 113a) has large amounts of white corrosion product in the slots between crevice plateaus. Several of the aerated plateaus are heavily damaged by the growth of large pits, while others have only scattered pits. The ozonated sample (Fig. 113b) is characterized by a dark discoloration of the bulk sample, evidence of a coherent oxide layer. The slot regions of the ozonated sample are light gray in color, covered by small scattered amounts of white corrosion product. Many of the crevice plateaus of the ozonated sample are their original silver color, with a dark discoloration around their edges, while other plateaus are stained by the discoloration flowing in from the edges.

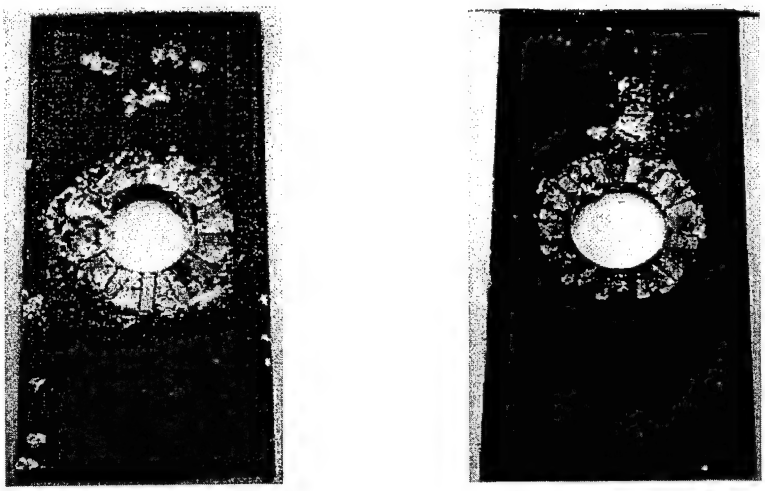

(a) (b)

Figure 113. Small AL1100 crevice samples, 2.5x5.1 cm (1.0x2.0 in) exposed for 4 weeks: (a) aerated artificial seawater, (b) Ozonated artificial seawater. Note lack of white corrosion product in crevice region for ozonated condition.

Wire Samples Electrochemical testing of AL1100 wires in the tanks showed that the corrosion potential of wires in ozonated solutions is shifted 0.25-0.50 V active to the potential in aerated seawater (Fig. 114). These results are in contrast to the other metal alloys which showed a noble shift in corrosion potential.

Comparing the corrosion rates calculated from LPR measurements for AL1100 in aerated and ozonated seawater, it is clear that corrosion rates are markedly lower with ozonation. The aerated case shows a maximum of 23 μm/y (0.9 mpy) at 4 weeks, decreasing to approximately 10 μm/y (0.4 mpy) by 16 weeks exposure. Corrosion rates in ozonated seawater reach a maximum of only 2 μm/y (0.08 mpy) decreasing with time to ≤ 1μm/y (0.04 mpy) by 16 weeks.

Polarization experiments support the surface observations of reduced crevice corrosion in ozonated seawater, especially for the case of AL1100. Figure 116 shows a comparison of polarization curves in aerated and ozonated artificial seawater after 4 weeks. For the ozonated case a breakdown potential of 0.0 V_{SCE} is indicated by a slight knee in the ozonated curve, with a repassivation potential, noble to the zero current potential, of -0.75 V_{SCE}. For the aerated case, the sample shows no breakdown potential and the zero current potential is noble to the crossover of the return portion of the hysteresis loop, indicating severe crevice corrosion susceptibility. Current densities, measured at 0.3 V noble to the zero current potential, show that the ozonated current density is about two orders of magnitude less than the aerated current density. After 8 weeks of exposure the only change in

the aerated polarization curve (Fig. 117), was a decrease in the aerated current density (measured at 0.3 V noble to the zero current potential), showing a difference of only a factor of 10 higher than the ozonated case. The ozonated curve also showed little change from the 4 week curve, except that no breakdown potential was seen by the formation of a knee in the curve, as was evident at 4 weeks.

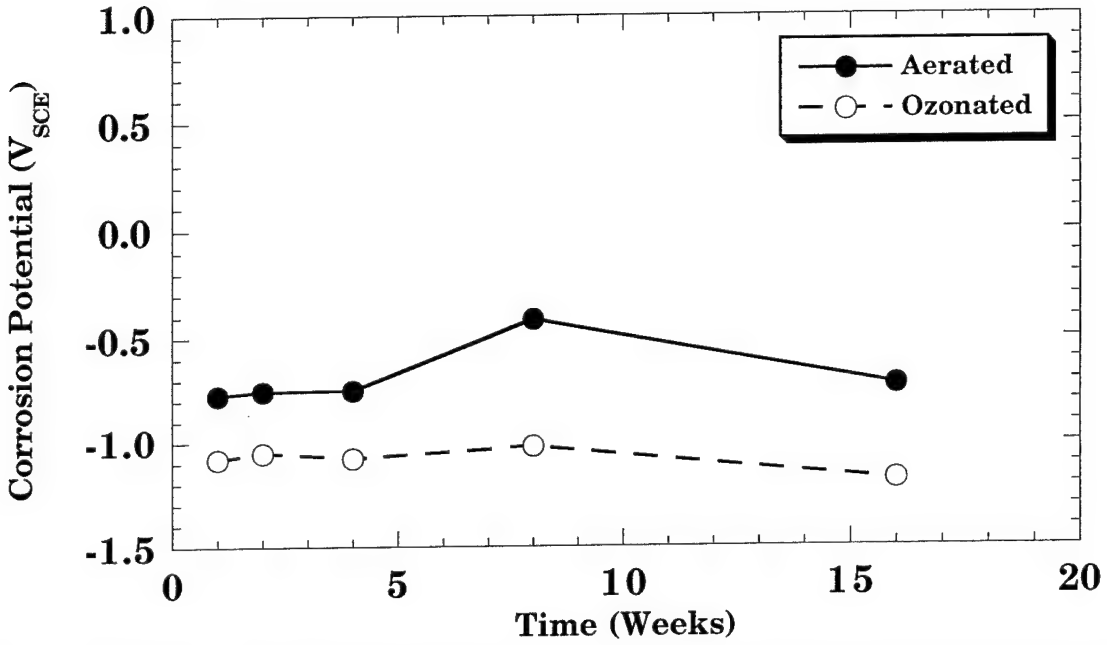

Figure 114. The steady state corrosion potential of AL1100 wires exposed to aerated or ozonated artificial seawater.

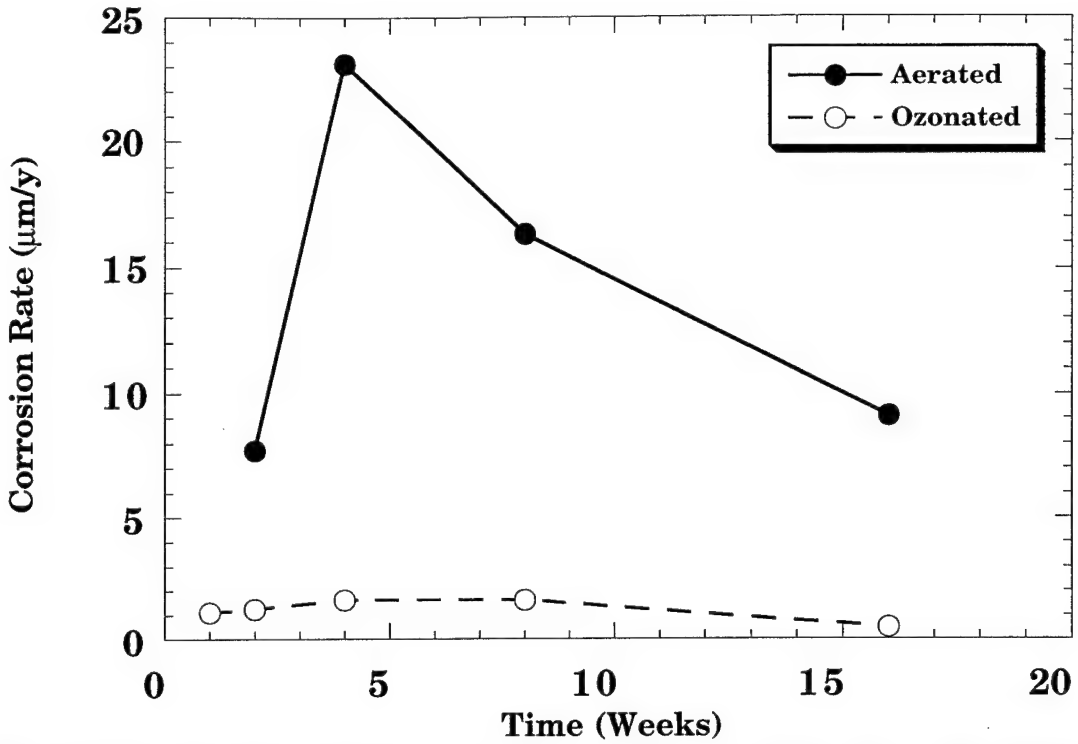

Figure 115. A comparison of the corrosion rates calculated from LPR measurements for AL1100 in aerated and ozonated artificial seawater.

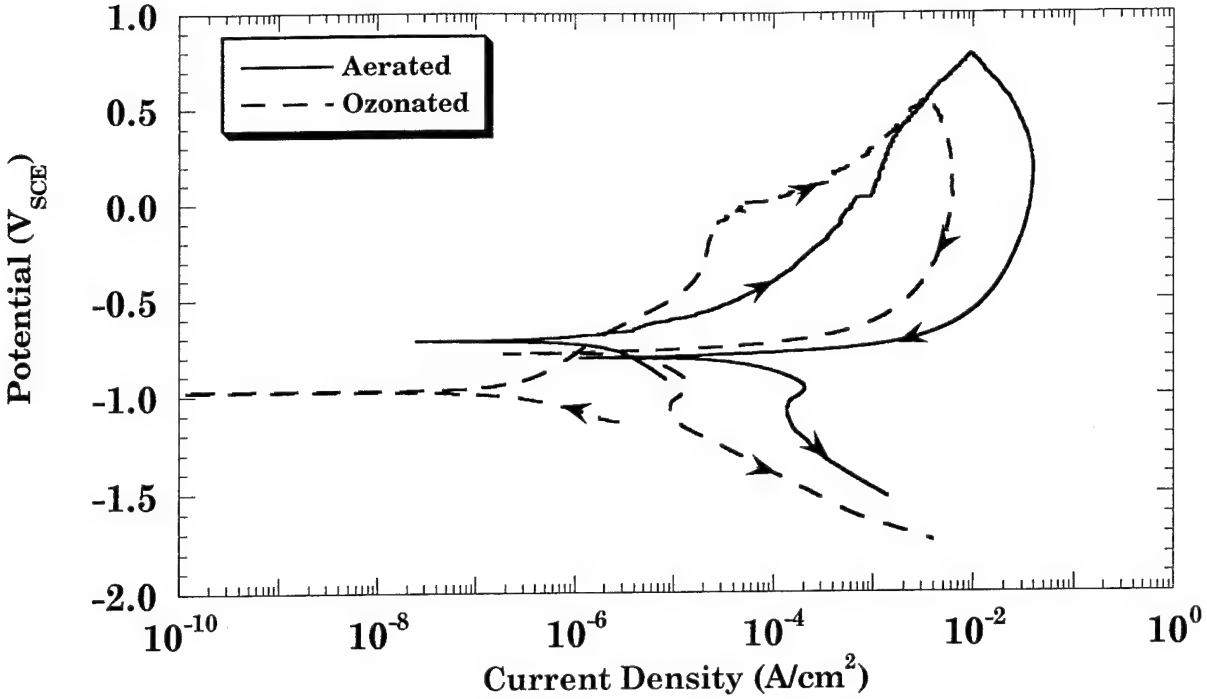

Figure 116. A comparison of polarization curves of AL1100 wires exposed to aerated or ozonated artificial seawater for 4 weeks. Notice that in the aerated case, the repassivation potential is below the zero current potential and there is no breakdown potential.

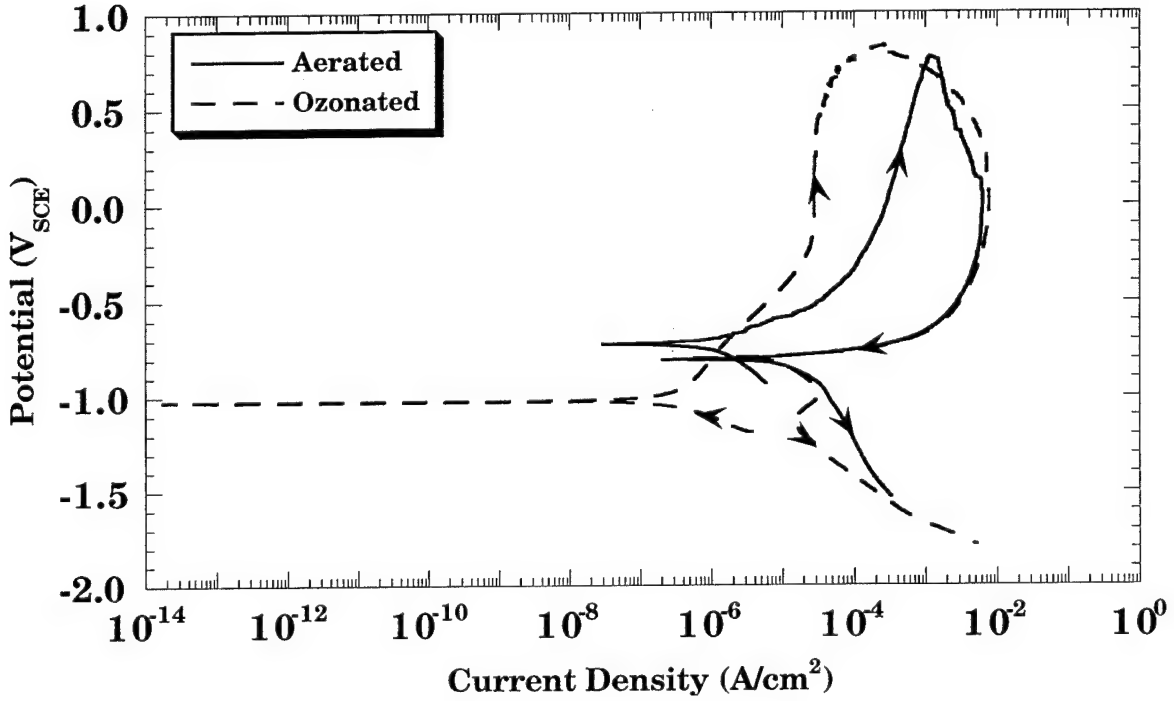

Figure 117. A comparison of polarization curves of AL1100 wires exposed to aerated or ozonated artificial seawater for 8 weeks.

AL5052/AL5356

Weight Loss Samples The exact corrosion rates of the aluminum alloys are difficult to ascertain at this time since no corrosion product has been removed. Figure 118 shows the percent weight loss (%WTL) of AL5052 in aerated *vs.* ozonated seawater. The %WTL for the aerated samples is negative, reflecting the weight gained by the precipitation of white corrosion product on the samples. In contrast, the %WTL for the ozonated case shows no real weight loss.

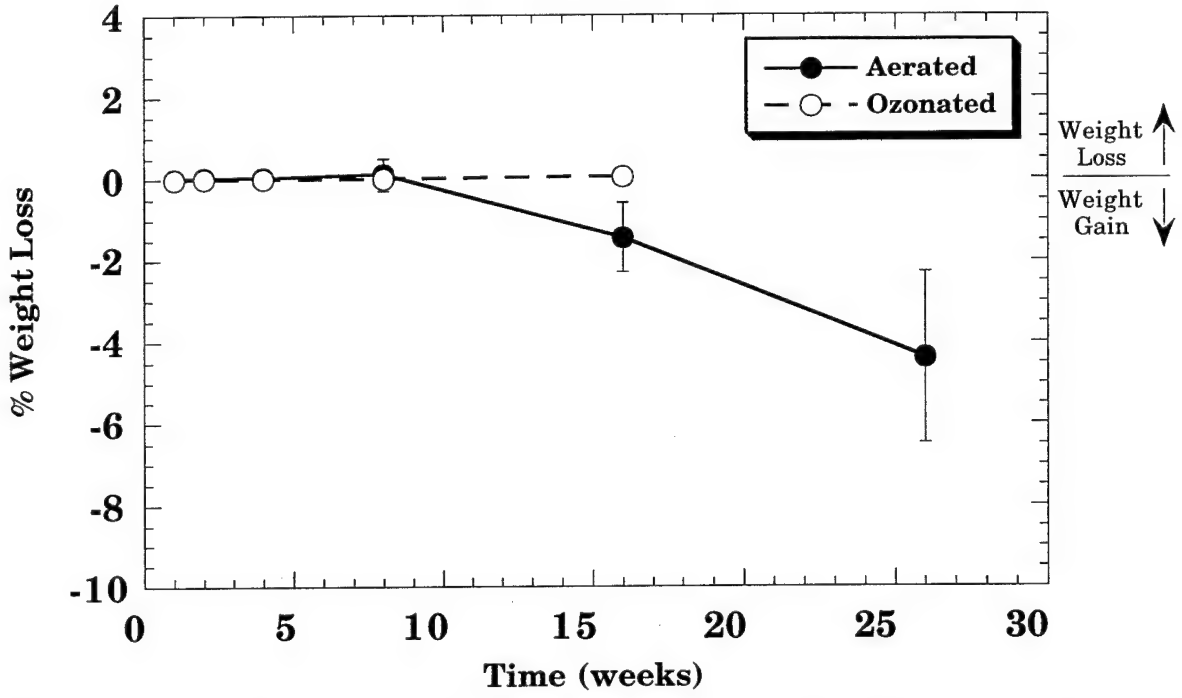

Figure 118. Percent weight loss of AL5052 in aerated and ozonated artificial seawater calculated from weight loss measurements. Note that the corrosion product was not removed because samples were re-immersed at each time period.

Crevice Samples Figure 119 shows the difference between aerated and ozonated samples of AL5052 after 4 weeks of exposure. Large amounts of white corrosion product are present in the slots of the aerated sample (Fig. 119a). Several plateaus on the aerated samples have large amounts of pitting damage, while others have only scattered pits. The ozonated sample (Fig. 119b) is characterized by a dark discoloration of the bulk sample, evidence of a coherent oxide layer. Several slot regions of the ozonated sample contain small scattered amounts of white corrosion product, while others are discolored by what appears to be the formation of the

coherent oxide of the bulk region. This discoloration has traveled under several plateaus, however many of the crevice plateaus are their original silver color. At 20x magnification, many small pits are seen scattered in both the plateau and slot regions.

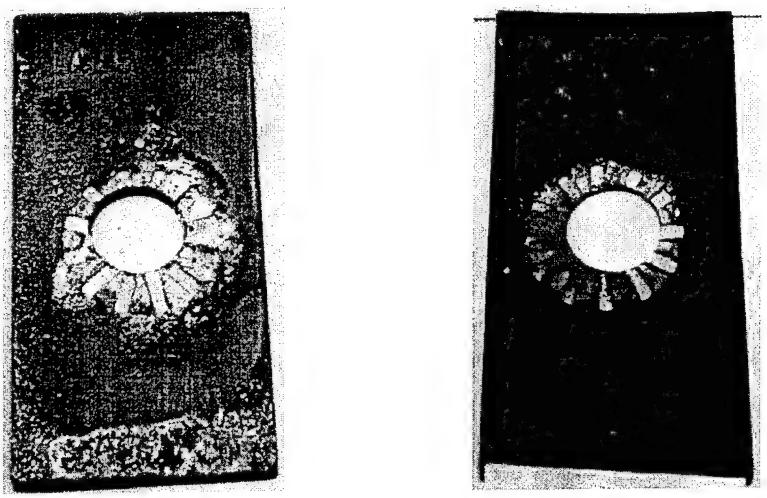

(a) (b)

Figure 119. Small AL5052 crevice samples, 2.5x5.1 cm (1.0x2.0 in) exposed for 4 weeks: (a) aerated artificial seawater, (b) Ozonated artificial seawater. Note lack of white corrosion product in crevice region for ozonated condition.

Wire Samples Electrochemical testing of AL5356 wires, close in composition to AL5052, showed that the corrosion potential of wires in ozonated solutions is shifted about 0.25-0.30 V more active than the potential in aerated seawater (Fig. 120). These results are in contrast to the other metal alloys which showed a noble shift in corrosion potential.

Corrosion rates calculated from LPR measurements of AL5356 wires in aerated and ozonated artificial seawater are shown in Figure 121. AL5356 under aerated conditions shows somewhat higher rates than under ozonated conditions, but the difference is not nearly as great as seen for AL1100. After reaching a maximum of 3.5 μm/y (0.14 mpy) at 8 weeks, the corrosion rate decreases to ≤ 1 μm/y (0.04 mpy) by 16 weeks. Corrosion rates in ozonated seawater increase to about 2 μm/y (0.08 mpy) by 8 weeks, similar to the behavior seen for AL1100.

Figure 122 shows a comparison of polarization curves of AL5356 wires in aerated and ozonated artificial seawater after 4 weeks. Unlike AL1100, there is little difference between the current density (measured 0.3 V noble to the zero current potential), the breakdown, and the repassivation potentials of wires in aerated *versus*

ozonated solutions. However, for the aerated case the repassivation potential is almost the same as the zero current potential, indicating crevice corrosion susceptibility. Due to the active shift in zero current potential with ozonation, the repassivation potential of the ozonated wire is about 0.25 V noble to the zero current potential, indicating improved resistance to crevice corrosion with ozonation.

After 8 weeks of exposure, there is little difference in the curves (Fig. 123), except that the zero current potential of the aerated wire is shifted 0.1 V noble to the repassivation potential, indicating severe crevice corrosion susceptibility.

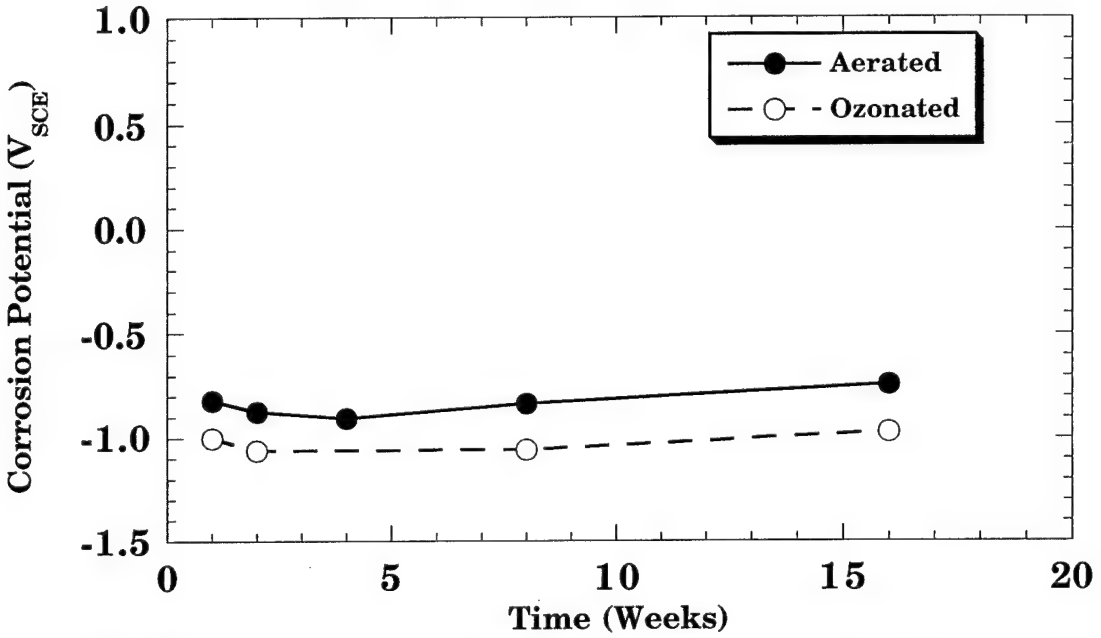

Figure 120. The steady state corrosion potential of AL5356 wires exposed to aerated or ozonated artificial seawater.

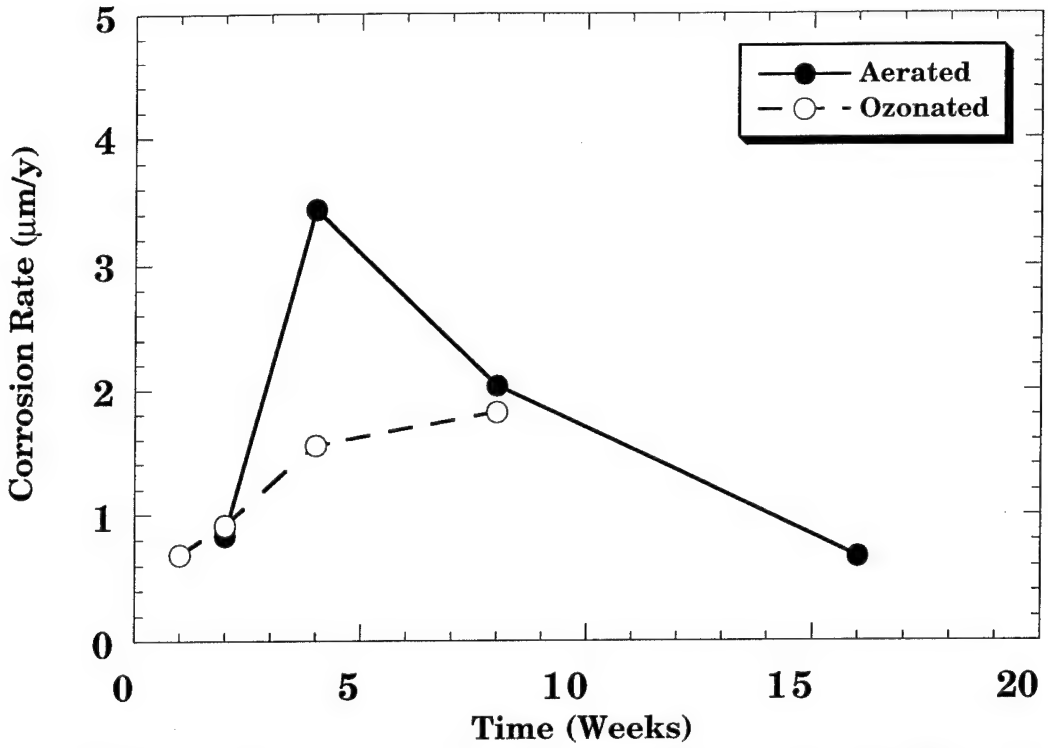

Figure 121. A comparison of the corrosion rates calculated from LPR measurements for AL5356 in aerated and ozonated artificial seawater.

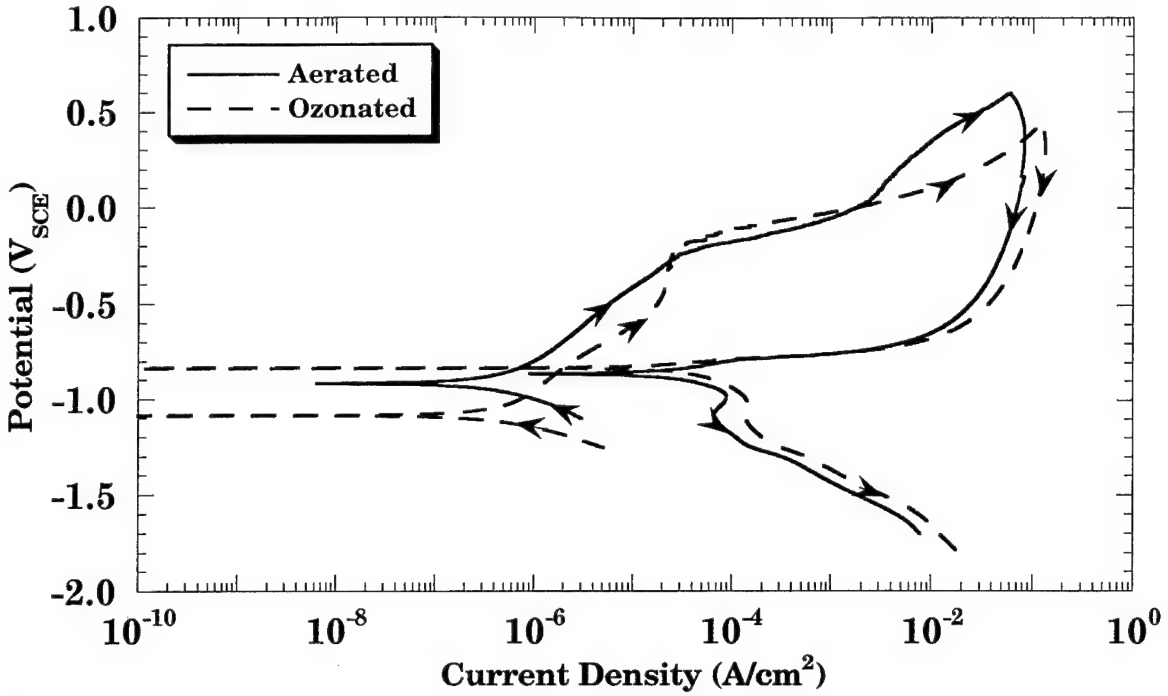

Figure 122. A comparison of polarization curves of AL5356 wires exposed to aerated or ozonated artificial seawater for 4 weeks. Notice that the aerated case the repassivation potential is approximately equal to the zero current potential.

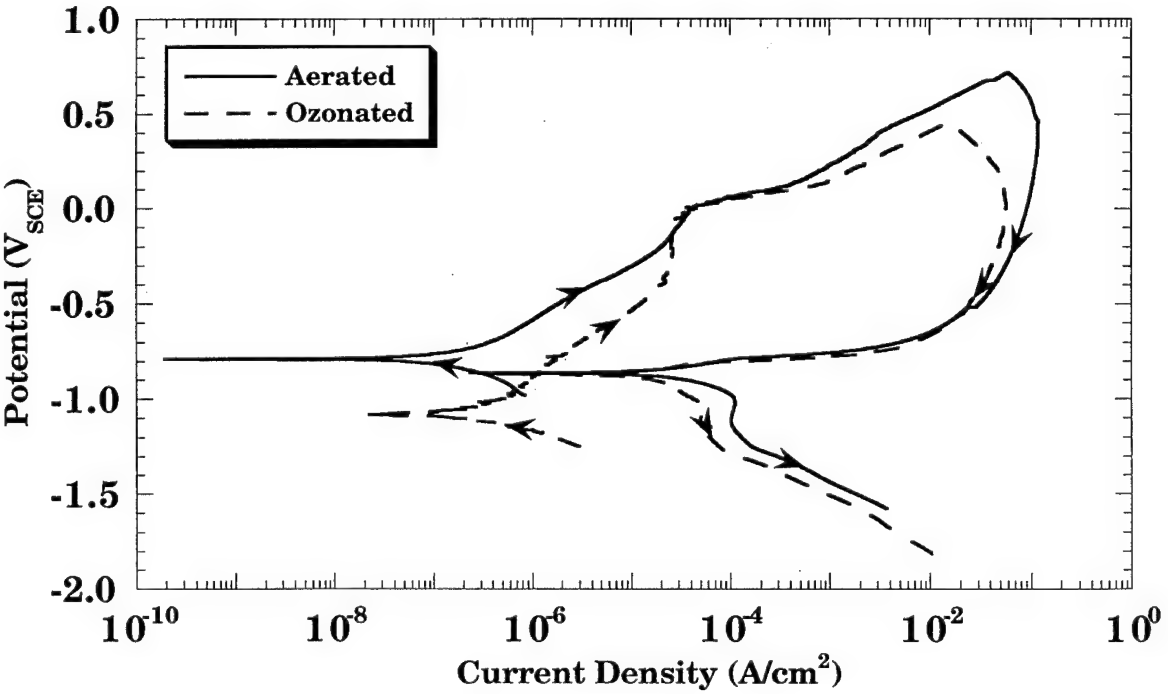

Figure 123. A comparison of polarization curves of AL5356 wires exposed to aerated or ozonated artificial seawater for 8 weeks.

AL6061

Weight Loss Samples Figure 124 shows the percent weight loss (%WTL) of AL6061 in aerated *vs.* ozonated seawater. The exact corrosion rates are difficult to ascertain at this time since no corrosion product has been removed. The %WTL for the aerated samples is negative, due to the precipitation of white corrosion product on the samples. However, the %WTL does not indicate as much weight gain as seen for AL1100 and AL5052. As is the case with AL1100 and AL5052, the %WTL for the ozonated case shows only a slight weight loss.

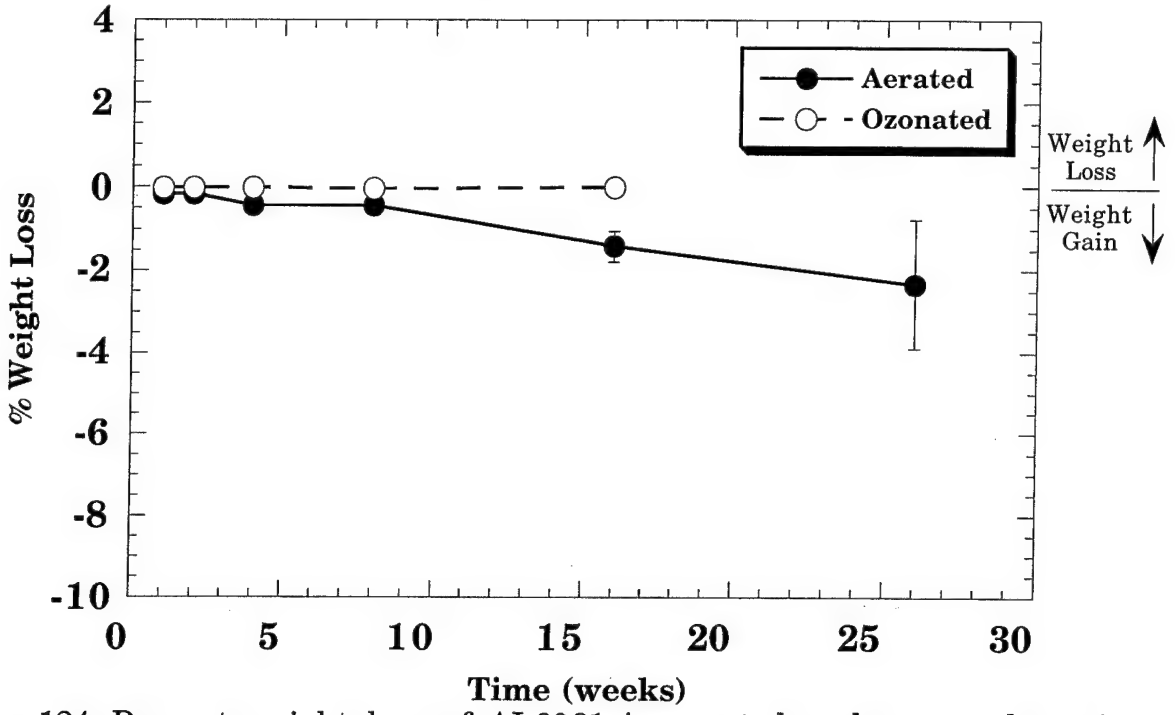

Figure 124. Percent weight loss of AL6061 in aerated and ozonated artificial seawater. Note that the corrosion product was not removed because samples were re-immersed at each time period.

Crevice Samples Figure 125 shows the difference between aerated and ozonated samples of AL6061 after 4 weeks of exposure. In contrast to the aerated sample, the ozonated sample is darker in coloration over its bulk, which is believed to be due to the formation of a coherent oxide. Both samples exhibit characteristic spots of corrosion over the bulk of the sample. However, the precipitation of white corrosion product on these spots for the aerated case appears to be more developed than the ozonated case. Large amounts of white corrosion product are present in the slots of the aerated sample. Several plateaus on the aerated samples have severe crevice corrosion damage, which has traveled into the slot region, while other plateaus have only scattered pits. Several slot regions of the ozonated sample contain small

scattered amounts of white corrosion product, while others are discolored by what appears to be the formation of the coherent oxide of the bulk region. This discoloration has traveled under several plateaus, however many of the crevice plateaus are their original silver color with only a few small scattered pits.

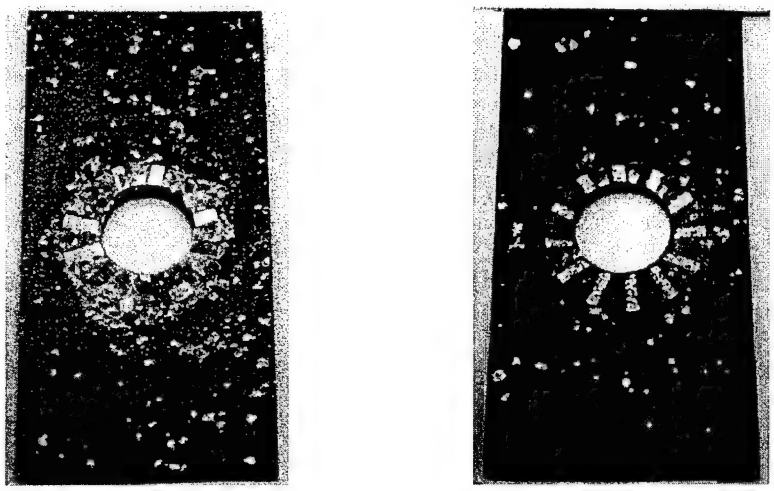

(a) (b)

Figure 125. Small AL6061 crevice samples, 2.5x5.1 cm (1.0x2.0 in), exposed for 4 weeks: (a) aerated artificial seawater, (b) Ozonated artificial seawater. Note lack of white corrosion product in crevice region for ozonated condition.

AL7075

Weight Loss Samples Figure 126 shows the percent weight loss (%WTL) of AL7075 in aerated *vs.* ozonated seawater. As with AL6061, the %WTL for the aerated samples is negative, but does not indicate as much weight gain as seen for AL1100 and AL5356. Again, the %WTL for the ozonated case shows only a slight weight loss. The exact corrosion rates are difficult to ascertain at this time since no corrosion product has been removed.

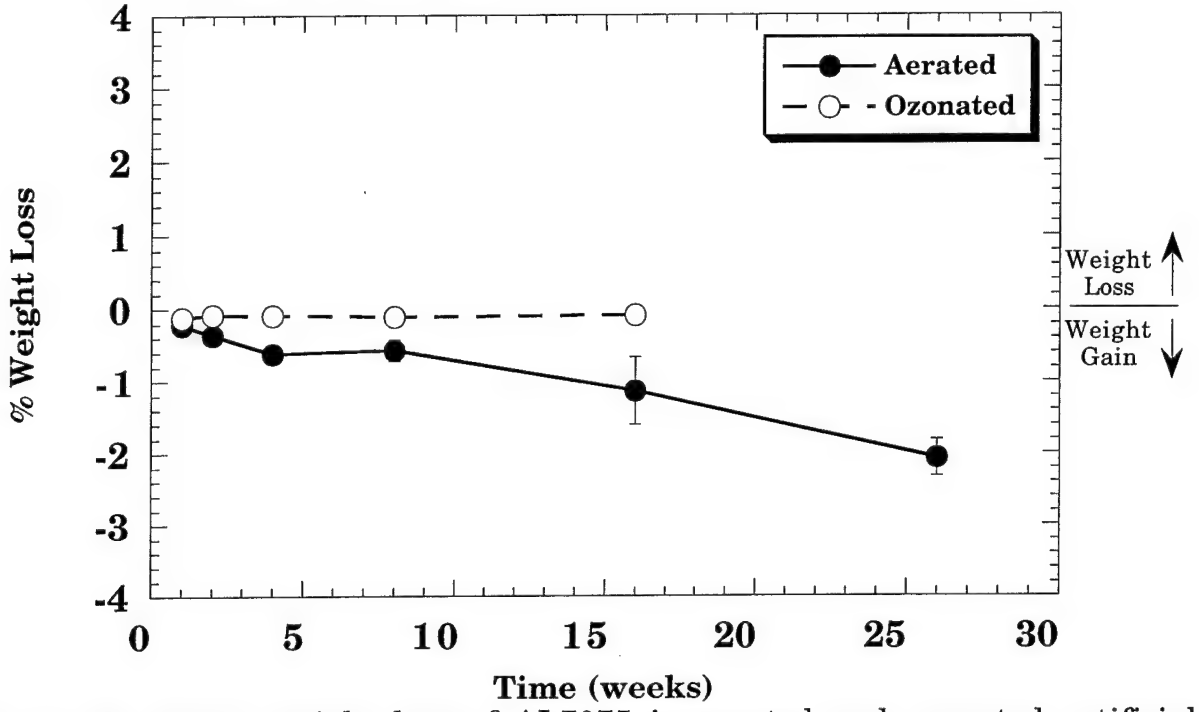

Figure 126. Percent weight loss of AL7075 in aerated and ozonated artificial seawater calculated from weight loss measurements. Note that the corrosion product was not removed because samples were re-immersed at each time period.

Crevice Samples Figure 127 shows the difference between aerated and ozonated samples of AL7075 after 4 weeks of exposure. In contrast to the aerated sample, the ozonated sample is darker in coloration over its bulk, which is believed to be due to the formation of a coherent oxide. The susceptibility to crevice corrosion of AL7075 in aerated seawater is shown by the large buildup of corrosion product where the sample stamped with numbering (Fig. 127a). There is no similar buildup on the numbers on the ozonated sample, however, there is white corrosion build-up on one edge of the sample. Large amounts of white corrosion product are present in the slots of the aerated sample. Several plateaus on the aerated samples have severe crevice

corrosion damage, which has traveled into the slot region, while other plateaus have only large scattered pits. Several slot regions on the ozonated sample contain small scattered amounts of white corrosion product, while others are discolored by what appears to be the formation of the coherent oxide of the bulk region. This discoloration has traveled under several plateaus, causing a marbled effect on the surface. Scattered pitting was found in both the slot and plateau regions of the ozonated sample.

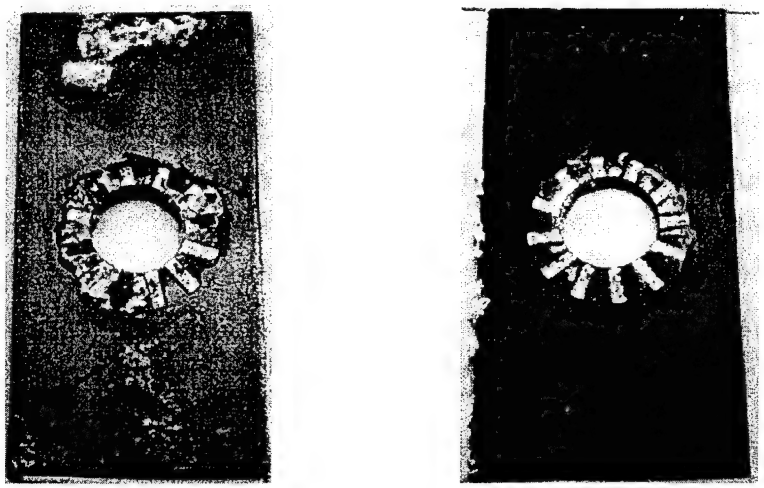

(a) (b)

Figure 127. Small AL7075 crevice samples, 2.5x5.1 cm (1.0x2.0 in), exposed for 4 weeks: (a) aerated artificial seawater, (b) ozonated artificial seawater. Note lack of white corrosion product in crevice region for ozonated condition.

Copper Alloys

For purposes of this discussion, active alloys are considered to be those that do not exhibit an electrochemical active-to-passive transition in seawater, either spontaneously or during anodic polarization. In this program, the primary active alloy family being investigated is that of the copper based alloys.

ETP Copper

Weight Loss Samples Figure 128 shows that the percent weight loss (%WTL) of CDA 110 (electrolytic tough pitch [ETP]) copper is lower in ozonated *vs.* aerated seawater. The aerated condition shows steadily increasing %WTL with time, but in contrast, the %WTL does not change significantly with time after 8 weeks. Note, however, that these values reflect weight loss measurements taken with the corrosion product still on the surface of the sample.

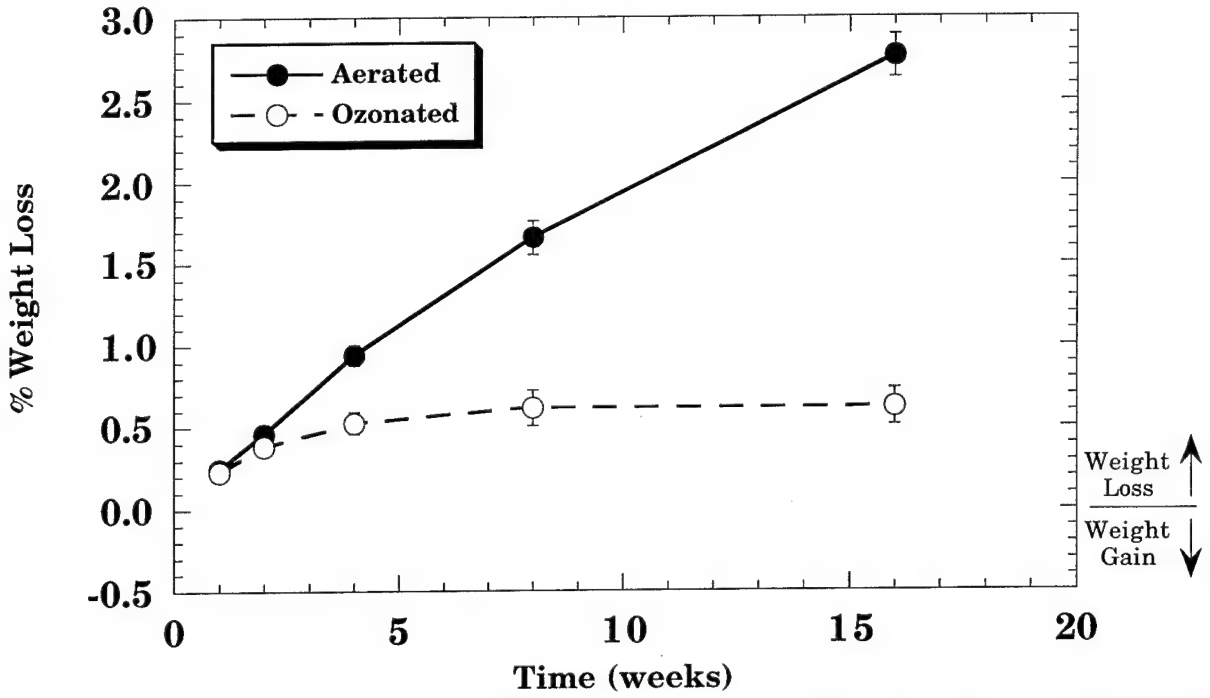

Figure 128. Percent weight loss of ETP copper in aerated and ozonated artificial seawater. Note that corrosion product was not removed because samples were re-immersed at each time period.

Crevice Samples Figures 129-130 show the changes in aerated and ozonated ETP copper crevice samples at 4 and 16 week exposures. At 4 weeks, the bulk of the ozonated sample is dark brown in color, while the surface of the aerated sample is mottled copper and dark brown. Surrounding the crevice region on both samples is an area where copper appears to have plated out. SEM/EDS analysis of this region on

the ozonated sample confirms the formation of pure copper crystallites (Fig. 131). On the ozonated sample, the phenomena of pure copper plating out extends into the slot regions, as it does for the aerated sample. In the ozonated case, however, a blue-green precipitate is also present in several of the slot regions. The plateau regions of both samples are very similar, showing a bright copper surface, marbled with black areas of corrosion product.

At 16 weeks, the bulk surface of the ozonated sample is brown-black in coloration, while the aerated surface is dark brown. There is no longer a region of plated out copper surrounding the crevice area of the ozonated sample, however, there is a large region for the aerated sample. Dispersed on the aerated sample is also a light dusting of blue-green corrosion product, which mostly surrounds the region of plated out copper. Most of the slots of the ozonated sample are bright blue-green in color, with a bright copper coloration towards the narrow end of the slot and surrounding the plateaus where crevice corrosion has exposed grains of the base metal. The slots of the aerated sample are either the brown color of the bulk material, copper colored from copper replating, or gray in color. The plateaus of the aerated sample show little difference from at 4 weeks. The ozonated plateaus, however, appear to be outlined by grains of copper exposed by crevice corrosion which has occurred at the interface with the slot region, with some plateaus almost completely engulfed by crevice corrosion.

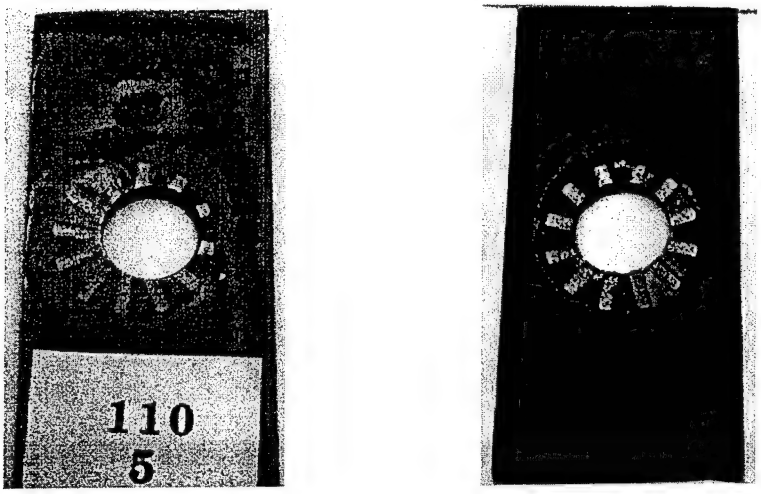

(a) (b)

Figure 129. Small ETP copper crevice samples, 2.5x5.1 cm (1.0x2.0 in), exposed for 4 weeks: (a) aerated artificial seawater, (b) ozonated artificial seawater.

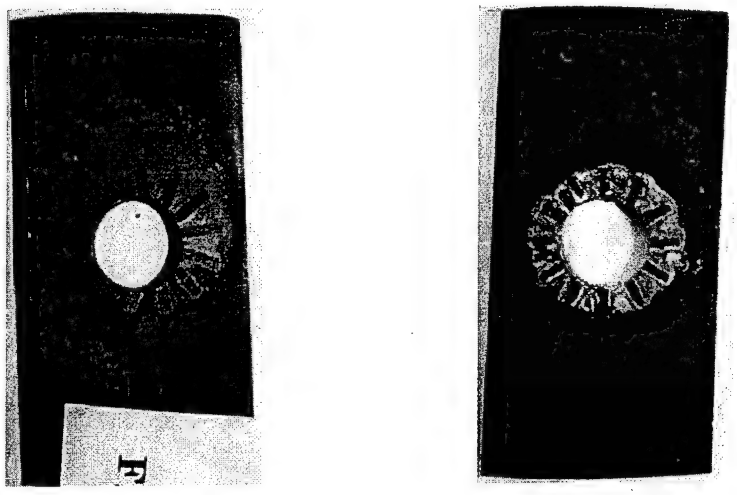

(a) (b)

Figure 130. Small ETP copper crevice samples, 2.5x5.1 cm (1.0x2.0 in), exposed for 16 weeks: (a) aerated artificial seawater, (b) ozonated artificial seawater.

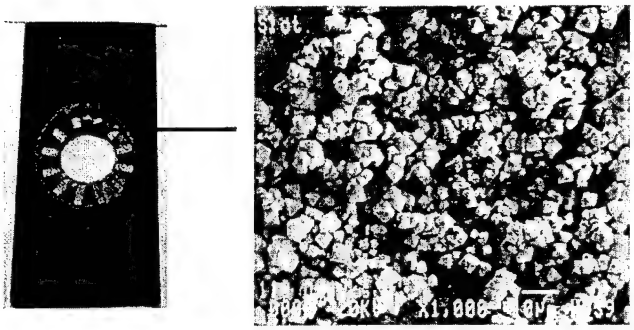

Figure 131. ETP copper 2.5x5.1 cm (1.0x2.0 in) crevice sample after 4 weeks of exposure to ozonated artificial seawater. SEM photograph on the right depicts the pure crystallites of copper which have plated out in the slot regions and the area surrounding the crevice.

90Cu-10Ni

Weight Loss Samples Figure 132 shows that the percent weight loss (%WTL) of 90Cu-10Ni (CDA 706) is lower in ozonated *vs.* aerated seawater. The %WTL in ozonated seawater does not change substantially after 2 weeks exposure, but the %WTL in aerated seawater increases at a greater rate. Note, however, that these corrosion rates are calculated from weight loss measurements taken with the corrosion product still on the surface of the sample.

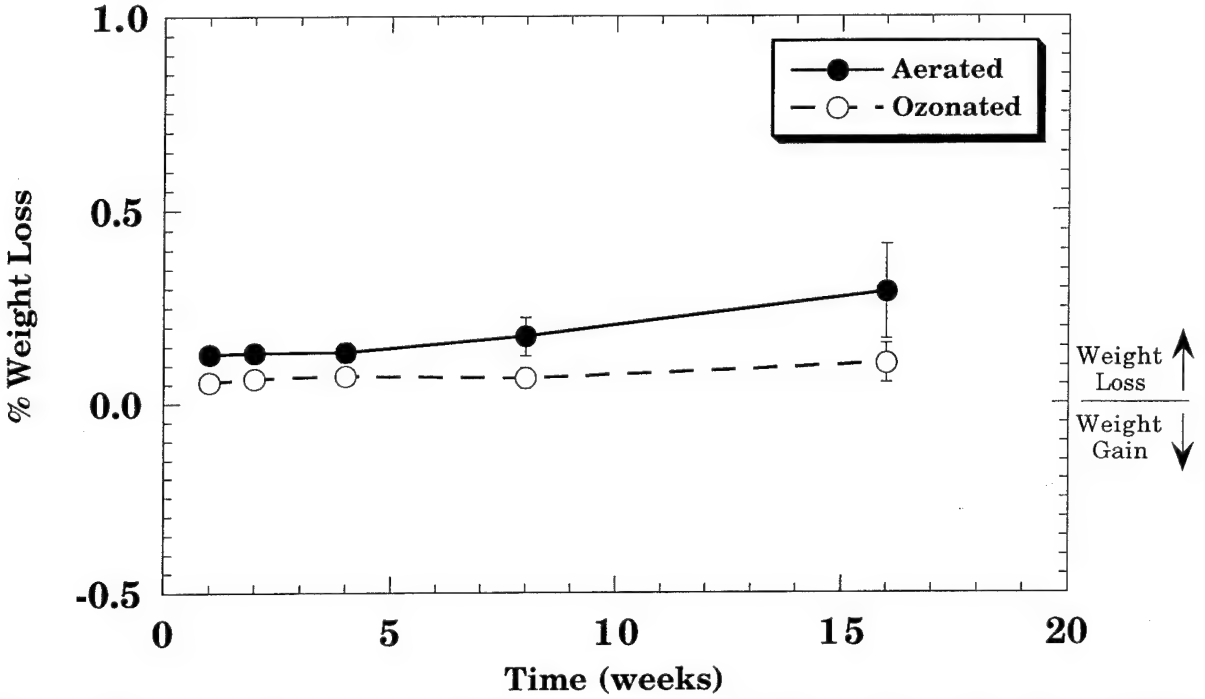

Figure 132. Percent weight loss of 90Cu-10Ni in aerated and ozonated artificial seawater. Note that corrosion product was not removed because samples were re-immersed at each time period.

Crevice Samples Figure 133 shows the changes in aerated and ozonated 90Cu-10Ni crevice samples at 4 weeks of exposure. At 4 weeks, the bulk of the ozonated sample is dark brown/black in color, while the surface of the aerated sample is gray-brown speckled with dots of dark corrosion product. On the aerated sample, a dark brown region of corrosion product surrounds the crevice region, and progresses into the slot region. The slots of the ozonated sample are dark brown in color, with a loose blue-green precipitate in several of the slot regions. The plateau regions of both samples are very similar, showing a bright silver surface, marbled with black areas of corrosion product.

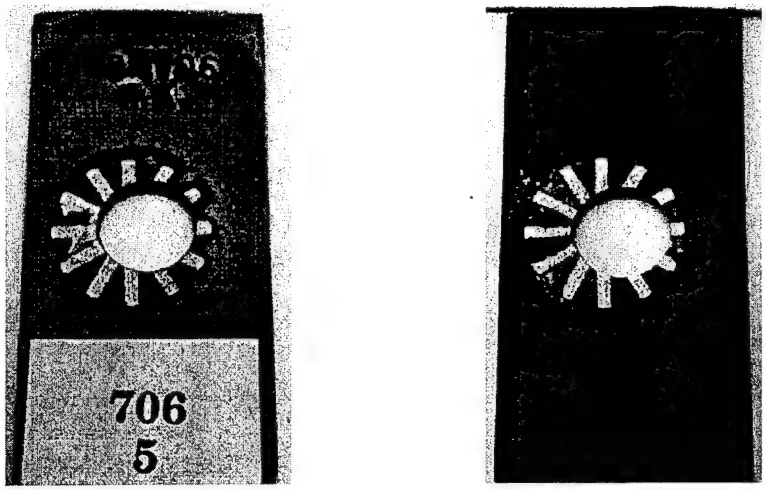

(a) (b)

Figure 133. Small 90Cu-10Ni crevice samples, 2.5x5.1 cm (1.0x2.0 in), exposed for 4 weeks: (a) aerated artificial seawater, (b) ozonated artificial seawater.

Hiduron 191

Weight Loss Samples Figure 134 shows little difference in the percent weight loss for Hiduron 191 in ozonated *vs.* aerated seawater. In both cases, the weight loss is very low when compared to ETP copper. Note, however, that these corrosion rates are calculated from weight loss measurements taken with the corrosion product still on the surface of the sample.

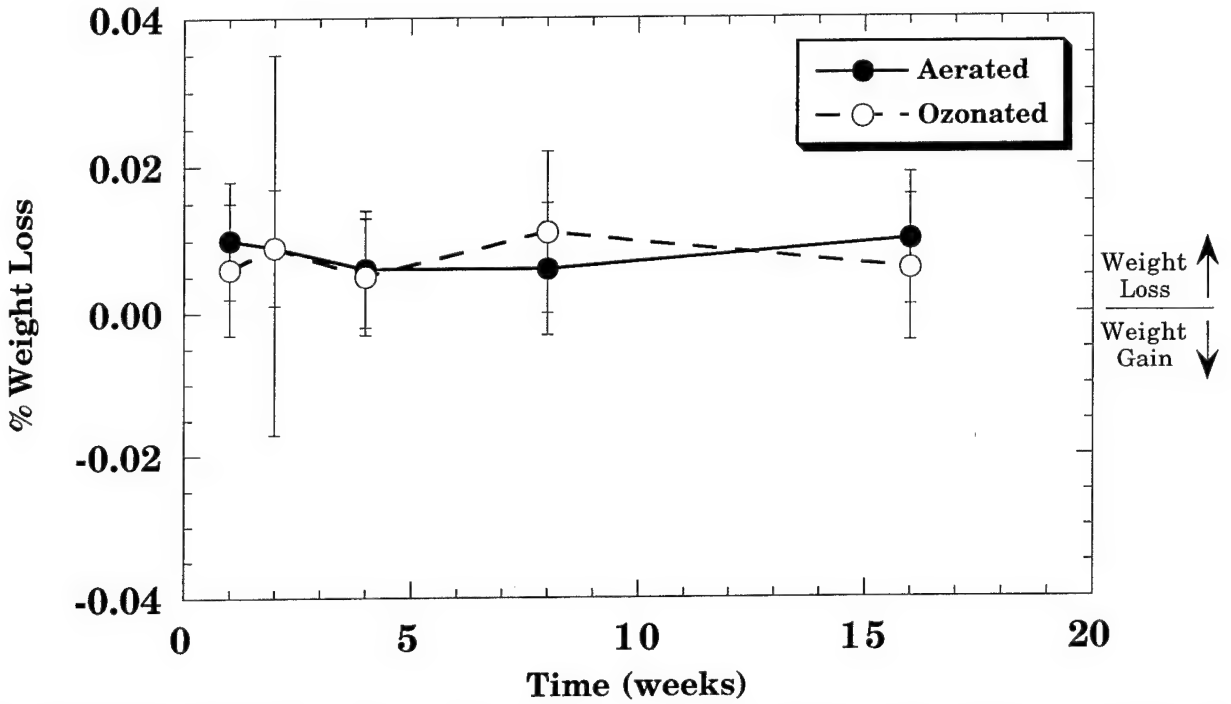

Figure 134. Corrosion rates of Hiduron 191 in aerated and ozonated artificial seawater calculated from LPR measurements. Note that corrosion product was not removed because samples were re-immersed at each time period.

Crevice Samples Figures 135-136 show a comparison of the corrosion product produced on Hiduron 191 in aerated *vs.* ozonated artificial seawater at 4 and 16 week exposure times.

At 4 weeks, the sides of the aerated sample were a light brown tarnish color, while the sides of the ozonated sample were darker brown in coloration. The majority of the slot regions of the aerated sample were filled with a brown-black corrosion product layer, with the rest of the slots appearing to be unaffected, remaining metallic silver in color. All of the slots of the ozonated sample contained dark brown corrosion product, with several having blue-green precipitates near the narrow end of

the slot. Underneath the corrosion product in several slots, evidence of crevice corrosion was found in the form of exposed metallic grains of the base metal. The crevice corrosion in the slots of the ozonated samples extended into several of the plateau regions, but was mainly concentrated around the edges of the plateau. The plateaus of both samples were brass colored, however, the aerated plateaus contained spots of silver on the majority of the plateaus. All of the plateaus of the ozonated sample were marbled with spots of dark brown corrosion product.

At 16 weeks, there was not much change in the coloration of the sides of the samples. Crevice corrosion was found in the slot and crevice regions in both aerated and ozonated samples, exposing grains of metal. The crevice corrosion of the ozonated samples was more severe, leaving hardly any regions untouched under the crenelated washer. The aerated sample, however, showed a smaller amount of crevice corrosion, which began mainly at the interface between the slot and plateau regions, progressing into the plateau region.

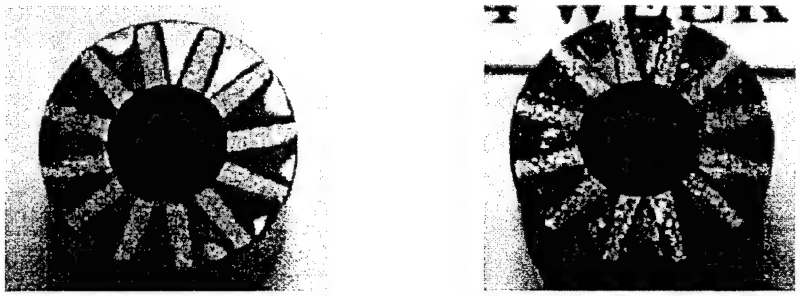

(a) (b)

Figure 135. Hiduron 191 crevice samples, LxD=1.2x1.6 cm (0.5x0.62 in), exposed for 4 weeks: (a) aerated artificial seawater, (b) ozonated artificial seawater.

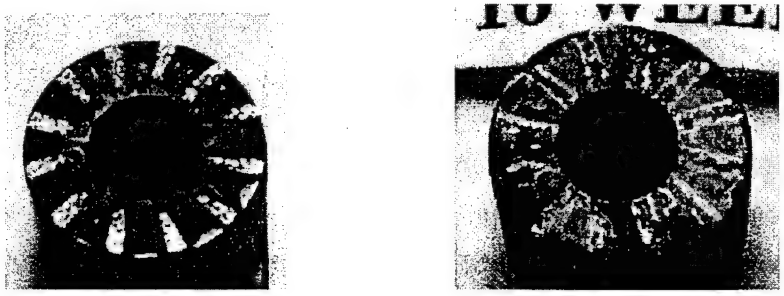

(a) (b)

Figure 136. Hiduron 191 crevice samples, LxD=1.2x1.6 cm (0.5x0.62 in), exposed for 16 weeks: (a) aerated artificial seawater, (b) ozonated artificial seawater.

Marinel

Weight Loss Samples Figure 137 compares the percent weight loss (%WTL) for Marinel in aerated and ozonated seawater. In both cases, the %WTL is very low when compared to ETP copper. There is a slight increase in weight loss for ozonated *vs.* aerated seawater from 4 to 8 weeks, however the %WTL values are not significantly different by 16 weeks. Note that these values were calculated from measurements taken with the corrosion product remaining on the surface of the sample.

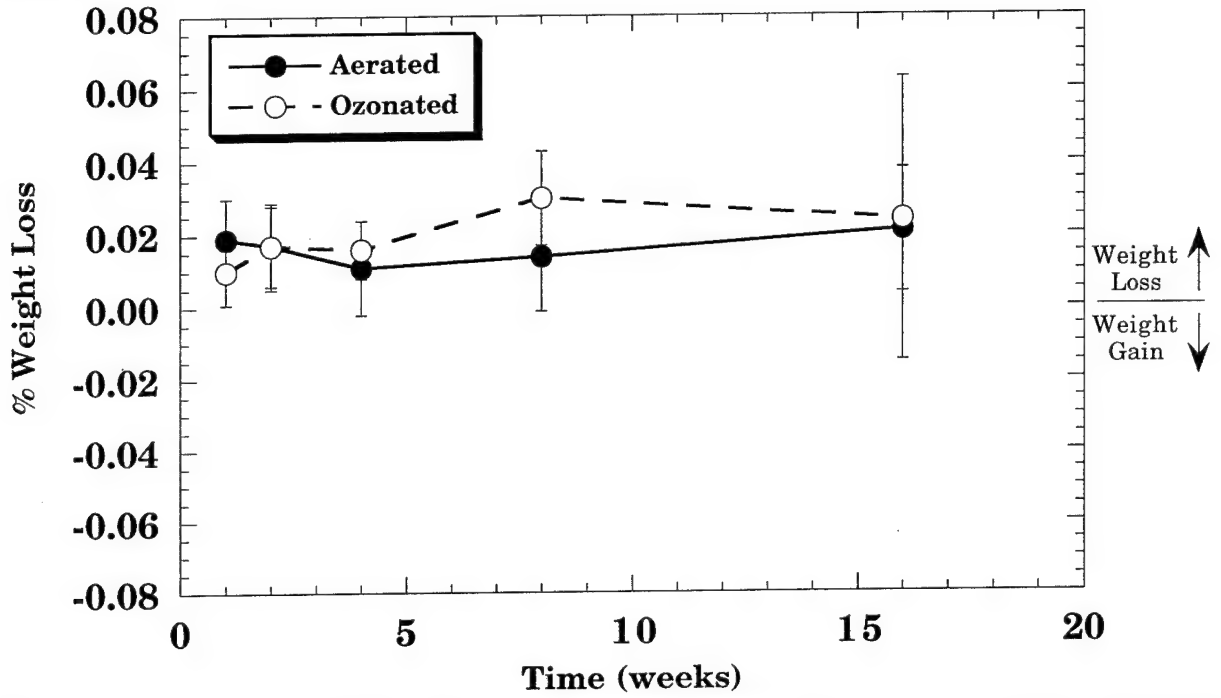

Figure 137. Percent weight loss for Marinel in aerated and ozonated artificial seawater. Note that corrosion product was not removed because samples were re-immersed at each time period.

Crevice Samples Figure 138 shows a comparison of Marinel crevice samples in aerated *vs.* ozonated artificial seawater after 4 weeks of exposure.

At 4 weeks, the sides of the aerated sample are a dark brown tarnished rainbow color, while the sides of the ozonated sample are dark brown-black in coloration. The majority of the slot regions of the aerated sample have a thin layer of brown-black corrosion product, with the rest of the slots appearing to be slightly darker but generally unaffected. All of the slots of the ozonated sample contain a thick layer of dark brown corrosion product, in some cases covered by a blue-green corrosion product. Underneath the corrosion product of the ozonated sample, several

slots showed evidence of crevice corrosion though out the slot, exposing metallic grains of the base metal. This crevice corrosion in the slots of the ozonated samples extends into several of the plateau regions, but is mainly concentrated around the edges of the plateau. Aerated samples also show evidence of crevice corrosion, but mainly on the edges of the plateaus. Regions of the plateaus that were not affected were brass colored on both samples, with dark colored corrosion product creating a marble-like appearance on the surface.

(a) (b)

Figure 138 Marinel crevice samples, LxD=1.2x1.6 cm (0.5x0.62 in), exposed for 4 weeks: (a) aerated artificial seawater, (b) ozonated artificial seawater.

70Cu-30Ni

Weight Loss Samples Figure 139 shows that the percent weight loss of 70Cu-30Ni (CDA 715) is somewhat higher in ozonated *vs.* aerated seawater. In ozonated seawater, the rate of weight loss is high at earlier times, but the curve levels off at longer times. The %WTL in aerated seawater shows a steady, slow increase to 0.05% by 16 weeks exposure.

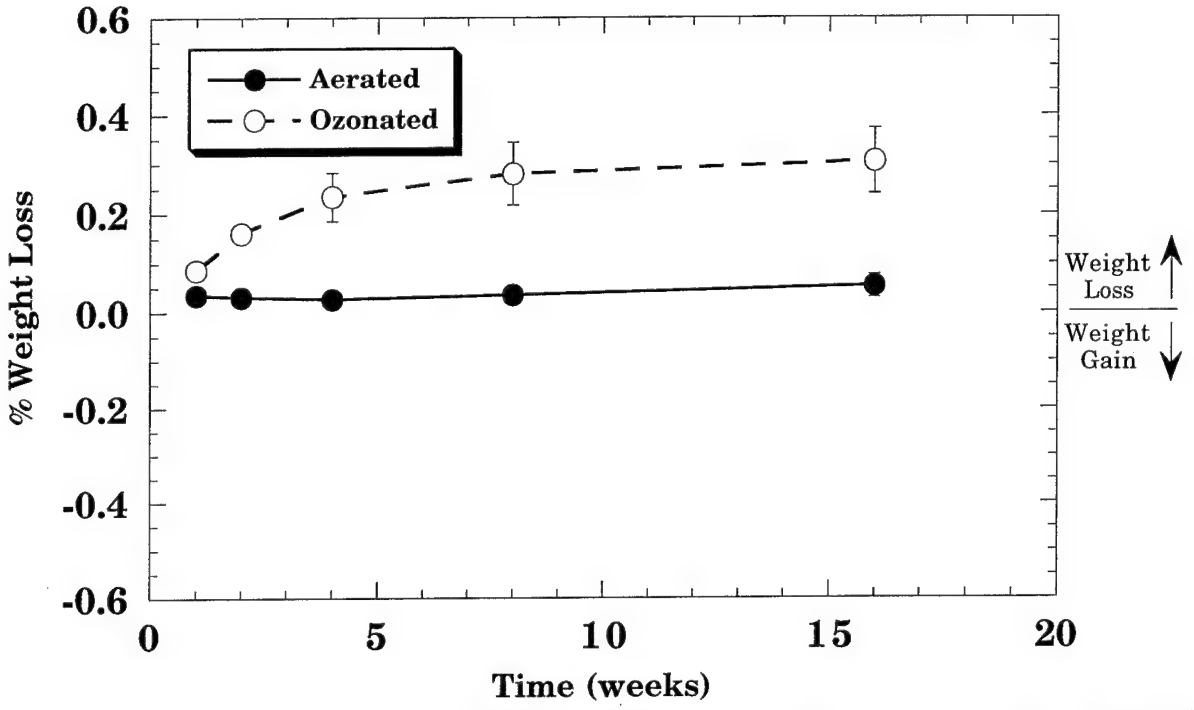

Figure 139. Percent weight loss of 70Cu-30Ni in aerated and ozonated artificial seawater. Note that corrosion product was not removed because samples were re-immersed at each time period.

Crevice Samples General corrosion, as well as enhanced crevice corrosion, in ozonated seawater solutions was found to occur as the nickel concentration of the copper alloy was increased. For copper nickel alloys, preferential and enhanced dissolution of nickel is observed in ozonated solutions, with a non-adherent black corrosion product being produced, as described for the nickel based alloys.

Figures 140-141 show the difference in the corrosion at the crevice surface for aerated and ozonated samples at 4 weeks and 16 weeks.

At 4 weeks (Fig. 140) the bulk of the aerated sample has a thin layer on the surface, creating an "oil slick" rainbow coloration. Dispersed over the surface of the aerated crevice sample are green dots of corrosion product where pits had formed. The bulk surface of the ozonated sample is a mottled coloration of dark green, brown,

and gray; the gray spots being regions where pitting has occurred on the surface. The amount of pitting on the bulk surface is much greater for the ozonated rather than aerated sample. Only a few slots of the aerated sample appear to be undergoing crevice corrosion, exposing metal grains of the base metal. Other slots have brown corrosion product at the interface between the slot and plateau, where crevice corrosion has started to manifest itself. All of the slots of the ozonated sample have crevice corrosion occurring, revealing grains of the base metal under a layer of brown and green corrosion product. Crevice corrosion in the slot region of the ozonated sample extends slightly beyond the region covered by the crenelated washer. In contrast to the slot regions, the plateaus of both aerated and ozonated samples are free of corrosion, although in some cases crevice corrosion appears to be edging in from the interface with the slot region.

At 16 weeks (Fig. 141) the bulk of the aerated sample has a layer of green corrosion product over most of its surface. The bulk surface of the ozonated sample has a thick layer of brown and green corrosion product, which has spalled off in places to reveal metal grains underneath. The majority of the slots of the aerated sample are filled with green corrosion product. All of the slots of the ozonated sample have crevice corrosion occurring, revealing grains of the base metal, with a sprinkling of copper colored corrosion product over the exposed base metal. The plateaus of the aerated sample are relatively unaffected, with some corrosion occurring at the interface with the slot region. The plateaus of the ozonated samples are similar to the aerated samples, except the crevice corrosion from the slot region has reached under the edges of all of the plateaus, leaving only the very center portion of the plateaus untouched.

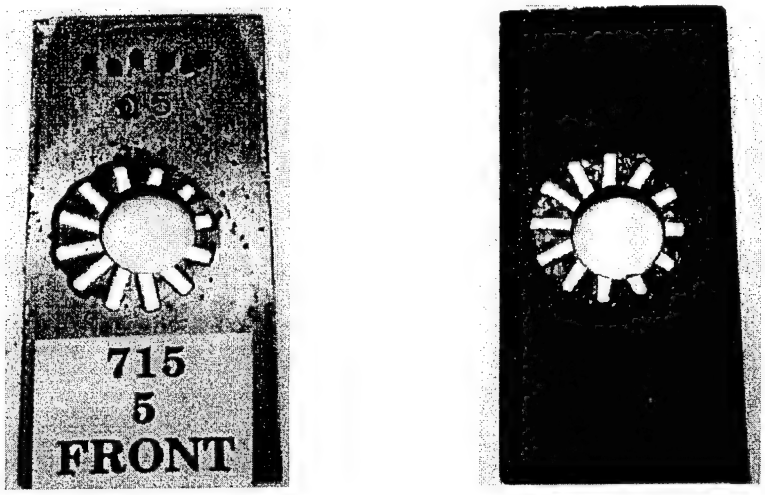

(a) (b)

Figure 140. Small 70Cu-30Ni crevice samples, 2.5x5.1 cm (1.0x2.0 in), exposed for 4 weeks: (a) aerated artificial seawater, (b) ozonated artificial seawater.

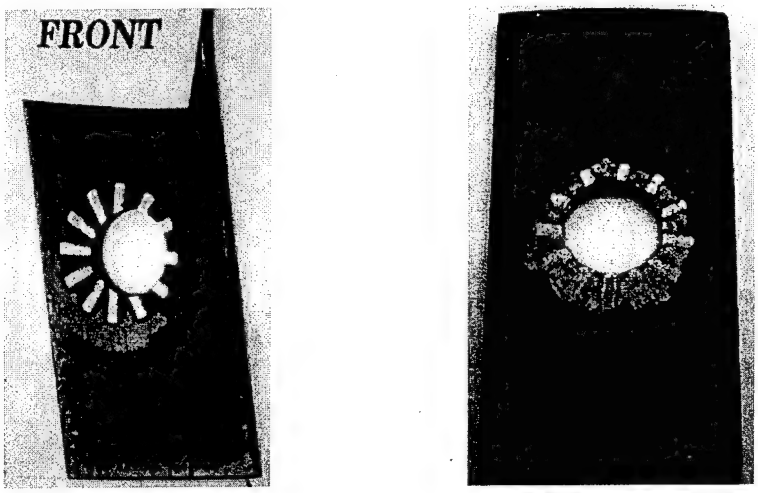

(a) (b)

Figure 141. Small 70Cu-30Ni crevice samples, 2.5x5.1 cm (1.0x2.0 in), exposed for 16 weeks: (a) aerated artificial seawater, (b) ozonated artificial seawater.

Wire Samples As is the case for passive alloys, the corrosion potential of copper based alloys shifts in ozonated seawater compared to aerated seawater, but only by approximately 0.15-0.20 V in the noble direction and after several weeks of exposure (Fig. 142).

A comparison of the corrosion rates calculated from LPR measurements in aerated and ozonated seawater is shown in Figure 143. Initially, the corrosion rate of ozonated 70Cu-30Ni increases from 110 to 140 μm/y (4.4 to 5.6 mpy), however this decreases to 40 μm/y (1.6 mpy) after 16 weeks of exposure. The corrosion rate or the aerated condition is relatively low at each time interval, approximately 5 μm/y (0.2

mpy).

The polarization curves of 70Cu-30Ni (Fig. 144) show a noble shift of about 0.2 V in the zero current potential of wires exposed to ozonated solution, as well as an increase in the current density as compared to aerated solutions. However, ozone does appear to increase the slope of the anodic portion of the curve such that the current density is lower at the higher potentials as compared to aerated conditions, indicating a form of passivity.

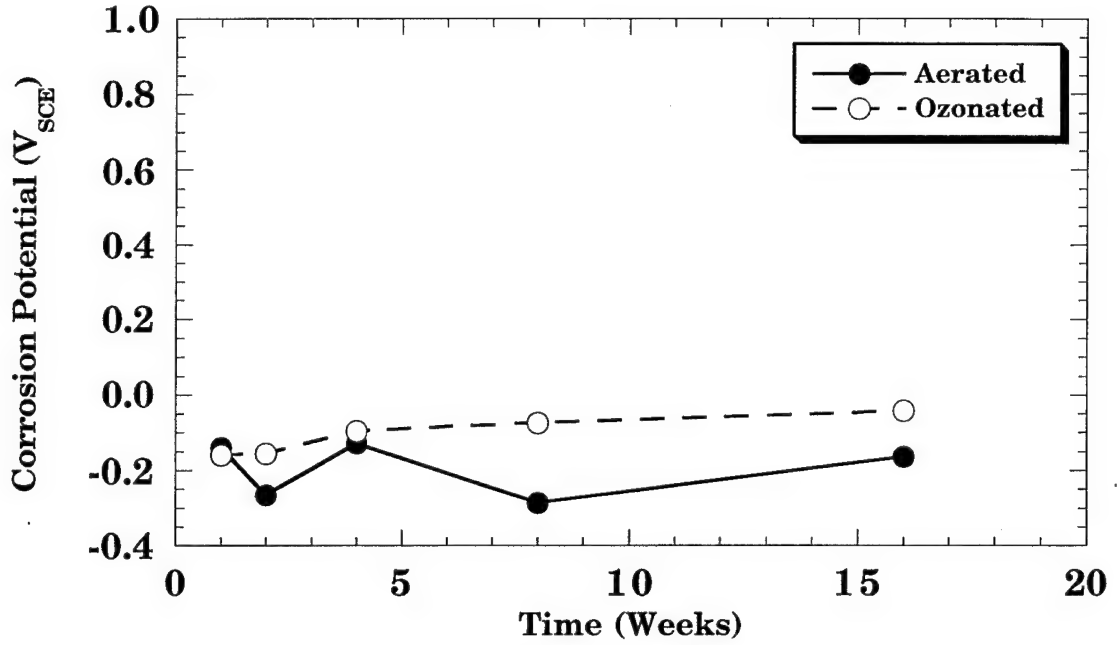

Figure 142. The steady state corrosion potential of 70Cu-30Ni wire exposed to aerated or ozonated artificial seawater.

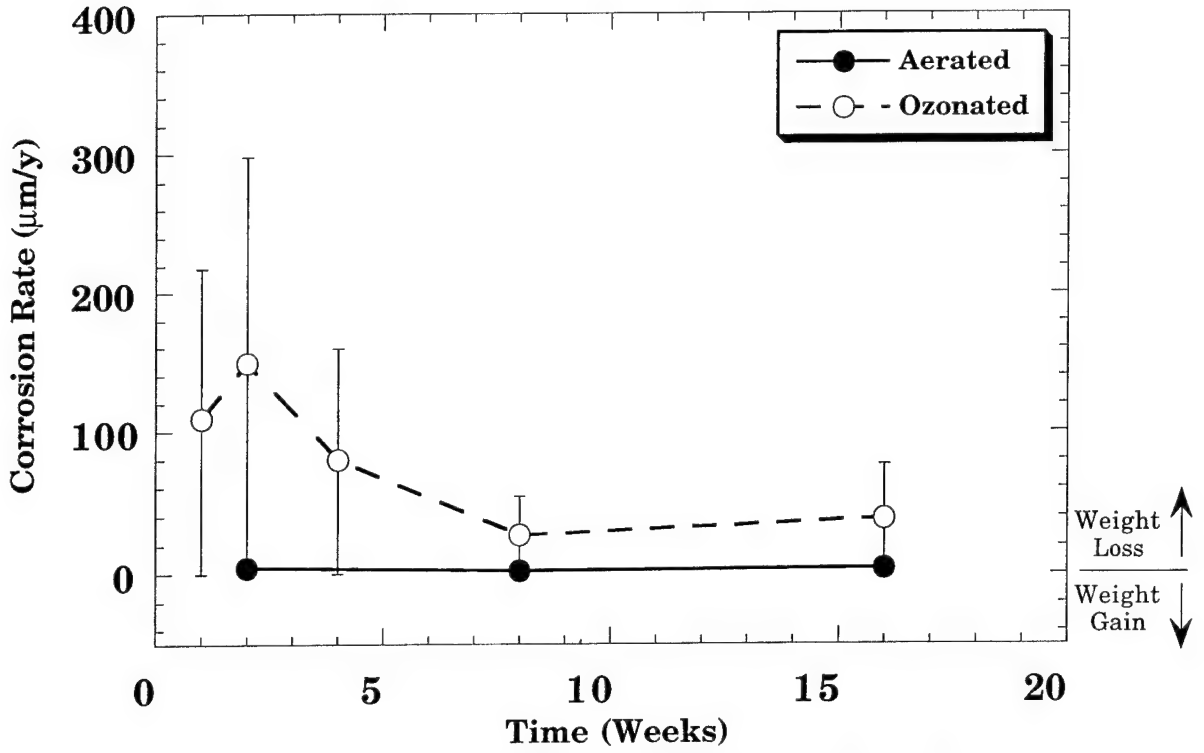

Figure 143. A comparison of the corrosion rates calculated from LPR measurements for 70Cu-30Ni in aerated and ozonated artificial seawater.

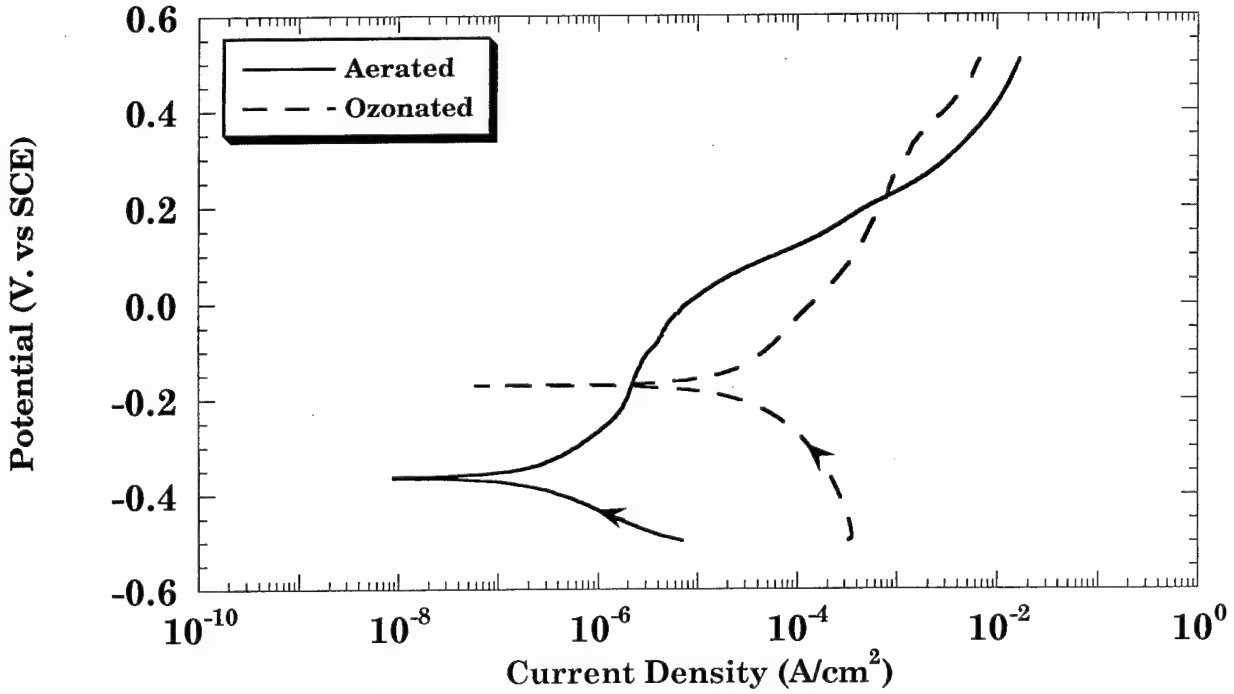

Figure 144. A comparison of the polarization curves of 70Cu-30Ni wires exposed to aerated or ozonated artificial seawater for 4 weeks.

DISCUSSION

The results to date represent data collected up to an interim period of 16 weeks. Analyses of the data are not complete, and this discussion includes probable mechanisms which will be explored in greater detail and presented in the next report.

Solution Chemistry

After samples were immersed, a decrease in the amount of residual ozone was measured in all of the tanks. This is believed to be due to an increase in ozone demand created by metallic corrosion of the samples. This ozone demand reflected reduction of ozone at cathodic areas to support the anodic reaction on the alloys present in the ozonated seawater. As time progressed, residual ozone concentrations rose for the passive metals, related to the decreased corrosion rates as well as the decreased ozone demand associated with lower unreacted Br^- ion concentration.

Little change was observed in the pH of either ozonated or aerated tanks with time after sample immersion. This reflects the normal buffering capacity of seawater, which has been maintained by refreshing 6L of the tank volume weekly.

Passive Alloys

Potential Shifts

Passive alloys are under anodic control; the marked anodic polarization of the passive alloys sets the corrosion potential near the cathodic half-cell potential.[25] For ozonated solutions, the cathodic reaction is ozone reduction, with the half-cell potential (e) = 1.55 V_{SHE}; in aerated seawater, the half-cell potential for oxygen reduction is 0.73 V_{SHE}.

The potential shift observed on the passive alloys is approximately the same (+0.8 to +0.9 V) as the difference between the calculated reduction potentials for ozonated *vs.* aerated seawater, $\Delta e = 1.55 - 0.73 = +0.82$ V from Table I. This correlation shows that the corrosion potential of the alloys in ozonated seawater is influenced strongly by the presence of ozone rather than oxygen. At the oxygen content in the feed gas (P_{O_2} = 0.90-0.95 atm), the calculated reduction potential for oxygenated seawater is 0.75 V_{SHE}, only 0.02 V noble to the aerated seawater value. Accordingly, higher oxygen concentrations in ozonated seawater are not the cause of the corrosion potential shifts.

Nickel alloys

The voluminous, flocculent, black corrosion product observed in the tanks is

due to nickel dissolution as Ni^{++} and its interaction with ozone in seawater. This conclusion is based on the presence of the black product in ozonated tanks containing alloys with substantial nickel content, (all Ni-base alloys, 70Cu-30Ni, and AL6XN [24 wt.% Ni]) and its absence in ozonated tanks of alloys with no nickel content (titanium and aluminum alloys). The formation of the black product tends to form most readily at areas of high ozone concentration (i.e., the fritted glass bubbler). Black corrosion product was collected from the ozonated tank containing the nickel alloys, filtered and dried. Based on analyses using energy dispersive spectroscopy (EDS) and x-ray diffraction, the product consists of calcium oxide, sodium chloride, and hydrated nickel chlorate. The chlorate ion in ozonated seawater forms by oxidation of Cl^- -> ClO^- -> ClO_3^- by ozone. Nickel dissolves ionically, reacts with ozone and precipitates in a mixed compound with CaO and NaCl. It is also possible that the black product is amorphous $NiO_2 \bullet 2H_2O$, as predicted by the potential-pH diagram[42] at pH 8 - 9 under the oxidizing conditions of ozonated seawater. In the amorphous state, the compound would not be identifiable by x-ray diffraction.

Despite the appearance of voluminous black product, the weight losses of nickel alloys in ozonated seawater are still very low. Comparing the behavior of nickel alloys in ozonated *vs.* aerated seawater, ozone causes a phase oxide layer to grow over time. This is based on the observation that, in ozonated solutions, the only adherent corrosion product on nickel alloys is characterized by the presence of thin oxide films exhibiting interference type coloration. This oxide varies in apparent thickness from alloy to alloy and with time of exposure to ozonated solutions based on its changes in coloration. Concurrently, dissolution is evident in ozonated seawater. Based on the green color of seawater, ozonation results in the dissolution of nickel as Ni^{++}.[42]

Further confirming this, cyclic potentiodynamic polarization (CPP) testing of C276, C22, and IN625, show that these alloys are transpassive in ozonated seawater. The open circuit corrosion potentials in ozonated seawater are in a transpassive region of the polarization curves when superimposed on the aerated CPP data, after 4 weeks exposure to ozonated seawater. In aerated seawater, CPP testing indicates that these alloys are resistant to crevice corrosion; the CPP curves do not show breakdown or hysteresis. However, pitting is observed on the surface of C276 wires after polarizing in aerated artificial seawater.

After 8 weeks exposure to ozonated seawater, significant differences are observed in the CPP curves of C276 and C22 when compared to the aerated data. The secondary passive regions are more pronounced, with approximately a 10-fold

decrease in current density in these regions. However, a defined breakdown potential as well as hysteresis is clearly evident upon reversal of the scan. The CPP data for IN625 is the exception to this; there is no hysteresis observed under ozonated *vs.* aerated conditions after 4 weeks or longer exposures. Examination of the ozonated C276 and C22 wire samples after they had been polarized showed the appearance of corrosion similar to the crevice corrosion observed on ozonated C276 crevice samples, with the formation of a dark brown corrosion product which spalled away to reveal shiny metallic base metal. The C22 wire exhibited only very small regions of this type of corrosion over the surface of the wire, with no evidence of pitting. In the case of C276 wires, this corrosion occurred at the waterline, in addition to extensive pitting on the wire surface that was submerged. The results obtained from CPP curves of these alloys were confirmed by the enhanced corrosion of C276 and C22 weight loss samples in the slight crevice area formed by contact with the glass rod and Teflon spacers, after 8 weeks of exposure to ozonated seawater.

Corrosion rates of the Ni-Cr-Mo alloys, calculated from LPR values, show ozonated corrosion rates in the range of 2 to 10 μm/yr (0.08 to 0.4 mpy) after 16 weeks exposure *vs.* less than 1 μm/yr (0.04 mpy) in aerated artificial seawater. Comparing these rates to the literature, the Ni-Cr-Mo-W alloy Hastelloy C is considered immune to general and localized corrosion in seawater, with corrosion rates of less than 1 μm/yr (0.04 mpy);[24] general corrosion rates for IN625 in seawater have been reported as 0.4 μm/yr (0.016 mpy), with no pitting or crevice attack.[27] This shows that although the corrosion rates of nickel alloys in ozonated seawater are slightly higher compared to rates in aerated artificial seawater, and literature values in natural seawater, they are still relatively low.

In both aerated and ozonated seawater, the nickel alloys show resistance to classical crevice corrosion. The exception to this is the case of IN690 in ozonated seawater, which does exhibit classical crevice corrosion; the initially passive surface actively corrodes under the tight crevice plateaus. In aerated seawater, crevice corrosion was also noted for IN690, although to much lower degree. IN690 does not contain molybdenum, which is necessary for resistance of nickel alloys to the reducing acidified chloride environment that develops in tight crevices.[25] It may be noted that the Ni-Cr-Fe alloys such as IN690 are usually selected for resistance to oxidizing conditions rather than for resistance to crevice corrosion in seawater.

The significance of molybdenum as an alloying element for reducing crevice corrosion susceptibility is clearly demonstrated by the results for IN690. Although the molybdenum-bearing nickel alloys in this test program show resistance to

classical crevice corrosion, they do exhibit a different form of localized corrosion behavior. The plateau creviced regions of the samples exposed to ozonated seawater are uncorroded, exhibiting resistance to reducing environments characteristic of molybdenum containing alloys. However, the corrosion morphology of the slot regions exhibit the formation of a dark brown corrosion product. This behavior indicates that a differential oxidation cell develops between the high ozone activity at the bulk surfaces and the low ozone activity in the slot regions of the creviced washers.

Stainless Steel Alloys

In the case of stainless steels, 304 and 316 stainless steels show an increase in percent weight loss (%WTL) in ozonated *vs.* aerated seawater (Fig. 53 and 62). The other alloys studied, AL6XN, 654SMO, and Remanit 4565S, show very low %WTL values, with little or no difference between ozonated and aerated artificial seawater. This result reflects the higher chromium contents of these alloys, which impart resistance to the oxidizing ozonated seawater environment.

Cyclic potentiodynamic polarization (CPP) results after 4 weeks exposure indicate that 304 stainless steel should be more susceptible to crevice corrosion in ozonated *vs.* aerated seawater. This is confirmed by the appearance of the creviced immersion samples. At 8 weeks exposure and beyond, the CPP results do not show breakdown or hysteresis, and no pitting is observed in the CPP test. These samples behave as oxygen electrodes on both the forward and reverse scans. Similar behavior was observed for 316 stainless steel. However, exposure in the ozonated tank resulted in pitting under corrosion product at the original waterline. The conclusion is that exposure to ozonated seawater for extended time periods enhances resistance to pit initiation, but if crevices exist, the driving force for crevice attack is greater.

Enhanced passivity of 304 stainless steel in ozonated seawater was noted in earlier work.[32] This may be due to greater incorporation of oxygen into the passive film by ozone reduction, or by enhancing passive film thickness at the noble corrosion potentials. Results for 316 stainless steel indicate secondary passive film formation as the cause of enhanced passivity. After 8 weeks exposure to ozone, both the open circuit corrosion potential and zero current potential were positioned in the secondary passive range of the aerated CPP curve (Fig. 69).

The results of CPP tests in aerated artificial seawater indicate that AL6XN is completely resistant to crevice corrosion, and crevice samples illustrate this conclusion. The creviced AL6XN samples immersed in ozonated seawater do not exhibit any classical crevice corrosion at the plateau regions, instead, differential oxidation cell corrosion results in discoloration in slot regions between crevice

plateaus. However, the CPP tests reveal a pitting potential and hysteresis for AL6XN, and small hemispherical pits are observed. The hysteresis and pitting are not observed in CPP tests after anodic polarization under aerated conditions. No similar pitting is observed on ozonated weight loss or creviced immersion samples, nor on the wire samples prior to the CPP tests. This indicates that the open circuit conditions in ozonated seawater are active to the pitting potential. Based on the current data, the observed pitting is due to localized secondary transpassive dissolution of nickel during the CPP tests, enhanced by ozone.

Both 304 and 316 stainless steels show very severe crevice corrosion with ozonation *vs.* aeration. The type of crevice corrosion attack for 304 and 316 stainless steels takes the form of severe gouging under the crevice plateau. The number of sites attacked and the severity of attack generally increases with increased exposure time in ozonated seawater. The effect of a larger cathode area seems to result in earlier initiation in ozonated seawater compared to the smaller area samples, but at 4 weeks and later, the degree of crevice attack is generally independent of the cathode area. It appears that initiation of crevices follows a stochastic process; the initiation of crevice corrosion at a given site is random and independent of active crevice corrosion at adjacent sites.

Alloys containing higher amounts of chromium and more than 4 wt.% molybdenum (AL6XN, 654SMO, and Remanit 4565S) show less crevice corrosion damage, following the conventional trend of resistance to crevice corrosion in seawater.[28] The appearance of the creviced areas for these higher alloyed stainless steels is a green/yellow oxide surrounding the plateaus of the crevice, with a buildup of darker, thicker oxide and black corrosion product in center of the slot regions. Increased exposure to ozonated seawater results in increased corrosion, manifested as thickening and cracking of the oxide in the center of the slots. The corrosion behavior in the slots is due to differential oxidation cells between free surfaces and the slots, as noted on the nickel alloys.

Titanium Alloys

The corrosion behavior of uncreviced titanium alloys shows no effect of ozonation *vs.* aeration. The percent weight loss for titanium alloys in both aerated and ozonated artificial seawater were either zero or negligible (being below the accuracy of our balances).

Corrosion rates calculated from LPR data for Grade-2 and -5 are consistent with the low percent weight loss data, with less than 1 μm/y in both aerated and ozonated seawater.

Cyclic potentiodynamic polarization data for Grade-2 and -5 did not show any detrimental effects of ozone at potentials up to 4 V_{SCE}. In fact, ozonation resulted in lower current densities during the entire potential scan, most notably for Grade-2. This data does not indicate crevice corrosion susceptibility in ozonated seawater, consistent with the crevice sample results using metal-to-metal crevices.

Titanium Grade-2 crevice samples exhibited small amounts of pitting at the edge of the plateaus of Teflon crevice washers in ozonated seawater, but not in aerated seawater. More highly alloyed titanium alloys show greater effects of ozonation on creviced behavior when compared to aerated conditions. Results from immersion tests with Teflon washers show that the beta-stabilized alloys, titanium Grade-12, Beta-C, and Beta-21S, (which contains substantial amounts of molybdenum), exhibit more discoloration and pitting in crevices than did the alpha-stabilized Grade-2 and -5. The crevice effects were visible after 4 weeks of exposure in ozonated seawater, whereas crevice corrosion damage initiation was delayed to at least 8 weeks of exposure for Grade-2 and -5. The data indicate that presence of the beta phase, in a two-phase alpha+beta or completely beta phase microstructure, increases the susceptibility to crevice corrosion in ozonated seawater.

Metal-to-metal crevices on titanium Grade-2 exposed to ozonated seawater did not exhibit pitting, as observed at crevices formed with Teflon crenelated washers. The data indicate that pitting is due to the breakdown of the Teflon, releasing fluoride ion and forming hydrofluoric acid (HF). Analysis with EDS revealed fluorine in the corrosion product at crevices of titanium Grade-2 after exposure to ozonated seawater, but not after exposure to aerated seawater. The passive film of titanium is known to break down in HF.[26] It is suspected that Teflon degradation influenced the crevice corrosion of the other titanium alloys as well. In view of this, future crevice corrosion testing of all titanium alloys in ozonated seawater will be performed with metal-to-metal crevices.

The degradation of Teflon in the presence of ozone is an issue that must be addressed. Teflon is generally considered to be inert in oxidizing environments. It is commonly used as a gasket material in contact with corrosion resistant alloys, replacing other polymeric gasket materials that are less resistant to degradation. Release of fluorine from Teflon in the presence of ozone would require readily breakable C-F bonds or unbonded fluorine in the polymer. These conditions are favored if non-virgin (recycled) PTFE is used in fabrication, where impurities could alter the integrity of the Teflon. However, the supplier of the crenelated washers verified that virgin PTFE was used. As such, Teflon degradation in the presence of

ozone remains an open issue and requires further investigation.

Active Alloys

Aluminum Alloys

In aerated seawater, all of the aluminum alloys show light gray surface color, extensive pitting, and the production of large amounts of white aluminum hydroxide corrosion product. However, after exposure to ozonated seawater, the aluminum alloys show a much darker, more adherent oxide layer. Ozonation of aluminum alloys results in lower corrosion rates, less pitting, and much less buildup of aluminum hydroxide compared to aerated seawater. The ozone-enhanced oxide or passive film appears to act as a self-limiting diffusion barrier, decreasing the %WTL compared to aerated conditions.

The corrosion potential of AL1100 is active in aerated seawater compared to other alloy classes, reflecting the active nature of aluminum. The active corrosion potential also indicates that the corrosion behavior of aluminum is under cathodic control, where the cathodic reaction is polarized such that the corrosion potential is close to the half-cell potential for the actively corroding metal.[25] In contrast to the other alloy systems which showed noble shifts in corrosion potential with ozonation, the aluminum alloys exhibited a shift of 0.2-0.5 V active to the corrosion potential with aeration. Assuming that the diffusion limited cathodic reduction controls the corrosion rate, a lower diffusivity of the ozone-enhanced oxide would decrease the limiting current density, resulting in a lower corrosion current. Moving to a lower current along the Al -> Al^{3+} Tafel line results in an active corrosion potential shift. Support for this can be seen in the CPP data for AL1100; the current densities, measured at 0.3V noble to the zero current potential, are an order of magnitude lower and the zero current potentials are shifted active with ozonation compared to aeration (Fig. 116-117).

The steep slope of the ozonated CPP curves indicates enhanced passivity with ozonation. Although the curves show hysteresis, the ozonated CPP data for AL1100 and AL5356 confirm that crevice corrosion is not expected in ozonated seawater since the zero current potentials are active to repassivation potentials by nearly 0.3 V.

The crevice plateaus on aerated crevice samples are corroded in the form of large pits, accompanied by large volumes of white aluminum hydroxide. In contrast, the crevice plateaus in ozonated seawater are only mildly affected. Alloys AL5052 and AL7075 showed the greatest differences between the two environments, with

samples exposed to ozonated solutions showing greatly decreased amounts of crevice corrosion damage.

Copper and Copper-Nickel Alloys

The percent weight loss data, with the corrosion product remaining, indicate a beneficial effect of exposure of ETP copper to ozonated *vs.* aerated seawater. The data show that the rate of weight loss in ozonated seawater decreases significantly after 4 weeks exposure, where the aerated data show a steady rate of increase in the weight loss as the exposure time increases. This indicates that the corrosion product in ozonated seawater is a more effective diffusion barrier to copper dissolution than the product formed under aerated conditions.

In aerated seawater, corrosion of polished copper surfaces[43] occurs as an oxidation to the cuprous ion (Cu^+) forming a cuprous chloride ion complex ($CuCl_2^-$). This reaction is coupled to oxygen reduction at cathodic sites. Hydrolysis of $CuCl_2^-$ to cuprous oxide (Cu_2O) follows (except in the presence of high Cl^- ion concentrations), where Cu_2O is a protective layer.

$$2CuCl_2^- + 2OH^- \rightarrow Cu_2O + H_2O + 4Cl^-$$

Further oxidation leads to formation of a cupric compound, $Cu_2(OH)_3Cl$ (atacamite, green). Other researchers[44] noted that the atacamite layer is less protective than the underlying Cu_2O. Regarding the low weight losses in ozonated *vs.* aerated seawater, the corrosion product layer due to ozonation is more protective that Cu_2O + atacamite, perhaps as cupric oxide (CuO) forming over Cu_2O.

Extensive copper dissolution occurred in the slot regions of creviced samples in ozonated seawater. At this stage of analysis, the enhanced crevice corrosion in ozonated seawater appears to be related to differential oxidation cells, however the complete mechanism is not understood. Evidence of copper crystals re-plating outside of slot regions was also noted in both aerated and ozonated solutions. Cupric ions (Cu^{++}) form by oxidation of $CuCl_2^-$ in the bulk solution to soluble $CuCl_2$. Cathodic reduction of Cu^{++} outside of the slot regions results in deposition of copper.

In aerated seawater, the presence of nickel in copper is beneficial, generally decreasing the %WTL compared to ETP copper. The lowest weight losses are seen for Hiduron and Marinel, which, in addition to nickel, are also alloyed with aluminum and manganese. Conversely, for Cu-Ni alloys in ozonated seawater, increasing nickel content results in increased weight loss. In fact, 70Cu-30Ni showed nearly an order of magnitude increase in weight loss with ozonation *vs.* aeration. This observation, coupled with the large volumes of black corrosion product associated with nickel,

indicates denickelification in the presence of ozone.

The enhanced corrosion of 70Cu-30Ni is also observed in the corrosion rates calculated from LPR data and the anodic current density from polarization curves. In contrast to the passive alloys, the electrochemical behavior of 70Cu-30Ni indicates active corrosion. Where the passive alloys exhibited a corrosion potential shift of + 0.8 to 0.9 V with ozonation, the corrosion potential of 70Cu-30Ni is only shifted by approximately 0.2 V noble to the aerated potential. The corrosion behavior is under cathodic control, where the ozone reduction reaction is polarized to the corrosion potential near the potential of the actively corroding anode. Assuming that the diffusion-limited reduction of oxidant controls corrosion, the limiting reduction current density on 70Cu-30Ni is approximately 2 orders of magnitude greater with ozonation than with aeration, which is shown by the polarization curves in Figure 144.

With increasing nickel concentration, copper alloys showed increasing crevice corrosion damage in ozonated *vs.* aerated solutions. This damage was mainly concentrated at the interface between the plateau and slot region, moving into the plateau regions with increasing time.

CONCLUSIONS

1.) For the case of non-creviced passive alloys, ozonation is found to stabilize the passive films of titanium and stainless steel as well as the oxide film of aluminum. However, in the case of nickel alloys, ozonation causes the alloys to behave in a transpassive manner.

2.) For the case of non-creviced active copper alloys, the layer of copper corrosion product formed in ozonated solutions appears to be more protective than that formed in aerated solutions. As the nickel concentration of the alloy is increased, this trend reverses, becoming significant at nickel concentrations of 30 wt.%.

3.) For all the non-creviced alloys, the material loss that occurs in ozonated artificial seawater appears to be sufficiently low such that general corrosion is not considered to be a problem.

4.) From polarization curves and crevice samples, 304 and 316 stainless steel alloys are very susceptible to crevice corrosion in ozonated solutions. High chromium, high molybdenum stainless steels are resistant to classical crevice corrosion, but exhibit differential oxidation corrosion in ozonated seawater. The extent of this type of corrosion is not severe.

5.) Creviced nickel alloys containing molybdenum do not exhibit classical crevice corrosion behavior. Crevice corrosion occurred at the interfacial regions, leaving the actual crevice (plateau) protected due to differential oxidation. This crevice corrosion, however, is by no means severe. The absence of molybdenum in a nickel alloy, as in the case of IN690, however, displays normal crevice corrosion behavior which was on the order of severity of that seen with the low molybdenum stainless steels.

6.) A large cathode area has little effect on the crevice corrosion of stainless steel and nickel alloys.

7.) From polarization curves and crevice samples, aluminum alloys show a significant decrease in susceptibility to crevice corrosion in ozonated artificial seawater.

8.) Creviced copper and copper-nickel alloys are more severely attacked in ozonated artificial seawater than aerated artificial seawater. This is believed to be due to differential oxidation.

9.) The differences noted in crevice samples of titanium alloys exposed to ozonated seawater as compared to aerated seawater, are believed to be due to the breakdown of Teflon crenelated washers. Metal to metal crevice samples and EDS analysis support this conclusion.

APPENDIX I
TITRATIONS

Hypohalite and Bromate Titration

Hypohalite and Bromate Titration

Modified from: Haag, W. R. Technical Note on the Disappearance of Chlorine in Seawater. Water Research, Vol. 15, 1981. p 937).

Modified by: Gordan Grguric, 1991, Barbara Brown 1995.

Reagents:

1.) **0.3 M Potassium Iodide**. Dissolve 25 g of potassium iodide in 5OO mL of distilled-deionized water. Store in a dark bottle to prevent photo-oxidation of the iodide. Discard the solution when it becomes faintly yellow.

2.) **Ammonium Molybdate Catalyst**. Dissolve 7.5 g of ammonium molybdate in 250 mL distilled-deionized water.

3.) **pH 3.8 Acetate Buffer**. Dissolve 31.23 g of hydrated sodium acetate CH3COONa• 3H20 and 120 g (114 mL) of glacial acetic acid in 250 mL of distilled-deionized water.

4.) **9 N Sulfuric Acid**. Fill a 500 mL volumetric flask half-full with distilled-deionized water. Carefully add 125 mL concentrated sulfuric acid. Fill to the 500 mL mark with distilled-deionized water. Mix well and let the flask cool to room temperature (use an ice bath if necessary). When cooled, fill to the mark again.

5.) **Starch Solution (indicator)**. Dissolve 2 g of soluble starch in 200 mL of distilled-deionized water. Heat the solution to boiling. After letting it cool to room temperature, filter the solution and use only the clear filtrate. This solution is stable for 1-2 weeks and can be preserved with 1 mL of phenol.

6.) **Potassium Bromate Standard**. Analytical grade potassium bromate is dried at 180°C for several hours. After cooling in a desiccator overnight, weigh

exactly 16.70 g and dissolve in 1 L of distilled-deionized water. This is your 0.1M bromate standard.

7.) **Sodium Thiosulfate Titrant**. Prepare 0.01 M sodium thiosulfate by dissolving cca. 1.24 g hydrated sodium thiosulfate in 500 mL of distilled deionized water. Store in a dark bottle. It can be preserved with 0.5 mL of amyl alcohol. Alternately, 0.01M sodium thiosulfate can be prepared by diluting standard 0.1 N (=0.1M) sodium thiosulfate stock solution, if available.

Standardizing the Sodium Thiosulfate Solution:

1.) Pipet 20 mL of distilled-deionized water in a 50 mL Erlenmeyer flask. Add exactly 0.1 mL of potassium bromate standard solution.

2.) While stirring, add the following reagents in succession: 1 mL of potassium iodide, 0.1 mL of ammonium molybdate, 1 mL of 9 N sulfuric acid and 1 mL of the starch solution.

3.) Titrate this solution with sodium thiosulfate until the blue color completely disappears. You will need approximately 6 mL of the titrant to reach the endpoint.

4.) Calculate the molarity of the thiosulfate solution from the equation:

$$M(Na_2S_2O_3)=0.06/V(Na_2S_2O_3 \text{ used, in mL})$$

Procedure

A.) Hypohalite Titration:

1.) Place a stir bar in a 50 mL Erlenmeyer flask. Pipet exactly 20 mL of the sample into a 50 mL Erlenmeyer flask.

2.) While stirring, add the following reagents in succession: 1 mL of potassium iodide, 0.1 mL of ammonium molybdate, 1 mL of pH 3.8 acetate buffer and 1 mL of the starch indicator. If there is hyochlorite or hypobromite present, the solution will turn blue. Titrate with your standardized sodium thiosulfate until the blue color completely disappears. Make sure you don't overshoot the endpoint as the same titration is continued at pH 1 to determine the bromate concentration. If you do overshoot the endpoint and want to determine the bromate concentration in the sample, you have to redo the hypohalites titration.

3.) Calculate the concentration of hypohalites (hybromite and hypochlorite) using the equation:

$$mM(\text{hypohalites}) = 25{,}000 * V(Na_2S_2O_3) * M(Na_2S_2O_3)$$

Where: $V(Na_2S_2O_3)$ is the volume of titrant used, in mL
$M(Na_2S_2O_3)$ is the molarity of sodium thiosulfate

B.) Bromate titration:

1.) To the sample just titrated, add 1 mL of the sulfuric acid. The blue color will reappear if there is bromate present. Titrate with sodium thiosulfate again until the blue color disappears.

2.) The bromate concentration is calculated from the equation:

$$mM(BrO_3^-) = V(Na_2S_2O_3) * M(Na_2S_2O_3) / 120{,}000$$

Where: $V(Na_2S_2O_3)$ is the volume of titrant used, in mL.
$M(Na_2S_2O_3)$ is the molarity of sodium thiosulfate

Bromide Titration

Bromide Titration

Modified from: K. Grasshoff, *Methods of Seawater Analysis*, NY, Verlag Chemie, 1976.

Modified by: Gordan Grguric, 1991; Barbara Brown, 1995.

Reagents:

1.) **Sodium Chloride Solution.** NaCl 10% (w/v). Dissolve 50g of NaCl in 500 mL of distilled deionized water.

2.) **Phosphate Buffer.** $NaH_2PO_4 \bullet H_2O$. Dissolve 25 g of sodium dihydrogen phosphate (sodium phosphate monohydrate) in 250 mL of distilled deionized water and dilute to 500 mL.

3.) **Sodium hypochlorite solution.** NaOCl. Prepare a 0.1N solution of NaOH by adding 1 gram of NaOH in 250 mL of distilled deionized water. Fill a 250 mL flask with 70 mL of 4-6% sodium hypochlorite solution. To this flask add 30 mL of 0.1N NaOH solution.

4.) **Sodium Formate Solution.** HCOONa. 50% (w/v). In a 250 mL flask, dissolve 30 g of NaOH in 50 mL of distilled deionized water. Cool solution in an ice bath. While stirring, add 32 mL of 90% formic acid. Fill flask to 100 mL mark with distilled deionized water.

5.) **Potassium Iodide Solution**. SAME AS HYPOHALITE and BROMATE TITRATION

6.) **Ammonium Molybdate Catalyst**. SAME AS HYPOHALITE and BROMATE TITRATION

7.) **6 N Sulfuric Acid**. H_2SO_4. Fill a 1 liter flask with 330 mL of 9N sulfuric acid solution (from hypohalite and bromate titration). Add 170 mL of distilled deionized water.

8.) **Starch Solution (indicator)**. SAME AS HYPOHALITE and BROMATE TITRATION

9.) **0.01M Sodium Thiosulfate Titrant**. SAME AS HYPOHALITE and BROMATE TITRATION

Procedure
Bromide Titration:

1.) Pipet 10 mL of seawater into a 250 mL flask. Add the following reagents in succession: 10 mL of sodium chloride, 10 mL of phosphate buffer, and 2 mL of hypochlorite solution.

2.) Heat solution on a hot plate for 6 minutes at a setting of 4 on a Corning® hot plate. Boil for 5 seconds maximum and then remove from heat. Carefully add 5 mL of sodium formate solution while stirring. Cool to room temperature.

3.) Add the following reagents in succession: 5 mL of potassium iodide, 0.2 mL molybdate solution, 10 mL of 6N sulfuric and 10 mL of starch indicator. Start titration after 30 seconds with sodium thiosulfate until solution is colorless.

4.) Calculate the concentration of bromide using the equation:

$$mM(Br^-)=V(Na_2S_2O_3)*M(Na_2S_2O_3)*16667$$

Where: $V(Na_2S_2O_3)$ is the volume of titrant used, in mL
$M(Na_2S_2O_3)$ is the molarity of sodium thiosulfate

REFERENCES

1. P. C. Singer, "Assessing Ozonation Research Needs in Water Treatment," Journal of American Water Works 82, Oct. (1990) p. 77-88.
2. D. L. LaBonne, "Ozonation of Marine Mammal Pool Waters," National Aquarium in Baltimore, 1990.
3. R. Sugam, J. H. Singletary, W. A. Sandvik and C. R. Guerra, "Condenser Biofouling Control with Ozone," Ozone Science and Engineering 3, (1981) p. 95-107.
4. A. J. Bard and L. R. Faulkner, Electrochemical Methods: Fundamentals and Applications, (New York, New York: John Wiley & Sons, 1980) 700.
5. A. G. Hill and R. G. Rice, Ozone: Historical Background, Properties and Applications, (Ann Arbor: Ann Arbor Science Publishers, 1982)
6. F. L. Evans, Ozone in Water and Waste Water Treatment, (Ann Arbor, MI: Ann Arbor Science Publishers, Inc., 1972) 83.
7. P. M. Williams, R. J. Baldwin and K. J. Robertson, "Ozonation of Sea Water: Preliminary observations on the Oxidation of Bromide, Chloride, and Organic Carbon," Journal of Water Research 12 (1978) p. 385.
8. W. J. Blogoslawski, L. Farrell, R. Garceau and P. Derrig, "Production of Oxidants in Ozonized Sea Water," Proceedings of the Second International Symposium on Ozone Technology, (Jamesville, NY: Ozone Press, 1976) 671-681.
9. P. Pichet and C. Hurtubise, "Proceedings of the Second International Symposium on Ozone Technology," Symposium on Ozone Technology, (Montreal, Canada: International Ozone Institute, 1976) 664-670.
10. E. A. Crecelius, "Measurement of Oxidants in Ozonized Seawater and some Biological Reactions," J. Fish Res. Board Canada 36, (1979) p. 1006-1008.
11. W. R. Haag and J. Hoigné, "Ozonation of Bromide-Containing Waters: Kinetics of Formation of Hypobromous Acid and Bromate," J. Environ. Sci. Technol. 17, 5 (1983a) p. 261-267.
12. J. Hoigné and H. Bader, "Rate Constants of Direct Reactions of Ozone with Organic and Inorganic Compounds in Water-I. Non-Dissociating Organic Compounds," Water Research 17 (1983a) p. 173.
13. R. P. Rice, "Fundamental Aspects of Ozone Chemistry in Recirculating Cooling Water Systems," Paper No. (Houston, TX: NACE International, 1991).
14. P. K. Mitchell, "Bromination: Two Methods Available of Sanitizing," Pool & Spa News April 15 (1985) p. 128-129.

15. W. R. Haag, J. Hoigné and H. Bader, "Improved Ammonia Oxidation by Ozone in the Presence of Bromide Ion during Water Treatment," Water Research 18, 9 (1984) p. 1125-1128.
16. L. B. Richardson, D. T. Burton, G. R. Helz and J. C. Rhoderick, "Residual Oxidant Decay and Bromate Formation in Chlorinated and Ozonated Seawater," Water Research 15, (1981) p. 1067-1074.
17. U. von Gunten and J. Hoigne', "Factors Controlling the Formation of Bromate Ion During Ozonation of Bromide-Containing Waters," J. Water SRT--Aqua 41, 5 (1992) p. 229-304.
18. J. Hoigné, H. Bader and J. Staehelin, "Rate Constants of Reactions of Ozone with Organic and Inorganic Compounds in Water III," Water Research 19, 8 (1985) p. 993-1004.
19. W. R. Haag and J. Hoigné, "Ozonation of Water Containing Chlorine or Chloramines. Reaction Products and Kinetics," Water Research 17, (1983b) p. 1397-1402.
20. A. Bousher, P. Brimblecombe and D. Midgley, "Rate of Hypobromite formation in Chlorinated Seawater," Water Research 20, (1986) p. 865-870.
21. G. Grguric, Relative Importance of Several Inorganic Pathways for Ozone Decomposition in Closed Seawater Systems, Florida Institute of Technology, 1993)
22. W. E. Wyllie II, B. E. Brown and D. J. Duquette, "Unpublished Research," Rensselaer Polytechnic Institute, 1994.
23. J. J. Keaffaber, C. J. Costen and e. W.G. Ham, "Redox Chemistry of Closed Ozonation Systems: Modeling Bromine and other Redox Active Species," The use of Ozone in Aquatic Systems, (Greenwich, Connecticut: The International Ozone Association, 1992) 82-97.
24. M. G. Fontana, Corrosion Engineering, 3rd Ed., (New York: McGraw-Hill, Inc., 1986) 374.
25. H. H. Uhlig and R. W. Revie, Corrosion and Corrosion Control, (New York: John Wiley & Sons, 1985)
26. ASM International, Metals Handbook, V.13: Corrosion, (Metals Park, OH: ASM International, 1987)
27. F. W. Fink and W. K. Boyd, The Corrosion of Metals in Marine Environments, (Colombus, OH: Bayer & Co., Inc., 1970)
28. M. A. Streicher, "Analysis of Crevice Corrosion Data from Two Sea Water Exposure Tests on Stainless Alloys," Materials Performance 22, May (1983)

p. 37-50.
29. B. A. Shaw, P. J. Moran and P. Gartland, "Crevice Corrosion of a Nickel-Based Superalloy in Natural and Chlorinated Seawater," 12th International Corrosion Congress, NACE, 1993) 1915-1928.
30. A. J. Sedriks, Corrosion of Stainless Steels, (New York, NY: John Wiley & Sons, Inc, 1979)
31. H. H. Lu and D. J. Duquette, "The Effect of Dissolved Ozone on the Corrosion Behavior of Cu-30Ni and Type 304L Stainless Steel in 0.5N NaCl Solutions.," Corrosion 46, 10 (1990) p. 843.
32. B. E. Brown and D. J. Duquette, "A Review of the Effects of Dissolved Ozone on the Corrosion Behavior of Metals and Alloys," Paper No. (Houston, TX: NACE International, 1994).
33. R. W. Schutz, "Titanium: The Technically Correct Metal for Offshore Seawater Service," 10th Anniversary Conference on Corrosion and Materials Offshore, (Oslo, Norway: NITO/NKF, 1994)
34. W. L. Adamson and R. W. Schutz, Naval Eng. J. 103, (1987) p. 124.
35. A. J. Sedriks, "Advanced Materials in Marine Environements," Materials Performance 33, 2 (1994) p. 56-63.
36. R. W. Schutz, RMI Titanium Co., Personal Communication, March 1994.
37. K. A. Chandler, Marine & Offshore Corrosion, (London: Butterworth & Co., 1985) 117-134.
38. D. B. Anderson, "Statistical Aspects of Crevice Corrosion in Seawater," Galvanic and Pitting Corrosion - Field and Lboratory Studies, ASTM STP 576, F. Baboian Rowe, and Rynewicz (Philadelphia, PA: American Society for Testing and Materials, 1976) 231-242.
39. ASTM D 1141-90, "Standard Specification for Substitute Ocean Water," (Philadelphia, PA: ASTM, 1990).
40. H. Bader and J. Hoigne', "Determination of Ozone in Water by the Indigo Method," Water Research 15 (1981) p. 449-456.
41. H. Bader and J. Hoigne, "Colorimetric Method for the Measurement of Aqueous Ozone based on the Decolorization of Indigo Derivitives," Ozonation Manual for Water and Wastewater Treatment, W. J. Masschelein (Chichester: John Wiley & Sons, 1982) 169-172.
42. M. Pourbaix, Atlas of Electrochemical Equilibria in Aqueous Solutions, (Houston, TX: National Association of Corrosion Engineers, 1974)
43. G. Bianchi, G. Fiori, P. Longhi and F. Mazza, ""Horse shoe" Corrosion of Copper

Alloys in Flowing Seawater: Mechanism, and Possibility of Cathodic Protection of Condenser Tubes in Power Stations," Corrosion 34, 11 (1978) p. 396-406.

44. F. Mansfeld, G. Liu, H. Xiao, C. H. Tsai and B. J. Little, "The Corrosion Behavior of Copper Alloys, Stainless Steels and Titanium in Seawater," Corrosion Science 36, 12 (1994) p. 2063-2095.